



**HAL**  
open science

# Surface and subsurface structures of the Greater Caucasus flexural basin in Georgia, reconstruction of its tectonic inversion since the Early Cretaceous

Zoé Céleste Candaux

► **To cite this version:**

Zoé Céleste Candaux. Surface and subsurface structures of the Greater Caucasus flexural basin in Georgia, reconstruction of its tectonic inversion since the Early Cretaceous. Earth Sciences. Université Côte d'Azur, 2021. English. NNT : 2021COAZ4053 . tel-03426246

**HAL Id: tel-03426246**

**<https://theses.hal.science/tel-03426246>**

Submitted on 12 Nov 2021

**HAL** is a multi-disciplinary open access archive for the deposit and dissemination of scientific research documents, whether they are published or not. The documents may come from teaching and research institutions in France or abroad, or from public or private research centers.

L'archive ouverte pluridisciplinaire **HAL**, est destinée au dépôt et à la diffusion de documents scientifiques de niveau recherche, publiés ou non, émanant des établissements d'enseignement et de recherche français ou étrangers, des laboratoires publics ou privés.

# THÈSE DE DOCTORAT

Structure en surface et subsurface du  
bassin flexural du Grand Caucase en  
Géorgie, reconstitution tectonique  
depuis le Crétacé Inférieur

**Zoé Céleste CANDAU**

Géoazur

**Présentée en vue de l'obtention  
du grade de docteur en** Sciences de la  
Planète et de l'Univers  
d'Université Côte d'Azur  
**Dirigée par :** Sosson Marc, Dr, HDR  
**Co-dirigée par :** Guillaume Duclaux, Dr.,  
MCF  
**Soutenue le :** 27 juillet 2021

**Devant le jury, composé de :**  
Jon Mosar, PR, HDR, Université de  
Fribourg, Suisse  
Eric Barrier, Dr d'Etat, Sorbonne Université,  
France  
Victor Alania, Dr, I. Javakhishvili State  
University, Géorgie  
Marie Françoise Brunet, Dr, Sorbonne  
Université, France  
Carole Petit, HDR, PR, Université Côte  
d'Azur, France  
Jean-Marc Lardeaux, PR, Dr, Université  
Côte d'Azur, France  
Christian Blanpied, Dr, Sorbonne  
Université, France



# Structure en surface et subsurface du bassin flexural du Grand Caucase en Géorgie, reconstitution tectonique depuis le Crétacé Inférieur

Surface and subsurface structures of the Greater Caucasus flexural basin in Georgia, reconstruction of its tectonic inversion since the Early Cretaceous

## Rapporteurs

Jon Mosar, PR, HDR, Université de Fribourg, Suisse

Eric Barrier, Dr d'Etat, Sorbonne Université, France

## Examineurs

Victor Alania, Dr, I. Javakhishvili State University, Géorgie

Marie Françoise Brunet, Dr, Sorbonne Université, France

Carole Petit, HDR, PR, Université Côte d'Azur, France

Jean-Marc Lardeaux, PR, Dr, Université Côte d'Azur, France

## Invités

Christian Blanpied, Dr, Sorbonne Université, France





# Structure en surface et subsurface du bassin flexural du Grand Caucase en Géorgie, reconstitution tectonique depuis le Crétacé Inférieur

---

## **Résumé**

Le Grand Caucase est une chaîne de montagne correspondant à un bassin Jurassique moyen à Crétacé supérieur, inversé durant le Cénozoïque (âge encore débattu). Les structures de cette chaîne et de son bassin flexural illustrent une combinaison complexe de déformations impliquant la couverture, on parle de « thin-skinned tectonic », et de déformations pouvant impliquer le socle, on parle alors de « thick-skinned tectonic ».

Le bassin flexural s'est développé durant deux collisions successives entre le continent Eurasie ainsi que le bloc Tauride-Anatolide-Sud-Arménie depuis le Crétacé Inférieur (collision dans le Petit Caucase), et se poursuit encore actuellement en liaison avec le poinçonnement de l'Arabie au sud.

Cette région présente un double intérêt. A un niveau purement fondamental, il est évident que la compréhension de la propagation des déformations entre la zone de collision du Petit Caucase au sud et le Grand Caucase permet de mieux contraindre l'évolution tectonique de ce secteur de la chaîne téthysienne et de comprendre le processus d'inversion tectonique et son moteur. D'un point de vue appliqué, l'étude des structures du bassin flexural et des lithologies impliquées dans la déformation est essentielle pour mener des explorations afin d'étudier les systèmes à hydrocarbures comme cela est le cas à l'Est du bassin en Azerbaïdjan.

Cette étude présente de nouvelles données de terrain sur les structures de surface (cartographie, analyse structurale et lithostratigraphique), complétées d'analyses de profils sismiques et de données de forages permettant de contraindre en profondeur les interprétations. Le but de ce travail a été de localiser les structures profondes et les potentiels niveaux de décollements afin de mieux contraindre la géométrie des structures supra-crustales. De plus, l'identification et l'analyse des dépôts sédimentaires syn-tectoniques ont permis de contraindre la chronologie des déformations.

Nous présentons tout d'abord l'étude du bassin flexural de Rioni, situé à l'est de la Mer Noire et à l'ouest du Grand Caucase. Nous avons mis en évidence la présence d'un bassin résultant d'une extension depuis le Barrémien jusqu'au Turonien sous le bassin flexural Cénozoïque de Rioni, et qui se prolonge vers l'Est dans le Bloc Géorgien. Ensuite, dans un second temps nous présentons les résultats concernant le style et la chronologie des déformations dans les bassins de Rioni et de Kura pendant la compression qui se déroule en deux temps : au Paléocène-Eocène puis à partir du Miocène Supérieur. Nous montrons par comparaison entre les bassins flexuraux de Rioni à l'ouest, et de Kura à l'est, que la présence des failles normales du Crétacé qui sont présentes sous Rioni influent grandement sur le style et la localisation de la déformation. Enfin, nous présentons nos résultats concernant la structure et l'histoire tectonique du rift avorté et inversé d'Adjara-Trialeti qui longe au sud le bassin flexural. Ce bassin est aussi affecté par les failles normales du Crétacé au sud de Rioni, mais se développe vers l'est au sud du de Kura de manière superposée durant le Paléocène et l'Eocène. Nous montrons alors que la structure de ce bassin est liée à l'inversion des failles normales, mais aussi de déformations résultant de niveaux de décollements dans les sédiments syn et post-rift. Pour présenter nos résultats, nous proposons trois coupes de plus de 50km traversant du sud au nord toute la région du Transcaucase reliant le Petit et le Grand Caucase, ainsi qu'une reconstitution tectonique depuis le Crétacé Inférieur.

---

Mots Clés : Grand Caucase, Inversion Tectonique, Tectonique, Géologie Structurale

---



# Surface and subsurface structures of the Greater Caucasus flexural basin in Georgia, reconstruction of its tectonic inversion since the Early Cretaceous

---

## ***Abstract***

The Greater Caucasus Mountain Belt is a rifted basin that formed during the Middle Jurassic to the Upper Cretaceous and has been inverted during the Cenozoic (age still debated). The belt is deformed by a complex combination of thick and thin-skinned tectonic. We talk about thick-skinned tectonic when the basement is involved in the deformations, and thin-skinned deformation when the cover is deformed.

The flexural basin of the Greater Caucasus developed since the Lower Cretaceous during the collision in the Lesser Caucasus between the Taurides-Anatolides-South-Armenian microcontinent and the Eurasian plate, and is still active because of the collision with the Arabian Plate to the south.

The Caucasus frame present a key area for two reasons. First, the propagation of the deformations from the Lesser Caucasus to the south, and toward the north in the Greater Caucasus allow us to better constrain the tectonic evolution of this Tethysian belt'part, and to better understand the inversion tectonic mechanisms.

Then, the study of the flexural basin structure, and the involved lithologies, offers the possibility to lead explorations about the oil and gaz resources systems, such as in the Eastern Azerbaijan basin.

We propose new field data (cartography, structural and lithostratigraphic analysis) to constrain the shallow structures, and we combine it with seismic lines interpretations and wells data analysis to constrain the deeper structures. The study was lead following two paths: first, we have localised the deformations and their related style and geometries. Then, the identification of the pre-, syn-, and post-tectonic deposits by the identification of growth strata allowed us to propose the chronology of the deformation during the multi-stage tectonic history in different structures of the flexural basin.

The first part concerns the study of the Rioni flexural basin that borders the Eastern Black Sea and is located south of the western Greater Caucasus. We highlighted a Barremian to Turonian basin beneath the Rioni flexural basin, and which continues eastward in the Georgian Block.

In the second part, we present our results related to the style and the timing of the deformations in the Rioni and the Kura flexural basin during the Paleogene and the Neogene. We highlight a two-stage compression: the first stage is during the Palaeocene-Eocene, and the second since the Upper Miocene. The study of the style of deformation allows us to compare the structural evolution of two basin with regard to the structural inheritance. The Rioni flexural basin structure and the localisation of the deformation are driven by the inherited normal faults, while the Kura flexural basin structure presents only thin-skinned tectonic. Finally, the third part presents our results about the avorted rifted Adjara-Trialet basin. This basin borders to the south the flexural basin, and is affected by the Lower to Upper Cretaceous extension in its western part, south of Rioni. During the Palaeocene-Eocene a superimposed basin was formed and developed eastward, south of the western Kura basin. This extension is coeval with the compression observed in the flexural basin. We show that the structure of this basin is related to the inversion of the inherited normal faults, but is also deformed by thin-skinned tectonic because of some decollement levels in the syn- and post-rift deposits. Our results are presented in three cross-sections and reconstitutions of more than 50km and that cross the whole Trancaucasian area and constrain the structures and the timing of the deformations between the Lesser and the Greater Caucasus since the Lower Cretaceous

---

Keywords : Greater Caucasus, Inversion tectonic, tectonic, structural geology

---





## *Remerciements, Thank you*

Je souhaite par la présente remercier les personnes qui ont permis ou m'ont aidée à mener cette thèse jusqu'au bout. Tout d'abord je remercie l'Ecole Doctorale des Sciences Fondamentales Appliquées (EDSFA) de m'avoir financée pendant mon contrat doctoral, à l'université de Nice Sophia Antipolis puis l'Université Côte d'Azur de m'avoir financée et permis d'enseigner pendant plusieurs années. Je remercie TOTAL Paris d'avoir financé les campagnes de terrain et de m'avoir permis l'accès à des lignes sismiques. Je remercie Victor Alania de l'Institut de géophysique de Tbilisi pour les données de forages ainsi que les anciennes lignes sismiques. Je remerci enfin Alexandre Chabukiani de l'agence Géorgienne du pétrole et du gaz (State agency for Oil and Gas) pour l'accès aux lignes sismiques. Je remercie l'équipe géorgienne, en particulier Shota Adamia, Nino Sadradze, Victor Alania, Onise Erukidze, Aleko Gventsadze, Alexandre Chabukiani, Tamar Beridze et Nata Zviadadze ainsi que Eric Barrier et Christian Blanpied d'être allés sur le terrain avec moi, d'avoir pu observer et m'apporter leurs points de vue.

Je remercie les membres du jury : les rapporteurs Eric Barrier et Jon Mosar, ainsi que les examinateurs Carole Petit, Victor Alania, Jean-Marc Lardeaux, Marie-Françoise Brunet, Christian Blanpied d'avoir accepté de lire et faire partie du jury de cette thèse. Je remercie plus spécifiquement d'avance vos retours et remarques que je considérerai afin de présenter un travail de meilleure qualité, tant à l'oral lors de la soutenance, qu'après la soutenance lorsque je ferai les corrections.

Ce sujet de thèse a été pensé et proposé par Marc Sosson pour qui j'ai toujours eu un grand respect depuis que je l'ai rencontré lors d'un cours de géodynamique en licence. Dès mon stage de licence avec lui, sujet sur la péninsule d'Azuerro au Panama qui s'était très bien passé, nous avons parlé de pouvoir collaborer de nouveau dans le cadre d'une thèse de doctorat. En fin de master, Marc est venu jusqu'à Lausanne où nous avons pu parler plus concrètement du possible sujet de thèse. Une année plus tard, la thèse commençait. Durant les trois premières années de thèse j'ai fait du terrain et j'ai traité et interprété les données. Plusieurs fois j'ai été bloquée et j'allais voir Marc, qui en général en quelques phrases ou directives me menait à pouvoir moi-même résoudre mes problèmes. Il est même arrivé que je ne comprenne pas une phrase, que je la note dans mon carnet de travail, et que j'y revienne plus tard, car il avait déjà compris que j'aurai un souci d'ici quelques semaines. Ce travail a mené à des présentations et posters à l'EGU et à un workshop de l'AAPG. Je dois vraiment appuyer sur le fait que les commentaires scientifiques de Marc sont rigoureux et justes. Il a une capacité, de par son expérience, mais pas que, à voir quels sont les défauts, quels sont les points à améliorer, où se poseront les futurs problèmes. Ce point de vue permet scientifiquement, d'améliorer la qualité de mon travail de manière indiscutable et efficacement.

Pour avoir pensé ce travail et m'avoir aidée scientifiquement pendant ce projet, mais aussi plus généralement de m'avoir inspirée à faire de la géologie structurale une passion, je souhaite donc remercier Marc Sosson. Je souhaite aussi le remercier pour les moments où j'ai eu de gros coups durs dans ma vie personnelle, d'avoir été si compréhensif et d'avoir su me dire que dans ces moments là, on met le travail de côté, et d'y revenir plus efficacement quand les problèmes seront traités.

Mon travail scientifique présenté dans des abstracts pour des oraux et des posters, a aussi été relu et corrigé pour l'EGU et l'AAPG Workshop par Yevgeniya Sheremet que je remercie pour cela. Lors de ces conférences, Guillaume Duclaux et Carole Petit avaient été d'un grand soutien et avaient aussi aidé à améliorer la qualité de mon travail par les corrections et avis sur mes posters et présentations orales.

La suite de ma thèse, la rédaction a été plus difficile et lorsque je n'arrivais alors plus à ouvrir un document, que je n'arrivais plus à même lire un article pour le plaisir, c'est par l'intermédiaire de Frédérique Leclerc et Boris Marcailloux que j'ai pu alors commencer à travailler avec Guillaume Duclaux, avec le soutien de Carole Petit. Déjà, pour m'avoir aidée à ce moment-là je souhaite remercier ces quatre personnes. Pour Guillaume et Carole cela ne s'arrête pas ici. Ils n'ont sans doute pas réalisé à quel point la suite allait être difficile, moi non plus, et ils ne m'ont pas lâchée tant que j'avais besoin de leur aide. Je me souviens du premier confinement, lors de séances « à quatre mains » via zoom, Guillaume jonglait avec les aléas du télétravail, et le fait de rester avec moi en visio parfois pendant 2h de temps, pour corriger et faire avancer le travail. Ainsi, au final, Guillaume et Carole ont pu m'aider mais dans une tâche qui est vraiment très difficile, même s'ils ont aussi évidemment contribué à la science, il s'agissait surtout de méthode, de motivation, d'encadrement de la partie peut-être la moins intéressante en recherche, du moins la moins agréable : devoir encadrer une doctorante en cours de route et qui a failli abandonner, dans un sujet qui n'est pas le leur, avec des méthodes qui ne sont pas les leurs. Franchement chapeau. Aucun de nous ne pouvait se rendre compte de l'année qui allait suivre et des difficultés qui allaient être rencontrées. Ce travail est donc plutôt ingrat et j'espère par ces quelques lignes vous remercier Guillaume et Carole pour ce travail que vous avez fait, j'en suis très reconnaissante. Je tiens aussi à remercier Emmanuelle Hommonay et Gildas Beauchamps d'avoir corrigé un chapitre de ma thèse lorsque le timing devenait trop serré.

Pour la préparation de la soutenance je remercie d'avance Marc et Guillaume, ainsi que les collègues et amis qui me feront répéter et me donneront leurs avis afin de préparer ce travail.

Ces dernières années m'ont permis de faire des rencontres professionnelles teintées de nuances d'amitié. Sur le terrain en Géorgie, j'ai eu le plaisir de pouvoir partager en plus de la

science, des repas, des apéros, des aventures et donc des souvenirs. Les lignes suivantes sont donc en anglais afin que les personnes concernées puissent les lire et les comprendre.

Victor, you have been my “mentor” when we were in the field, I will always remember your sympathy and your smile. I hope one day we will watch a rugby game together.

Nino, you even have invited me at your home, I remember the taste of the fruits of your beautiful garden. Together with Tamara, we went in Tbilisi to visit the city, I still have the memory of you two, replicating the “just married” picture on the bridge. You never let me go to sleep without a “sweet dreams Zoé” and I really appreciated this nice feeling to be in good hands. Onise, you bring me to the museum where your wife is a specialist and learn me the history of Georgia, you explained to me many Georgian traditions. Alexandre Chabukiani you went with me In the field during a rainy day, you bring me from places to places for different meetings and you were always nice to me. Aleco Gventadze, we have been to different places in the field, many pictures, many memories, and I remember your complicity with Nino Kvavadze, you made me laugh both of you. We have also shared a week of field in the south of Georgia with Nata and his grand-daughter. You take care of me, of my needs and your sympathy went directly to my heart. Emzhari, our driver, so nice to me to, he scared me many times on the road, but always put some musics and said nice things. Finally, I am very happy to have met Shota, quelques mots de français de temps en temps, always so kind to me. I hope I will see you again, all of you, and I want to thank you. Take care of you, your families, and Gaumarjous.

Sur le terrain, j’ai aussi pu partager quelques jours avec Éric et Christian. Ils ne connaissaient pas cette région, et je les ai donc emmenés à divers endroits traités par ma thèse. Leurs observations et interprétations sur le terrain ont été très intéressantes pour moi. En plus de la géologie, ils ont pu me raconter diverses expériences (je retiens que je dois absolument aller voir les hippopotames et les éléphants en Ouganda, qu’il faut éviter les crudités et aliments non cuits lorsque l’eau n’est pas forcément très saine dans le coin, ainsi que mon premier « seep ». J’ai apprécié ces quelques jours avec vous deux et vous en remercie.

En plus du terrain, j’ai pu voyager lors de congrès et conférences. Mes deux EGU je les ai faits en étant accompagnée de Carole, Anthony que j’appelle Tony depuis la licence, de Guillaume et de Jean. J’ai apprécié ces journées avec vous et vous m’avez encouragée, guidée à travers ces premières expériences de congrès. Je ferai une mention spéciale des « petits déj’ Viennois » de Carole, étape importante car « c’est trop bon » (chez Wendy par exemple) ces souvenirs, avec tes yeux qui brillent entre deux arrêts de métro ainsi que ton rire face aux pubs « The New Bralette » dans le métro. Tony et les soirées avec « les inconnus » pour se détendre, et Guillaume et Jean avec quelques bières, rien de plus normal, pour se détendre aussi, en fin de journée.

Marc Hassig m'a accompagnée pendant le workshop à Batumi, avec notre petite terrasse pleine de raisins.

J'ai pu aussi recroiser les copains de master pendant ces conférences, Laure Cindy Gino et Thibault entre bière et cafés du matin, et évidemment Dori (Dorotha) avec qui nous avons déjà tant partagé en master, et encore dans le palais de Sisi.

Je souhaite faire une mention spéciale pour Boris, Frédérique et Bernard qui m'ont aidée pendant une période difficile. Je vous remercie d'avoir été de tels soutiens. De plus, Angélique Derambure a été d'une grande aide, tant niveau méthodologique que personnellement, et peut-être prochainement avec la défense, qui m'a beaucoup aidée à travailler et à retrouver la confiance en moi. Elisabeth Taffin de Givenchy m'a aussi soutenue en cours de thèse, me donnant la force de ne pas abandonner.

J'ai été financée depuis le début de la thèse pour enseigner. Ceci m'a permis de croiser le chemin de divers enseignants-chercheurs. Sur le terrain, nous avons partagé de bons moments et des bonnes bières en fin de journée avec Stéphane Bouissou, Bertrand Delouis, Huyen Chan et Maxime Godano. En plus du travail d'enseignant, vous m'avez permis de « boucler la boucle » dans le Verdon

Les cours en pétrologie m'ont permis de collaborer avec Marie Revel, Guy Libourel, Chrystèle Verati, Christophe Renac, Emmanuelle Homonnay et Asmae El Bakili. Nous avons dû faire face aux demandes liées aux réformes de l'université et aux problèmes d'organisation. Je me souviendrai toujours des TDs où l'on se retrouvait à faire nos trajets entre deux bâtiments avec des cadies remplis de roches. J'ai aussi travaillé avec Emanuelle, Guillaume, Carole et Frédérique lors de sorties terrain, et je me souviens particulièrement bien de la journée dans l'Estérel lorsque les étudiants se plaignaient de marcher 25minutes en fin de journée et que « ce n'était pas humain » de demander de tels efforts en fin de journée.

Hors de mes fonctions, j'ai pu aussi profiter de la vie du labo. Nous avons des soirées belotes en première année, évidemment parmi les personnes les plus importantes se trouvent mes compères Tony, Sara et Luc, et je souhaite faire un clin d'œil à toute la team Belote de Géoazur car les soirées belotes étaient vraiment agréables.

Nous avons aussi eu l'occasion de faire des apéros les midis dans le cadre des « Vino'Azur », organisés par Marianne Saillard, c'était vraiment de bons moments autour de vins présentés chacun notre tour. Je vous avais amenés des vins blancs suisses pour la découverte, et nous amenions tous de bons entremets, entre fromages et gourmandises, j'ai eu de bonnes discussions avec plusieurs personnes du labo dans ces moments.

D'ailleurs, lorsque je revenais dans mon bureau, il faut savoir que j'ai eu différents co-bureaux : tout d'abord Sargis Vardaniyan, avec qui on se suit, toujours de loin mais j'aime cette connexion avec toi. Puis avec Nicolas Wynant-Morel, avec qui ce partage de bureau n'a été qu'un début d'amitié forte, Yanchuan avec qui j'ai partagé quelques mois dans ce bureau au



dernier étage isolée, puis avec les filles Manue, Sara et Caro. J'ai vraiment apprécié être avec vous dans les bureaux. Laurie nous n'étions pas dans le même bureau, même si le tien faisait office de QG, tu as aussi été d'un grand soutien et j'espère que nous aurons plus de temps (heureux) à l'avenir, car il est important de se serrer les coudes dans les mauvais moments, et on a eu notre dose, maintenant, place aux bons moments. D'ailleurs, j'y repense, avec Emmanuelle et Laurie, notre week-end à taper des talons en Irlande pour la fête de la musique traditionnelle, les chaussures n'ont pas survécu et cela a offert de beaux souvenirs. D'autres amitiés se sont créées, Pierre, Diego, Quentin, Alain, Gentiane, Stephen et plein de monde que j'oublie de mentionner c'est certain.

Dans ma vie extra-labo, j'ai pu découvrir de nouveaux hobbies et de nouvelles passions. Tout d'abord les jeux de société, les BDs avec Gilles, Octave et Nolwenn qui m'ont initiée, et le relais a été pris par Caro, Nico, Serge, Flo, Ophélie et Lionel. Romain et Clémence sont aussi passés par là, mais ils avaient d'autres projets.

D'ailleurs les jeux n'étaient pas notre seule activité hors-les-murs, et nous avions nos apéros en fin de journée en bord de plage ou aux sommets des montagnes. Gaspard, même en partant loin, nos chemins se sont et vont encore se recroiser pour profiter de la nature pour changer des appels téléphoniques.

Je fais une spéciale mention pour Christophe Matonti, Manue, Gildas, Maria José, Hector et Sébastien qui étaient présent durant l'été 2020, ainsi que le groupe de Geomusic, dont principalement Caro Serge et Nico avec qui nous avons fait équipe pour gagner un belle bouteille de gin, non pas au quizz car d'autres étaient meilleurs que nous, mais en musique (lobbying) pour ACDC/Gorillaz.

En parlant musiques, le labo ainsi que l'observatoire étaient rythmés par deux groupes majeurs : Waiting 4 Ze Bus et the WatHerMelons. Je ne saurais vous dire si j'allais les voir pour leur musique ou par amitié, mais ils savaient tous mettre l'ambiance pour passer de très bonnes soirées, à Mouans Sartoux, à Géoazur, ou encore à l'observatoire de Nice, face au coucher de soleil, sous la pluie, rien ne les arrêtait.

De jolies randonnées avec Emmanuelle et Gildas pour bien s'aérer, parfois avec Asmae, Flo, Romain, Clémence, Jean et Stella. Manue, d'ailleurs m'avait initiée au fitness, en mode « gazelle ».

Personnellement, j'ai partagé le quotidien de pas mal de personnes. La coloc de Garebejaire (Octave, Gilles, Nolwenn and co), la coloc de Magnan avec Sabine, Matthieu, Valère, Emilie qui m'ont donné envie de trouver la mienne. A Biot, malgré les tristes évènements qui sont survenus, j'ai pu rencontrer des personnes incroyables, spécialement en Aurore, Hubert et Oussama qui m'ont marquée et que j'apprécie énormément. Plus tard j'ai partagé le quotidien avec Asmae El Bakili, je pense que toutes les deux nous aurions préféré partager des moments plus faciles qu'une fin de thèse, on en profitera bientôt. Enfin, ma coloc à Nice, avec

plus spécifiquement Anne qui terminait sa thèse aussi, et Camille qui est une personne pleine d'amour, m'a suivie jusqu'à ce que je rentre à la maison « dans mes montagnes ». La maison du bonheur m'a aussi souvent accueillie, avec David Dédé mon très cher ami et ses compères Carlo, Andy, Alison et amis Marcus, Marion et Robin (Audrey).

Je pense que ma plus grande révélation durant ces années a été la découverte du rugby. Je serai toujours reconnaissante que Patrick m'ait emmenée sans le dire sur ce chemin. Je me souviens de ce premier entraînement où je pensais être dans une équipe de toucher, lorsque l'on s'est échauffé les cervicales, mis les protèges-dents, et qu'il m'a dit « t'inquiète pas, c'est pareil ». J'ai donc débuté avec cette équipe à Mandelieu où j'ai pu rencontrer des personnes importantes, dont Bee, Prit, Lucile = Coquelicot (très douce en effet, et fragile), Ratatouille, et Carine, ainsi que Damien. J'ai ensuite poursuivi dans le rugby en m'engageant auprès de l'équipe du RCASA à Antibes, avec nos coachs Pierre dit « le barbu » et Tintin. J'ai pu rencontrer des femmes fortes et battantes, dont Camille, Sini la warrior, lorsque nous n'avons pas repoussé les méduses en maillot de bain lors d'une baignade au cap d'Antibes.

Je ne sais pas si c'est le rugby qui m'a mis sur leur chemin, ou le fait d'avoir croisé leur chemin qui m'a donné envie de progresser encore en rugby. Pour le cas d'Aurélien, il était déjà mon enseignant en planétologie comparée en licence, et du coup je pense qu'il s'agit d'un hasard, un beau hasard de pouvoir fouler la pelouse à ses côtés. En tout cas, je me suis retrouvée à partager d'abord des terrasses, avec Guillaume, Michel, Laure, Aurélien, Eric, Eva et Mamadou (Champions du monde !!!), et cela, de fil en aiguille m'a amenée à faire chanter le cuire avec certains d'entre eux. Le Riviera Rugby Club a été pour moi un refuge pendant plusieurs années, et pourtant aussi un grand défi physique et féministe. J'ai pu durant plusieurs années faire ma place dans cette équipe de rugby, au milieu de Castor, d'enclume et de poney. Le week-end de 6 nations à Rome m'avait réellement permis un apparté dans ma vie de thésarde, et je ne crois qu'aucun des joueurs de cette équipe ne se rend compte à quel point ils ont été importants pour moi. Ben Stevens m'avait aussi permis de jouer avec les barbarians. La Rivier Family, avec son bordeaux des Arboras a été un des piliers de ma vie pendant plusieurs années. De là sont sortie des amitiés avec des personnes, des souvenirs. Je fais évidemment une mention spéciale à mes deux comparses de la triplète Ben et Py qui m'ont permis de beaucoup rire pendant près d'une année. Nous avons eu aussi des équipes de belote avec Bob, Py, Hervé, Ben, Victor et Fabien au Corner. La dernière belote en date montre une victoire de Victor et Zoé contre Py et Ben. J'ai pu d'ailleurs être initiée au yoga avec Laure, sur la colline du château, face à la mer et cela m'a beaucoup apporté car j'essaie encore aujourd'hui.

Evidemment, il ne s'agit pas uniquement de rencontres, les personnes qui me connaissent depuis toujours ont été d'un très grand soutien, la Team Morzine avec en particulier des appels plus ou moins réguliers avec Antho, athlète de haut niveau dont les conseils d'ami proche

m'ont toujours été utiles, la motivation et l'amour donné par Maëlle et Clo, Thibault, et quelques apéros avec Yo. Le week-end à Bristol « chez » Vince était lui aussi un moment mémorable. Mes amis en Suisse, en particulier les copains de Master croisés de temps en temps, et le groupe de copines avec Marine mon amie de toujours, Audrey, Christèle, Cindy et Magali qui sont pendant que j'écris ces lignes entrain de fêter nos 30ans. J'espère être bientôt plus présente avec vous tous et vous montrer comme vous êtes tous importants pour moi. J'ai eu du soutien de ma famille aussi, Valoue, Juju, Laurane, Catherine.

Aurélien m'a aidée de près ou de loin pendant les moments les plus durs et je suis heureuse d'avoir pu compter sur quelqu'un qui pouvait aussi bien me comprendre et me soutenir dans ces moments.

Enfin pour terminer, ceux qui ont suivi au plus près toute ma vie mes sacrifices, mes peines et déceptions et qui ont été présents et source d'une force incroyable, ma maman, mon papa, et surtout mon petit frère Moutte.

Merci à tous, vous avez été très importants pour moi.



## Table des matières, Table of contents

<b>Résumé</b> .....	5
<b>Abstract</b> .....	7
<b>Remerciements, Thank you</b> .....	11
<b>Table des matières, Table of contents and list of figures</b> .....	19
<b>Chapter 1: Introduction: Deformation of inherited structures during collisions: insights from the Greater Caucasus flexural basins</b> .....	27
I. Deformations styles in inverted basins .....	28
Abstract .....	29
1. Introduction on deormations styles in fold-and-thrusts belts .....	28
2. What controls the style of deformation? .....	31
3. Why is it important? .....	33
II. Case-study: the Greater Caucasus basins .....	38
1. The Tethys Ocean and the related back-arc basins .....	38
2. The Greater Caucasus: the Alpine history .....	39
3. Tectonic questions and timing of the multi-stage tectonic history .....	40
4. Structural interpretations related to the style of deformation .....	44
III. Objectives of the study and methodology .....	49
1. The problematic .....	49
2. Objectives .....	49
3. Methodology and data .....	50
<b>Chapter 2 : Identification of inverted Mesozoic back-arc basins in the internal zone of the Caucasus Orogen, insights from the Transcaucasus area, western Georgia</b> .....	55
Abstract .....	56
I. Introduction.....	57
II. Geological context.....	61
1. The structures of the Northwestern Transcaucasus domain.....	61
a. Foreland basins .....	61
b. The Southern Greater Caucasus .....	62
c. The Georgian Block.....	63
d. The Dzirual Massif and the Adjara-Trialeti Fold-and-thrusts belt .....	63
e. The Eastern Black Sea .....	64
2. The stratigraphy in the northwestern Transcaucasus .....	64
III. Structural and stratigraphic observations in the Rioni .....	67
1. Foreland Basin and the Georgian Block .....	67
2. Western Section across the Rioni area .....	67

a.	Rioni Foreland Basin: South of the Tsaishi Anticline .....	69
b.	Rioni Foreland Basin: the Tsaishi Anticline .....	70
c.	Greater Caucasus Southern Slope Zone: the Jvari Anticline .....	76
d.	Mesozoic deposits thickness variations along the Rioni transect .....	80
3.	Eastern transect across the Georgian Block.....	82
a.	The Dzirula Massif.....	84
b.	The Georgian Block .....	86
c.	The Ambrolauri Flexural Basin.....	95
d.	Thickness variations along the Georgian Block transect .....	98
IV.	Tectonostratigraphic interpretations.....	100
1.	The Georgian Block.....	100
2.	The Ambrolauri Flexural Basin .....	101
3.	Across the Rioni FB.....	101
4.	Beneath the Rioni FB.....	102
5.	The Jvari area.....	103
V.	Conclusion .....	105
1.	Reconstitution from the Lower Jurassic .....	105
2.	Role of the inherited structures during syn-collisional deformations .....	109
3.	Main tectonic events .....	109

***Chapter 3: Style and timing of collision-related deformations in the flexural basins along the southern Greater Caucasus*** .....

I.	Introduction.....	112
II.	Geological setting .....	115
1.	The foreland basins .....	116
2.	Rioni and Ambrolauri flexural basins .....	116
3.	Kura and Kartli foreland basins .....	118
III.	Field observations .....	120
1.	The Paleogene deposits .....	121
a.	Localisation of deformation and growth strata: the structures .....	121
b.	Jvari - north of Jvari .....	124
c.	Ambrolauri .....	128
d.	South of Rioni .....	131
e.	Kura foreland basin .....	138
2.	The Neogene deposits .....	146
a.	Rioni-Ambrolauri .....	148
b.	Kura and Kartli basins .....	149
c.	The Adjara-Trialeti fold-and-thrust belt .....	149
IV.	Interpretations .....	149
1.	In the Rioni-Ambrolauri flexural basins .....	150

a. The Paleogene deposits .....	151
b. The Neogene deposits .....	152
2. In the Kura-Kartli flexural basins .....	154
a. The Paleogene deposits .....	154
b. The Neogene deposits .....	156
V. Discussion, comparison from west to east .....	155
1. The Paleogene deposits .....	156
2. The Neogene deposits .....	157
Conclusion .....	157

**Chapter 4: The structure of the Adjara-Trialeti Fold-and-thrusts belt .....** 159

I. Introduction .....	161
II. Geological Setting.....	163
III. Observations.....	165
1. Nature and thickness of the deposits along the AT.....	166
a. The Cretaceous deposits.....	166
b. The Paleogene deposits.....	168
c. Wells data in the Western-Central AT .....	171
2. The structures.....	171
3. Thin-skinned and small scale tectonic.....	172
4. Thick-skinned tectonic and major fold-and-thrusts structures of the belt.....	175
a. The borders.....	175
b. Dzirula.....	178
IV. Interpretations - discussion .....	179
1. The general structure of the belt.....	180
2. Reconstitutions.....	187
a. Adjara-Trialeti during the Mesozoic.....	187
b. Adjara-Trialeti during the Paleogene.....	187
c. Adjara-Trialeti during the Neogene compression.....	187
V. Conclusion .....	188

**Chapter 5: Discussion .....** 190

I. Introduction.....	191
II. The main results of the study.....	192
1. Interpretation of tectonic events during the Mesozoic.....	193
a. The Rioni foreland basin and the Georgian Block: the western section.....	193
b. The Kura foreland basin and the Central Greater Caucasus: the eastern section.....	194
2. Interpretation of post-Mesozoic tectonic events.....	194
a. In the western section.....	194
b. In the eastern section.....	194
3. Differences from west to east.....	195
a. Differences during the Mesozoic.....	195
b. Differences after the Mesozoic.....	195
4. The Adjara-Trialeti from basin to fold-and-thrusts belt.....	196

a. The tectonic history of the AT fold-and-thrusts belt.....	196
b. The structure of the AT Fold-and-thrusts belt.....	196
III. The flexural basins of the GC in Georgia: highlights of the tectonic history.....	199
1. Reconstitutions.....	200
2. Tectonic units and tectonic stages in space.....	201
IV. Highlights of the open questions pointed out and discussion.....	202
1. Eastern Black Sea structures continuation.....	204
a. The Adjara-Trialeti basin, Dzirula and the Georgian Block.....	204
b. The Ambrolauri horst.....	204
2. The relation of the Jvari area and the Greater Caucasus.....	205
3. The superimposed basins in Adjara-Trialeti.....	205
4. Tectonic during the Paleogene.....	206
a. Relation between the Paleogene Eastern Black Sea and Rioni basins.....	206
b. Extensional stage during the Palaeocene Eocene collision.....	207
c. The Oligocene deposits.....	208
5. Styles of deformation variations from west to east along the belt and relations with the inherited structures.....	208
V. Limits and perspectives.....	210
1. Styles of deformation variations from west to east and relations with strike-slip structures (inherited or neoformed).....	210
2. What controls the style of deformation? .....	213
3. Salt tectonic in the Maykopian deposits.....	214
4. The shortening rate.....	215
5. Resources.....	215
VI. Conclusion .....	216
<b>Bibliography</b> .....	2190



## List of figures

### Chapter 1:

Figure I.1: A-C: Schematic cross-sections from (Pfiffner 2017) and (Lacombe & Bellahsen 2016)

Figure I.2: Sketch from (Butler et al., 2006)

Figure I.3: Cross-sections from (Lacombe & Bellahsen 2016) and (Scisciani et al., 2019)

Figure I.4: Paleotectonic maps from Barrier et Vrielynck 2008 (MEBE project)

Figure I.5: Details on the paleotectonic maps from Barrier et Vrielynck 2008 (MEBE project)

Figure I.6: Paleotectonic reconstruction of the Caucasus area after (Rolland et al., 2020)

Figure I.7: Tectonic map and the related Cross Section after (Sosson et al., 2016)

Figure I.8: Data and localisations of the field observations on the Google Earth view of the Georgia

Figure I.9: Figures after (Ahmadi et al., 2013)

### Chapter 2:

*Figure II.1: Structural sketch of the Black Sea-Caucasus region in the general framework of the Middle East based on current work data and previous interpretations (Milanovsky & Khain 1963; Adamia et al., 1981, 2011a, 2017; Gamkrelidze 1986; Okay et al., 1994, 2015; Nikishin et al., 2003, 2010, 2015a, 2017; Sosson et al., 2010, 2016, 2017; Stephenson & Schellart 2010; Tari et al., 2018; Tari & Simmons 2018).*

Figure II.3: Synthetic stratigraphic log of the North-western Transcaucasus (Georgian Bloc)

*Figure II.3: Pictures along the western cross-section across the Rioni Foreland basin toward the Jvari area*

*Figure II.4: Cross sections of the Tsaishi Anticline near TsC on Fig.1, and Gakhomela anticline (Gk in Fig.1) with associated pictures along the transects.*

*Figure II.5: Seismic interpretation of the Tsaishi seismic line*

Figure II.6: Cross sections of the Jvari anticline “Jv” on Fig.1 with associated pictures and stereonet along the transect.

Figure II.7: *Stratigraphic log for the western section*

*Figure II.8: Pictures along the eastern cross-section.*

*Figure II.9: Dzirula area locations of the seismic lines, and the relative seismic interpretations.*

Figure II.10: Cross sections of the Koutaissi Anticline near Kt on Fig.1 with associated pictures along the transects.

Figure II.11: Cross section of the Tkibuli area, Tk on Fig.1 with associated pictures along the transect.

Figure II.12. Cross sections of the Kenashi anticlines near Zg “Zogishi” on Fig.1, with associated pictures and stereonet along the transects.

Figure II.13. Cross sections of the northern Ambrolauri area with the frontal GC deformation. Both cross sections are associated with the pictures along the transects.

Figure II.14: Stratigraphic log for the western section

Figure II.15: Geologic cross-sections based on field, well and seismic data

Figure II.16: Reconstitution of the Western Cross Section

Figure II.17: Reconstitution of the Eastern Cross Section

### *Chapter 3:*

*Figure III.1: Tectonic map of the Rioni and the Kura foreland basins and the neighbouring areas.*

Figure III.2: Stratigraphic log with thickness variations, modified after Adamia et al., 2011, a.

*Figure III.3: Pictures of observations mainly in the frontal deformation with the Uppermost part of the Cretaceous in the Jvari area and north of Ambrolauri area.*

*Figure III.4: Cross section of the Jvari area with the stereonets of bedding and associated pictures.*

Figure III.5: Cross section of the western part of Kenashi with the associated pictures. Interpreted Google Earth view of the area and the stereonet of the data of the Kenashi area.

*Figure III.6: Pictures of the area of Tsaishi*

Figure III.7: Interpreted scan of the Tsaishi old seismic line.

Figure III.8: Cross sections of the Gakhomela and Tsaishi anticlines and associated pictures.

Figure III.9: Pictures in the frontal deformation of the Greater Caucasus in the Kura area

Figure III.10: Cross section of the Ananauri area with the stereonet of bedding from the data along the section and associated pictures.

*Figure III.11: Cross section of the Zhinvali area with the stereonet from the bedding planes measurement along the section and associated pictures.*

*Figure III.12: Cross section of the Zhinvali area on the eastern part of the mountains with the stereonet from the bedding data along the section and associated pictures.*

Figure III.13: Pictures of the deposits in the Kura and Kartli foreland basins.

Figure III.14: cross sections located in Fig. III. 1.

Figure III.15: Reconstitution of the cross-section in the Rioni FB after the Mesozoic.

Figure III.16: Reconstitution of the cross-section in the Kura FB after the Mesozoic.

## Chapter 4:

Figure IV.1: Tectonic map of the Adjara-Trialeti fold-and-thrusts belt and the neighbouring areas.

Figure IV.2: Stratigraphic log with thickness variations, modified after Adamia et al., (2011a).

Figure IV.3: Pictures of the Mesozoic deposits observed along the AT.

Figure IV.4: Pictures of the Paleogene deposits in the Eastern AT.

Figure IV.5: Pictures of the Paleogene deposits in the Western and central AT.

Figure IV.6: Wells data in the Western-Central part of the AT, illustrated in stratigraphic log with thickness.

Figure IV.7: Pictures of small-scale deformations in different deposits along the AT.

Figure IV.8: Cross sections on the northern border of the AT with associated pictures.

Figure IV.9: Cross section south of the Dzirula massif, at the transition with the AT with associated pictures and interpreted seismic line.

Figure IV.10: Cross section of the central AT with the relative pictures.

Figure IV.11: Cross section and relative pictures of the Eastern AT.

Figure IV.12: Reconstitutions of the Adjara-Trialeti basin since the Upper Cretaceous from the Eastern to the Western part.

## Chapter 5:

Figure V.1: Evolutive cross-section of the Western Transcaucasus area, from the Adjara-Trialeti section, the Rioni foreland basins and southern Greater Caucasus.

Figure V.2: Evolutive cross-section of the Central Transcaucasus area, from the Adjara-Trialeti section, the Dzirula horst, the Georgian Block "basin", the Ambrolauri horst / foreland basin and the southern Greater Caucasus.

Figure V.3: Evolutive cross-section of the Eastern Transcaucasus area, from the Adjara-Trialeti section, the Kura foreland basins and southern Greater Caucasus.

Figure V.4: Tectonic reconstitution sketches of the western and central Georgia during the Lower Cretaceous, the Palaeocene-Eocene and the Upper Miocene.

Figure V.5: Recapitulative table of the observations and interpretations resulting of the study for the eastern Transcaucasus area

Figure V.6: Recapitulative table of the observations and interpretations resulting of the study for the western Transcaucasus area



***Chapter 1: Introduction: Deformation of inherited structures during collisions: insights from the Greater Caucasus flexural basins***

## I. Deformations styles in inverted basins

### Abstract

Aborted continental rifts' structures are defined by normal and strike-slips faults. In orogens, these old structures can be identified but are often covered or deformed by compressional deformations. We call it the structural inheritance which has been studied for decades in the main orogens because these mechanisms inform us on the continental lithosphere's rheology. The Greater Caucasus has not been studied with this idea. Our work give new results which highlight the role of these inherited structure in the localisation and the style of multi-stages deformations that lead to the inversion of continental back-arc basins.

First, I will present the different styles of deformations and the deformations observed in inverted basins, and then, the problematics related to the Greater Caucasus.

### 1. Introduction on deformations styles in fold and thrust belts

The style of deformation of fold-and-thrust belts has been subject of central studies during the last century as described in (Lacombe & Bellahsen 2016) who proposed a review of the subject. The discovery of nappes tectonics (Fig. I.1, A) have been the subject of many studies during the past decades and has given rise to a lot of questions about how to equilibrate these structures (Suppe 1983; Suppe & Medwedeff 1990; Epard & Groshong, 1993, 1995) among a lot of other.

The compressional deformation can occur not only within the main axial zones including nappes but also in tectonic zones located out of the main range: forearc basins and back-arc basins develop during the subduction (under extensional tectonics for back-arc basins), and when the collision occurs these structures are also deformed and inverted by the compression. In these areas, the style of deformation is very interesting because the inversion of these basins can be accommodated by three different mechanisms as proposed by Pfiffner (2017) (Fig. I.1): i) thick-skinned tectonics when normal faults are inverted as reverse faults which involve the basement (refs), ii) thick-skinned tectonics can also occur with some major detachments in the basement when the amount of shortening is large (as observed in the orogenic belts) and finally iii) thin-skinned tectonics occurs when the sedimentary cover is thrust onto a decollement level. (Davis *et al.*, 1983) developed this view by showing that the deformation will at first be triggered by internal deformations in the wedge, mainly by

thrusts. The horizontal deformation along the basal decollement level can only be active when the wedge has grown enough (depending on the basal friction and the internal friction, depending on Coulomb failure criterion and weakness linked to temperature and fluids pressures) (known as the critical taper theory). The superficial decollement levels can be rooted at depth along thrust at the basis of the sediment cover. This style of deformation generally implies important shortening in the orogenic belts (Fig. I.1, A, D).

Thick-skinned tectonic deformation involves the basement. It can imply the basement in thrusts that root in the upper crust (Fig. I.1, B), or deform the basement with steep fault (Fig. I.1, C). These styles of deformation can be linked together. As proposed by Lacombe & Bellahsen (2016) (Fig. I.1, D), the thick-skinned tectonics can be related to thin-skinned tectonics in space and time: for the space, the Fig. I.1, D: a and b show that the major deformations linked to the under-thrusting (orogeny scale), with an important shortening, affects the basement with crustal-scale rooted thrusting (Fig. I.1, B style). These thrusts then propagate towards the surface, along a decollement level located in the sedimentary cover and create thin-skinned tectonic structures. In Fig. I.1, D c, the major décollement level is located in the crust (also Fig. I.1, B style) while the cover is affected by thin-skinned along a decollement level (salt in this case). This shows that in the same area, or same structural unit, shortening can be accommodated by different tectonic styles. Finally, Fig. I.1, D, d presents a foreland basin, where thin-skinned tectonic occurs, but is “broken” (Lacombe & Bellahsen 2016) by an important uplift. This uplift is due to an inverted basin. The thick-skinned tectonic stops the propagation of the thin-skinned deformation. This example shows also that the vergence in the thin-skinned deformation is not controlled by the thick-skinned deformation as in Fig. I.1, D, a and b. The superimposed structural style during these deformations can occur simultaneously. (Lacombe & Bellahsen 2016) give an example of simultaneous thick-skinned and thin-skinned tectonic deformations in Zagros (the structure is in Fig. I.1, D, c), and in the first stage Sierras-Pampeanas-Laramides (Fig. I.1, D, d). The possibility to have the thick-skinned deformations followed by thin-skinned deformation (not necessarily induced), or the opposite with the thin-skinned tectonic followed by thick-skinned tectonic is also mentioned in their publication.

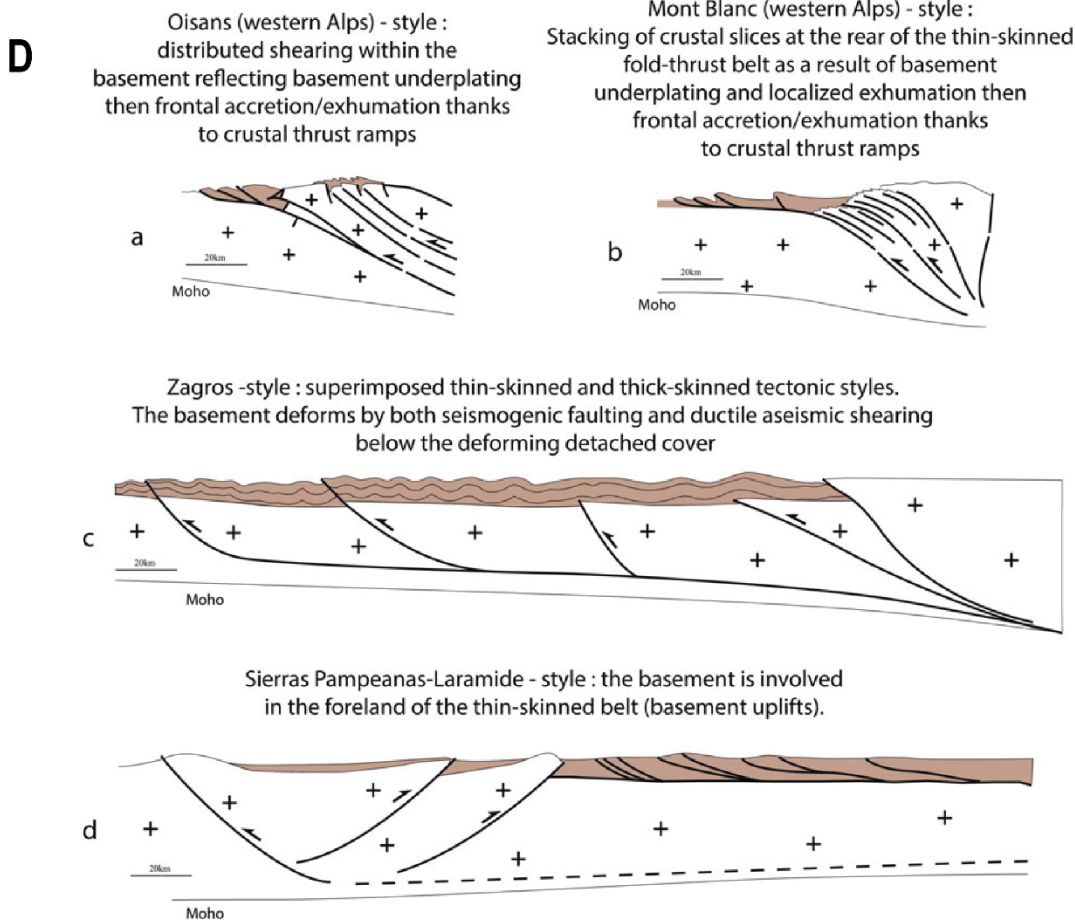
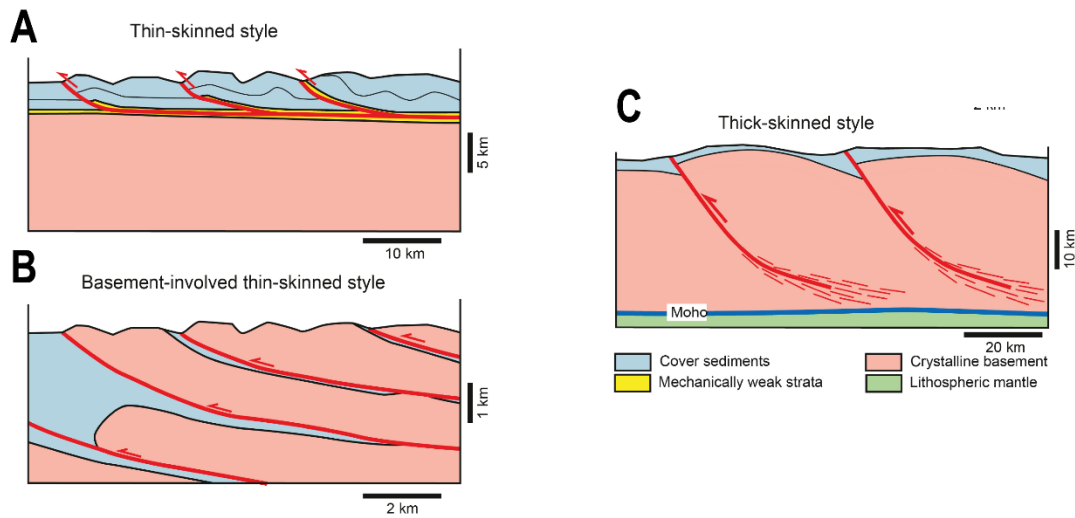


Figure I.1: A-C: Schematic cross-sections showing three styles of thin-skinned and thick-skinned tectonics from (Pfiffner 2017). Pictures D from (Lacombe & Bellahsen 2016) proposes different examples of interplays of different deformations styles in a same tectonic unit



## 2. What controls the style of deformation?

Since different styles of deformation can occur at the same place, it is important to better understand what controls the occurrence, the style, and the localization of compressional deformations. The review of (Lacombe & Bellahsen 2016) proposes to discuss the parameters which could control the styles of deformations observed. They proposed that the parameters that control the mechanisms of deformation are the structural inheritance and the rheological aspects, which were discussed already in (Davis *et al.*, 1983). The temperature in the crust plays a major role in the weakness of the materials (i). The weaker is the crust, the possibility to deform it as a whole and thus with thick-skinned tectonic is important, while a strong and cold lithosphere could imply localisations of the deformation in thin-skinned tectonic. The slab retreat, the extension in the back-arc area or a young passive margin are examples of increased weakness in the crust that can involve thick-skinned deformations. The second main mechanism proposed is the possibility of preferential localisation of the deformation linked to the coupling with the mantle (ii): the higher the coupling, the less the crust can be deformed as a whole, which creates thin-skinned tectonic. If the coupling is low, the crust can thus be deformed with thick-skinned tectonic. This mechanism is different when we have a look in the intraplate coupling (iii). The intraplate coupling is linked to the stress transfer occurrence. The higher is the intraplate coupling, the higher is the stress transfer and can lead to deform the basement, and thus create thick-skinned deformations. When the intraplate coupling is low, the deformation will be thin-skinned tectonic. The intraplate coupling is linked to the amount of syn-tectonic sedimentation because of the degree of friction it can generate. When the syn-tectonic sediment amount is high, the friction increases and thus the intraplate coupling increases and creates more thick-skinned deformations. When the amount of sediments is low, the friction decreases, and the intraplate coupling is low and new thrusts can be created with efficient decollement levels.

Fig. 1.2 summarizes the different possibilities of structures when the deformation is localized onto inherited normal faults. Depending on the dipping of the faults, if the normal faults was curved low-dipping listric-style normal fault, the possibility to inverse it is higher than with high-dipping normal faults. The inversion of listric fault could evolve in a major frontal thick-skinned thrust and involve a shortcut. The inversion of high-dipping normal faults is linked to the friction localized on the fault. If the friction is high, the normal fault can't be inverted, and

a “buttressed cover against the wall” can be observed. With a low friction, the fault can be inverted with minor displacement of the cover (“minor faults”), or with major displacement which creates some major thrusts “fully inverted normal faults” in the Fig. I.2. We can wonder if the major thrusts and thus fully inversion could develop on minor normal faults, and minor inversion could occur on major normal faults to know if the degree of inversion is linked to the degree of importance of the normal fault. It is also proposed that the normal fault can be inverted at depth but creates a shortcut at surface. Finally, the friction on the faults could be triggered also by the temperature in the crust, and thus the age of the latest tectonic event. The same inherited structures in a rigid and cold craton could not have the same behaviour than the inherited structures in a young and warm lithosphere.

The deformation style can thus be a combination of thick and thin-skinned tectonics in the same FTB, and as well in the same structural unit (as an inherited rifted basin), and the relationship between thick and thin-skinned deformation can vary. This seems to vary with the crustal “basement involved thin-skinned” (Fig. I.1, B), which will easily affect the surface in the FTB as well as in the flexural basins where the deformation can progress following the same structures or by creating new in thin-skinned tectonic deformations. It can also be controlled by the inherited structures, as the normal faults, since these are linked to thick-skinned tectonic deformations (we don’t consider the different styles of rifted basins here (Stampfli *et al.*, 1991) as the normal faults based on detachment levels could be interpreted as in the Fig. I.1, B as “basement involved thin-skinned” in order to clarify the problematic. This is also due to our poor possibility to constrain these structures at depth).

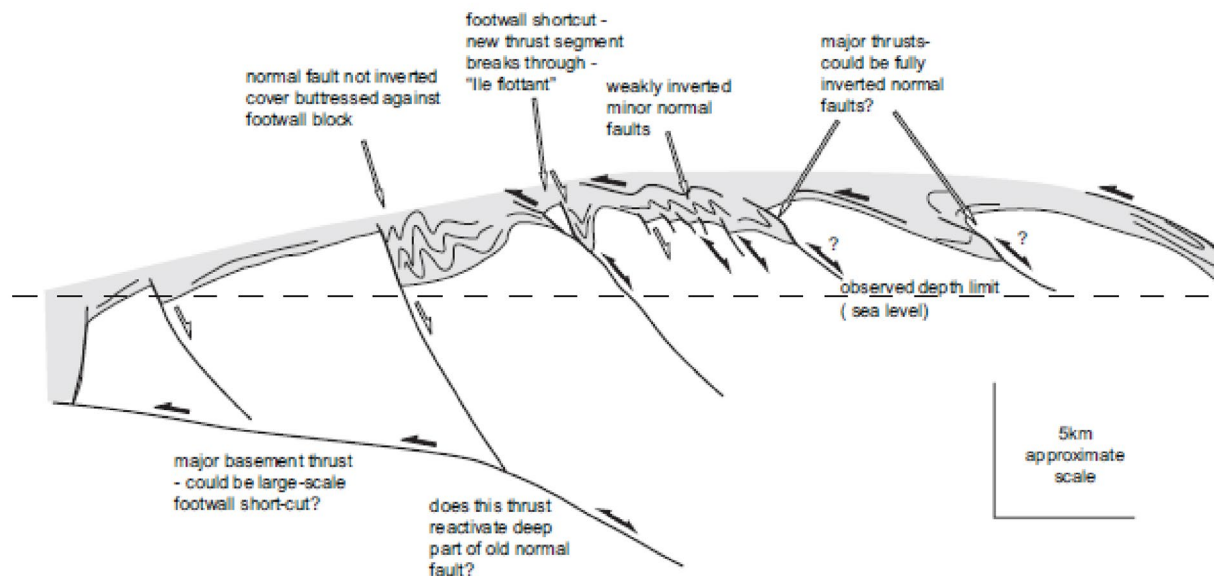


Figure I.2: Sketch from Butler et al., (2006) who propose different structural style to invert the inherited normal faults in a same unit (in the Ecrins Massif).

### 3. Why is it important?

The Apennines belt is a good example of a FTB where the interpretation in terms of tectonic style has been matter of debates, especially the Umbria-Marche Ridge structure.

Fig. I.3, A-D after the review paper of (Lacombe & Bellahsen 2016) summarize the main different interpretations that have been proposed. Fig. I.3, E-F after (Scisciani *et al.*, 2019) proposes an interpretation based on the seismic lines. They consider the presence of an inherited rifted basin in the studied area (Paleozoic-Mesozoic extensional multi-stages before the Apennines Orogeny). This paleo-structure is thus highlighted in Fig. I.3, F where the cross-section is reconstructed from the balanced cross-section.

The Apennines FTB is affected by the Variscan history, followed by the Alpine orogeny (Scisciani *et al.*, 2019). The interpretation of the style of deformation strongly affects the estimation of the shortening rate. It is so important, that it seems useless to balance a cross section if the style of deformation itself is poorly constrained. Based on the interpretations proposed in Fig. I.3, A, the structure can be interpreted as a thin-skinned tectonic deformation and results in a nappe stack which root in a Triassic decollement level located above the basement (not deformed on this cross-section). In this interpretation, the layers are duplicated eight times with nappes of about 30km long. The amount of shortening is about 200km. The reconstruction involves a 300km cross-section to an actual 100km long cross-

section (nearly 66% of shortening). In the interpretations of the Fig. I.3, B and C, the structure is alternatively interpreted as a thick-skinned tectonic style, which affects the basement and the cover along steeply dipping thrusts. The reconstruction of such a cross-section leads to a much smaller amount of shortening than in the Fig. I.3, A. The Fig. I.3, D and E present an interpretation based on the presence of inherited normal faults/extensional basins which will be inverted during the compression. The Fig. I.3, E suggests that the main normal faults are inverted as major thrusts which affect the basement with thick-skinned tectonics, and to the borders of which occur intense deformations interpreted as “basement involved thin-skinned tectonics” (Fig. I.1, B). This propagation of the deformation toward the East causes some thin-skinned deformations in the foreland basins. This interpretation of the structure of the Umbria-Marche Apennines region shows a complex structure, driven by thick and thin-skinned tectonics, and with different shortening amount along the cross-section (more shortening at the borders of the paleo extensional basin). The reconstruction proposed in the Fig. I.3, F shows that the Umbria-Marche Ridge area is not affected by strong shortening. The inheritance of the rifted basin controls the location of the deformations during the compression. There is nearly no shortening. Toward the east, the deformation is not controlled by the inherited normal faults and has been more affected by the shortening. In this area, the deformation roots also at depth in the basement. The shortening rate is about 50%.

Following a style or another in the interpretation of the structure of FTB can lead to very different conclusions about the amount, the location and even the quality of oil and gas resources (Stampfli *et al.*, 1991; Robinson *et al.*, 1996; Tari *et al.*, 2020) .

The Umbria-Marche Ridge is an inverted basin. The inversion of inherited rifted basin presents a good opportunity to constrain the mechanisms of the deformations and the style of deformations. The back-arc basins can be in the future collision areas. Their ages can trigger the style of deformations whether these are still hot and related to weak lithospheres, or cold and rigid, the inversion could change from the central part to the borders (Nalpas 1994; Butler *et al.*, 2006; Espurt *et al.*, 2014; Lacombe & Bellahsen 2016). The amount of sediments in the basin which controls the friction controls also the style of deformation (Nalpas 1994; Erdős *et al.*, 2015; Lacombe & Bellahsen 2016). The viscosity ratios between the cover and the basement or the viscosity ratios inside the cover depends on the lithologies and controls also the style of deformation (Bauville & Schmalholz 2015). The lithologies could thus create a

good decollement level, and its thickness controls the coupling inside the crust and thus the style of deformation. The more the decollement levels is thick, the more the coupling inside the crust drops and can creates decollements and result in thin-skinned deformations (Nalpas 1994; Lacombe & Bellahsen 2016). Finally, the directions of the different tectonic stages and the related structures controls the possibility to inverts the basins and controls the strike-slip amount along the structures too (Nalpas 1994). In the case of the back-arc basins, if the structures are parallel to the subduction and the collision, the possibility to invert the basin is higher. Moreover, the age of the back-arc basin can be young if the basin is rifted until the collision.

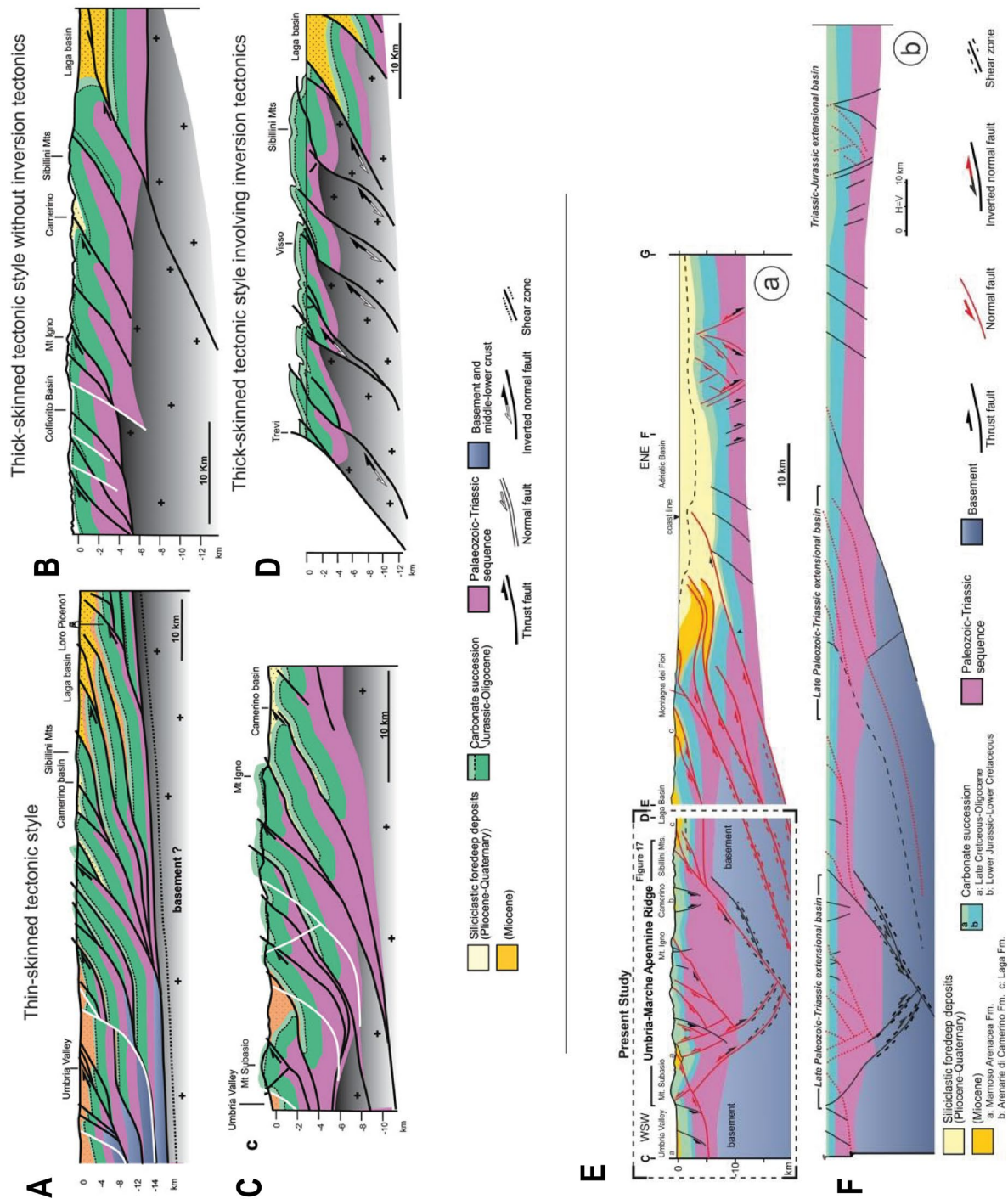


Figure I.3: Sketches A-D from (Lacombe & Bellahsen 2016) presenting the different interpretations about the structural style of the Umbria–Marches domain of the Northern Apennines: A Thin-skinned tectonic style with décollement along the Triassic evaporites. The basement remains undeformed. B: Thick-skinned tectonic style without deforming the basement. C: Basement involved Thin-skinned tectonics after the interpretation of Pfiffner 2017 (Fig. I.1). D: Thick-skinned tectonic style resulting from the inversion of inherited structures. Pictures E and F from (Scisciani et al., 2019) E is the cross-section of the Umbria-Marche Apennine Ridge and F its restoration. This shows the importance of the interpretation of the structure on the shortening rate and the localisation of the deformation.

Norian



Toarcian



Aptian



Burdigalian



Back-arc extension area



Inverted back-arc basins



Figure I.4: Paleotectonic maps from Barrier et Vrielynck 2008 (MEBE project). The extensions resulting from a back-arc setting are in yellow during the Mesozoic subduction of the Tethys and the location of the inversion of these basins in red during the Neogene collision.

## II. Case-study: the Greater Caucasus basins

The Caucasus area has been affected by the Variscan collision during the Paleozoic e.g. (Adamia *et al.*, 2011; Rolland *et al.*, 2011). The Variscan orogeny has been followed by the subduction of the Tethys ocean beneath Eurasia, and then the closure of the Tethys resulted in the Alpine orogeny. We propose to follow the tectonic history of the area to highlight the location and the timing of the formation of the different extensional structures, which could then be affected by compressive tectonics.

### 1. The Tethys Ocean and the related back-arc basins

The Tethys Oceans have an history since the Devonian with a former oceanic formation (Paleotethys), followed by the Cimmerian rifting and the Alpine-Atlantic rifting (Neotethys) (Stampfli *et al.*, 1991).

The closure of the Paleotethys leads to the Variscan orogeny and the closure of the Neotethys to the Alpine orogeny.

In the Fig. I.4 we show some reconstructions of the Peri-Tethyan tectonic history from the MEBE and DARIUS projects, published in 2008 and 2017 (Barrier & Vrielynck 2008; Barrier *et al.*, 2018). Back-arc basins related to tethysian subductions have an important role on the style of deformation when the collisions occur (Ricou *et al.*, 1986). Indeed, the structure of the back-arc basin can control the localisation and the style of the deformation during the further collision. During the Mesozoic the areas under extension are the Caucasus area (back-arc setting), and the Atlantic (rifting) (Stampfli & Borel 2002; Barrier & Vrielynck 2008). The Black Sea can be related to a back-arc basin. It has developed on an active margin setting since the Permian and is thus affected by multi-stage history of back-arc extension and inversions e.g. (Nikishin *et al.*, 2012). The same interpretation can be made for the Greater Caucasus basin (Khain 1975, 2007; Adamia *et al.*, 1977, 2011; Rolland *et al.*, 2011). To better understand how inherited structures can affect the style of deformation during the collisions, we propose to take a closer look at the Caucasus-Black Sea area.



## 2. The Greater Caucasus: The Alpine history

The Alpine orogeny in the Caucasus range involves three plates and two suture zones. The Lesser Caucasus to the north results from the collision between the Eurasian Plate and the Taurides-Anatolides-South-Armenian Microcontinent (TASAM) (Sosson *et al.*, 2010). The Zagros belt to the south results from the collision between the Eurasia and the Arabian Plate (Ricou *et al.*, 1977) among many others.

Fig. 1.5 illustrates the Alpine history interpreted by Barrier & Vrielynck (2008) based on the multidisciplinary results of the MEBE project, and we will use this illustration to introduce the different units of the Caucasus area in the next paragraphs.

During the Callovian, the Tethys ocean subducted northward beneath the Laurasia continent (Eurasian Plate). An arc developed along the active margin. The different basins located along the active margin (Fig. 1.5) are the Küre Basin (affected by thermal subsidence since the Norian), the South Balkan Basin (affected by active extension in a back-arc setting since the Norian and by thermal subsidence during the Callovian), the Greater Caucasus basin (affected by active extension in a back-arc setting during the Mid. Toarcian and by thermal subsidence during the Callovian), and finally the South Caspian and the Kopet Dagh basins affected by active extension in a back-arc setting during the Callovian.

During the Middle Aptian, the Greater Caucasus and the South Caspian basins are affected by thermic subsidence, while the Eastern and Western Black Sea and the Karkinit Rifted basins were affected by rifting tectonics which continued during the Cenomanian (Fig. 1.5). The Western Greater Caucasus basin is affected during the Cenomanian by active rifting as well. Meanwhile, the volcanic arc was still active along the active margin.

During the Early Campanian, the Greater Caucasus and the South Caspian basins were still undergoing subsidence. Some extension is observed in the Central Pontides Volcanic Arc, in the Crimean Platform, the Emine Basin and the Srednogorie Rift Basin.

During the Lutetian, the Armenian basin was affected by subsidence in a flexural basin setting because of the collision between the TASAM and the Eurasian Continent. Strike-slip regime is documented in the Crimean Peninsula, while some compression occurred in the Greater Caucasus basin and along the Suture zone from the south of the Moesian Platform to the south of the Black Sea and continued toward the East south of the Southern Caspian Sea basin. Two areas are affected by active extensional tectonics: the Adjara-Trialeti Basin (located north

of the Artvin-Bolnisi volcanic arc) and the Orumieh-Dokhtar volcanic arc (located in the Karaj Basin). The Adjara-Trialeti basin is bordered by bivergent thrusts.

During the Burdigalian, the domains located in the internal zone of the Greater Caucasus range were affected by compression interpreted to be due to the southern collision with the Arabian Platform. Some flexural uplifts and subsidences occurred in the northern part of the Eastern Black Sea and in the southern part of the Greater Caucasus. The Pontides volcanic arc was bordered by bivergent thrusts, the Alborz Range was also affected by major thrusts, as well as the southern Greater Caucasus basin.

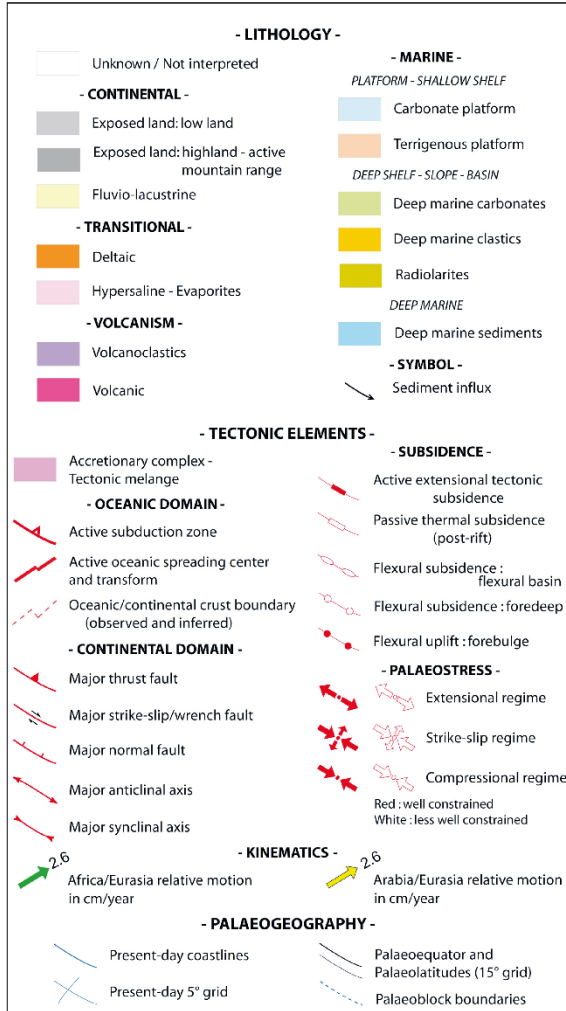
During the Piacenzian, the collision of the Arabian Plate resulted in a global compressive stage. The compression affected the whole Caucasus area. Some flexural basins developed all along the Southern Greater Caucasus in the northern Black Sea, the Rioni foreland basin and the Kura foreland basin and in the northern part of the Southern Caspian Basin. Many thrusts affected the internal zone. Most of them are south-verging thrusts, except the northern part of the Pontides Volcanic arc, the Adjara-Trialeti Range, and the northern part of the Greater Caucasus Range. Some strike-slip occurred south of the Lesser Caucasus, but it is not documented in the internal zone. We can also point out that the Dzirula Massif is exposed at the surface during the whole alpine history.

The evolution proposed in Barrier and Vrielynck 2008 is mainly accepted. An orogenic phase, the Cimmerian orogeny is proposed by Gaetani *et al.*, (2005), McCann *et al.*, (2010) during the Middle Jurassic. This followed the observation of folded and tilted blocks in the Transcaucasus. (Saintot *et al.*, 2006) proposes that this tectonic stage affected the study area more to the East, near the Iranian terranes. Some interpret it to not be an orogeny but just the development of flexural foredeeps during the Mid-Jurassic (Kaz'min & Tikhonova 2006) due to local compression.

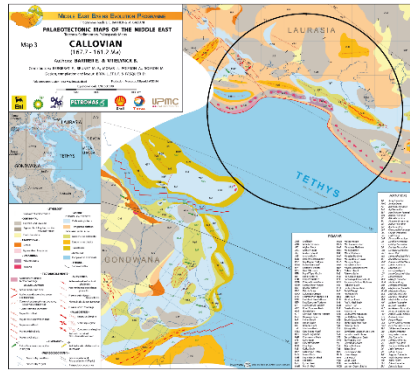
### 3. Tectonic questions and Timing of the multi-stage tectonic history

The presence of different tectonic units imply that the deformation of the Caucasus area is not completely cylindrical. (Khain 2007, 2009) pointed the mistake to try to find arguments for the whole area while its formation present differences from west to east, and that inherited structures in the Transcaucasus area located in the internal zone could play a role in the tectonic evolution of the area. (Mosar *et al.*, 2010) show that along the strike of the GC,

the shortening and uplifting rates and amounts are heterogeneous. They propose that the convergence rates and the inherited structures could play a major role in the heterogeneity of the tectonic deformations along the GC. (Okay *et al.*, 1994) point out the importance of rotational tectonics, with the contribution of strike-slip and related deformations in the BS area. It is not clear whether the BS is a “classical” Back-arc basin trending in the same direction as the subduction ((Sosson *et al.*, 2016; Tari *et al.*, 2020) or is related to other mechanisms involving the change in the mechanical parameters of the back-arc area.



### Callovian



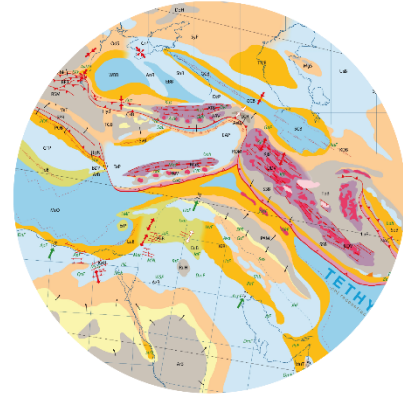
### Middle Aptian



### Early Campanian



### Lutetian



### Burdigalian



### Piacenzian

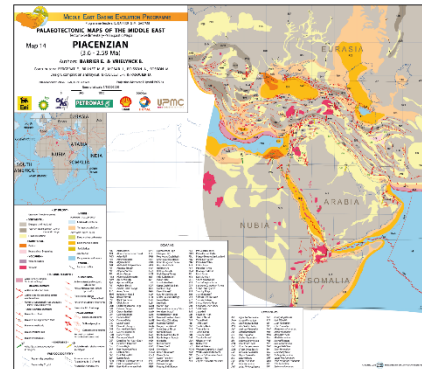


Figure I.4: Details on the paleotectonic maps from Barrier et Vrielynck 2008 (MEBE project) from the Callovian until the Piacenzian.

The geodynamic context related to the basin development involves possible non-cylindrical deformations and is thus very important to take in account. The Fig. I.6 shows that the continuity from of the basins localized in the back-arc area is important. The indenting of the TASAM takes place only in the western part. The east of the Black Sea is a key point in the area to observe how this can controls the deformations behaviour toward the east since the Cretaceous.

The Lateral variations can be followed by highlighting the timing of the tectonic stages. This offers the possibility to identify the main structural units and follow them through the different tectonic stages to point the possible variations along strike.

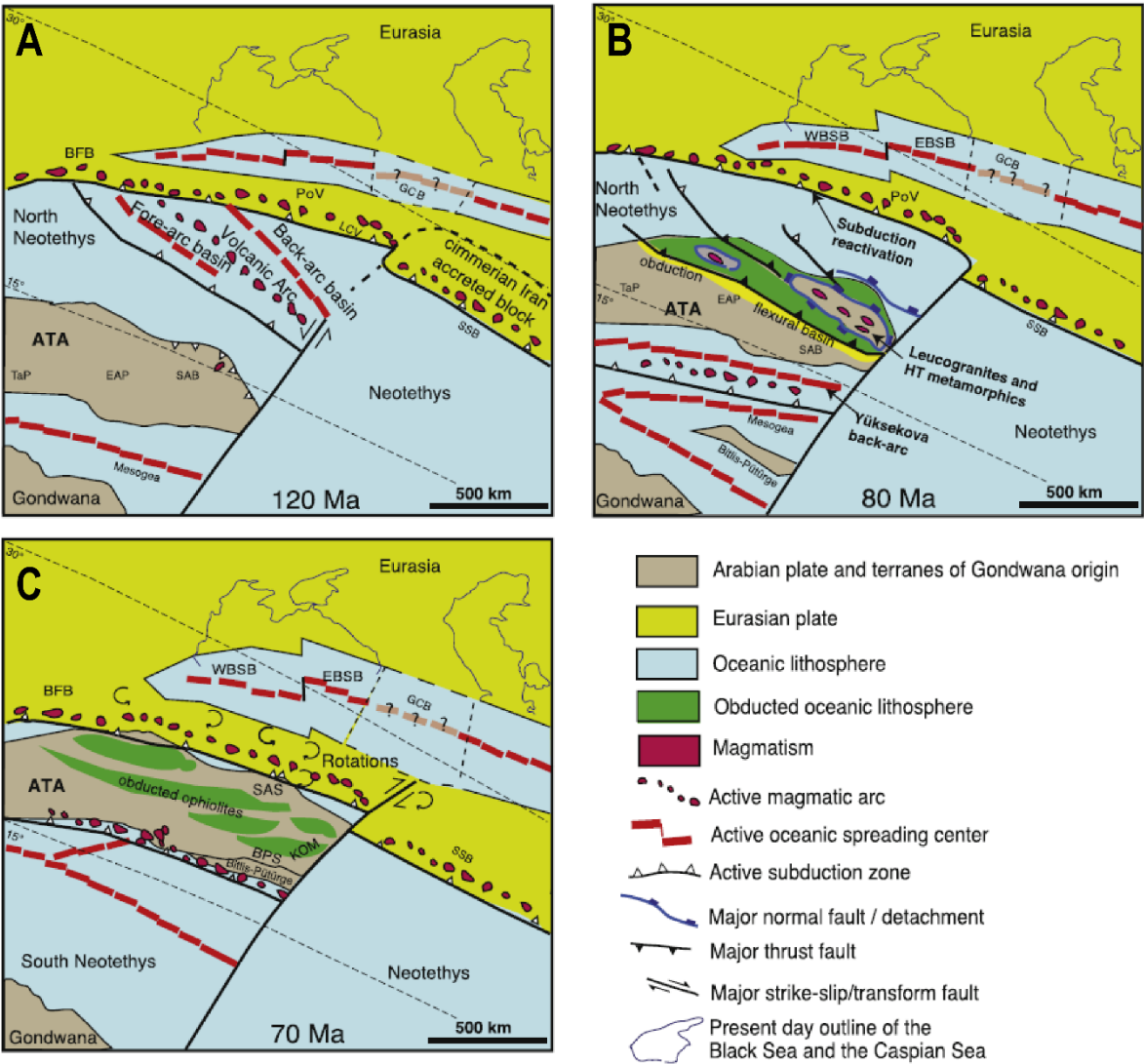


Figure I.6: Paleotectonic reconstruction of the Caucasus area after (Rolland et al., 2020). We can highlight the importance of rotational tectonics and of possible lateral differences in the structures and timing between the Black Sea area to the west and the Southern Caspian Basin to the East. This highlights the key area located between these basins.

#### 4. Structural interpretations related to the style of deformation

The main tectonic units of the Caucasus area have been first described in (Milanovsky & Khain 1963; Gamkrelidze 1964, 1986; Khain 1975; Adamia *et al.*, 1977, 1981, 2015 p. 201). These ideas are summarized here and are the basis of the studies in the area. From north to south we can observe: The shelf of the Scythian Platform, the Greater Caucasus Basin and Range, the Transcaucasus area (an island arc), which contains the Black Sea to the west, and the Southern Caspian Sea to the east as well as the Rioni and Kura foreland basins. The Rioni basin located east of the Black Sea shore is interpreted to be deformed by thin-skinned tectonics (Banks *et al.*, 1998; Morariu & Noual 2009; Tibaldi *et al.*, 2017b,a; Tari *et al.*, 2018), but some normal basement faults have been reported beneath the decollement levels (Banks *et al.*, 1998; Tari *et al.*, 2018). The Kura foreland basin is located west of the Caspian shore and is interpreted to be deformed by thin-skinned tectonics (Banks *et al.*, 1998; Alania *et al.*, 2009; Forte *et al.*, 2010, 2013, 2015; Alania *et al.*, 2017a). The Dzirula Massif separates both foreland basins and is made of paleozoic basement rocks. It is interpreted to be a remnant of the variscan orogeny e.g. (Rolland *et al.*, 2011, 2016).

The Adjara-Trialeti domain is located south of the Greater Caucasus foreland basins and north of the suture zone of the Lesser Caucasus. The suture zone of the Lesser Caucasus contains obducted ophiolites which were part of the Tethys Ocean lithosphere. The Greater Caucasus basin was the main basin situated in the Caucasus area, and is elongated in a NW- SE direction. Other basins are present in the study area: the Black Sea is constituted of two basins: the western and the eastern basins. These basins are in a key area, near the suture zone of the Lesser Caucasus. The Black sea contains oceanic crust and highly extended continental crust ((Nikishin *et al.*, 2015b,a).

The structural relationships and styles of deformation between the units can be observed along NS transects (Yilmaz *et al.*, 2013) or on the transect proposed in the Fig. I.7 (Sosson *et al.*, 2016).

Fig. I.7 shows the main structural domains of the Caucasus area interpreted by Sosson *et al.*, 2016, based on different projects and a decade-long study (Sosson *et al.*, 2013, 2017). The structures are interpreted to be mainly due to thin-skinned tectonics along the borders of the Greater Caucasus, while thick-skinned tectonics is observed in the Central Greater Caucasus. The thin-skinned deformation propagated into the foreland basins. The Adjara-Trialeti unit is

interpreted as affected by a thick-skinned deformation with the inversion of the inherited basin structures. This interpretation highlights the interplay between different styles of deformation along the transect.

This interpretation of the cross-section from the northern Greater Caucasus to the Southern Lesser Caucasus shows variations in the deformation styles along the cross-section. The Greater Caucasus interpreted as an inverted basin is deformed to the south by a major thrust rooted in the basement. Most of the shortening is thus localised along this structure. The Transcaucasus is deformed with thin-skinned tectonic in the foreland basin along the same structure at the basis until the Adjara-Trialeti inverted basin which is an inverted rifted basin where the normal faults are inverted. This unit is thus poorly affected by the shortening. Between the foreland basin and the Adjara-Trialeti inverted basin, the structural style is different, as well as the vergence of the deformations. This creates a triangular zone. Towards the south, the Lesser Caucasus is affected by thin-skinned tectonic, and by major thrusts linked to the obducted ophiolites. Some major thrusts also root into the basement, but based on this interpretation, the shortening is mainly localized on the suture zone.

The different structural units can be interpreted in different ways that we will summarize below, but mainly, we need to follow the structural style along-strike (from W to E) in the Transcaucasus area.

(Saintot *et al.*, 2006) points out that the inherited structures in the area can lead to local stress variations and change the style of deformation from thick to thin skinned tectonics.

These authors also propose that different styles of deformation can occur simultaneously. The thin-skinned deformations are dominant in the Western and Eastern Greater Caucasus, while thick-skinned deformation occur in the central part of the basin.

The Transcaucasus area can be interpreted in different ways, which results in very different interpretations of the tectonic styles. It can be interpreted as a platform/block which separates different foreland basins where thin-skinned tectonic deformations occur, or as an accretionary prism (Khain 1975, 2007). Some interpret that there is an oceanic lithosphere in the TC (Okay *et al.*, 1994; Cowgill *et al.*, 2016) and then and interpret the accretionary prism as a subduction-related (Cowgill *et al.*, 2016). Some authors interpret it as resulting from a continental subduction (Gamkrelidze *et al.*, 2018, n.d. p. 201), or from an intense crustal underthrusting beneath the Greater Caucasus (Saintot *et al.*, 2006; Mosar *et al.*, 2010). The

Transcaucasus area is considered to be deformed by south and north verging nappes by Adamia *et al.*, (2002). All these interpretations involve thin-skinned deformations.

(Khain 2007) points out west to east variations in the structure of the TC: while the eastern part is intensely deformed with nappes and thin-skinned thrusts (with more than 10km of shortening), the western TC is less deformed because of inherited inverted structures and thick-skin deformation. (Mosar *et al.*, 2010) show that the uplifting and shortening rates are heterogeneous, and that it could be the consequence of differences in the style of deformations also because of inherited structures. Some authors alternatively interpret the western part as related to thin-skinned deformation (Tibaldi *et al.*, 2017b,a).

The Tethyan evolution involves the presence of several suture zones in the Lesser Caucasus. According to the interpretation of Rolland (in (Rolland *et al.*, 2011, 2016; Rolland 2017) the Adjara-Trialeti basin is the eastern continuation of the Black Sea basin, with the Dzirula Massif and the Khrami Massif as horst structures.

The Adjara-Trialeti (AT) basin/fold and thrust belt can be related either to the Transcaucasus unit and the Eastern Black Sea, to the Lesser Caucasus suture zone or to the Pontides volcanic arc. The AT is a volcanic zone during the Paleogene (Banks *et al.*, 1998; Alania *et al.*, 2017b). The problematic of this unit is that, as for the example of the Umbria Marche Ridge (Fig. 1.3), the interpretation of its structure and history can lead to very different reconstructions and shortening rates. On Fig. 1.7, Sosson *et al.*, 2016 interprets it as affected by thick-skinned tectonic deformations, while usually the structure is interpreted with thin-skinned tectonics (Banks *et al.*, 1998; Alania *et al.*, 2017b).

The Black Sea can be interpreted as deformed by thick-skinned tectonics on its bordures and thin-skinned tectonics in its central part after (Espurt *et al.*, 2014; Hippolyte *et al.*, 2015, 2018), who show that 33% of shortening affect the Pontides while nearly no shortening affects the central part of the Black Sea. This interpretation highlights localisation of the deformation on the borders of the basin as it was shown with detailed structural studies in Crimean Mountains (Sheremet *et al.*, 2016a,b; Korniyenko-Sheremet *et al.*, 2021)

The interpretation of the style of deformation, together with the interpretation of the timing of the deformations during the multi-stage history of the area has an important implication concerning the resources. Answering these question is thus important to constrain the presence of structural traps , the inversion of the inherited structures, and the propagation of



the deformation into post-rift deposits (Stampfli *et al.*, 1991; Robinson *et al.*, 1996; Tari & Simmons 2018; Tari *et al.*, 2020).

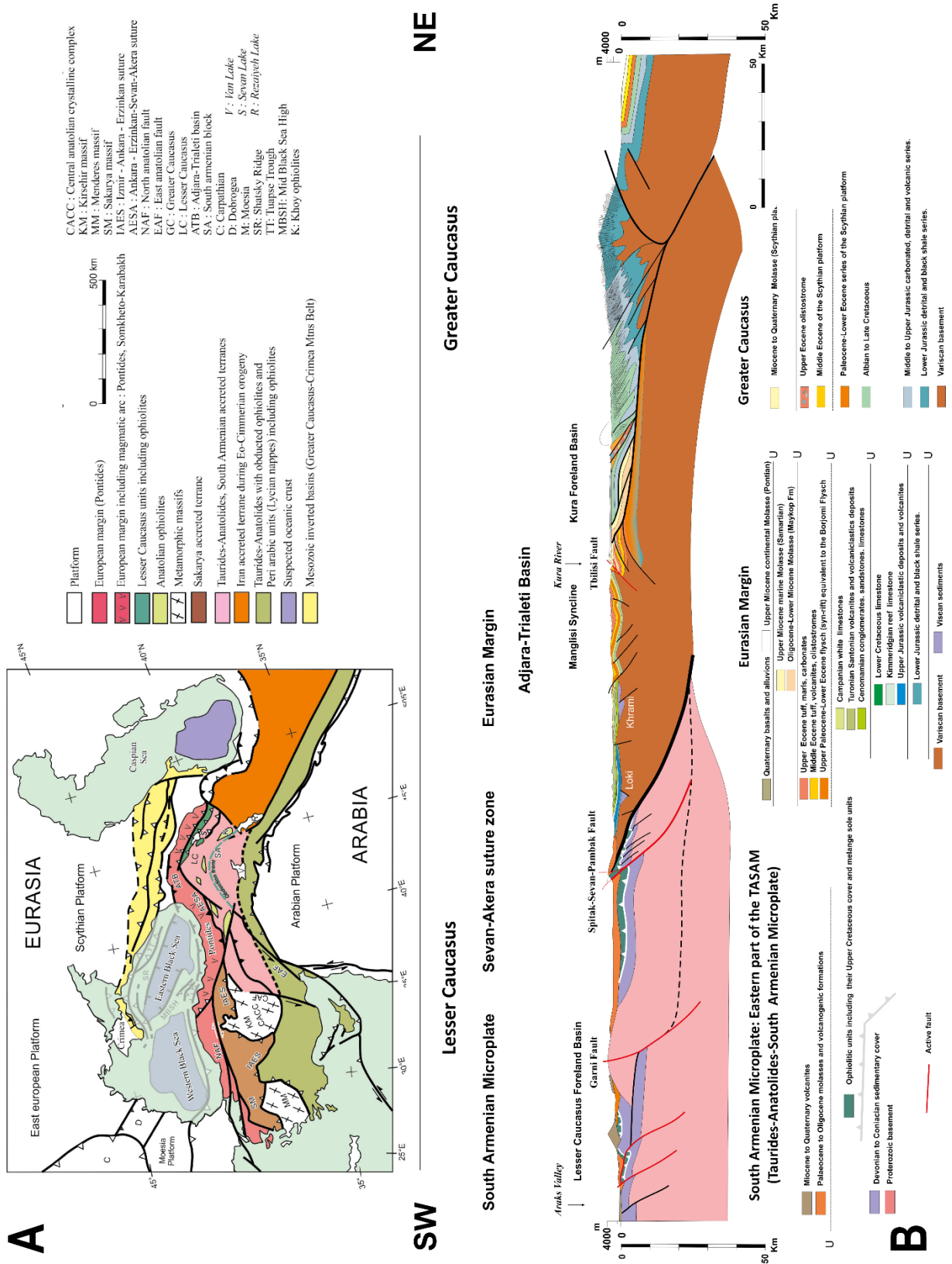


Figure I.5: Tectonic map and the related Cross Section after (Sosson et al., 2016) from the Scythian Platform to the Lesser Caucasus Suture Zone

### III. Objectives of the study and methodology

#### 1. The problematic

The Caucasus area presents a large variability in the style of deformations. Its location on the upper plate near the active margin before the collision is key to observe the role of inherited extensional structures on the compressional deformation. During the subduction, rifting in the back-arc areas results in the opening of different basins. The geodynamic origin of these basins (xx or yy) often debated in the literature, is independent from their general structure with major normal faults at their borders. One thing that can change however is the presence of strike-slip faults if the basins were opened in a transtensional setting.

The style of deformation is a central question to constrain the role of the inherited structures. Moreover, in a polyphase and complex tectonic history such as in the Caucasus, the chronology and the timing of the different tectonic stages must be constrained as well as the related structures.

The area presents non cylindrical evolution along the active margin, and compression and extension can affect at the same time different areas. The possible imbrication and superimposition of the structures with time is a difficulty we need to consider. This results in a possible heterogeneity in the evolution during the collision processes and thus, the timing and the structures must be followed and delimited along strike.

#### 2. Objectives

The objectives of this study are thus to delimit the different structures and reconstruct their tectonic evolution in space and time. We seek at proposing new interpretations regarding the polyphased tectonic history of the GC by taking in account the possible superimposition of different tectonic stages and thus structural units.

The lateral variations of the different tectonic units can be highlighted by parallel NS-trending cross-sections across the western and eastern parts of the study area.

### 3. Methodology and data

The main novelty of our study is the acquisition of numerous field observations and data. We have been in the field during five trips of two to five weeks long. The location of field observations is compiled in the Fig. 1.8.

We had access to some private seismic line across the Adjara-Trialeti fold-and-thrust belt from TOTAL, Paris. The interpreted line is the 05 XIA (Depth), 09XIA (MIG), 06 XIA (MIG). We could return with the line drawings (locations in Fig. 1.8). The old seismic lines of Tsaishi anticline have been given by Victor Alania (Tbilisi State Agency) and are the same published and interpreted by Tibaldi *et al.*, (2017a). Some seismic lines situated near Koutaisi and the Dzirula Massif (location in Fig. 1.8), SOG 03 RSS (MIG), SOG 19 RSS (MIG), SOG 20 RSS and SOG23 RSS (depth) have been proposed for interpretation at the State Agency for Oil and Gas in Georgia with Alexandre Chabukiani. We could return with the line drawings.

We had also access to wells data which includes the ages, facies, and depth of the formations (locations in Fig. 1.8) given by Alexandre Chabukiani (State Agency for Oil and Gas in Georgia). The names of the wells are: Samtredia 1/58, Bziauri 1, Lesa 5, Sagvamichao 6 and 16, Tsaishi 3, 4, and 8, Zugdidi 3, Choloki 1, Chokhatauri 4 (are located on the Fig. 1.8).

The wells data and the seismic lines are very useful and have been the subject of different studies in the Caucasus (Banks *et al.*, 1998; Tibaldi *et al.*, 2017b,a; Tari *et al.*, 2018; Tari & Simmons 2018). The opportunity to combine these data with field allowed us to constrain the geometry of the different tectonic units and follow their structures from the surface to depth in order to offer new interpretations.

Our field observations were driven by the need to identify the main tectonic structures in order to constrain the timing and location of the deformations. We have analyzed sediment thickness and facies variations in order to constrain the tectono-stratigraphic units and the environment of deposition.



Moreover, the style of deformation impacts the geometry of growth strata (Suppe 1983, 1997; Suppe & Medwedeff 1990; Suppe *et al.*, 1992; Mercier *et al.*, 2007) (Fig. I.9, a vs b vs c). The observation of the geometry of the growth strata offers thus the possibility to constrain the style of deformation. The inversion of inherited normal faults is not proposed in the Fig. I.9. We think that the inversion of normal faults can be compared to the fault-propagation folds regarding the growth strata geometries (Fig. I.9, b and b'). The thin-skinned tectonic deformations observed in the area can be related to the geometries of growth strata observed on fault-bend-folds (Fig. I.9, a and a'). The geometry of the ramps impacts the geometry of the growth strata (Fig. I.9) (Ahmadi *et al.*, 2013).

The field observations of the growth strata and their geometries can offer an interpretation on the timing of the tectonic events and also the style of deformation at depth. We will observe first the geometries of the unconformities of the syn-tectonic deposits onto the pre-tectonic deposits. This observation gives keys to interpret if the uplift rate or the sedimentation rate is the higher (case 1 or case 2, Fig. I.9). The sedimentation rate neither the uplift rate is constant with time: the tectonic can lead to an increasing uplift rate, which can create more erosion and thus more sedimentation. The models here are based on one case but it is likely that both cases can take part of the tectonic history.

Then, the differentiation of the observations at the back and at the front of the folds will be important. The geometry of the growth strata will help us to better constrain the style of deformation.

We have constructed three cross sections across the Transcaucasus area, from the Adjara-Trialeti Fold and thrust belt to the south, toward the southern Greater Caucasus to the north. We made a cross section east of the Black Sea, across the Rioni Foreland basin, another one located eastward near the Dzirula Massif, and finally another one in the eastern ending of the Adjara-Trialeti fold and thrust belt, west of Tbilisi.

We make some simple restorations by keeping the length of the formations between each tectonic deformation.

The cross section situated in the Rioni basin has been made with the Move software (Petroleum Experts). The combination of wells, seismic lines and field observations in the Rioni foreland bring important constraints on the geometry and thus the style and timing of deformations in the area. The use of the Move software allows us to create balanced cross-

sections and a better constrained restoration. We based the thick-skinned geometries proposed in the cross sections on the geometry of the growth strata as well.

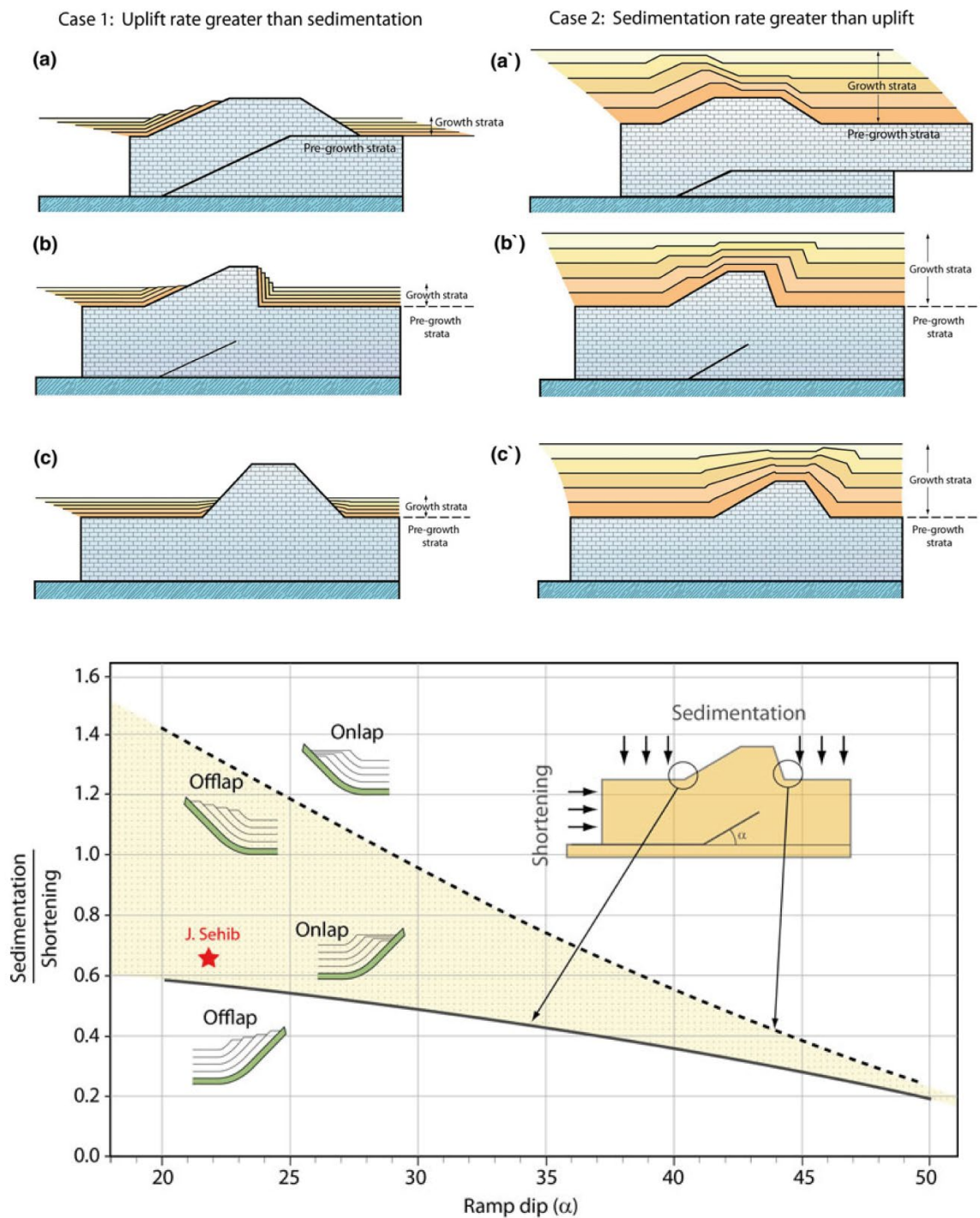


Figure I.9: Figures after (Ahmadi et al., 2013) summarizing the different parameters that affect the geometry of growth strata. The ratio of sedimentation vs. deformation rate affects the way the deposits will cover or not the anticline. The style of deformation affects the geometry of the growth-strata. Finally, the geometry of the deformed structure will also affect the geometry of the growth strata: the back-limb or the front limb will present offlaps or onlaps depending on the vergence of the fold.





## *Chapter 2*

*Identification of inverted Mesozoic back-arc basins in the internal zone of the Caucasus Orogen, insights from the Transcaucasus area, western Georgia*

Draft to publish in Journal of Asian Earth Sciences

## Abstract

The Black Sea - Greater Caucasus region is a natural laboratory that gave birth to many models attempting to reconstruct the tectonic evolution of collision zones during the long-lived closure of the Tethys ocean. Many studies have interpreted most of the structures in this region as resulting from Cenozoic collision. However, extensional structures formed during either the Lower Cretaceous rifting of the Black Sea, or during the Greater Caucasus back-arc basin opening in the Early-Middle Jurassic, or even during earlier extension in the Triassic could have played a role in the subsequent collisional deformation but are generally overlooked.

Based on new detailed field observations and structural analyses of the Mesozoic rocks in key areas of the Transcaucasus region, we traced out the major deformation zones and the continuity of structures from the Eastern Black Sea to the Georgian Block, including the Mesozoic deposits lying beneath the Cenozoic forelands basins of Rioni and Ambrolauri.

We complement these observations with seismic lines and well data in order to propose two cross-sections through the Transcaucasus area: one in the western part across the Rioni foreland basin, and one to the east across the Georgian Block. Comparing the main stratigraphic discontinuities and the tectonic structures allows us to unravel the timing and location of the deformations since the Early/Middle Jurassic. Our analyses highlight three main tectonic stages during the Mesozoic in the study area: 1) an extensive phase during the Middle Jurassic marked out during Bajocian by volcanic activity and during the Bathonian by a more deltaic related subsidence. The Upper Jurassic – Lower Cretaceous is a period of rebalancing of the constraints, with small localized subsidence. 2) an extensive phase during Late Lower Cretaceous and early Upper Cretaceous marked out by the Barremian deltaic rifting, and the Aptian to Cenomanian subsidence localized near the normal faults. The Upper Cretaceous is concerned by gentle subsidence near the faults, erosion, and punctuated by volcanic activity during Turonian. 3) the Cenozoic orogenic stage involving the current folded structures of the Transcaucasus area.

We then propose 2D cross-section reconstructions as well as structural schemes in order to correlate the main structures below the Cenozoic deposits of the Rioni foreland basin.

The interpretations are well correlated with the tectonic stages observed in the Greater Caucasus during the Jurassic but seems to correlate with the Eastern Black Sea evolution during the Cretaceous.

We discuss about the role of these inherited extensional structures during the Cenozoic orogenic stage, and their role concerning the foreland basins formations.

## I- Introduction

The Caucasus mountains belt originates from the successive closures of the Paleotethys and Neotethys oceanic plates during the Variscan, Cimmerian and Alpine Orogenies, respectively (Adamia *et al.*, 1981; Gamkrelidze 1986, 1991; Saintot & Angelier 2002; Khain 2007; Barrier & Vrielynck 2008; Sosson *et al.*, 2010; Mosar *et al.*, 2010; Adamia *et al.*, 2011b; Rolland *et al.*, 2011; Vincent *et al.*, 2014; Adamia *et al.*, 2015; Vincent, Stephen J *et al.*, 2016; Rolland *et al.*, 2016; Cowgill *et al.*, 2016; Barrier *et al.*, 2018).

However the occurrence of the Cimmerian orogeny and thus, the origin of the folded Jurassic deposits is not well constrained in the area of the Transcaucasus while it is identified in the Greater Caucasus (Nikishin & Cloetingh 1998; Gaetani *et al.*, 2005; Kaz'min & Tikhonova 2006; Khain 2007; McCann *et al.*, 2010; Nikishin *et al.*, 2012).

During the Alpine orogeny in Cenozoic times, the Caucasus range formed due to the collision between the Arabian plate to the south, the Taurides-Anatolides-South Armenian continental Micro-plate (TASAM), and the Eurasian plate to the north (Khain 1975; Adamia *et al.*, 1977, 2011a; Gamkrelidze 1986; Barrier & Vrielynck 2008; Sosson *et al.*, 2010; Yilmaz *et al.*, 2013; Rolland 2017).

The overall geometry of the Caucasus orogen is controlled by major thrusting and some strike-slips deformations (Philip *et al.*, 1989; Okay *et al.*, 1994; Koçyiğit *et al.*, 2001; Saintot & Angelier 2002; Saintot *et al.*, 2006). The continental collision took place after the closure of the main Tethyan ocean and other marginal Tethyan basins (either back-arc or subduction-related) (Ricou *et al.*, 1986; Stampfli *et al.*, 1991; Robertson *et al.*, 1996, 2009; Stephenson & Schellart 2010; Sosson *et al.*, 2016).

From south to north, the different tectono-stratigraphic units which constitute the Caucasus range are organised as follows (Fig. I. 7 and Fig. II.1), mainly based on

(Sosson *et al.*, 2016) work: In the TASAM (external zone) i) foreland basins related to either obduction or collision, ii) obducted ophiolites, iii) the Lesser Caucasus range where the suture zone is located; North of the TASAM, in the Eurasian plate (internal zone), i) the Transcaucasus area formed by the bivergent Adjara-Trialeti fold-and-thrust belt and its foreland basins (Kura to the East, Rioni to the West) (Khain 2009), and ii) the Greater Caucasus inverted back-arc basin. West of the Transcaucasus area, the semi-inverted Black-Sea basin (Espurt *et al.*, 2014; Hippolyte *et al.*, 2015) is located between the Adjara-Trialeti-Pontides (to the south) and the Greater Caucasus (to the north). The internal zone is thus composed of a series of inverted basins.

The internal zone of the orogenic domain, north of the Lesser Caucasus suture zone, is divided into different tectonostratigraphic units. They have been defined following the current spatial distribution of terranes (Khain 1975; Adamia *et al.*, 1977, 1981; Gamkrelidze 1986) and paleogeographic reconstructions (Khain 1975; Adamia *et al.*, 1977; Gamkrelidze 1986; Barrier & Vrielynck 2008), and permit to highlight the different stratigraphic units of this area (see fig 1 for locations): the Adjara-Trialeti fold-and-thrust belt (Adjara-Trialeti), the Rioni Foreland basin (RFB), the Dzirula massif (DZ), the Georgian Block (Georgian Block), the Greater Caucasus (GC) which is separated into the Slope zones and the Main Range basin. To the west, the Black Sea is separated into the Western and Eastern Black Sea basins (WBS and EBS, respectively).

The Mesozoic tectonic history in this area involves several episodes of extensional and compressive tectonics (Khain 1975; Saintot *et al.*, 2006; Kaz'min & Tikhonova 2006) because of the multiple orogenic cycles (possible Cimmerian orogen, followed by the alpine orogen in two stages: the collision between Eurasia and TASAM, and the collision with Arabia), and because of the successive opening of back-arc basins (the Greater Caucasus and the BS), and their inversions. How these successive tectonic stages are imprinted in the different blocks is unclear. In this paper, we seek at providing constraints about the geometry of the tectono-stratigraphic units and their structural relationships, in order to determine if there is a relation between the location of the foreland basins and the underlying (pre-Cenozoic) structures and constrain the tectonic evolution in this area. In particular, we try to understand how tectonic

inheritance linked to the inversion of extensional basins could have influenced the structural style (thin or thick-skin) of the orogen and foreland.

This question raised by many authors during past decades (Somin 1996; Saintot & Angelier 2002; Saintot *et al.*, 2006; Khain 2007, 2009; Trexler *et al.*, 2020) has triggered very different interpretations of the structures in the area, from thick-skinned/vertical tectonic (Khain 1975), to thin-skinned tectonic with decollement levels (Gamkrelidze 1991; Somin 1996). The structures are currently interpreted to be formed by thick and thin-skinned tectonics (Banks *et al.*, 1998; Tibaldi *et al.*, 2017b,a; Tari *et al.*, 2018; Trexler *et al.*, 2020) but are still matter of debate. These questions have direct consequences on the industrial oil and gas potential of the area (Adamia *et al.*, 2002) because the main source rocks are known to be the coal-bearing Bathonian deposits, and the Eocene-Oligocene Maykop series (Robinson *et al.*, 1996), both sealed by shale deposits (Morariu & Noual 2009), and the Upper Cretaceous syn-rift deposits of the EBS (Vincent *et al.*, 2014; Nikishin *et al.*, 2015b; Tari & Simmons 2018).

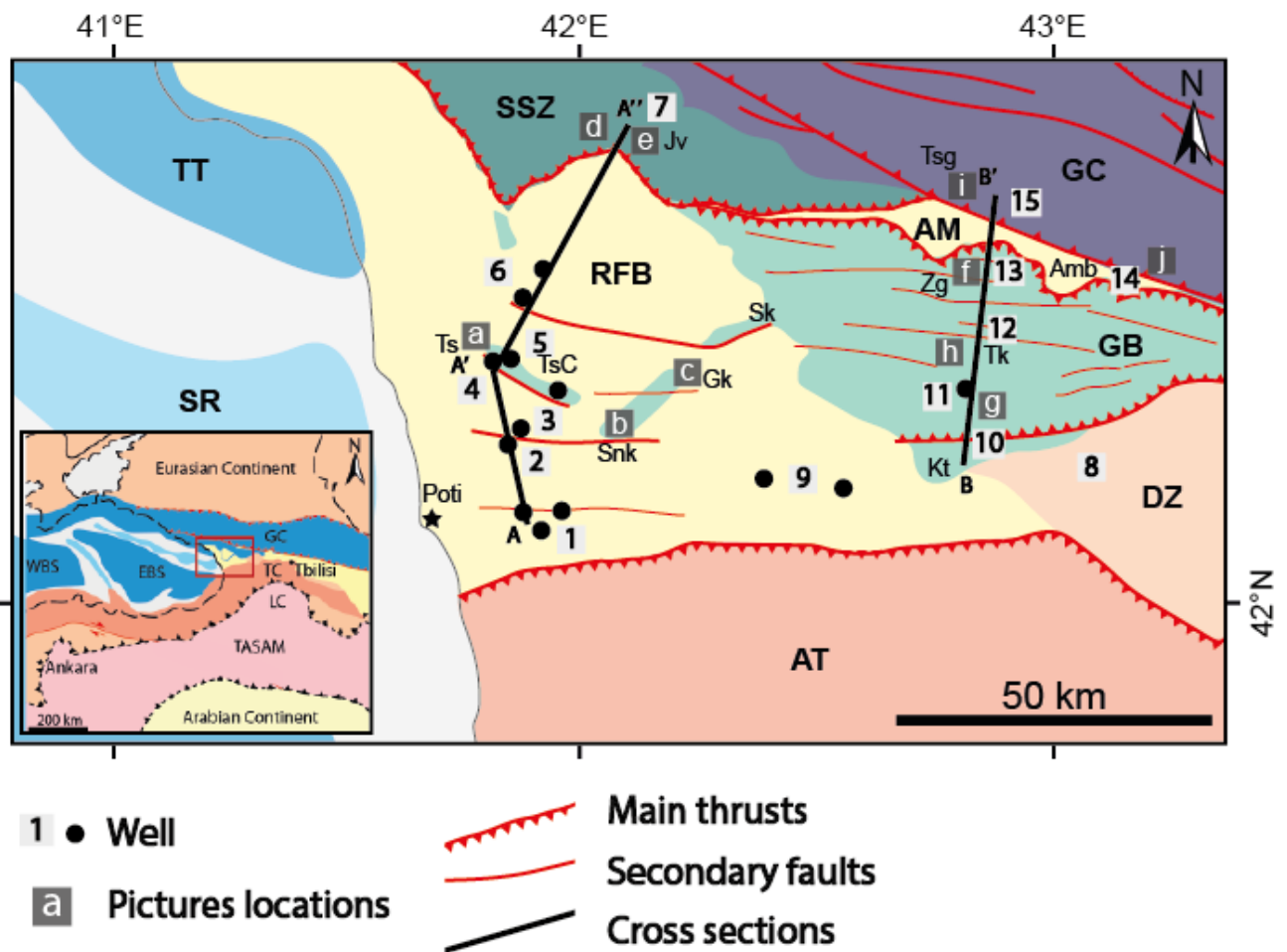


Figure II.1: Structural sketch of the Black Sea-Caucasus region in the general framework of the Middle East based on current work data and previous interpretations (Milanovsky & Khain 1963; Adamia et al., 1981, 2011a, 2017; Gamkrelidze 1986; Okay et al., 1994, 2015; Nikishin et al., 2003, 2010, 2015a, 2017; Sosson et al., 2010, 2016, 2017; Stephenson & Schellart 2010; Tari et al., 2018; Tari & Simmons 2018). The colors delimit the different units. Main figure: TT: Tuapsee Though, Southern Slope Zone: Southern Slope Zone, GC: Greater Caucasus, GB: Georgian Block, RFB: Rioni Foreland Basin, DZ: Dzirula, Adjara-Trialeti: Adjara-Trialeti. Inset: WBS and EBS: Western and Eastern Black Sea basins, TC: Transcaucasus, LC: Lesser Caucasus, TASAM: Taurides Anatolides South Armenian Microcontinent. Squares with letters a-j are the locations of the pictures of Fig. II.3 and 8. Squares with the numbers 1-15 are the locations of the stratigraphic logs (Fig. II.7 and 14). Ts: Tsaishi anticline, Jv: Jvari area, Zg: Zogishi and Kenashi area, Tk: Tkibuli area, TsC: Tsaishi Centre, Snk: Senaki, Gk: Gakhomela, Kt: Koutaissi, Tsg: Tsageri, Amb: Ambrolauri.

The Rioni Foreland basin lies at the connection between the Greater Caucasus mountain belt to the north, the Eastern Black Sea structures to the west, the Georgian block and the Dzirula massif to the east, and the Adjara-Trialeti fold-and-thrust belt to the south (Fig. II.1) Because of its central location it represents a key piece to the understanding of the tectonic evolution of this region. Indeed, the prolongation of Mesozoic tectonostratigraphic units beneath the Rioni basin is unclear, although

previous studies based on seismic data suggest that Mesozoic deposits continue beneath the Cenozoic deposits (Banks *et al.*, 1998; Tari *et al.*, 2018).

In this contribution, we aim at characterizing the Mesozoic tectonic evolution of the northern Transcaucasus and its relationships with surrounding units. The units are characterized along two cross-sections trending SSW-NNE and crossing either the Rioni foreland basin or the Georgian Block and the southern flank of the Greater Caucasus (see Fig. II.1). We focus on the Mesozoic deposits and propose a set of new tectono-stratigraphic logs compiled from well data and field observations along the cross-sections. These logs, along with reinterpretation of published seismic lines allow us to propose new geological cross-sections of the study area. We then discuss the correlation and continuity of the structures between both cross-sections, as well as the relationships with the adjacent Mesozoic basins (i.e., the Greater Caucasus and the Eastern Black Sea).

## II- Geological context

The Northwestern Transcaucasus area (NTA) (Fig. II.1, Fig. I.7) located between the Greater and the Lesser Caucasus mountains belt gathers different tectono-stratigraphic units originated by their tectonic evolution since Triassic. North of the Taurides-Anatolides-South Armenia Microplate (TASAM)-Eurasia suture zone, NTA shows a series of basins of various origins: the extensional basin of the Eastern Black Sea (EBS) to the northwest, the inverted back-arc basin of the Greater Caucasus (GC) to the northeast and flexural basins of Rioni and Ambrolauri (FB). These basins are surrounded by the Georgian Block (a tectonic unit), the inverted Adjara-Trialeti basin and the Dzirula Massif (DM).

In the following part, we propose a review about the main characteristics of these tectonostratigraphic units.

### 1. The structures of the Northwestern Transcaucasus domain

#### a- Foreland basins

Two flexural basins, Ambrolauri and Rioni, developed between the southern GC, the Georgian Block, the Adjara-Trialeti, DM, and the EBS tectono-stratigraphic units (Fig. II.1, Fig. I,7). Major thrusts generating kilometric amplitude folds delimits the borders of these basins (Adamia *et al.*, 2002). The Rioni flexural basin developed during the

Cenozoic, while the compression between Eurasia and TASAM created topography in the GC and in the Adjara-Trialeti belts as evidenced by the tracking of sediment sources (Vincent *et al.*, 2007, 2011; Adamia *et al.*, 2010, 2015; Cowgill *et al.*, 2016). The Ambrolauri foreland basin has the same history as the Rioni Foreland Basin but is physically separated from it by the uplifted Georgian Block. The sediments of the Rioni Foreland Basin are deformed up to the Meotis-Pontian deposits (Banks *et al.*, 1998; Tibaldi *et al.*, 2017b; Tari *et al.*, 2018). Some fault-bend-folds are documented: from north to south the Tsaishi and the Khobi south verging anticlines, the Kvaloni north-verging anticline, the Sagvamichao/Chaladidi south-verging anticline and the Lesa Anticline (Banks *et al.*, 1998; Tari *et al.*, 2018). Below, we will refer to these structures as the Tsaishi anticline and its prolongation (Fig. II.1).

The Ambrolauri Flexural Basin is fed to the north by the south-verging thrusting of the Southern Greater Caucasus (Gamkrelidze *et al.*, 1991, 2018), and to the south by the north-verging thrusting of the Georgian Block (Adamia *et al.*, 2002). The Cenozoic deposits are folded in this area and Mesozoic deposits outcrop in the eastern prolongation of the basin. The structure formed by the southern Greater Caucasus and the northern Georgian Block thrusts/folds continues along the western Ambrolauri Flexural Basin then disappears under the Rioni Foreland Basin (Philip *et al.*, 1989; Gamkrelidze 1991; Adamia *et al.*, 2002).

#### b- The Southern Greater Caucasus

The Greater Caucasus belt (GC) is divided into the Southern and Northern Slope Zones (SSZ, NSZ) which represent the transitions between the Mesozoic carbonate platforms located north and south of the GC, and the Main Range (MR) located in the center of the mountain belt (Adamia *et al.*, 1981, 2011b, 2017). The MR is composed of a large thickness of Mesozoic flysches which deposited in the deepest part of a basin: the Greater Caucasus (Adamia *et al.*, 1981, 2011b).

We focus here on the Southern Slope Zone because it constitutes the boundary between the southern Greater Caucasus and the Transcaucasus area. The Southern Slope Zone is folded with kilometric south-verging folds all along its border with the other tectono-stratigraphic units.

We will distinguish the Jvari area (on the western transect) and the Ambrolauri one (on the eastern transect). In both areas we can observe the same south-verging fold



structure, but its relationship with the Rioni Foreland Basin, the Georgian Block, and then the Ambrolauri Foreland Basin is a matter of debate and can have an important impact on the tectonic interpretation of the area. We will discuss the interpretation of this structure below.

#### c- The Georgian Block

The Georgian Block is a tectonostratigraphic unit defined by Adamia *et al.*, (1981) and is usually interpreted as a Mesozoic carbonate platform sparsely covered by Bajocian, Turonian and Campanian volcanic arc deposits (Adamia *et al.*, 1981, 2011a, 2017). The Georgian Block presents a bivergent structure with major kilometric folds at its boundaries. It is covered to the north by the Ambrolauri Flexural Basin and thrust by the Greater Caucasus Southern Slope Zone. It is thrust to the south onto the Dzirula Massif. It is covered to the west by Cenozoic deposits of the Rioni Flexural Basin. The southern limit of the Georgian Block, close to the Dzirula Massif, shows a steep south-verging fold limb, including Bajocian to Paleogene deposits. This south-verging fold thrusts over some horizontal deposits including Upper Cretaceous ones (map from (Abesadze *et al.*, 2004)).

The northern limit of the Georgian Block with the Ambrolauri Foreland Basin is characterized by a northward tilting of the sedimentary layers. In its central part, the Georgian Block is affected by some faults (map from Abesadze *et al.*, 2004) which based on their dip, relative displacement and stratigraphic thicknesses variations can be interpreted as normal faults that affect the Jurassic and the Lower Cretaceous deposits. To the west, Cenozoic deposits of the Rioni Foreland Basin mask older structures (Abesadze *et al.*, 2004) (Fig. II.1) and it is not clear whether the Georgian Block corresponds to the autochthon of the Rioni Foreland Basin or not.

#### d- The Dzirula Massif and the Adjara-Trialeti Fold-and-thrusts belt

The Dzirula Massif is located south of the GB and east of the Rioni Foreland Basin (Fig. II.1). It consists of the crystalline variscan basement (e.g. (Rolland *et al.*, 2011, 2016) among other) partly covered with thin Upper Paleozoic and Mesozoic and Cenozoic series. It is overthrust to the south and north by adjacent tectonostratigraphic units (Georgian Block and Adjara-Trialeti) (Trexler *et al.*, 2020). The Lower Jurassic, the Lower Cretaceous and the Upper Cretaceous deposits are deposited onto the crystalline rocks forming a major unconformity.

The Adjara Trialeti belt is located south of the Rioni Foreland Basin and the Dzirula Massif. It is interpreted as a tectonically inverted thick volcanoclastic basin or arc

(Khain 1975; Adamia *et al.*, 2010, 2015; Yilmaz *et al.*, 2013; Tari & Simmons 2018) that was active during the Paleogene. The deposits are then thrust and folded during the Cenozoic collision: the Middle Cretaceous to Oligocene deposits of Adjara Trialeti basin thrusts over to the north the Dzirula Massif and the Rioni Foreland Basin (Khain 1975; Gamkrelidze 1986; Adamia *et al.*, 2011a).

#### e- The Eastern Black Sea

West of the NW Transcaucasus domain, the Eastern Black Sea is bordered to the South East by the Adjara Trialeti, to the East by the Rioni Foreland Basin and to the north by the Greater Caucasus Southern Slope Zone. It is composed of three main structures elongated in a NW-SE direction. To the north, the Tuapsee Though is usually interpreted as a deep Cenozoic foreland basin (Robinson *et al.*, 1996; Nikishin *et al.*, 2015a) which developed south of the Greater Caucasus (Okay *et al.*, 1994; Banks *et al.*, 1998; Nikishin *et al.*, 2003, 2010, 2015a, 2017; Vincent *et al.*, 2007; Cowgill *et al.*, 2016; Tari *et al.*, 2018). South of the Tuapsee Though, the Shatsky Ridge was a topographic high since the beginning of the rifting of the EBS (end of Lower Cretaceous) (Okay *et al.*, 1994; Nikishin *et al.*, 2003, 2010, 2015b) and as a consequence is characterised by thinner Mesozoic deposits. The Shatsky Ridge is then covered by Neogene deposits (Nikishin *et al.*, 2003; Tari & Simmons 2018).

The main EBS basin is located south of the Shatsky Ridge. It is deeper than the northern basin of the EBS and shows deeper basin-type deposits (Okay *et al.*, 1994; Banks *et al.*, 1998; Nikishin *et al.*, 2003, 2010, 2015a, 2017; Vincent *et al.*, 2007; Cowgill *et al.*, 2016; Tari *et al.*, 2018). The continuation of these structures beneath the Rioni Foreland or their relationship with the Adjara-Trialeti is still unclear.

## 2. The stratigraphy in the northwestern Transcaucasus

Taking into account the previous studies (Morariu & Noual 2009; Adamia *et al.*, 2011a; Tari *et al.*, 2018), we present a synthetic log of the North-Western Transcaucasus (Fig. II.2). Cenozoic deposits of the foreland basins are unconformably overlying Mesozoic deposits (Banks *et al.*, 1998; Vincent *et al.*, 2007, 2014; Adamia *et al.*, 2010; Vincent, Stephen J *et al.*, 2016; Tibaldi *et al.*, 2017b). We summarize the stratigraphy of the area in Fig. II.2 in the following paragraph: Paleogene deposits begin with marly to sandy deposits during Paleocene and Eocene (Fig. II.2). Oligocene deposits are

known in the area because of their oil potential: they consist of dark clays, gypsum and salt (Morariu & Noual 2009). Neogene sediments are detrital deposits, marked by variations of paleo-environment from marine to continental. The thickness of these deposits can reach about 3000 m in some areas (Nikishin *et al.*, 2003; Morariu & Noual 2009; Adamia *et al.*, 2010).

Upper Cretaceous Turonian to Maastrichtian deposits consist of either fine-grained limestones and white-pink limestones and marls with concretions, with a thickness ranging from 0 to 600 m, or of 0 to 800 m thick tuffs and tuff-breccia-sandstones.

Aptian-Cenomanian deposits are mainly marls, tuffs and end with glauconitic sandstones, marls and limestones. There is an unconformity at the basis of Cenomanian, and in some places also at the top of the Barremian. The whole Aptian-Cenomanian series is 0 to 360 m thick.

Barremian-Hauterivian sediments consist of massive limestones of 0 to 120 m thick for the upper part. Valanginian deposits are dolomitised limestones with concretions. Berriasian deposits are sandstones and argillites. The thickness of the sedimentary column from Berriasian to Hauterivian can vary between 500 and 1200 m. There is an unconformity at the basis of the Berriasian deposits.

Upper Jurassic deposits consist of evaporites alternating with sandstones and shales. The lower part are detrital-lagoonal deposits locally named the multicolored sequence (Adamia *et al.*, 1981, 2011a). The whole Upper Jurassic sequence has a thickness which ranges from 0 to 150 m and lies unconformably onto the Bathonian deposits.

Bathonian sediments are detrital deposits (conglomerates to argillites) and their thickness varies from 0 to 200 m. These deposits have an industrial interest with coal mines near Tkibuli (Fig. II.1, point 12 for location) because the organic deposits contained in the sandstones are turning into coal in this area. Bathonian age is known to be linked to a major climate change which allowed the deposition and preservation of organic deposits (such as plants) which will produce coal and black shales. Then, during the Upper Jurassic the arid climate triggers the production of evaporite and reef limestones (Khain 2007; Guo *et al.*, 2011).

Bajocian deposits are made of volcanogenic deposits: volcanoclastic tuffs, lava flows and intrusive rocks. Their thickness varies from 1300 to 2000 m. The Bajocian deposits sometimes overlay Aalenian deposits with an unconformity. Aalenian-Hettangian deposits are made of 1500 to 2200 m thick detrital, fine grained deposits (shales and argillites and sandstones). They rest on Triassic deposits or directly overlay the

Variscan crystalline basement. The Triassic and other pre-Mesozoic deposits are made of volcanoclastics rocks and are deposited onto the Variscan basement.

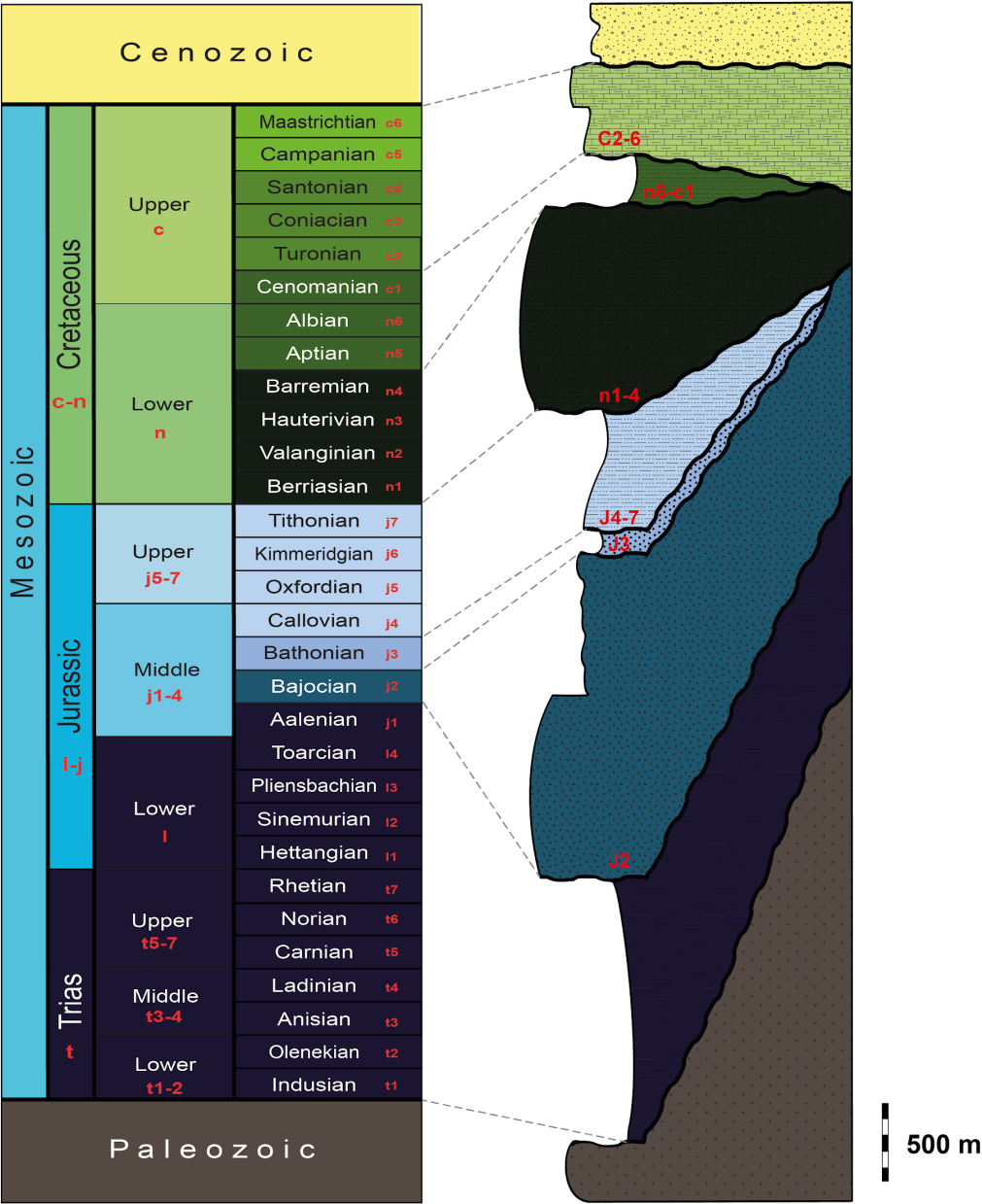


Figure II.2: Synthetic stratigraphic log of the North-western Transcaucasus (Georgian Bloc) modified after (Morariu & Noual 2009; Adamia et al., 2011a; Tari et al., 2018)

### III- Structural and stratigraphic observations in the Rioni

#### 1. Foreland Basin and the Georgian Block

Field observations have been carried out in the area of the Rioni Foreland Basin and Georgian Block (Fig. I, 8). In this paper, we focus on observations concerning the Mesozoic deposits characteristics (facies, geometry, and thickness variations). Mesozoic deposits outcrop in the Rioni Foreland Basin, east of the Black Sea along the Tsaishi anticline and its prolongation to the east near Senaki (Fig. II.1). Along this anticlinal structure, deposits from Middle to Upper Cretaceous are exposed. To the East, in the Georgian Block, Bajocian to Maastrichtian Mesozoic deposits crop out. The location of field observations used to constrain the A-A'-A'' cross section is along the Tsaishi anticline and the eastern prolongation of anticlines in the Rioni Foreland Basin. The Jvari area is cut in a N-S axis by a road located west of Jvari until the dam, and east of Jvari toward the north. About the B-B' cross section, two roads go across the Georgian Block in a NS direction. We have also gathered field data in gorges south of Zogishi (Fig. II.1).

Field observations have been completed with existing seismic and well data in order to highlight and interpret the structure of Mesozoic sediments beneath the Cenozoic cover. The structures linked to the Cenozoic compression deformation are first identified and located in order to discriminate them from the ones linked to Mesozoic deformations. We then correlate and compare these observations in the Rioni Foreland Basin and in the Georgian Block in order to unravel the Mesozoic deformation history of this region.

#### 2. Western Section across the Rioni area

The first section trending SSW-NNE crosses the western Rioni Foreland Basin and reaches the Greater Caucasus Southern Slope Zone (see Fig.1). This section of the Rioni Foreland Basin is mainly occupied by Cenozoic deposits, but we could gather some field observations on Upper Cretaceous deposits.

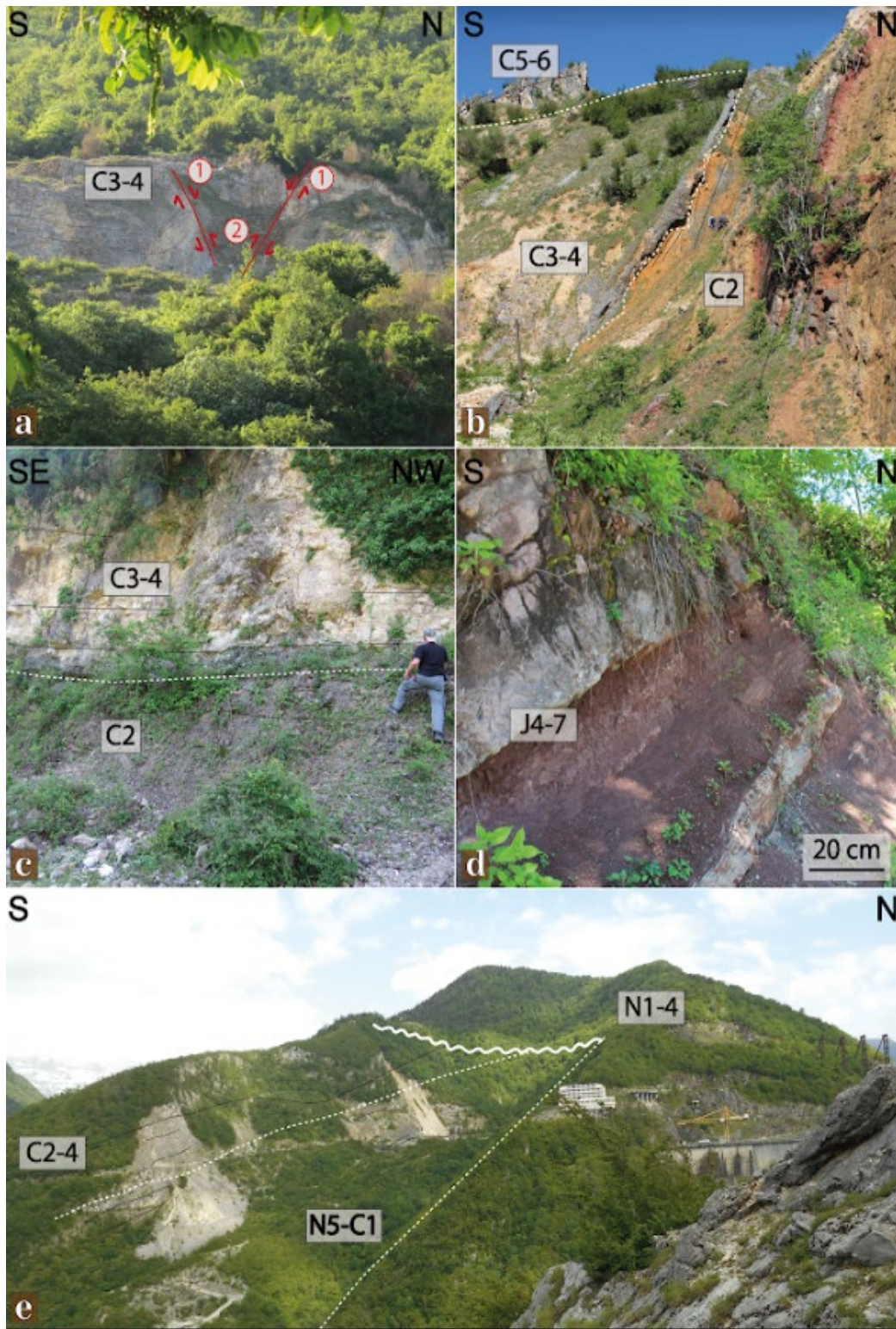


Figure II.3: Pictures along the western cross-section across the Rioni Foreland basin toward the Jvari area (Fig. II.1). Letters are the references to the position in the Fig. II.1. a: *reactivated normal* faults in the Upper Cretaceous (C3-4, Coniacian-Santonian) in the Tsaishi anticline. b: fan-shape with onlap in the Upper Cretaceous deposits (C2 Turonian, C3-4 Coniacian-Santonian and C5-6 Campanian-Maastrichtian) east of the Tsaishi anticline. c: horizontal normal contact in the Upper Cretaceous deposits east of the Tsaishi anticline (Coniacian (3) with glauconite on top of the Turonian C2). d: Upper Jurassic (J4-7 Callovian-Tithonian) deposits near Jvari area, “multicolored sequence” which is going

coarser at the top. e: panoramic view of the Jvari area showing the onlap fan-shape of the Aptian-Cenomanian deposits onto the Barremian.

#### a- Rioni Foreland Basin: South of the Tsaishi Anticline

The main observations concerning the deposits south of the Tsaishi anticline are made from the wells data (Fig. II.1 for the location) and are described from south to north (Fig. II.7).

Lesa 5 well (locality 1 in Fig. II.7): This well is very similar to wells Lesa 3, 6 and 12. Upper Cretaceous deposits between Turonian and Campanian are not distinguished and are together 140m thick. Albian-Cenomanian deposits are about 600m thick. Well data show that the facies of these deposits is a little different from usually observed: the deposits are made of detrital and clays, with some volcanic deposits.

Berriasian-Aptian deposits are about 800m thick, with at least 500m of clayish deposits in the upper part: we can interpret this upper sequence as corresponding to the Aptian deposits.

Upper Jurassic evaporites are 60 m thick. Middle Jurassic volcanogenic deposits are about 400 m thick. As well data describe tuff-greywacke sandstones in this part of the well we interpret the age of these deposits as Bathonian.

The Sagvamichao 6 well (locality 2 in Fig. II.7): The Upper Cretaceous is undivided between Turonian and Campanian. The whole deposits are 270 m thick. These are made of clayish limestones and detrital sediments. Cenomanian deposits are less than 100m thick. The 120 last meters are made of sandy tuffs of probable Bathonian age.

The Sagvamichao 16 (locality 3 in Fig. II.7) well is separated into two parts delimited by a thrust. The upper 3' log presents Turonian-Danian formations less than 250 m thick, ~500 m thick Albian-Cenomanian formations, and finally 170 m thick Aptian-Neocomian hard limestones.

The lower part of the log 3 shows more than 400 m of grayish-white limestones with alternation of friable and hard limestones of undifferentiated Upper Cretaceous age.

The undifferentiated Lower Cretaceous is about 220 m thick (maximum). It consists of dark dolomitized limestone and black marls.

Upper Jurassic evaporites, sand, clays and the colored sequence is more than 660m thick.

Bathonian volcanic tuffs have a maximal thickness of 730 m.

The 300 last meters of this well are very hard magmatic rocks that we can interpret as related to the Bajocian magmatic formations.

#### b- Rioni Foreland Basin: the Tsaishi Anticline

The main observations concerning the Mesozoic deposits in the Rioni Foreland Basin are located on the E-W Tsaishi anticline and its eastern prolongation along a WSW-ENE trend (Fig. II.1, Fig. II.4). Interpretations concerning other structures located along section A-A' (Fig. II.1) are taken from the literature and based on seismic lines (Banks *et al.*, 1998; Morariu & Noual 2009; Tibaldi *et al.*, 2017b; Tari *et al.*, 2018) (Fig. II.5) and/or constrained by well data (Fig. II.7).

The Tsaishi anticline (Locality 4 on the Fig. II.7) is a well-studied structure (Banks *et al.*, 1998; Morariu & Noual 2009; Tibaldi *et al.*, 2017b,a; Tari *et al.*, 2018) because of its oil-gas potential offshore of the Black Sea (Adamia *et al.*, 2002; Morariu & Noual 2009; Nikishin *et al.*, 2015b; Tari & Simmons 2018) and also a structure where active tectonics has been evidenced (Tibaldi *et al.*, 2017b,a; Trexler *et al.*, 2020). Upper Cretaceous sediments outcrop in the core of the anticline, but the fold also deforms the Lower Cretaceous (Banks *et al.*, 1998; Tibaldi *et al.*, 2017a; Tari *et al.*, 2018). Usually described as a thin-skinned tectonic structure (Gamkrelidze 1991; Tibaldi *et al.*, 2017b,a), with the location of the decollement level into the Upper Jurassic deposits (Banks *et al.*, 1998; Morariu & Noual 2009), the anticline is south-verging, as evidenced by its steeply dipping southern limb and gently dipping northern limb (Fig. II.3, d, Fig. II.4). Published seismic lines (Banks *et al.*, 1998; Tibaldi *et al.*, 2017a; Tari *et al.*, 2018) (Fig. II.5) show some small-offset normal faults in the Jurassic and Cretaceous deposits (until Albian-Cenomanian) of this anticline (Banks *et al.*, 1998; Tibaldi *et al.*, 2017a; Tari *et al.*, 2018). Along the anticlinal structure, we observed Upper Cretaceous deposits (Fig. II.3 a-d). Campanian-Maastrichtian limestones are present at the front of the foreland and disappear progressively at the rear of the fold, the Paleocene lying directly on the Lower Cretaceous deposits (section central Tsaishi on Fig. II.4). Coniacian-Santonian sandy and marly limestones present some normal faults and are observed only on the frontal fold limb (Fig. II.3, a). On the back limb, these deposits are very reduced and consist of recrystallized limestones (<20m) (Fig. II.4, 12). On the seismic line



presented on figure 5 which cross the anticline, these deposits appear to onlap onto Lower Cretaceous ones at the rear of the fold and thicken towards the north (Fig. II.5). This corresponds to the unconformity of the Upper Cretaceous deposits on top of the Lower Cretaceous ones. The fan-shape structures, highlighted by observation of onlaps and thickness variations, seem to concern only the frontal part of the anticline (Fig. II.5). Some onlaps of the Turonian-Santonian deposits are observed on the seismic lines at the rear of the anticline (Fig. II.5).

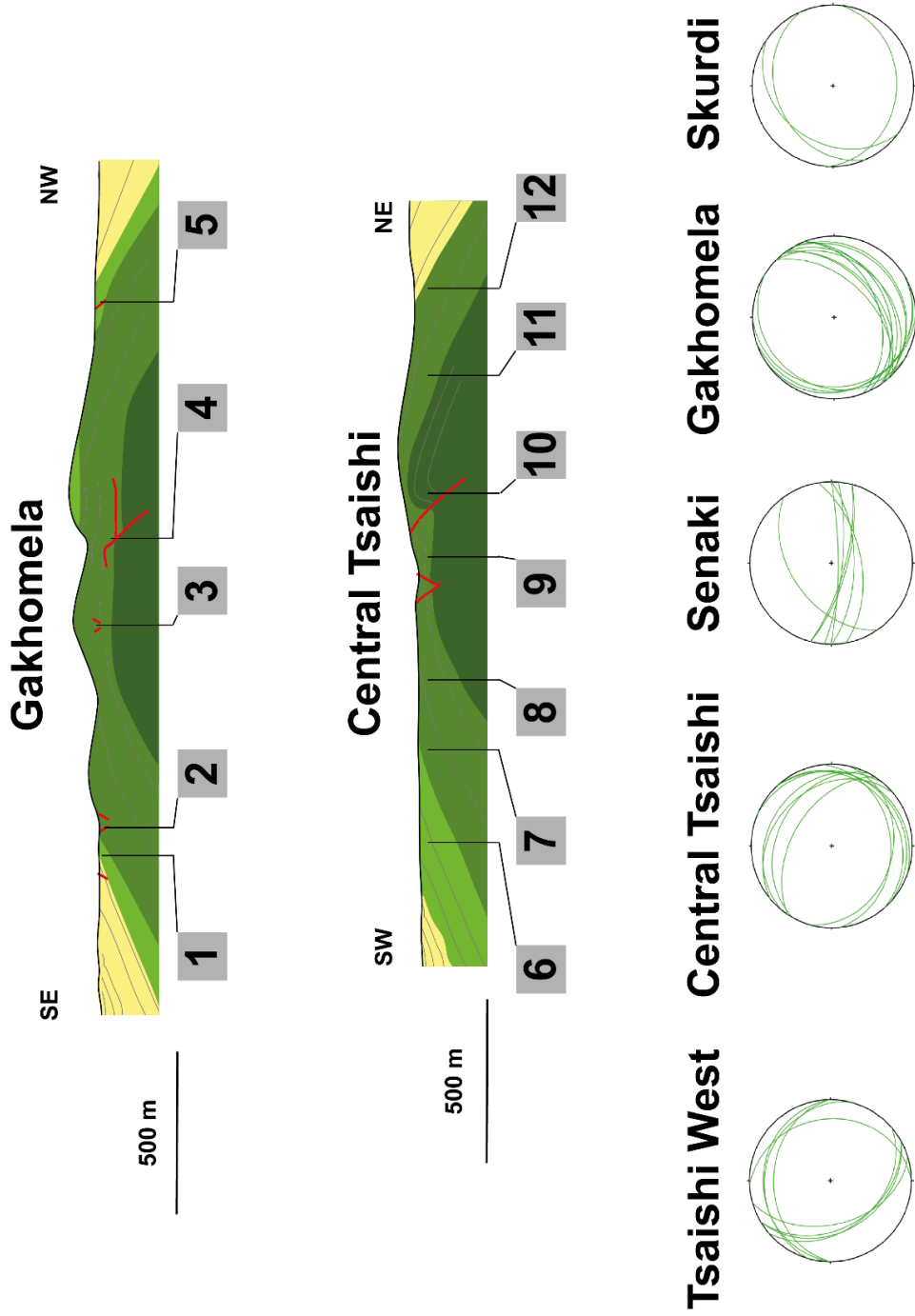


Figure II.4: Cross sections of the Tsaishi Anticline near TsC on Fig.1, and Gakhomela anticline (Gk in Fig.1) with associated pictures along the transects. The stereonets concern the dipping in the Mesozoic deposits in the different anticlines observed in the western Tsaishi (Ts), the central Tsaishi (TsC), Senaki (Snk) Gakhomela (Gk) and Skurdi (Sk) anticlines. The stereonets show the main constraints of the folds which change across the Rioni area. This can be observed on the geological maps with the axis of the folds. The most western anticlines have a NE-SW compression, while it changes to N/S in Senaki, and NW-SE to the east. A major strike-slip fault can be expected west of Tsaishi, going towards Zugdidi to the north.



1



1'



2



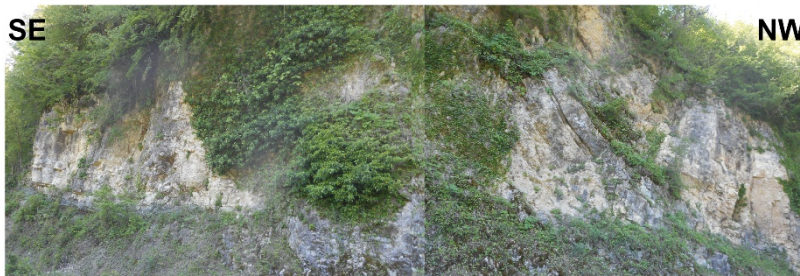
2'



3



3'



4



5



6



7



8



9



10



11



12

Figure II.4 bis. Pictures along the cross sections presented in in Fig. II.13: 1: Uppermost part of Upper Cretaceous limestones near the transition with Paleocene marls. The deposits contain pyrite nodules. 1': Typical Upper Cretaceous shaly limestone with nodules of cherts . 2 and 3: Senonian deposits which present some parts of breccias with angular reworked materials. 4: Senonian deposits on the top of the Turonian volcanogenic deposits: we observe a normal transition from Turonian deposits to the Senonian deposits with some glauconitic deposits at the transition. However, we observe on the picture a decollement level which create a fault-bend-fold into the Senonian deposits. It's the only example observed, but we can expect it in another places. 5: The same deposits of the Uppermost part of the Upper Cretaceous as in picture 1, situated at the back of the fold. 6: The Upper Cretaceous deposits to the south of Tsaishi, these limestones can present cherts lenses. 7 and 8 present the Senonian deposits: the deposits in 7 are more reddish than the ones in the 8 picture which are whiter and are changing in the deposits more marly observed in the picture 9. The deposits in the pictures 9 have some interbedding with marls. The picture 10 illustrate the river-eroded lower Cretaceous massive limestones. The deposits in the picture 11 are the Senonian deposits with thinner bedding, which evolve in the very recrystallised deposits observed in the picture 12. The Paleogene marly deposits are deposited directly on these deposits.

To the East, the same kind of fan shape is observed north of Senaki (Fig.1) where at the surface the south-verging fold exposes Turonian volcanogenic sandstone deposits (C2) in the core of an anticline. The Coniacian-Santonian deposits (C3-4) lie unconformably onto these Turonian sandstones (C2) (Fig. II.3b). In comparison, the overlying Campanian-Maastrichtian (C5-6) layers dip more gently to the south and forms also a fan-shape onto older deposits (Fig. II.3b). This stratigraphic architecture can be opposed to the conformable contact observed in the central part of the eastern prolongation of the anticline where Coniacian-Santonian sandy-limestones are deposited onto the Turonian volcanogenic sandstones (C2). The base of the Coniacian is marked by glauconitic sandy deposits (Fig. II.3c).

Well data describe lithological facies consistent with the usual stratigraphic interpretations found in the literature (Fig. II.7). We used these data in the next section to constrain thickness and facies variations along the cross-section.

Concerning the deposits along the Tsaishi Anticline, well data together with the seismic lines show thickness lateral variations in Lower Cretaceous deposits (Fig. II.1 and Fig 4, point 4 and 4', Fig. II.5). In the footwall of the Tsaishi thrust, the thickness of the deposits is more important than on the hanging wall. Moreover, the ones located on the rear of the fold are thicker too.

The seismic lines offer the possibility to observe the different anticlines which are

beneath the Cenozoic cover along the AA' cross section. Based on the seismic line interpretations, the decollement level of the folds seems to lay into the Upper Jurassic deposits (Banks *et al.*, 1998; Tibaldi *et al.*, 2017b,a; Tari *et al.*, 2018). Some normal faults affecting Jurassic sediments are evidenced (Tari *et al.*, 2018).

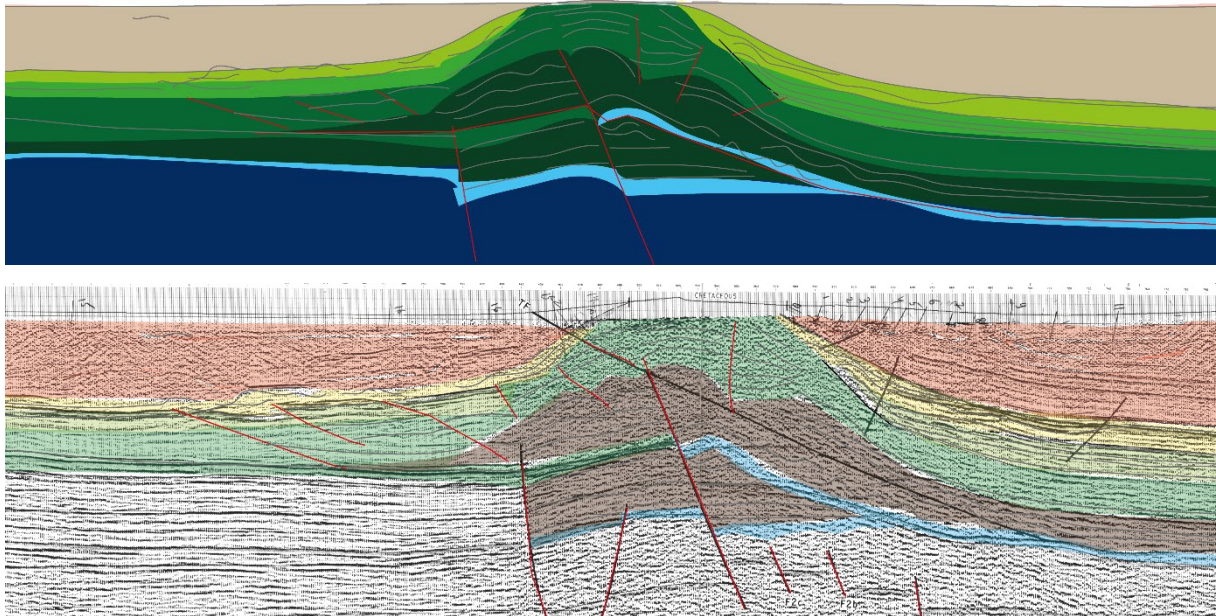


Figure II.5: Seismic interpretation of the Tsaishi seismic line: the Paleogene and Neogene deposits are undifferentiated. We observe on this interpretation two normal faults. The thickness of the Lower and Upper Cretaceous deposits increase north of the normal faults. We can observe that the normal fault displacement is nearly cancelled by the inversion. The Cretaceous deposits are thrust along the Upper Jurassic decollement level. We can also highlight the unconformity of Upper Cretaceous onto the Lower Cretaceous. (See chap. 3 for the Paleogene and Neogene deposits interpretation).

The localities 5 and 6 expose similarities (Fig. II.1 and Fig. II.7). The Bajocian deposits are at least 500m thick, and there is thin (<50m) or absent Bathonian deposits. The Upper Jurassic deposits are <300m thick. The Barremian deposits are more than 2000m thick, and the Aptian-Cenomanian deposits up to 600m thick. This is the thickest part of Cretaceous deposits in the western cross-section. The Upper Cretaceous deposits are eroded at the point 4, and the seismic line of the Tsaishi anticline show onlaps of the Turonian deposits onto the Lower Cretaceous deposits (involving decreasing thickness locally). The well Tsaishi 8 show a thickness of Upper Cretaceous up to 600m thick (Fig. II.7).

The well “Zugdidi 3” (locality 6 in Fig. II.1 and 7) show similar observation concerning the Jurassic deposits as in the locality 5. The well show an important erosion of the

Cretaceous deposits, which correlate with the uplift of the deposits in this area. The Lower Cretaceous deposits could be estimated as at least 200m thick.

#### c- Greater Caucasus Southern Slope Zone: the Jvari Anticline

The Jvari anticline (Locality 7 in the Fig. II.1 and 7), located on the southern edge of the Greater Caucasus (Southern Slope Zone: SSZ), exposes a tilted and strongly deformed continuous section of the Mesozoic formations, younging from North to South (Fig. II.6).

There, Middle Jurassic formations are approximately 4000 m thick. They are constituted of 2000 m of Bajocian volcanoclastic deposits and lavas, and 2000 m of Bathonian coal-bearing sandstones (Fig. II.6 and 7).

Upper Jurassic deposits onlap unconformably over the Middle Jurassic formations and present local thickness (0 to 400m) and facies variations. In the northern part, conglomerates and reddish sandstones are the dominant lithologies for the Upper Jurassic. These formations evolve laterally to the South towards multicolored argillaceous sequences with some intercalated anhydrite layers (Fig. II.3d).

Lower Cretaceous (mainly Barremian) deposits are up to 2000 m thick. Thickness variations cannot be observed because of the lack of reliable stratigraphic limits in this formation and because the deposits are locally faulted and sheared (Fig. II.6). This deformed zone within the Lower Cretaceous formation corresponds to a major decollement level.

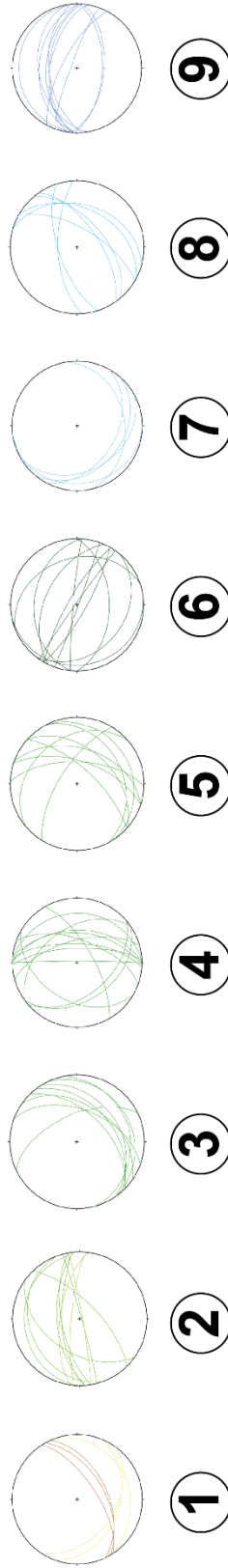
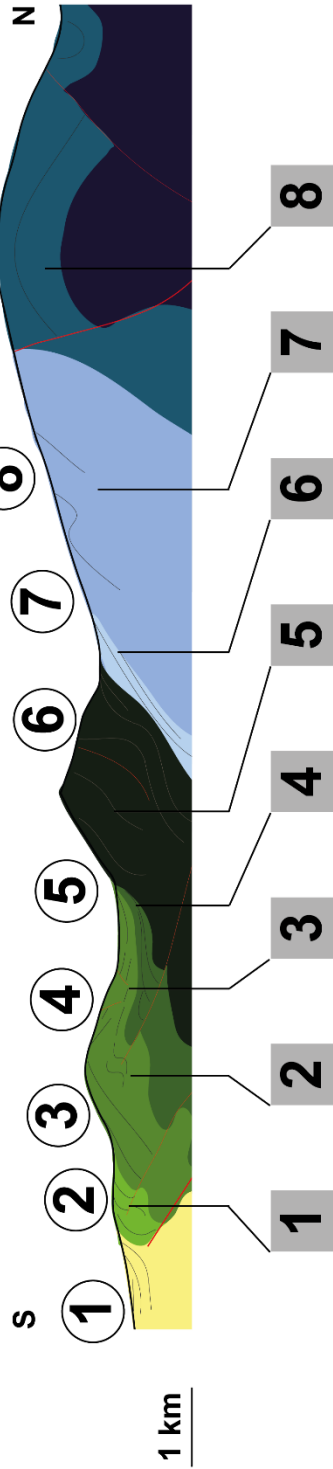
Albo-Cenomanian deposits can be observed on Barremian deposits (Fig. II.3e). They show a very rapid thickness variation from North to South from 0 to ~100 m, indicating a deepening of the deposition environment toward the south.

Turonian-Santonian deposits are unconformably overlying onto the Albo-Cenomanian or the Lower Cretaceous deposits (Fig. II.3e). These present some local dipping variations (Fig. II.6).

The western transect (Fig. II.1) therefore shows thicker deposits close to the front of the fold, which are then onlapped by younger deposits. In the southern part of the section, we observe these relationships in Upper Cretaceous deposits (Fig. II.3e). In the northern part of the transect, this is observed in Upper Jurassic and Albo-

Cenomanian deposits. Other thickness variations in Middle Jurassic and Barremian deposits can only be determined by looking at the geological map.

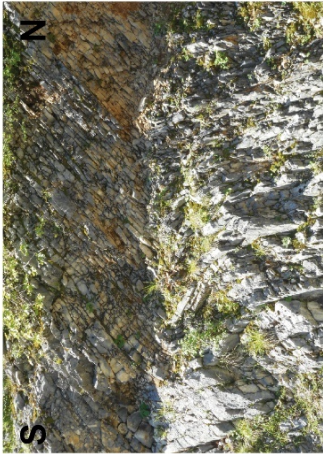
# Jvari







1



2



3



4



5



6



7



8

Figure II.6: Cross sections of the Jvari anticline “Jv” on Fig.1 with associated pictures and stereonet along the transect. 1: Upper Cretaceous deposits showing changes in the dipping in a <10m scale. 2 and 3 are the Senonian deposits, affected by breccias as observed in Fig.4. Picture 4 is the Aptian- Cenomanian deposits with black marls alternations. These deposits are not observed higher in the cross section (Fig. II.3e). Picture 5 is the Lower Cretaceous massive limestones. Picture 6 is the Upper Jurassic deposits. The picture 7 is the middle Jurassic Bathonian deposits, and finally the picture 8 are the Bajocian deposits.

The stereonet show the variations of the main constraints along the transect. The main stress show N/S direction in the Bajocian and Lower Jurassic deposits while it changes in NW/SE in the Bathonian deposits as for the Senonian and Upper Cretaceous - Paleogene deposits. The Lower Cretaceous – Upper Jurassic are in a NE/SW direction. The Lower Senonian and the Lower Cretaceous deposits are deformed in an EW direction.

#### d- Mesozoic deposits thickness variations along the Rioni transect

Together with well data, local field observations highlight deposits thickness variations within the Mesozoic sequence along a 50 km transect (Fig. II.1 and 7). We describe here the general thickness variation along this transect starting from the Bajocian up to the Campanian-Maastrichian.

The base of volcanogenic Bajocian deposits is neither exposed in the field, nor has been reached in the wells, so we cannot infer any thickness variations. These deposits reach a thickness of at least 500 meters along the transect, in the literature the thickness in the cross-section reach about 1200-1500m thick (Tari *et al.*, 2018) or about 5000m (Banks *et al.*, 1998).

The base of the Bathonian deposits cannot be observed at localities 1 and 2 (Fig. II.7) so we could neither directly observe any thickness variations in the field. However, as evidenced by wells data thickness varies along the transect. Under the Rioni Foreland Basin, Bathonian deposits thickness decreases from locality 3 (about 500 m) towards the north, where they disappear or are limited to about 100 m. Further north in the Jvari Anticline, Bathonian formations thicken considerably, reaching about 2000 m.

Post-Bathonian Jurassic deposits thicken generally from locality 2 (Fig. II.7), where they are totally absent, toward the north. At locality 1 these formations are thin (< 100 m). At localities 3 and 4 they reach more than 500 m. North of the Tsaishi anticline, the deposits thickness decreases from 400 m at locality 5 to 300 m at locality 6. Near the

Jvari anticline (locality 7), the deposits thickness varies from 300 m to 0 m, onlapping over Bathonian formations.

Barremian and older Cretaceous deposits are thicker south and north of the transect. Deposits are absent at locality 2 and then the thinnest at locality 3, where they reach only 200 m together with the Aptian-Cenomanian deposits. South of this point, they reach at least 300 m and less than 800 m at locality 1. From localities 3 and 3', the thickness of these deposits increases: they reach 900 m at locality 4, about 1200 m at locality 4', more than 2000 m at locality 5. The locality 6 involving a possible erosion of the top of the Mesozoic sequence cannot be used to infer the thickness of Lower Cretaceous deposits. At the Jvari anticline (locality 7), the thickness of the Barremian formations appears homogeneous and reaches about 2000 m.

Albo-Cenomanian deposits are also the thinnest at localities 2 and 3 (100 to 200 m together with the older Cretaceous deposits at point 3). Their thickness is rather constant (from 500 m to 750 m) along the transect in the Rioni FB north to the locality 3. Toward the north, in the Jvari anticline at locality 7, these deposits are thinner (0 to 400 m) and onlapping over older formations down to the Barremian.

These data evidence an increase of thickness in the whole Lower Cretaceous and Cenomanian deposits between localities 3 and 3', and between localities 4 and 4'.

Turonian-Santonian and Campanian-Maastrichtian deposits are not distinguished in most of the wells. These deposits are affected by erosion in the anticlines, so the thickness variation is not well constrained. The thinnest deposits are located at locality 1 (< 200 m), and then increase to reach thicknesses ranging between 200 m (locality 3') and 700 m (locality 5). At locality 7, to the north, the thickness of the deposits increases again and reach > 1300 m.

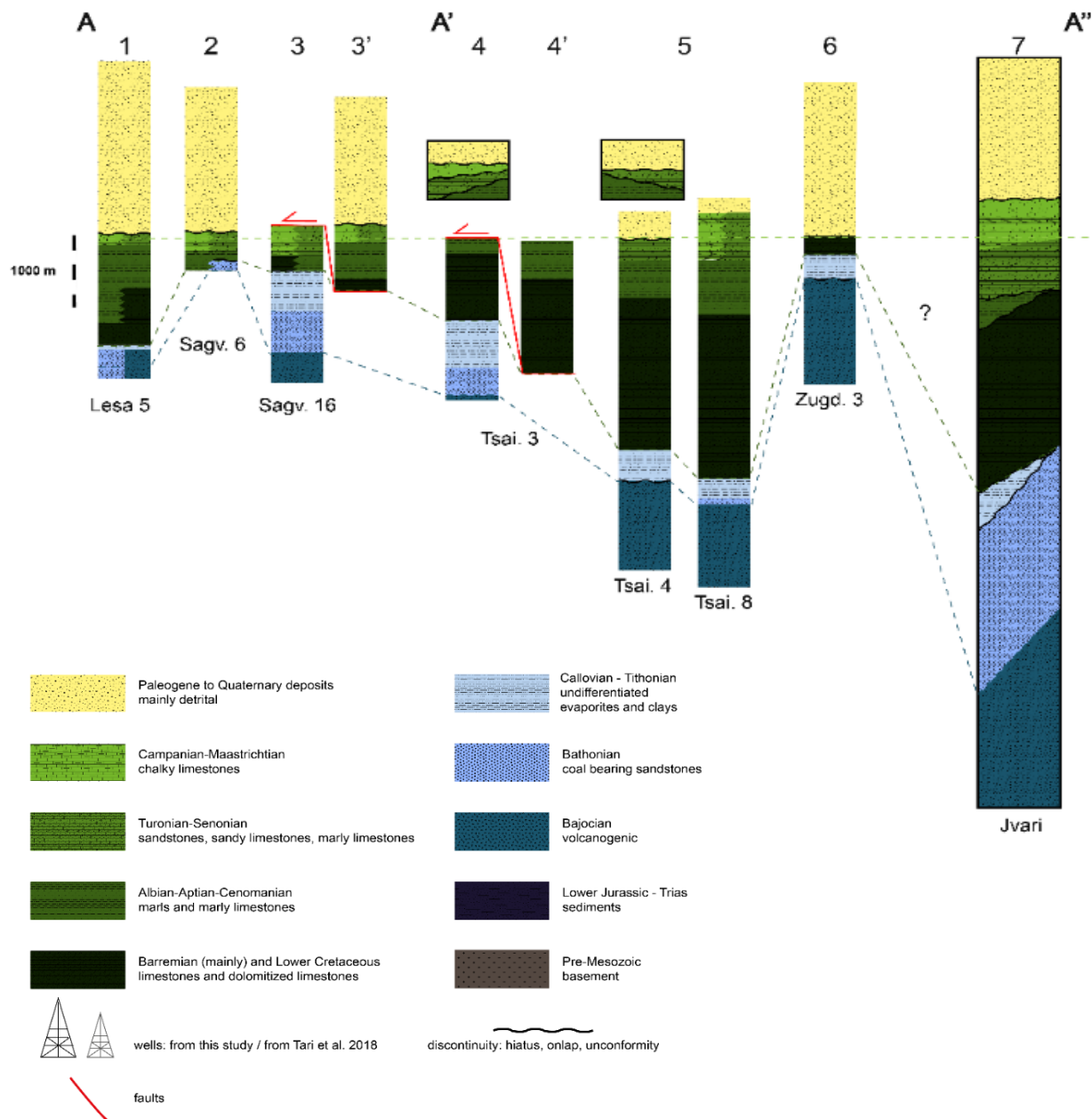


Figure II.7: Stratigraphic log for the western section (AA', see Fig. II.1). Same legend as Figure 2. The thinner log are the ones constrained by wells data. The thicker one (point 7), as well as the elongated boxes at point 4 and 5 are also constrained by field data.

### 3. Eastern transect across the Georgian Block

The second section crosses the Georgian Block, and extends over 50 km from SSW to NNE, from the Dzirula Massif to the Greater Caucasus Southern Slope Zone (see Fig.1). This transect is constructed using both direct field observations of the Mesozoic deposits (Fig. II.8), which are well exposed, seismic lines in the South (Fig. II.9), and

a well, *Bziauri1* (Fig. 11.14). Seismic lines help us constrain the transition between the Dzirula Massif and the Georgian Block, and the well, located in Jurassic deposits, constrains the minimal thickness of the Bajocian volcanogenic deposits (2500 m).

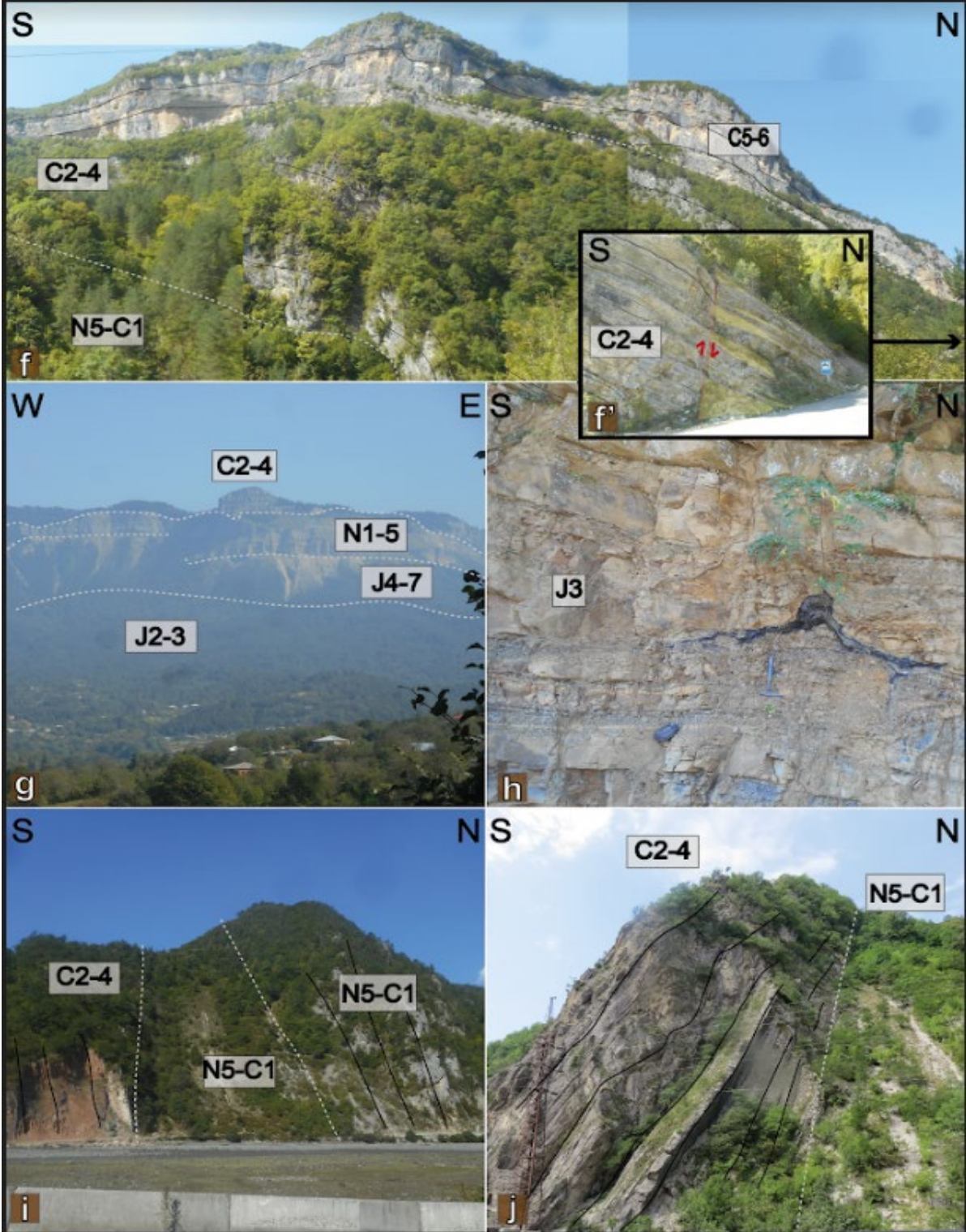


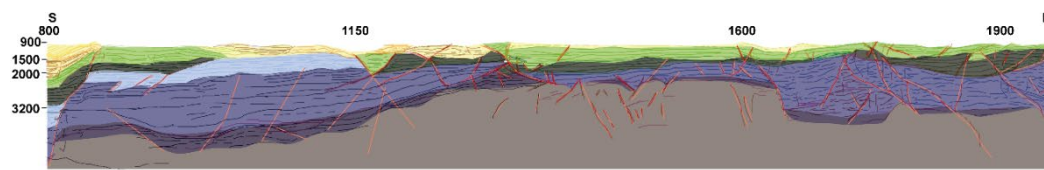
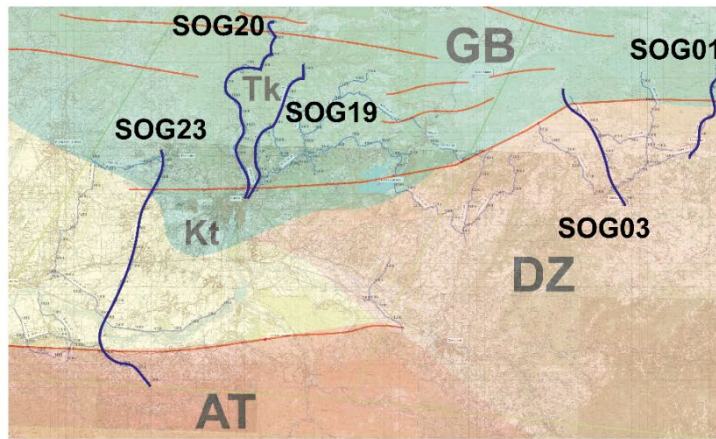
Figure II.8: Pictures along the eastern cross-section. Letters are the references to the position in the Fig. II.1.

f: Panoramic picture near the south-verging anticline which delimitates the Georgian Block and the Ambrolauri foreland basin. We can observe the unconformity of C5-6 on N5 to C4 and the fan-shape of the C2-4 deposits. g: panoramic picture showing the Mesozoic sequence near Tkibuli. h: Bathonian deposits where organic material (roots) is turning into coal. i: observation of the high dipping serie of the Greater Caucasus Southern Slope, east of the Ambrolauri foreland basin. j: observation of the south-verging anticline of the Greater Caucasus Southern Slope west of the Ambrolauri foreland basin.

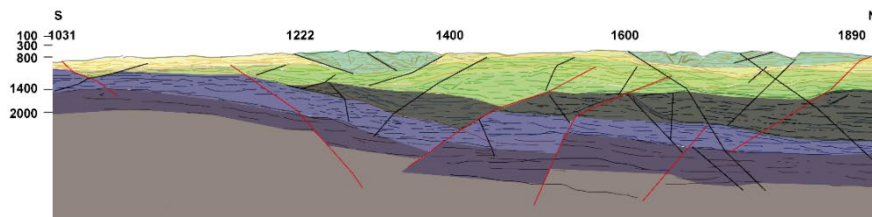
#### a- The Dzirula Massif

Here, we focus on the major unconformities observed on the northern side of this massif (Fig. II.1). We observed two important unconformities where either Upper Cretaceous or Middle Jurassic formations lie directly onto the basement.

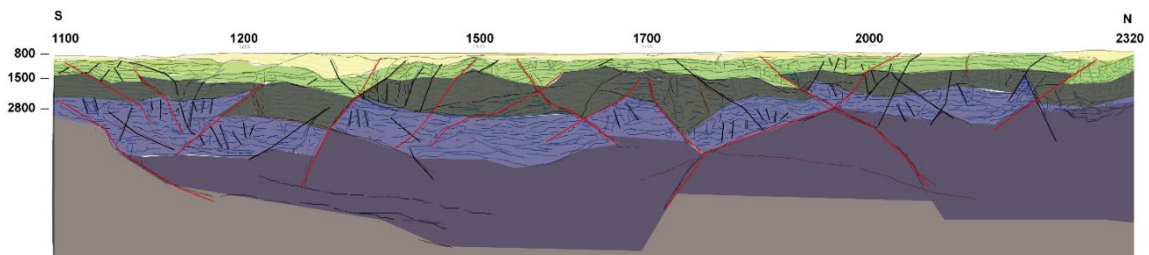
Three confidential seismic lines have also been used to investigate the geometry of the deposits at depth and highlight onlap of the Mesozoic deposits onto the basement, and a series of north-dipping normal faults further to the north (Fig. II.9). These observations are consistent with the geological maps (Abesadze *et al.*, 2004) indicating a thickening of the Mesozoic deposits against normal faults.



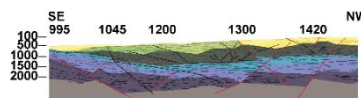
**SOG 23 RSS Depth**



**SOG 19 RSS Mig**



**SOG 20 RSS Depth**



**SOG 03 RSS MIG**

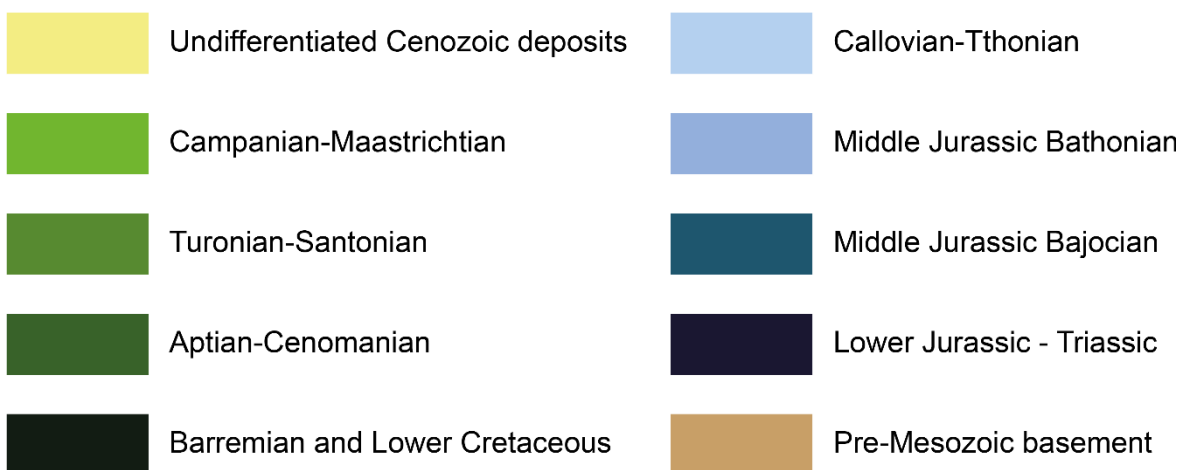
Figure II.9: Dzirula area locations of the seismic lines, and the relative seismic interpretations. Colors are speculative and no data constrain the ages of the formations.

## b- The Georgian Block

Mesozoic formations can be observed in the field eastward and northward of Koutaissi (Kt.in Fig. II.1). The structure presents a kilometric south-verging anticline (Fig. II.10), which involves a thrusting of the sedimentary cover over the crystalline Dzirula Massif unit (constituted of the basement and the autochthonous Mesozoic cover).

More to the north, Jurassic deposits are weakly deformed with some dip variations as long wave-length folding. Cretaceous deposits located north of the Jurassic formations are gently dipping toward the north (Fig. II.8, g, h). Similar structures are interpreted from the map (Abesadze *et al.*, 2004), where some faults are also described. Based on our observations (Fig. II.8 and 9), these faults can be interpreted as normal faults. Gently flexured Jurassic and Lower Cretaceous formations are overlain by the nearly horizontal Upper Cretaceous; hence, the pre-Upper Cretaceous deposits are slightly more deformed than the Upper Cretaceous (Fig. II.11).

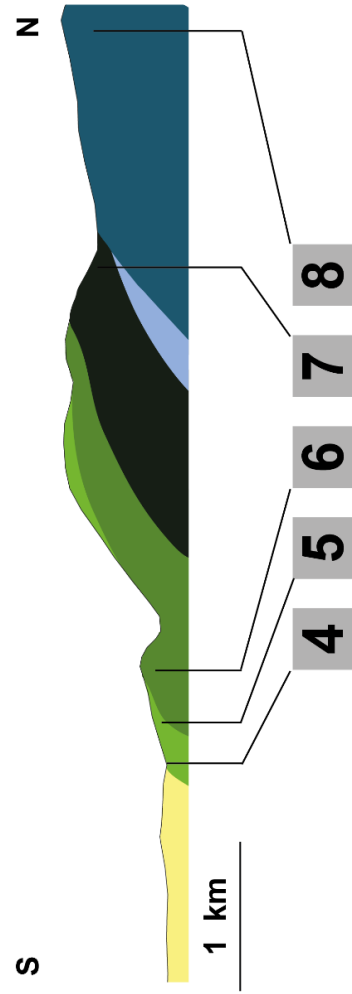
To the north, near Kenashi location (Fig. II.1) along a west-east direction going from Tsageri to Ambrolauri, we observed a north-verging kilometric-scale anticline (Fig. II.8 f, Fig. II.12). The core of the syncline preserves Upper Cretaceous Campanian-Maastrichtian formations. These anticlines are tilted towards the north. The Lower Cretaceous deposits are more tilted and their structure defines a fan shape typical of growth strata filling the normal-fault (Fig. II.8, f).



Legend for Fig. II. 9, 10, 11



# Koutaissi





1



1'



2



3



3'



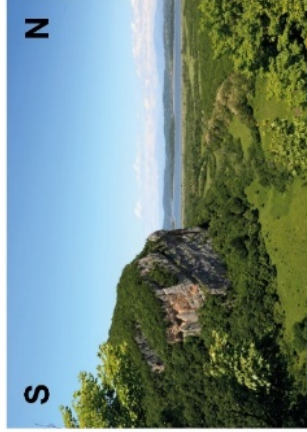
4



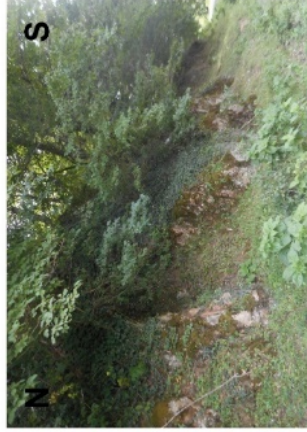
5



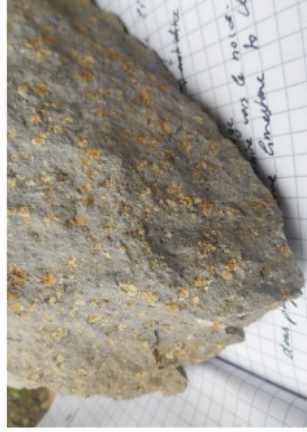
6



7



8



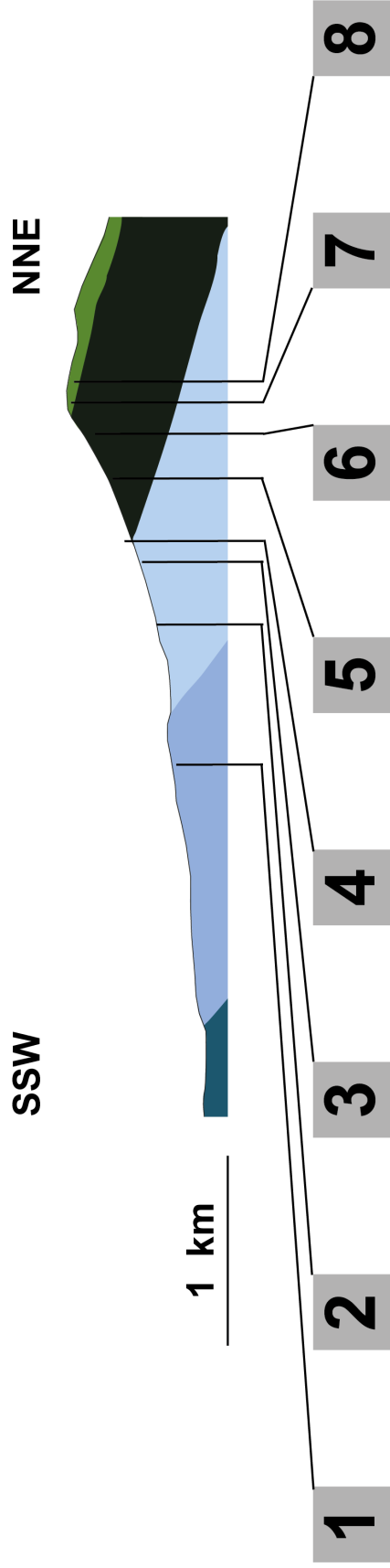
8'

*Figure II.10: Cross sections of the Koutaissi Anticline near Kt on Fig.1 with associated pictures along the transects. The second cross section is along strike 10 km to the east from the Kt.*

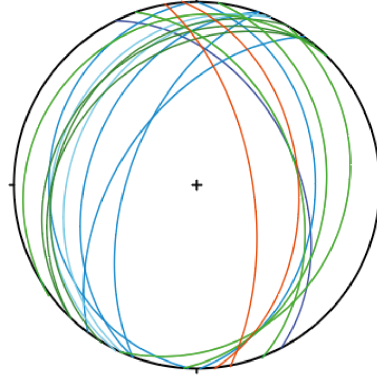
*Pictures 1 are the Paleogene deposits lying onto the very shaly limestones of the Upper Cretaceous. We don't observe here the alternation of limestone and detrital deposits as observed in Tsaishi and Gakhomela. 2: Picture from Google Earth \*\* showing the Lower Cretaceous massive limestones in the gorges. Pictures 3 show the Bathonian coal bearing deposits, with channel flows observed in the upper part. The pictures 4 and 5 show the Upper Cretaceous deposits of the frontal part of the anticline. The picture 6 shows the Senonian sandy deposits. The picture 7 from Google Earth \*\* shows in a landscape the Lower Cretaceous massive limestone and the Jurassic plain to the north, with the Tkibuli hills in the background (Fig. II.11).*

*The picture 8 shows the Bajocian deposits which are intruded by magmatic formations.*

# Tkibuli



# Koutaissi-Tkibuli





1



2



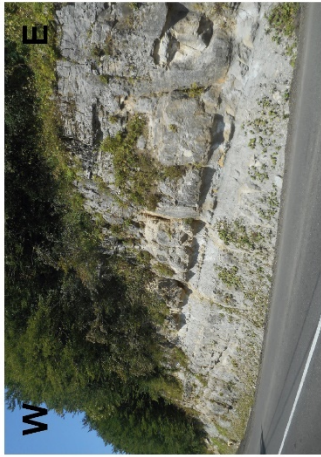
3



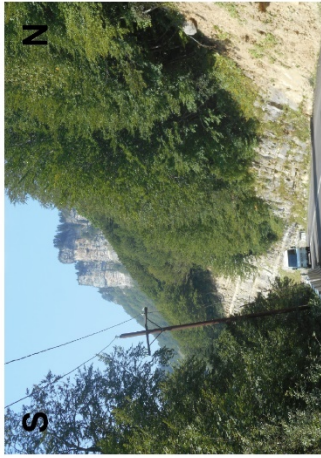
4



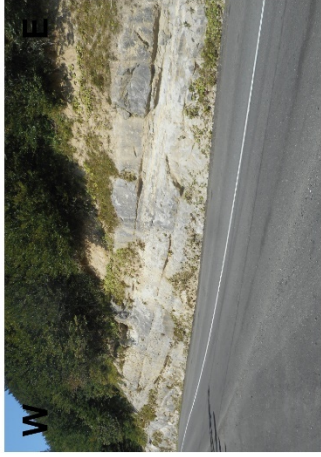
5



6

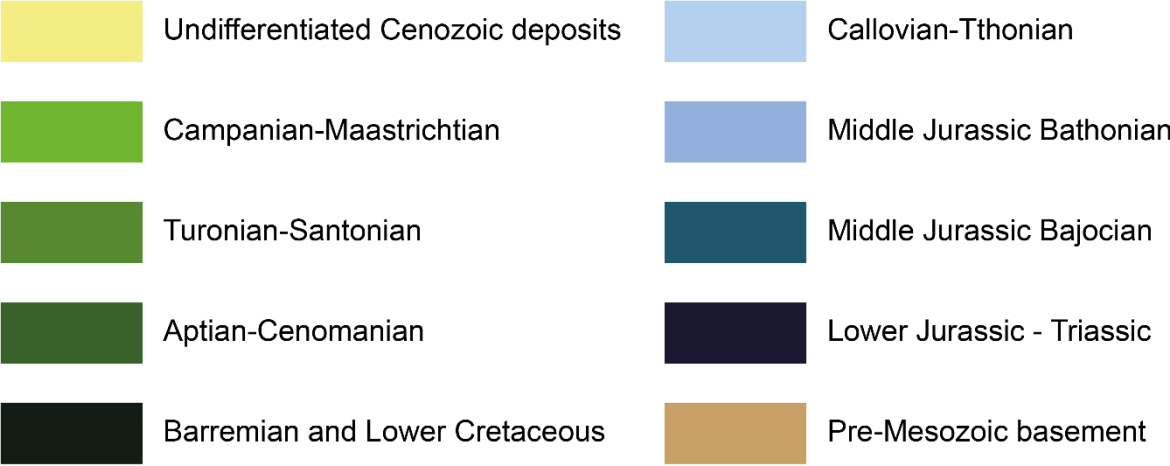



7



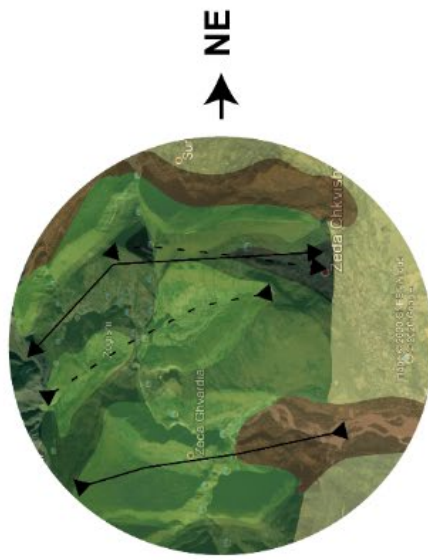
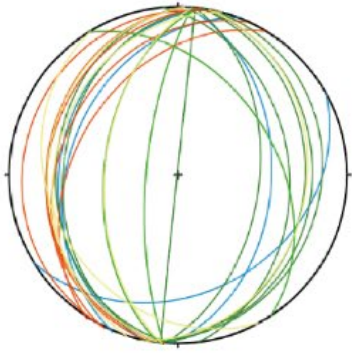
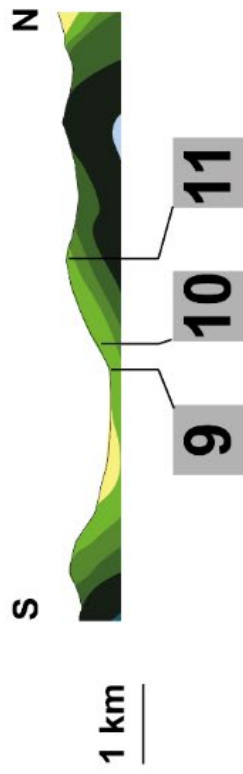
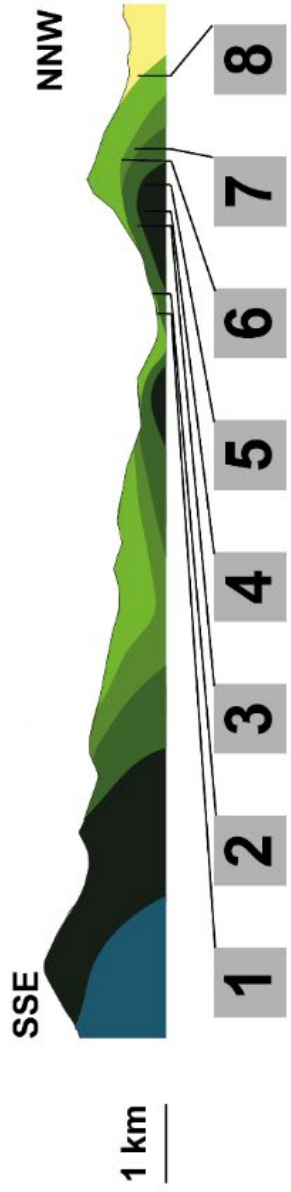
8

Figure II.11: Cross section of the Tkibuli area, Tk on Fig.1 with associated pictures along the transect. The stereonet concerns the dipping of the Mesozoic deposits in the whole area from Koutaissi to Tkibuli. Picture 1 show the Bathonian deposits which contain the coal in the area. Pictures 2 and 3 are the lagunal upper Jurassic deposits. The picture 4 show the limit of the lagunal colored suit of the Upper Jurassic. The pictures 5 and 6 show the lower Cretaceous which are not as massive as usual: here these contain some marls and blue shales. It is possible to be Aptian-Cenomanian facies in this place. Picture 7 and 8 are the Senonian deposits, with in the background the Upper Cretaceous deposits overlying the hills. The stereonet show that the direction of the deformation is mainly NNE/SSW from Koutaissi to Tkibuli hills.



 Faults      Legend for Fig. II. 12, 13, 14

# Kenashi





1



2



3



4



5



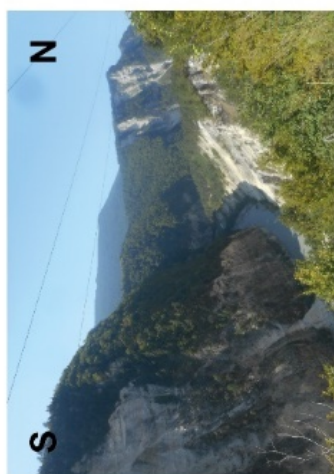
6



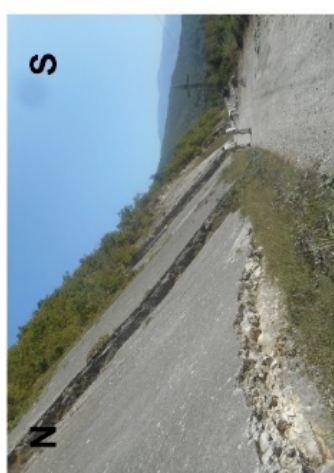
7



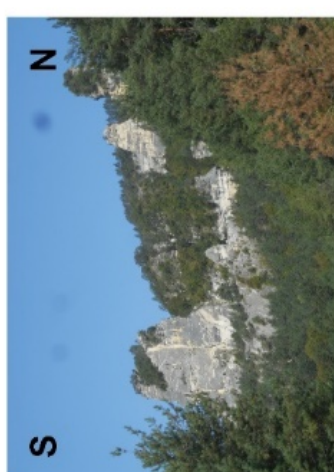
8



9



10



11



Figure II.12: Cross sections of the Kenashi anticlines near Zg “Zogishi” on Fig.1, with associated pictures and stereonet along the transects. Pictures 1, 2 and 9, 10, 11 are the Upper Cretaceous shaly deposits that we can observe in the syncline. The picture 3 present the Lower Cretaceous deposits with marly deposits: it can be Aptian-Cenomanian deposits. The pictures 4 and 5 show the Lower Cretaceous deposits which are not the massive limestones as in the Rioni foreland basin. Pictures 6 and 7 are the transition from Lower Cretaceous to Upper Cretaceous in the landscape, showing the variation of dipping. Picture 8 show the marine deposits of the Middle Miocene which are the first deposits we observe onto the Upper Cretaceous deposits. The stereonet show that the main compression is in a N/S direction in the area. The Google Earth Screenshot show in an W-E direction, the area concerned by the figure which show the synclines and anticlines well in the landscape.

### c- The Ambrolauri Flexural Basin

Cenozoic deposits are unconformably deposited onto the Mesozoic deposits. This flexural basin is the eastward continuation of the Rioni foreland basin (Fig. II.1). It is located in a triangular zone between the Georgian block which shows north-verging folds (Fig. II.8, f, Fig. II.12) near Kenashi, and the Greater Caucasus which shows south-verging folds (Fig. II.8, i, j, Fig. II.13) from Ambrolauri to Tsageri. The north and south-verging folds separates the Ambrolauri flexural basin from the Rioni foreland basin Ouest of Tsageri (Tsg in Fig. II.1).

The observations were made in the northern part of the Ambrolauri foreland basin and the Greater Caucasus Southern Slope Zone.

North of Ambrolauri Foreland Basin, the Rioni river forms a gorge that cross-cuts the structures. Steeply south-dipping strata of Cretaceous age can be observed (Fig. II.13). Going to the north, we observed overturned strata steeply north-dipping, marking more intense folding and shortening.

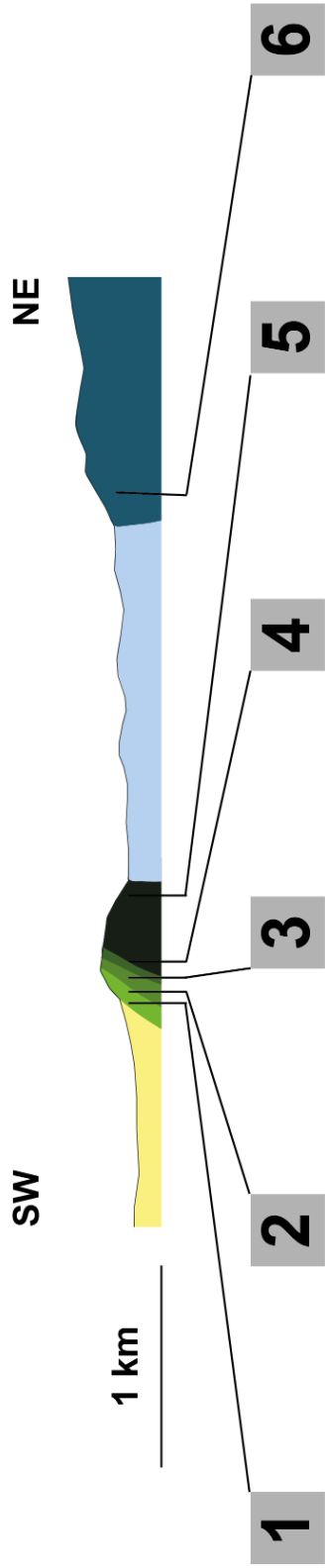
The south-verging pluri-kilometric fold affects the Cenozoic deposits that are observed to the south in Ambrolauri area.

To the north, we can observe the Jurassic deposits, less deformed.

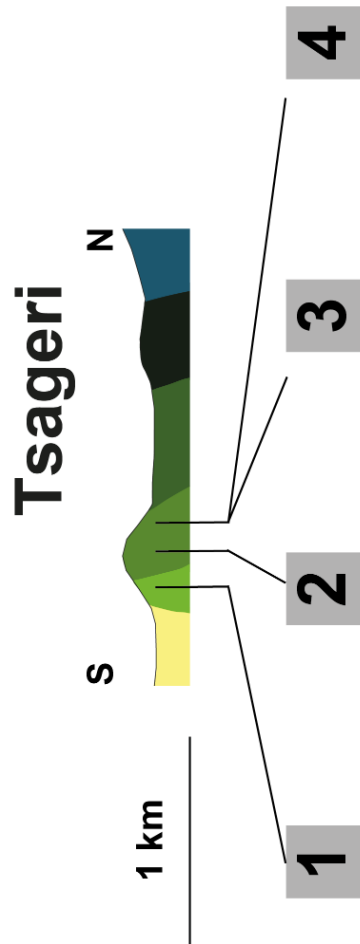
In this frontal part of the fold, the Cretaceous deposits are very different from what we observed in Georgian Block. Here, we have a condensed section of deeper deposits (Fig. II.8, i, j, Fig. II.13). The thickness is about 300m thick for the whole Cretaceous sequence, while in the Georgian Block, the sequence can reach more than 1500m south of the Ambrolauri foreland basin. The Jurassic deposits do not present major differences with the observations in the Georgian Block.

The lithologies are the lithologies used to be described in the Southern Slope Zone of the Greater Caucasus (Adamia *et al.*, 1981, 2011b,a).

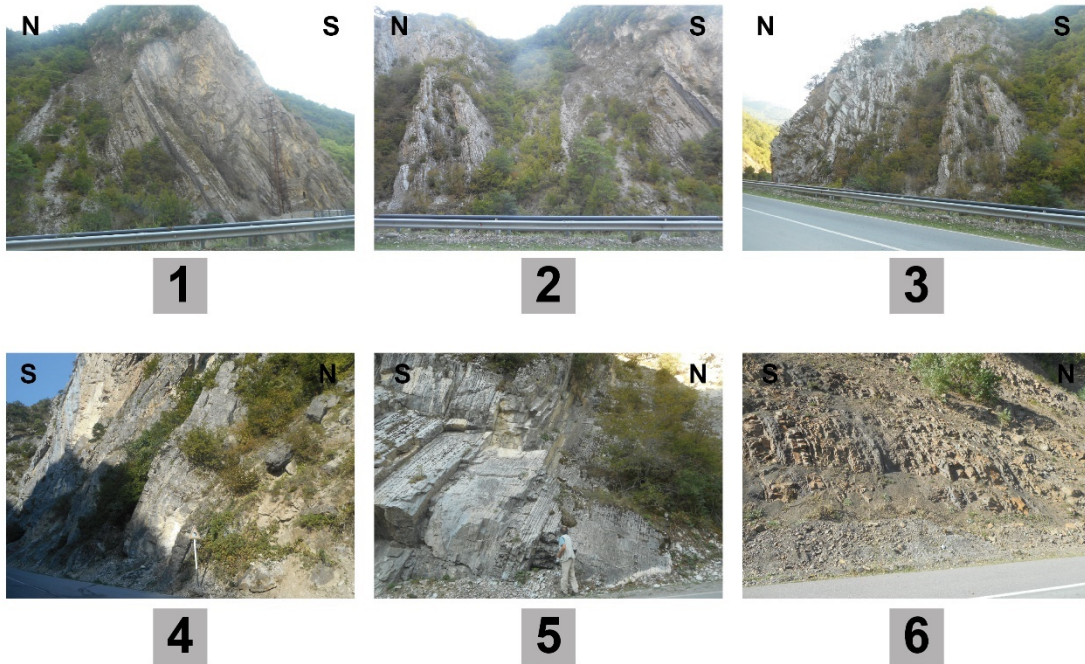
# Ambrolauri



# Ambrolauri - Tsageri



## Ambrolauri



## Tsageri

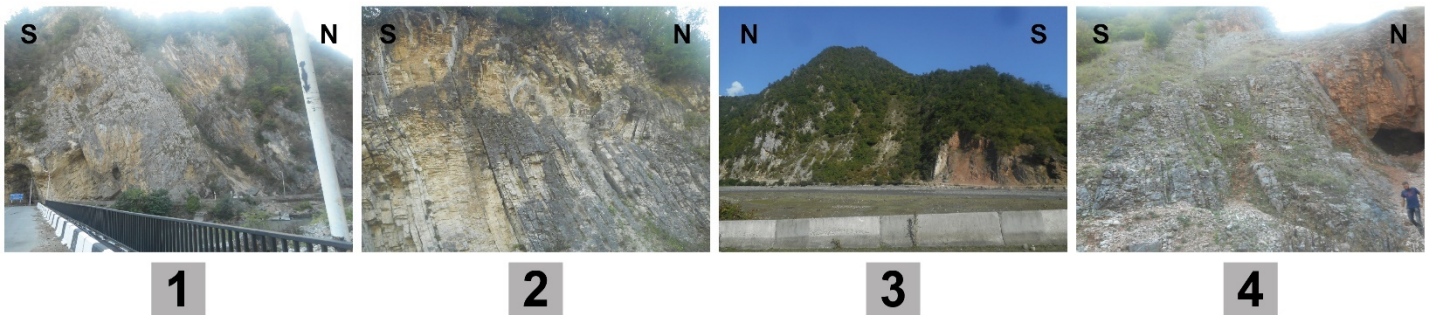


Figure II.13: Cross sections of the northern Ambrolauri area with the frontal GC deformation. The first one is situated at “Amb” on the Fig. II.1, and the second “Tg” on Fig.1. Both cross sections are associated with the pictures along the transects. The picture 1 of Ambrolauri show the Upper Cretaceous deposits. The picture 2 and 3 are the Senonian to Lower Cretaceous deposits. The picture 4 and 5 are the Lower Cretaceous deposits and the point 6 is the Bathonian deposits. The picture 1 of Tsageri is the Upper Cretaceous deposits, the 2, 3 and 4 are the Senonian deposits, which present internal geometries related to their formation. The reddish deposits are the Turonian deposit. The stereonet concerns the bedding in the Mesozoic of both areas together and show a N/S to NE/SW direction for the frontal anticline of the GC. The colors correspond to the ages.

d- Thickness variations along the Georgian Block transect

We compare the stratigraphy along the eastern transect based on the observations (fig 14).

In the Georgian Block we observed some local thickness variations (previous section) along the structures, especially at the frontal part of the anticlines. We also observed some larger scale variations along the transect when we take in account the different structures.

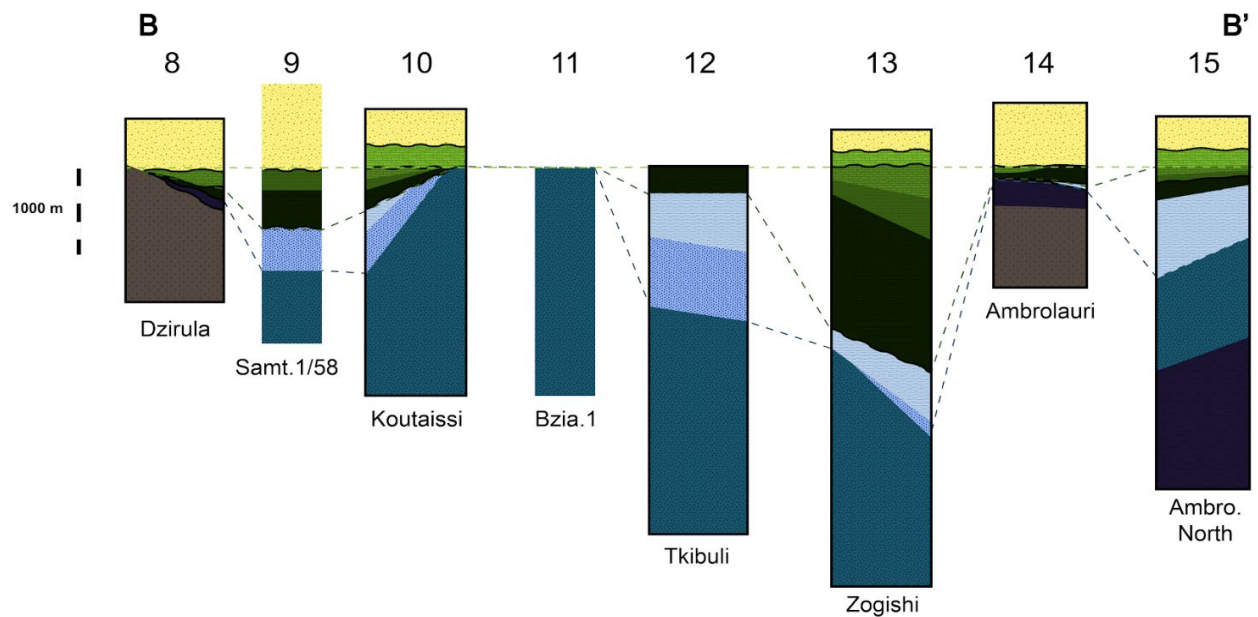
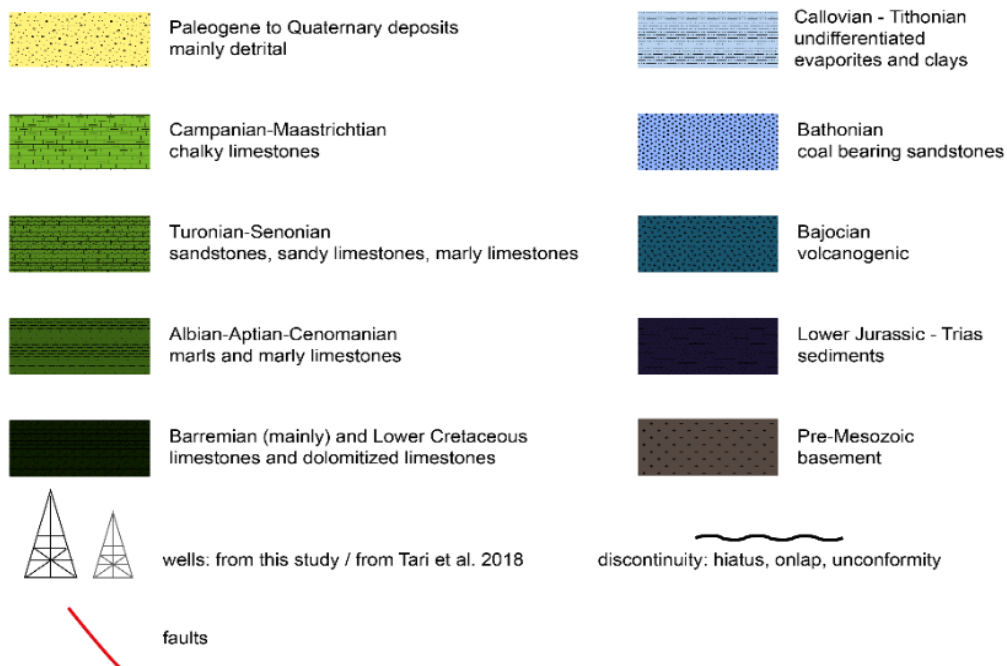


Figure II.14: Stratigraphic log for the western section (BB', see Fig. II.1). Same legend as Figure 2. The thinner log are the ones constrained by wells data (Samtredia 1/58 at point 9, Bziauri 1 at point 11). The thicker ones are constrained by field data.



Basement rocks and pre-Mesozoic deposits can be observed in the Dzirula Massif (Fig. II.9). The Cretaceous and Lower Jurassic deposits are deposited on the basement and show increasing thickness towards the north in the Georgian Block. The transition between the Georgian Block, the Ambrolauri Foreland Basin and the Greater Caucasus Southern Slope Zone is marked by the low thickness of Mesozoic sediments in the Ambrolauri Foreland Basin. The thickness increases to the south in the Georgian Block and to the north into the Greater Caucasus Southern Slope Zone.

The maps (Abesadze *et al.*, 2004) and the seismic lines that we analysed (SOG-03\_09, SOG-19\_09, SOG-23\_09) (Fig. II.9) show an increasing of the Mesozoic deposits thickness by tilting of normal faults northward from the Dzirula Massif. We do not have any information concerning the ages of the deposits observed on seismic lines, but we can correlate them with Mesozoic deposits observed on the field (with the stratigraphy described in Fig. II.2) and with the map (Abesadze *et al.*, 2004).

Lower Jurassic and Aalenian deposits are described on the map in the Ambrolauri Foreland basin, below the Cenozoic deposits.

According to the map (Abesadze *et al.*, 2004) and wells (Bziauri1) (Fig. II.14), the thickness of Bajocian deposits increases to the north of the Dzirula massif (from 0 m on Dzirula and up to 2500 m at locality 11). However these deposits are absent in the Ambrolauri area where the Lower Jurassic deposits are observed, and an unconformity of the Upper Jurassic and the Lower Cretaceous is mapped (Abesadze *et al.*, 2004) (Fig. II.14, location Ambrolauri).

Bathonian deposits follow the same tendency, with a maximum of thickness in the southern Georgian Block at point 12 (Fig. II.10, 11 and 14)

Middle Jurassic Bajocian and Bathonian deposits are observed in the Greater Caucasus Southern Slope Zone (locality 15), but these are not observed in the Ambrolauri Foreland Basin (locality 14). These deposits are thicker in the Greater Caucasus Southern Slope Zone than in the northern Georgian Block (locality 13). However, compared to point 12, they are thinner.

Post-Bathonian deposits described as Upper Jurassic in the wells are also thicker at point 12 and 15.

Well data (locality 9), map (Abesadze *et al.*, 2004) and field observations show that Lower Cretaceous deposits are also thicker directly north of the Dzirula massif, and their thickness continues to increase until the reaching a maximum at locality 13 (more than 1500m thick).

Lower Cretaceous and Cenomanian deposits are thicker in the Georgian Block, especially at point 13.

The Upper Cretaceous deposits are thinner in the Ambrolauri Foreland Basin (locality 14) than in the Georgian Block and the Greater Caucasus Southern Slope Zone. Their thickness is different between the Georgian Block and the Greater Caucasus Southern Slope Zone (localities 13 and 15). The deposits are thicker at the locality 13, but with deposits typical of shallower water environments (Fig. II.8, f compared to Fig. II.8, i and j).

#### IV- Tectonostratigraphic interpretations

Mesozoic tectonostratigraphic units allow us to interpret the basins geometry before the Cenozoic deformations and associated deposits.

We propose to compare the Mesozoic deposits and their structures along the Eastern Cross-section and compare it to the Mesozoic deposits of other tectonostratigraphic units.

##### 1. The Georgian Block

Along the Eastern Cross Section, we highlighted thickness variations in two different cases: outcrop-scale variations which create some local unconformities, and km-scale variations visible along the transect.

Global thickness variations highlight a zone of subsidence during the Jurassic and Cretaceous between the Dzirula Massif (locality 8) and the Ambrolauri Foreland Basin (locality 14). The northern Dzirula Massif structure suggests that this area was a hemigraben. The normal faults observed on the map affect the Mesozoic deposits and we propose that the Georgian Block was bordered to the north and south by normal faults, which separated it from the Dzirula Massif and the Ambrolauri Foreland Basin. Delimited by major normal faults, the Georgian Block thus forms a graben. The lithologies observed are not consistent with a rapidly subsiding basin, but rather with a moderately subsiding rift filled with deltaic and carbonaceous formations such as observed in Cretaceous deposits.

Local thickness variations seem related to normal fault activity. Near the boundaries of the Georgian Block, as well as in its central part, these variations are typical of tilted block sequences, with a deepening near the fault and shallower and thinner deposits away from the fault.

Regarding the local variations and the normal faults of the map (Abesadze *et al.*, 2004), we therefore highlight a horst and graben structure inside the Georgian Block (Fig. II.15).

## 2. The Ambrolauri Flexural Basin

Considering km-scale thickness variations, the Ambrolauri FB show very thin, or absent deposits during the Mesozoic (observations of Jurassic deposits beneath the Cenozoic cover on the map of Abesadze *et al.*, (2004) while the Georgian Block to the south, and the Greater Caucasus Southern Slope Zone to the north recorded sedimentation (Fig. II.14). The Greater Caucasus Southern Slope Zone was the major rift basin of the Greater Caucasus and shows deeper facies lithologies linked to a slope environment, compared to the southern area of the Ambrolauri FB which constituted a delta. We thus interpret that the Ambrolauri FB was a horst during the Mesozoic.

We cannot make any stratigraphic distinction during the Jurassic between the northern and the southern units. During the Jurassic both basins (Georgian Block and Greater Caucasus Southern Slope Zone) show extensional tectonics with similar deposits facies and geometries.

During the Lower-Middle Cretaceous, the northern Georgian Block records thicker deposits than in the Southern Slope Zone. The facies show shallower but more energetic deposition environments. We interpret this to be linked to the normal fault activity south of the Ambrolauri high.

## 3. Across the Rioni FB

Global thickness variations along the transect highlight a global deepening of depositional environments towards the north from point 1 to point 4, with a local thickening near Tsaishi, during the Upper and Middle Jurassic. The uniform lithology observed along the transect implies the formation of a single basin during the Jurassic, with normal faults creating some local thickness variations.

During Lower Cretaceous, locality 2, which is located south of the south-verging fold range was still a high topographic level, as during the Upper Jurassic. To the north (points 3 and 3' 3'' and 4), and to the south (point 1 and 2), the deposits are thicker.

Since Albian time, the topographic high seems to be closer to point 6, slightly more to the south from the fold range.

Since local variations affect the Lower Cretaceous and Albo-Cenomanian deposits we can argue that the normal fault activity was important during this time and created, as in the Georgian Block, some fan shapes geometries with thicker deposits near the faults.

Subsidence took place near these places after the Lower Cretaceous, as observed at point 2. The lack of field observations in Lower Cretaceous deposits makes it difficult to localize the normal faults responsible for this subsidence. However, we can reliably place a normal fault at the boundary with the Tsaishi anticline because of the thickness variation between point 2 and points 3.

#### 4. Beneath the Rioni FB

The Mesozoic structure along the Eastern Cross Section (Fig. II.15b) presents two major horst structures. The horsts are located in the Dzirula and the Ambrolauri FB units. These are separated by the Georgian Block graben. The Greater Caucasus Southern Slope Zone and the Main Range are located northward the Ambrolauri horst.

The western cross section, despite the lack of Mesozoic outcrops presents the same particularities (Fig. II.15a): the Mesozoic (especially the Cretaceous) deposits are thickening toward the north. We correlate this with the distancing to the north from the equivalent of the Dzirula horst, which should be located between the north-verging Lesa anticline and the Chaladidi south-verging anticlines (Fig. II.15, a).

The northern part of the western cross section (AA') is however a little bit different from the eastern one (BB'). The Jvari area seems to continue the deepening of the basin toward the north, while, in the eastern cross section, the Ambrolauri horst bounded the Georgian Block basin, and separates it from the Greater Caucasus.



## 5. The Jvari area

Near Jvari, local thickness variations are consistent with a normal fault delineating a basin deepening towards the north. The lack of observations between point 6 and 7 makes the correlation difficult the inference of a possible horst structure in between impossible.

However, the global basin deepening towards the north beneath the Rioni FB during the Mesozoic, and the similarities with the facies and local structures observed at point 4 are consistent with the simple continuity of the rift-related delta observed beneath Rioni FB.

Based on our observations, the stratigraphy of the western segment (locality 7) (Fig. II.3, e, Fig. II.7) is different from the one observed in the central part (localities 14 to 15) (Fig. II.8, l, j, Fig. II.14). We did not recognize the usual Southern Slope Zone stratigraphy, and no deepening to the north is observed in the Cretaceous deposits. The facies are similar to the ones observed in the Georgian Block (localities 3-6 and 9-13).

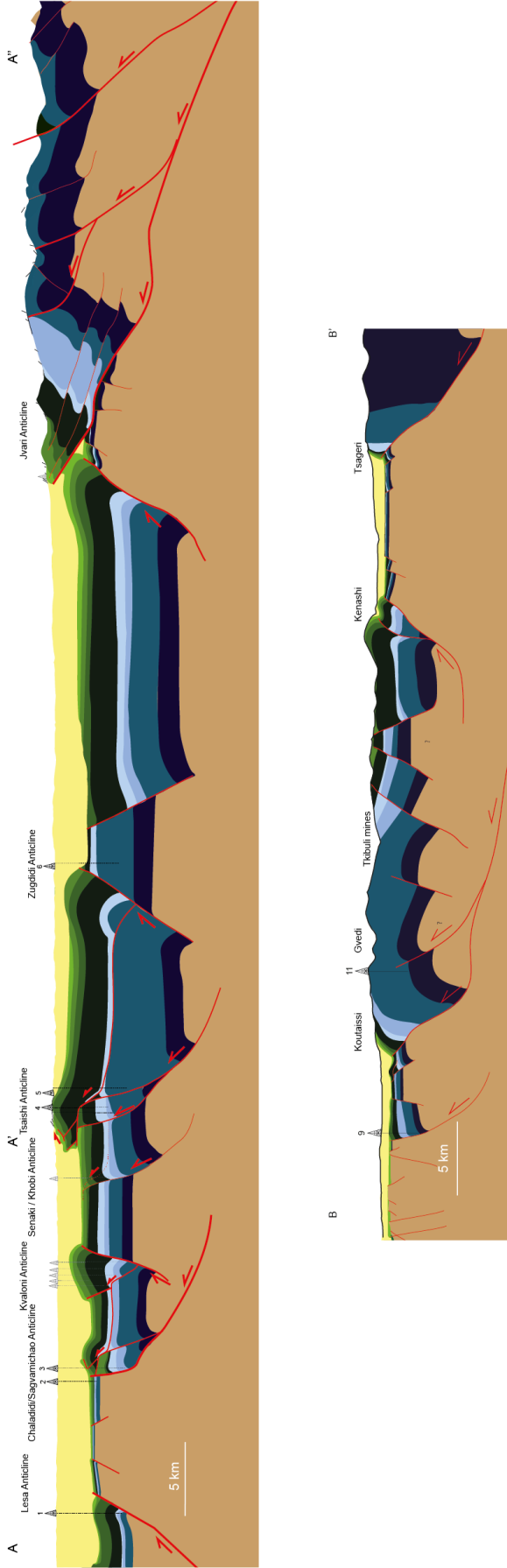


Figure II.15: Geologic cross-sections based on field, well and seismic data (see Fig. II.1 for locations). Same legend as figure 2. The main difference between both cross sections is that the western cross section relates to thick and thin-skinned tectonic, while the central cross section illustrates only thick-skinned tectonic deformations (except at the front near Koutaissi in a small-scale fold/thrust)

## V- Conclusion

Regarding the data compiled from field observations, old seismic lines, and wells, we propose that the Georgian Block continues beneath the Rioni FB Cenozoic deposits. The Georgian Block was a delta which rifted since the Jurassic until the Campanian. The Dzirula Massif and the Ambrolauri FB were horsts. The Greater Caucasus rifted during the same time and was characterized by basinal facies. During Mesozoic, a magmatic arc developed in the Adjara-Trialeti (Gamkrelidze 1986; Banks *et al.*, 1998; Adamia *et al.*, 2015).

Thanks to the two cross-sections we built and presented above (Fig. II.15) we attempt to balance the deposits thicknesses and deformation and can propose a reconstruction of the basin evolution during the Mesozoic. We attempt to reconstruct the system geometry for the upper Cretaceous and Upper Jurassic periods along the western (A-A'-A'': Fig. II.16) and eastern (B-B': Fig. II.17) sections.

### 1. Reconstitution from the Lower Jurassic

The Cenozoic deposits are made of detrital deposits during the collision (Fig. II.16, 17). During the Late Cretaceous (Fig. II.16, a, Fig. II.17, a), the environment is calm and shallow marine: the platform constituted of shaly limestones with some marls forms onto the whole pile of sediments. Some thickness variations could be related to the compensation of the paleotopography.

During the Turonian to Campanian the rifting and subsidence near the normal faults created growth-strata in the sediments.

The deltaic environment affects only the Georgian Block basin, or the beginning of the Greater Caucasus Southern Slope Zone on the western cross section in the Jvari area. Towards the north, in the Greater Caucasus, the Turonian-Campanian are made of flysch and testify to basinal rifting.

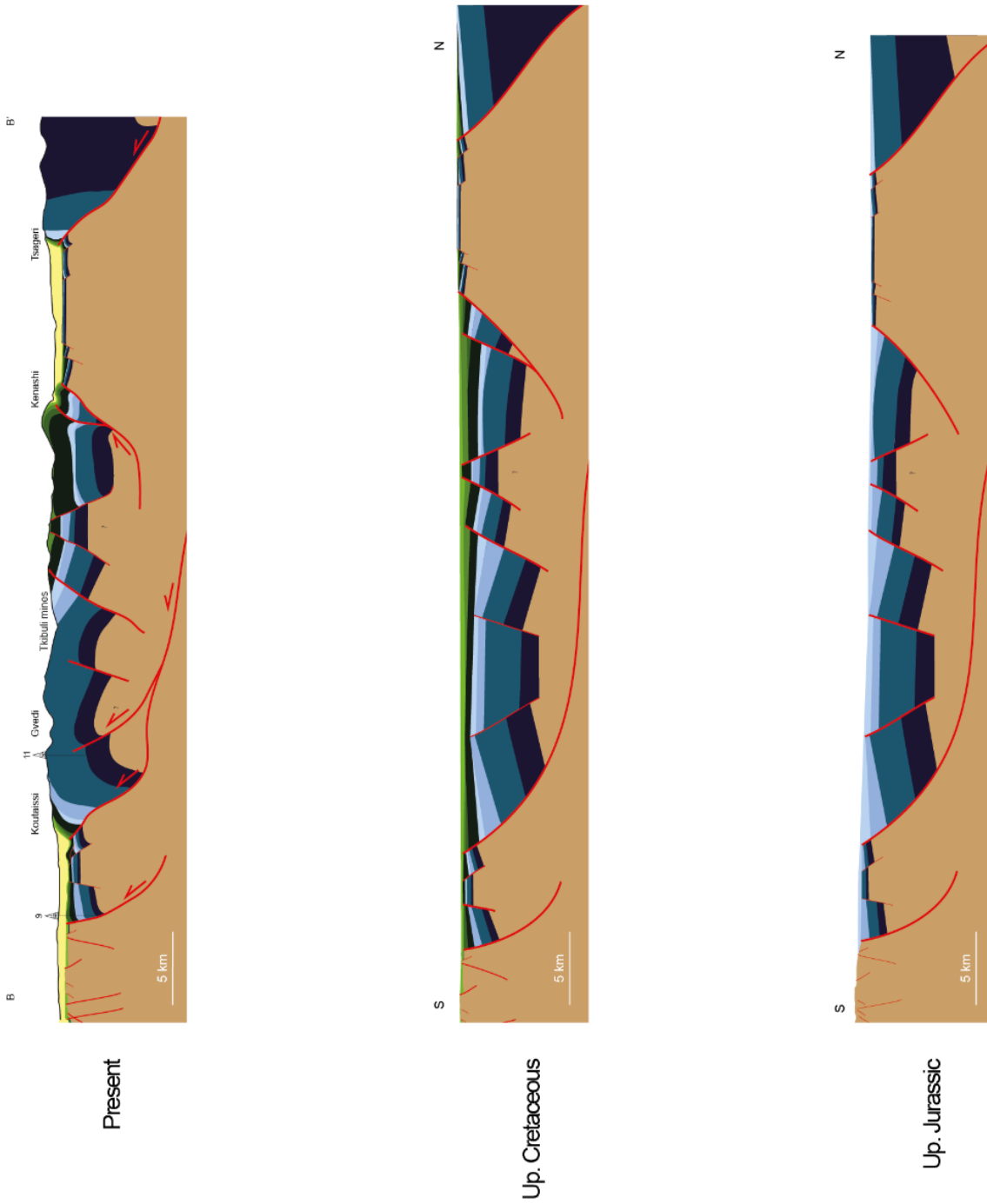


Figure II.16: Reconstitution of the Western Cross Section. We highlight here the role of the normal faults' inversions in the shortening of the Georgian Block.

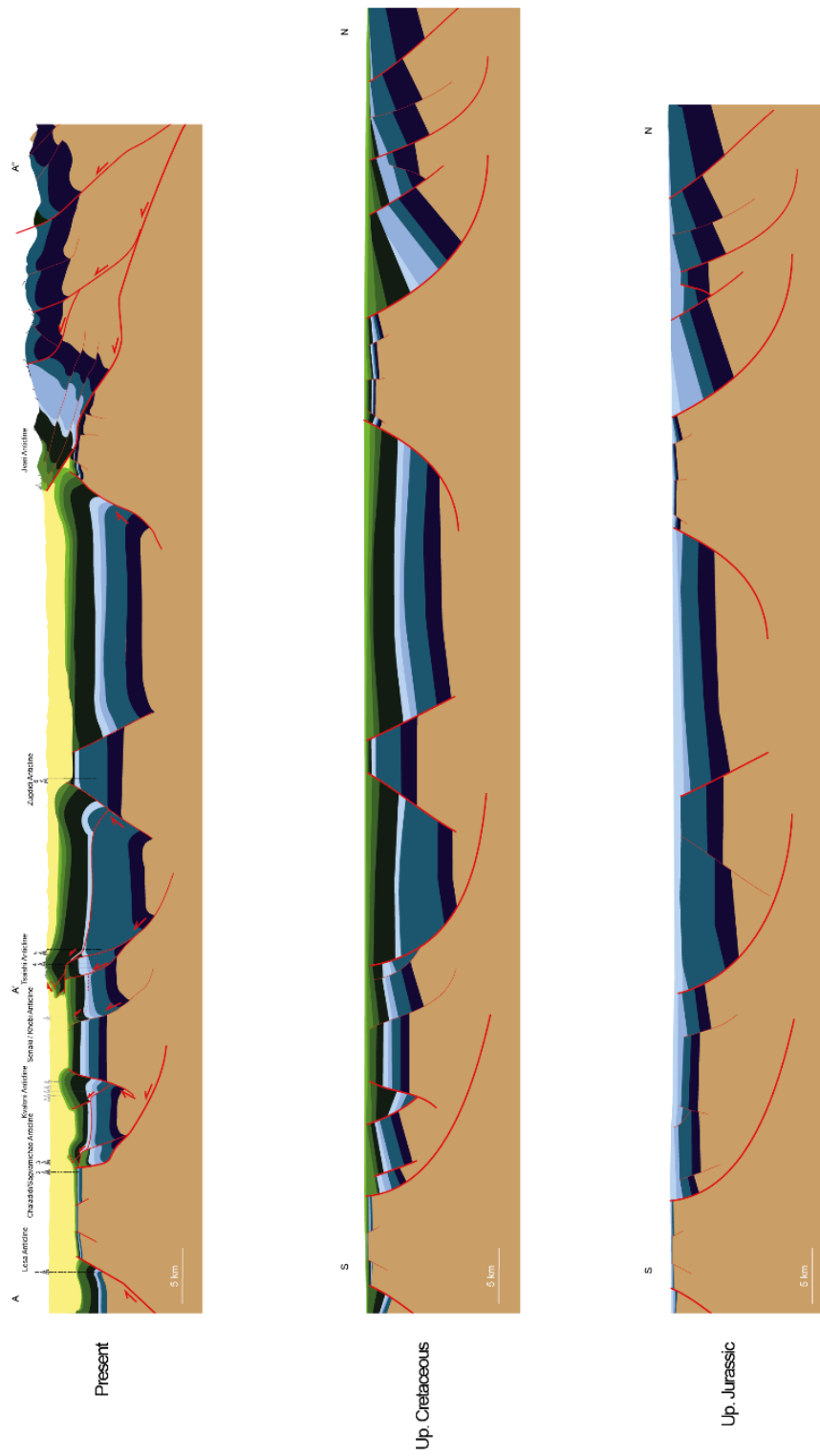


Figure II.17: Reconstitution of the Eastern Cross Section. We can observe that the normal faults are also inverted, but the role of the Upper Jurassic level in the style of deformation makes the structure different from the one presented in Fig. II.16.

During the Albo-Cenomanian, normal faulting south of the Ambrolauri FB seems to deform the area. The growth strata made of fan-shape figures witness to onlap testify of local subsidence due to the fault geometry. The local variations of thickness together with the location and the size of the growth strata tends to prove that the subsidence is important near the faults and is not widespread in the area. The strong fault-dependance of the deposits could be related to the fault geometry. The more marly, more fine-grained deposits than during Barremian depict a deeper or quieter environment.

During the Lower Cretaceous (mostly Barremian) (Fig. II.16, b, Fig. II.17, b), extensional tectonics is reactivated. Differences between the Greater Caucasus Main Range, the Greater Caucasus Southern Slope Zone, the Jvari area and the Georgian Block are observed since this time.

In the Greater Caucasus Southern Slope Zone the basin depth increases from the Ambrolauri FB toward the north into the GC. Thus, the main rifting seems to take place 30 km to the north from the Ambrolauri horst where the basinal flysch deposits are observed.

During the Upper Jurassic, the rifting is not active anymore. The deposits are lagunal or shallow marine deposits in the Georgian Block (Khain 2007; Guo *et al.*, 2011).

Some places are subject of erosion, in order to produce the material which constitutes the Upper Jurassic deposits.

The area was subject of extensional tectonics during Jurassic. The Dzirula Massif and the Ambrolauri FB were already horsts which separated some grabens (Fig. II.16, c, Fig. II.17, c).

Lower Jurassic basinal deposits are observed north of the Ambrolauri FB, as well as north of the Jvari area. We cannot constrain the position of the Georgian Block at this time.

However, Bajocian and Bathonian deposits are clearly deeper in the Georgian Block than in the horsts of Dzirula and Ambrolauri. These deposits are volcanoclastic and more detrital than during the early Jurassic. These thickness variations allow us to interpret the Georgian Block as a deltaic rift, which developed between the Dzirula and the Ambrolauri horsts. The same interpretation can be drawn for the Georgian Block beneath the Rioni foreland (Fig. II.16, b).

## 2. Role of the inherited structures during syn-collisional deformations

Structurally, we observe that the location of normal faults which limit the Mesozoic basins seems to control the localization of the compressional deformation (folding and thrusting) during the Cenozoic inversion, hence advocating for a thick-skin tectonic style.

However, we can relate that in the Rioni FB the sedimentary cover is affected also by thin-skinned tectonics (Adamia et al., 2002, Banks et al., 1997, Morariu et Nouhal 2009, Gamkrelidze et al., 1991, Tari et al., 2018, Trexler et al., 2020).

Regarding the location of the Tsaishi Anticline, which correlates with the presence of a normal fault highlighted by the thickness variations along the anticline, we propose that the presence of normal faults can control also thin-skinned deformations (chap 3). Gamkrelidze (1991), and Trexler et al., (2020) show that there is a problem with the accommodation of the structures if the deformation is accommodated by thin-skinned tectonic only.

## 3. Main tectonic events

- During the Bajocian the high topographic levels in Dzirula as well as in the Ambrolauri FB are already separated by a basin made of volcano-related.
- During the Bathonian, the deltaic rifting is more contained in the Georgian Block and near the horst structures (Dzirula and Ambrolauri FB).
- During the Upper Jurassic, the main reference is the study of Guo *et al.*, (2011). They show the global repartition of the deposits, and their facies variations. We can already observe that the deposits in the Georgian Block/Transcaucasus are different from the ones in the Greater Caucasus and the Black Sea where carbonates take place. We add some details concerning the location of the closed evaporitic basin. The location of the basin is important because it can control the location of the deposits which can constitute the decollement levels during the Cenozoic compressions.
- During the Barremian, the difference between the Greater Caucasus in one hand, and in the Jvari and the Georgian Block in the other hand lies in the deltaic type of basinal rifting in the Georgian Block and Jvari, while in the Greater Caucasus Southern Slope Zone the condensed deposits testify a deeper but with less subsidence environment. In the GC, the flysch deposits testify the main rifting of the GC.
- Then, during Albian, Aptian and Cenomanian, the Greater Caucasus continues its rifting, while the Georgian Block and Jvari area are concerned by localised subsidence controlled by the normal faults.

- During Turonian-Campanian, the rifting is more deltaic and calm. Erosion took place in the high topographic levels, and the deposits accumulate in the slopes.
- During the Late Upper Cretaceous, the area is calm, as a platform, which describes usually the Georgian Block.
- During Cenozoic, the area is compressed, and the shortening occurs onto the normal faults, as well as with decollement levels beneath the Rioni foreland basin.

We evidence the presence of a graben in the Rioni basin and in the Georgian block, bordered by two horsts to the north and the south (in the Ambrolauri area and the Dzirula Massif). We propose new interpretations about the timing and structural evolution of this area during the Mesozoic, and a new tectonic reconstitution, which takes into account the newly observed Mesozoic extension evidenced in the northern Transcaucasus area.

This highlights the importance of the inherited structures on the style of deformation occurring during later collision stages.



*Chapter 3: Style and timing of collision-related deformations in the flexural basins along the southern Greater Caucasus*

## I. Introduction

Along a N-S transect, from the Greater Caucasus to Arabia two suture zones have been described. In the Lesser Caucasus range (LC in Fig. III. 1) is located the Sevan Akera suture zone (prolongation of the Izmir-Ankara-Erzincan one's) resulting from the Latest Cretaceous-Early Eocene collision between the Eurasian continent to the north and the Taurides-Anatolides-South-Armenian micro-continent (TASAM in Fig. III.1) to the south. The Zagros range results from the collision further to the south of the Arabian continent and the TASAM (Fig. III. 1) during the Neogene. This structural pattern including Cenozoic major sutures zone witness for two collisions and for a history of 65 million year of shortening coupled with local possible extensional deformations.

The global convergence of the continents in the area is still active: the combination of the successive collisions and the indenting of the Arabian plate involves major thrusting and strike-slips in the Caucasian region. The deformations and the timing in the different areas which are parts of the Caucasus tectonic frame in the GC are not well constrained and results in disparities along the GC. The foreland basins situated north and south of the GC offer the possibility to constrain the timing of the compression in the area.

The first collisional event is well constrained along the suture of the LC where late Middle Eocene deposits unconformably lay over tilted obducted ophiolites and folded Cretaceous and Palaeocene deposits which highlights the timing of the collision (Sosson *et al.*, 2010, 2016; Rolland *et al.*, 2012; Hässig *et al.*, 2015). Similarly, in the Internal zone toward the north (Fig. III. 1), the timing of the first evidence of compression linked to the collision is contemporaneous to the timing observed in the LC: the BS is during Palaeocene (Nikishin *et al.*, 2015b,a; Sheremet *et al.*, 2016; Korniyenko-Sheremet *et al.*, 2021), in the Pontides the occurrence is observed during Early Eocene (Şengör 2003; Lefebvre *et al.*, 2013; Robertson *et al.*, 2013; Espurt *et al.*, 2014; Hippolyte *et al.*, 2015; Okay & Nikishin 2015). However, the timing is not the same all along the GC basins: in its western part, a Late Eocene age of the deformations related to collision is evidenced (Saintot & Angelier 2002; Saintot *et al.*, 2006), while in its central part, in Georgia, the timing is still matter of debate. The evidence is not directly observed nor in the Southern Frontal Greater Caucasus nor in the foreland basins where the timing is poorly constrained during the Paleogene and results in an interpretation

of a collision during the Neogene. The oldest occurrence could be during Oligocene (Vincent *et al.*, 2007; Vincent, Stephen J *et al.*, 2016) or Late Eocene (Mosar *et al.*, 2010) when the topography of the mountain range was already growing. This implies an earlier timing of compression resulting in a high topography during Oligocene than if we consider only the Neogene stage of collision. Toward the east near the Kura foreland basin, the oldest occurrence of compression is also debated. There, the exact age of some olistostrome/wildflysch deposits remains unclear because its actual formation process is not well understood (flexural or rifted basin). Further to the east, the Southern Caspian Sea presents a major unconformity at the boundary Cretaceous-Palaeocene and is interpreted to be related to the inversion of the southern Caspian margin (Brunet *et al.*, 2007; Shahidi *et al.*, 2011). The timing of this second compression event in the internal zone is more homogeneous than for the first one and is accepted as a succession of event during the Neogene: from west to east in the BS area, in the Pontides range, along the GC in the flexural basins, the growth strata and the unconformities are Upper Miocene in age. The growth strata south of the GC are well described in the Rioni and Kura foreland basins (Banks *et al.*, 1998; Alania *et al.*, 2009, 2017; Forte *et al.*, 2010, 2013, 2015). The compression continues until the present day in the whole Caucasus area (Philip *et al.*, 1989; Mosar *et al.*, 2010; Tibaldi *et al.*, 2017b; Sokhadze *et al.*, 2018; Trexler *et al.*, 2020).

The heterogeneous timing along the southern GC during the first collision is problematic. Because of the lack of clear identification of the onset of collision in the sedimentological records, the heterogeneity cannot be related neither to a methodical bias, neither to a local or even regional geodynamic mechanism.

In order to better constrain the timing and the style of deformation along the Southern GC, we propose to focus from west to east onto the Rioni-Ambrolauri, and the Kura-Kartli flexural basins. These basins are the product of the inversion of the GC during both collision events as well as of the AT during the second collision event. The identification of growth strata onto the main deformation fronts offers the opportunity to better constrain the timing of the compression. This task is carried on through a thorough mapping and identification of the pre-, syn- and post-compressional deposition sequences. Moreover, the style of the growth strata or the structure of the flysch deposits can be related to the style of deformation style at depth (See Chap. 1), and to the balance between the deformation and the sedimentation rate (see Chapter 1).

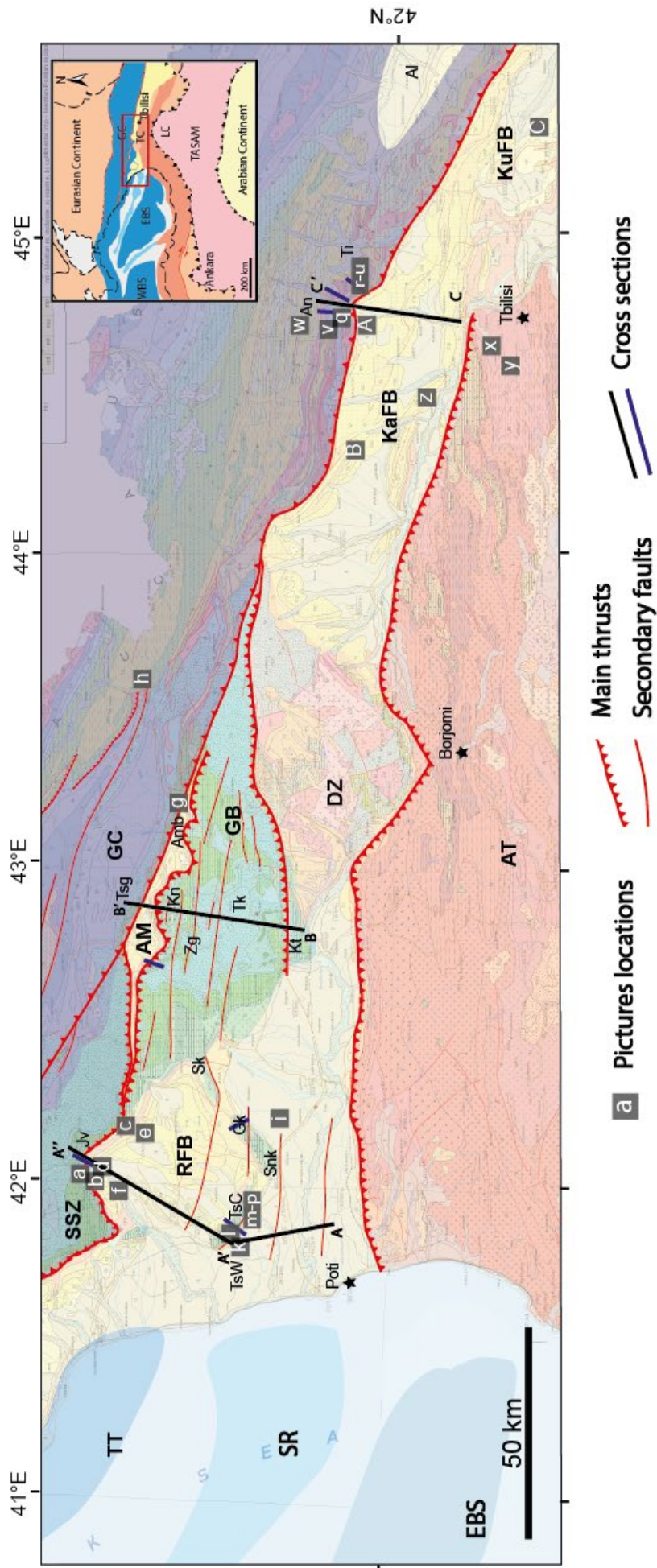


Figure III.1: Tectonic map of the Rioni and the Kura foreland basins and the neighbouring areas. Geological map is from Abesadze et al., 2004 TT: Tuasee Though, SR: Shatsky Ridge, EBS: Eastern Black Sea basin, SSZ: Southern Slope Zone of the Greater Caucasus basin. GB: Georgian block, AM: Amrbolauri flexural basin RFB: Rioni foreland basin, DZ: Dzirula massif, AT: Adjara-Trialeti fold-and-thrusts belt, KaFB: Kura foreland basin. Jv: Jvari, Ts: Tsaishi, Gk: Gakhomela, Tk: Tkibuli, Zg: Zogishi-Kenashi, An: Ananauri, Ar: Arguni, Ti: Tianeti, Al: Alazni piggy-back basin

## II. Geological setting

### 1. The foreland basins

The Greater Caucasus (GC) is elongated in a WNW-ESE trend (Fig. III. 1). Its southern border is constituted of the Southern Slope zone and the “Main Range” of the basin (Adamia *et al.*, 1977, 2011b,a). These deposits are deformed by south verging folds and thrusts (See the southern border of the GC in Fig. III. 1) all along the mountain range. The Adjara-Trialeti fold-and-thrusts belt (AT) (Fig. III. 1) is situated south of the foreland basins in a WSW-ENE trend from Poti to Tbilisi. The GC and the AT limit respectively to the north and the south the foreland basins from west to east: Rioni (RFB) and its sub-basin Ambrolauri (AM) (Fig. III. 1), and the Kura (KuFB) and its western sub-basin Kartli (KaFB) (Fig. III. 1). Those two foreland basins are separated by the Dzirula Massif (Dz). Westward, the Cenozoic deposits extend into the Black Sea, and eastward into the Caspian Sea. The DM is a massif where the Palaeozoic basement which results from the Variscan orogeny (Rolland *et al.*, 2016) crops out.

We will separate the observations in two parts: the RFB, the AM, and the KuFB and KaFB (Fig. III. 1).

The descriptions of the deposits in the foreland basins (Fig. III. 2) are from (Adamia *et al.*, 2010, 2011a) and (Tari *et al.*, 2018). The Palaeocene and Eocene deposits are described in the “Georgian Massif” and not specifically in the foreland basins in (Adamia *et al.*, 2010, 2011a). We propose to include the Palaeocene and the Eocene deposits in the foreland basins logs, as the Oligocene-Pleistocene deposits which are described separately between the Rioni and the Kura foreland basins. The aim of the figure is to summarize the thickness variations of the deposits with their ages.

### 2. Rioni and Ambrolauri flexural basins

The structure in western Georgia of the RFB (chap. 2) presents some southverging folds. To the north it presents a major fold near Jvari (Jv. In Fig. III. 1). The south-verging shortening propagates from the SSZ of the GC into the Rioni foreland basin situated southward (Fig. III. 1 and chapter 2). Further to the East, the northern Rioni foreland basin continues in the Ambrolauri. The Ambrolauri flexural basin is used to be considered as a part of the former Rioni basin but was then uplifted in the area (see the western continuation of the AM foreland

basin in Fig. III.1). The particularity of the Ambrolauri flexural basin is that it is situated in a shape of triangular zone: the northern part is constituted of a major south-verging fold which thrusts the GC deposits in the Ambrolauri flexural basin. To the south, the transportation of the deposits is northward. The north-verging folds displace the so-called “Georgian Block” deposits in the Ambrolauri flexural basin (see chapter 2).

In the Rioni and Ambrolauri basins, presented in Fig. III.2, the Palaeocene deposits begin with the Danian deposits which are the continuity of the Maastrichtian chalky limestones. The Danian deposits are more sandy-silty-marly white limestones which evolves in marls during the Paleocene. The maximal thickness is about 50m. The Thanetian-Ypresian deposits are about 100-250m of sandstones, siltstones and claystones (terrigenous turbidites) (100 to 250m thick). The Eocene deposits from Lutetian described as 700-1800m thick volcanogenic deposits (Adamia *et al.*, 2011a) have not been observed in the Rioni foreland basin. We have observed only the detrital, sandy to argillite deposits (see Observations section below) usually described as terrigenous carbonate turbidites up to 600m thick. We thus use this observation in the stratigraphic log. of the Fig. III. 2. The Oligocene – Lower Miocene is known to be the “Maykopian formation” which is in the area made of euxinic detrital to evaporitic facies constituted of dark argillite and gritstones, clays with some septarian nodules and gypsum (selenite) (low amount from our observations) from 100 to 500m thick, and evolves during the Lower Miocene, still in euxinic environment in gritstones and marls to conglomerates and sandstones, and again in gritstones and marls. The thickness of the Lower Miocene deposits is about 500m. The Middle Miocene is constituted of shallow marine detrital deposits as gritstones, marls and argillites which are then unconformably covered by conglomerates, marls and sandy limestones and then again gritstones and argillites still dated as Middle Miocene. The whole thickness of the Middle Miocene is about 400-600m. The Upper Miocene is separated in the “Sarmatian” and the “Meotian” and “Pontian”, called “Meotis Pontian” stratigraphic periods defined in Georgia (Messinian in the general stratigraphic chart). The Upper Miocene Sarmatian deposits are shallow marine detrital deposits constituted of conglomerates, olistostrome and gritstones. The thickness reaches about 1000m. The Meotis Pontian marine deposits cover unconformably the Sarmatian deposits with detrital deposits from conglomerates to argillites of 400 to 1500m thick. The Plio-Pleistocene deposits are marine and river-terraces deposits of 250 to 350m.

### 3. Kura and Kartli foreland basins

The continuity of the northward deformations disappears to the east of the Ambrolauri area, because the Ambrolauri flexural basin is covered by the overthrust GB basin (Fig. III.1). However, the south-verging deformation from the GC continues to the east until the Caspian Sea. East of the Dzirula massif, the south verging GC structures border the northern Kartli foreland basin (KaFB in Fig. III.1). This foreland basin is the western continuation of the Kura foreland basin (KuFB in Fig. III.1). Its particularity is that, unlike the eastern part, east of Tbilisi, the Kartli foreland basin is limited to the south by the Adjara-Trialeti folded belt (AT in Fig. III. 1) which ends near Tbilisi (see the location of KaFB between the GC and AT and the fronts of deformations in Fig. III.1). This creates also a triangular zone in the Kartli basin, which is tightened at the eastern termination of the AT and wider to the west, east of the Dzirula massif. The rest of the Kura foreland basin, east of Tbilisi, is deformed by the continuity of the south-verging folds and thrusts coming from the GC (KuFB in Fig. III.1) until the Azerbaijan border.

The Kura and Kartli foreland basins present different lithologies from the Rioni (and Ambrolauri) during the Paleogene. The Palaeocene deposits still show the same kind of formations during the Danian with marly fine-grained limestone. However, from the Thanetian, the Palaeocene-Eocene deposits are made of carbonate and then terrigenous turbidites. The thickness is from 300 to 550m. The Upper Eocene Priabonian deposits are described as terrigenous turbidites and olistostromes of 200m thick. The Oligocene – Lower Miocene Maykopian series are very similar to those observed in the Rioni foreland basin. These deposits also formed in an euxinic environment and their lithologies are composed of gritstones, siltstones, clays and gypsum, but compared to the Rioni-Ambrolauri basins they have more developed evaporitic facies with more gypsum and evaporites, especially in and south of the Adjara-Trialeti folds-and-thrusts belt. The thickness of the Maykopian series reaches 2000m. The Middle Miocene deposits unconformably cover the Maykopian series. Again, these are nearly the same as in Rioni basin, with shallow marine sandy argillites at the beginning and then a transition to marls and sandstones, conglomerates and gritstones of 600m thick. However, during the Upper Miocene, the Kura and Kartli basin show an evolution in continental deposits while the Rioni foreland basin still presents shallow marine environment deposits. The deposits during Sarmatian are made of 200m of conglomerates

and sandstones and then sandy limestones and argillites. The Meotis-Pontian which can be separated by an unconformity from the Sarmatian, are made of deposits of 2300-3000m thick. The deposits are constituted of lignites-coal bearing sandstones, clays, argillites and conglomerates. Finally, the Pliocene to Pleistocene deposits, cumulated are also continental environment deposits with fluvial, deltaic and lacustrine environment and river terraces of 4450-7250m thick when we add the maximal thickness from (Adamia *et al.*, 2011a).



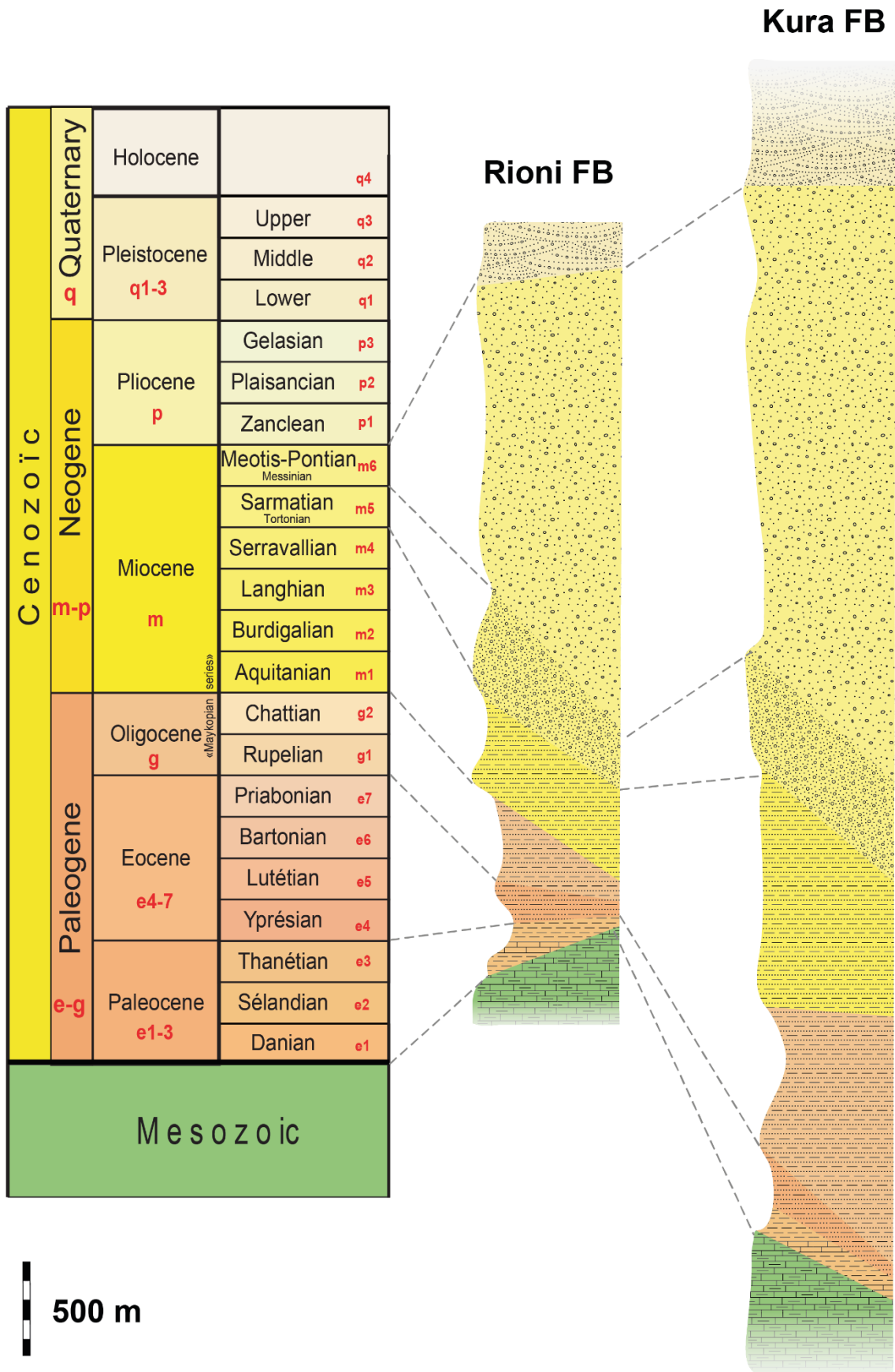


Figure III.2: Stratigraphic log with thickness variations, modified after Adamia et al., 2011, a.

To conclude, the Rioni and the Kura foreland basins evolve in different ways during the Paleogene after the Danian. Although, both show detrital environment, the Rioni foreland basin shows a calmer sedimentation environment than in the Kura foreland basin. The Maykopian series show a more closed environment in the Kura foreland basin with more evaporitic deposits. During the Miocene, the key difference is that the Kura foreland basin evolved to a continental sedimentary system during the Upper Miocene, while the Rioni foreland basin was still in a shallow marine setting (Adamia et al., 2010).

### III. Field observations

Usually, the locations to observe the growth strata or the unconformities related to the compression stages are at the front of the folds and the thrusts and at the back when a piggy-back basin is formed (See chap. 1). We focussed our research on the Paleogene deposits (which were deposited after a quiescent tectonic period during Late Cretaceous) (chapter 2) in order to precisely characterize the stages of compressional tectonics and their ages.

#### 1- Paleogene deposits

Paleogene deposits are observed in the foreland basins along the southern GC (Fig. III. 3, e, f). These deformed deposits display structures linked to the frontal thrusts of the GC (Fig. III. 3).

##### a- Localisation of deformations and growth strata: the structures

From WNW to ESE along the southern slopes of the Greater Caucasus range we observe differences in the style and the intensity of the deformation.

Near Jvari (Jv. In Fig. III. 1), the Southern GC is made of kilometeric scale south-verging anticlines. Even if the folding involves several kilometres of deposits, including the Mesozoic cover and its basement (chap. 2), strain remains rather diffuse and does not display clues of intense localisation (Fig. III. 3, a, c, d).

Further to the east, north of the Ambrolauri FB, the same observation is made: the whole pile of sediment is folded in a large-scale anticline which involves inversion of the deposit at the frontal part (Fig. III.3, g). However, further north on the road of Oni, when the deposits are part of the Main Range basinal flysch, the compression/deformation is more intense (Fig. III. 3, h). We observe the development of ductile fabrics including an axial planar schistosity. The

problem is that no Paleogene neither Neogene deposits are observed in this area to constrain the timing of the deformation.

In the Rioni FB the structures observed in the field are south-verging folds due to the inversion of pre-existing Mesozoic normal faults and thrusting of the Cretaceous deposits along the Upper Jurassic evaporite decollement level (chap.2).

The GB is linked to the thick-skinned inversion of normal faults. The global structure (GB and Rioni) is a bivergent structure bordered by growth strata at the frontal parts observed both north and south.

Finally, to the East, the Kartli and Kura foreland basins (KaFB, KuFB in Fig. III.1) are mainly used to constrain the geometry of Neogene growth strata. However, the study of the frontal part of the Ananauri area (An. in Fig. III.1), situated north of the foreland basin and which is part of the southern GC, presents structures that deform the Upper Cretaceous and the Paleogene deposits.

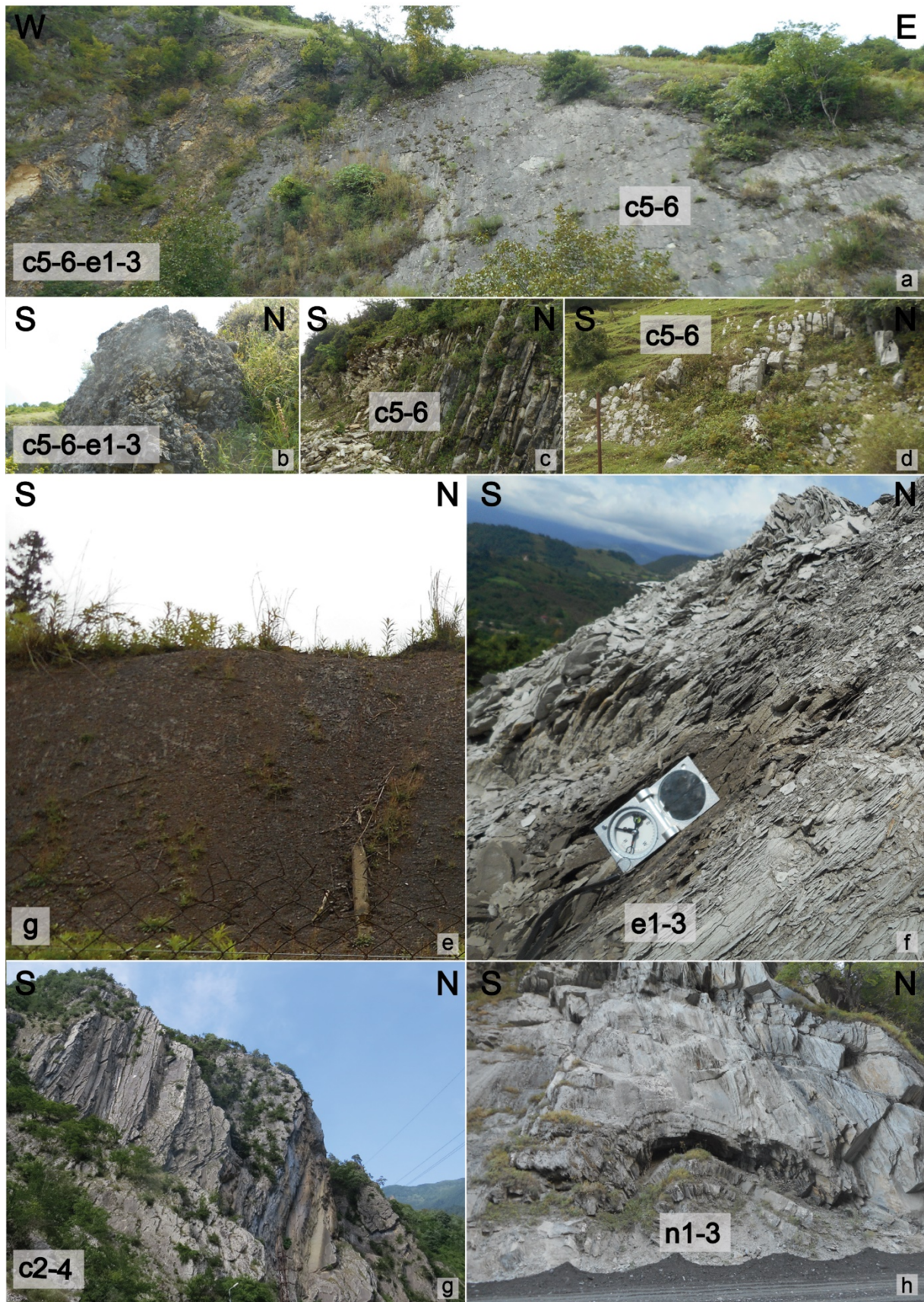


Figure III.3: Pictures of observations mainly in the frontal deformation with the Uppermost part of the Cretaceous in the Jvari area and north of Ambrolauri area, see locations on Fig. III.1.

a: picture of the transition from Upper Cretaceous to Paleogene deposits near Jvari. The Upper Cretaceous deposits are dipping toward the south and the transition to the Paleogene deposits is made of breccias. b: Picture of the deposits of reworked Upper Cretaceous in a breccias. c: Picture of the high angle deposits of Upper Cretaceous East of Jvari d: Picture of the high angle deposits of Upper Cretaceous at Jvari e: Picture of the Oligocene "Maykop" deposits east of Jvari. These deposits are not observed in the area of the picture a-d. f: Picture of the Paleocene marls which follow the deposits observed in a and b. g: Picture of the high angle Lower Cretaceous deposits north of Ambrolauri from the Greater Caucasus slope. h: Picture of the Lower Cretaceous deposits north of Ambrolauri from the Greater Caucasus basin. The deformation is stronger in this area.

#### b- Jvari - north of Rioni

The Jvari's area (Jv. on fig 1) allows us to observe a large scale structure marked by a south verging anticline constituted of Mesozoic deposits, which outcrop along with Cenozoic units on its southern inverse flank.

The study of the map (Abesadze *et al.*, 2004) together with the field observations show that the Eocene deposits drapes the contact of Upper Cretaceous and Paleocene and forms an unconformity (Fig. III. 4). The same observation is made with the Oligocene deposits which unconformably overlie the Eocene and the Upper Cretaceous onto the inverse flank of the anticline.

In the field we can observe the progressive transition from chalky Campanian-Maastrichtian limestone to the marlier Paleocene and detrital Eocene deposits, and finally the gypsum-rich and septarian concretion bearing dark shales of Oligocene age (Fig. III. 4, 7). However, observations toward to the hinge of the anticline indicate a different structure (fig 4, 3-6). There, we observe a zone of reworked material, with blocks of chalky limestones in a matrix (Fig. III. 4, 4-5) directly onto the upper Cretaceous cherts-bearing chalky limestones (Fig. III. 4, 6). The Paleocene marls are deposited at high angle onto this formation (Fig. III. 4, 3). A strong sandstones/conglomerate strata overlays unconformably the formation of reworked Upper Cretaceous (Fig. III. 4, 1-2). The age of this formation is unknown. This is not similar to the Eocene deposits and is probably of Neogene or quaternary age. No Palaeocene, neither Eocene nor Oligocene deposits are observed at the place with reworked material, but it is observed toward the west and east (Fig. III. 3, e,f). The lack of Paleogene deposits constitutes an unconformity.

The Jvari area is folded in a NW-SE trend. However, to the eastern continuation, the Cretaceous and Paleocene deposits are folded in a NE-SW (places 1, 2 in Fig. III.4), and WE (place 3 in Fig. III. 4) trend except for the Neogene deposits dipping. The Neogene deposits

seem to be deformed in a NE-SW to N-S compression. The origin of the changing in the trending of the deformation remains unclear and seems affect only the older deposits than the Neogene. The Paleogene deposits follow the same trend of deformation as the Cretaceous deposits.

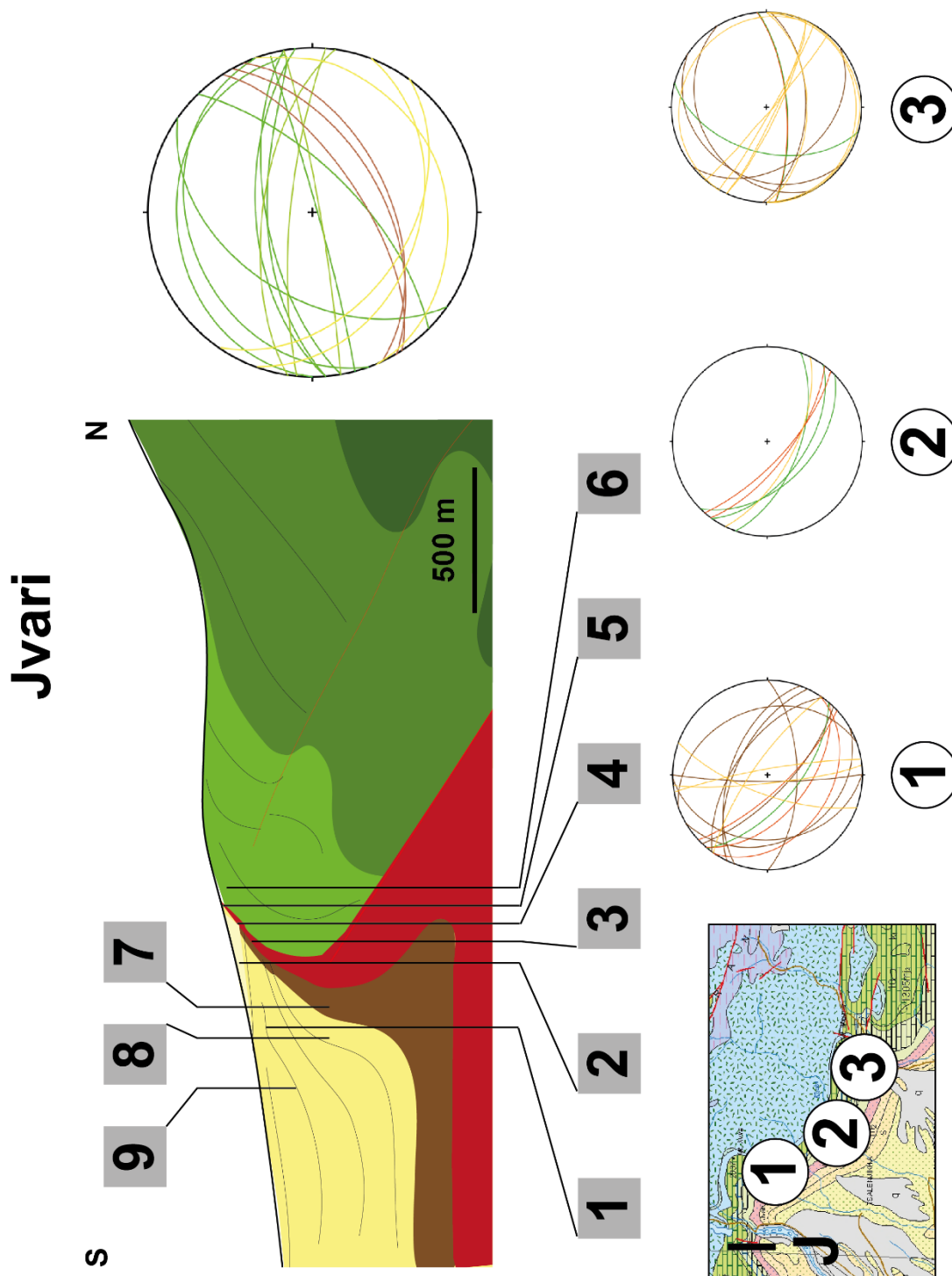


Figure III.4: Cross section of the Jvari area with the stereonets of bedding showing the Upper Cretaceous in Green, the Paleogene in red/brown and the Neogene deposits in yellow. The data have been plotted in a Lower Hemisphere projection with the North-East-Down coordinate system (NED) by using the “stereonet” software. The pictures illustrate the cross section. The three stereonets 1, 2, 3 are situated east of the cross section (map location from (Abesadze et al., 2004). (Legend before Fig. III.6)



1



2



2'



3



4



4'



5



5'



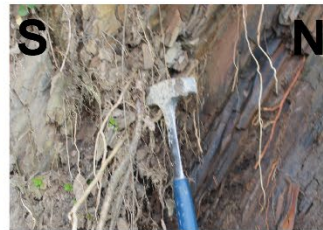
6



7



8



8'



9

Figure III.4 bis: pictures situated along the Jvari cross section. 1: sub-horizontal Neogene deposits, 2: the south-dipping conglomerate breccias, 3 the south-dipping Palaeocene deposits, 4: the transition from the Upper Cretaceous shaly limestones to the Palaeocene marls: the transition is made of more sandy limestones to breccias. This is the possible lateral evolution of the conglomerates of picture 2. 5: view of the transition as in picture 4, in the landscape, 6: the decimeter-bedding limestones of Upper Cretaceous, 7: the Maykopian deposits deformed, 8 and 9: the Lower and Middle Miocene deposits deformed

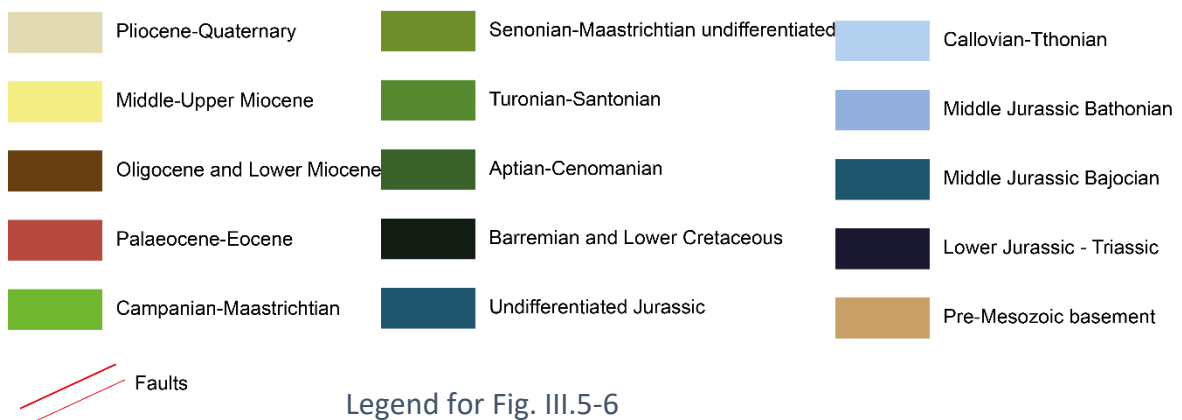


### c- Ambrolauri

In the Ambrolauri flexural basin, the Palaeocene deposits are present near Tsageri (Tsg in Fig. III. 1) on the southern border of the GC on the map (Abesadze *et al.*, 2004) but are not observed in the field. The Neogene deposits are deposited unconformably onto the Cretaceous deposits at the front of the deformation front.

However, along the northern GB, near Kenashi (Kn in Fig. III.1, and the cross-section location west of Kn) the deposits show the continuous sedimentation from Cretaceous to Neogene (Fig. III. 5). However, the Eocene and Oligocene deposits cover the Upper Cretaceous deposits in the upper part of the topography. This morphology is characteristic of an unconformity. This observation cannot be made all along the GC because Neogene deposits also cover the Upper Cretaceous directly and erase the record at many places. The map (Abesadze *et al.*, 2004) shows the unconformity of the Oligocene east of Kenashi in a syncline.

On Google Earth (Fig. III. 5), the deposits are followed, and we can observe the way they disappear under the Eocene and then under the Oligocene deposits. The lateral transition from continuous Up K to Oligocene, with variation in the thickness of Oligocene depositions when the Miocene deposits overlays the Upper Cretaceous deposits highlights the shape of the growth strata. The main direction of the folding is NNE-SSW.



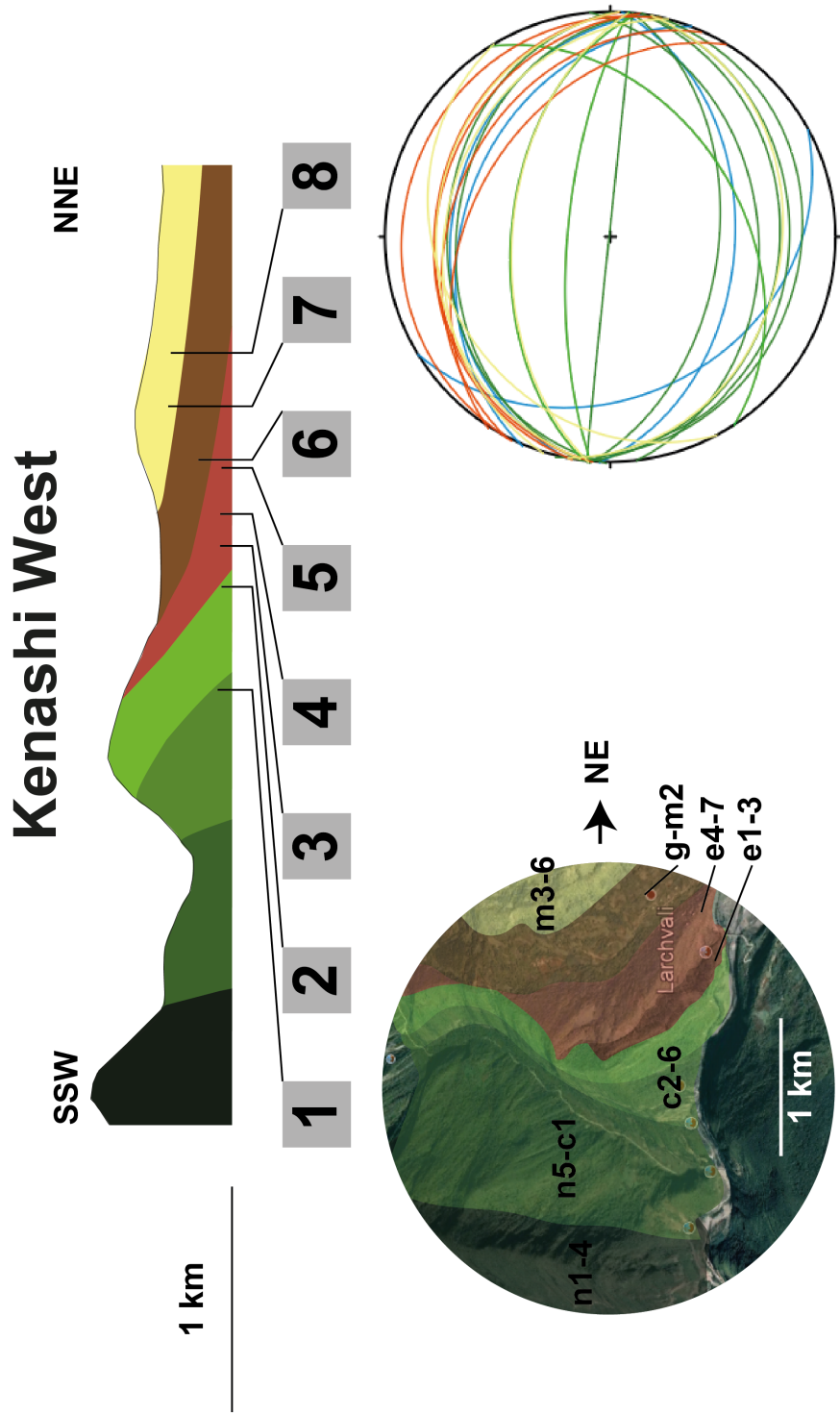


Figure III.5 : Cross section of the western part of Kenashi with the associated pictures. Interpreted Google Earth view of the area and the stereonet of the data of the Kenashi area.

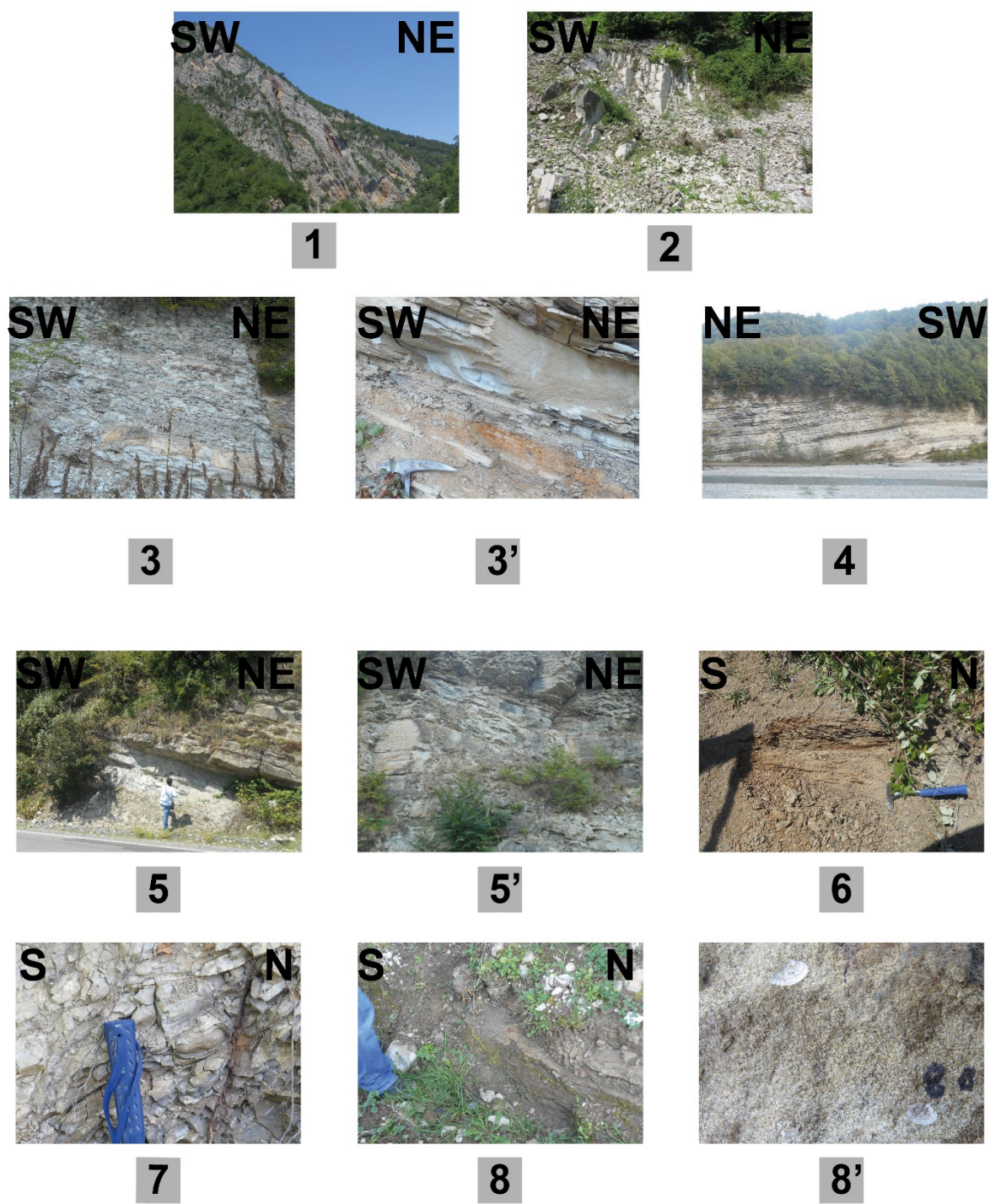


Figure III.5 bis : Pictures along the cross section of Fig. III. 5. 1: Upper Cretaceous deposits showing onlaps, 2: Uppermost part of the Upper Cretaceous deposits, 3 and 4: Palaeocene to Eocene deposits, 5: Eocene deposits, 6: Maykopian Oligocene deposits, 7 and 8: Middle to Upper Miocene deposits

#### d- south of Rioni

The observations on the growth strata in the Rioni foreland basin and in the Georgian Block is possible near the boundaries of the major inverted faults: for example, along the Tsaishi anticline and its eastern prolongation the Gakhomela anticline (TsC and Gk in Fig. III. 1).

The Tsaishi anticline and its eastern continuation offer a great opportunity to understand the Paleogene deposit formation because the foreland basin develops at the frontal part of the anticline and in a piggy-back basin (TsC and Gk in Fig. III.1).

Near Gakhomela, at the front of the anticline, we observe the transition from Upper Cretaceous chalky limestones which contains pyrite nodule and cherts to the more marly and detrital deposits (Fig. III. 6, i, j). We observe a syn-sedimentary normal fault (Fig. III. 6, j). Toward the south the deposits are more marly and do not show variations in the dipping to the south (Fig. III. 6, i).

At the back of the fold, the transition from Upper Cretaceous to Oligocene is nearly the same, with alternating limestones and marls, marls, sandstones and black shales which contain septarian. The Oligocene sediments are deposited onto the Upper Cretaceous limestones higher up toward the hinge of the anticline (Fig. III. 8, pictures 3-8) which highlights an unconformity (see Fig. III. 8 for more details on the Gakhomela anticline). The Tsaishi anticline also contains some outcrops of the Palaeocene deposits. In the field, on the forelimb of the anticline the Miocene deposits cover the UP K. To the west of the Senaki anticline (Snk in Fig. III. 1) we can observe the marls of Paleogene at the end of the eastern periclinal area.

The Cretaceous-Paleogene transition can be observed on the backlimb of the fold. Near the Rioni river we observe the Paleogene suite (Fig. III. 6, k-l) conformably deposited over the Upper Cretaceous Maastrichtian deposits. However, the dipping decreases in the younging direction the series.

In the more centre part of the anticline (TsC in Fig. III.1), a hard ground is observed at the limit between Upper Cretaceous and Palaeocene deposits (fig 6, o). The Upper Cretaceous deposits are made or recrystallised, thus very competent, pink limestones (Fig. III. 6, m). The hardground (fig III. 6, o) is made of glauconitic green shale deposits containing pyrite crystals. The limit is marked by a jump in the river. Then the deposit of alternating marls-limestones sequences is observed like in other places (Fig. III. 6, n, p). Locally, some volcanogenic tuffs are

observed intercalated within more detrital facies (Fig. III. 6, n). These evolve into sandstones during the Eocene (Fig. III. 6, p) and then some shales are observed before going into the Miocene detrital series (see Fig. III. 8 for more details on the Tsaishi Anticline).

The main direction of the compression is N-S to NE-SW, except for the westernmost part of the Tsaishi anticline which is in a NW-SE direction. This direction can be affected by a major strike slip faults with a dextral movement which seems to affect at least the Mesozoic and the Paleogene deposits (Abesadze *et al.*, 2004) and the Neogene deposits after the dipping observed on the stereonet in Fig. III. 8.

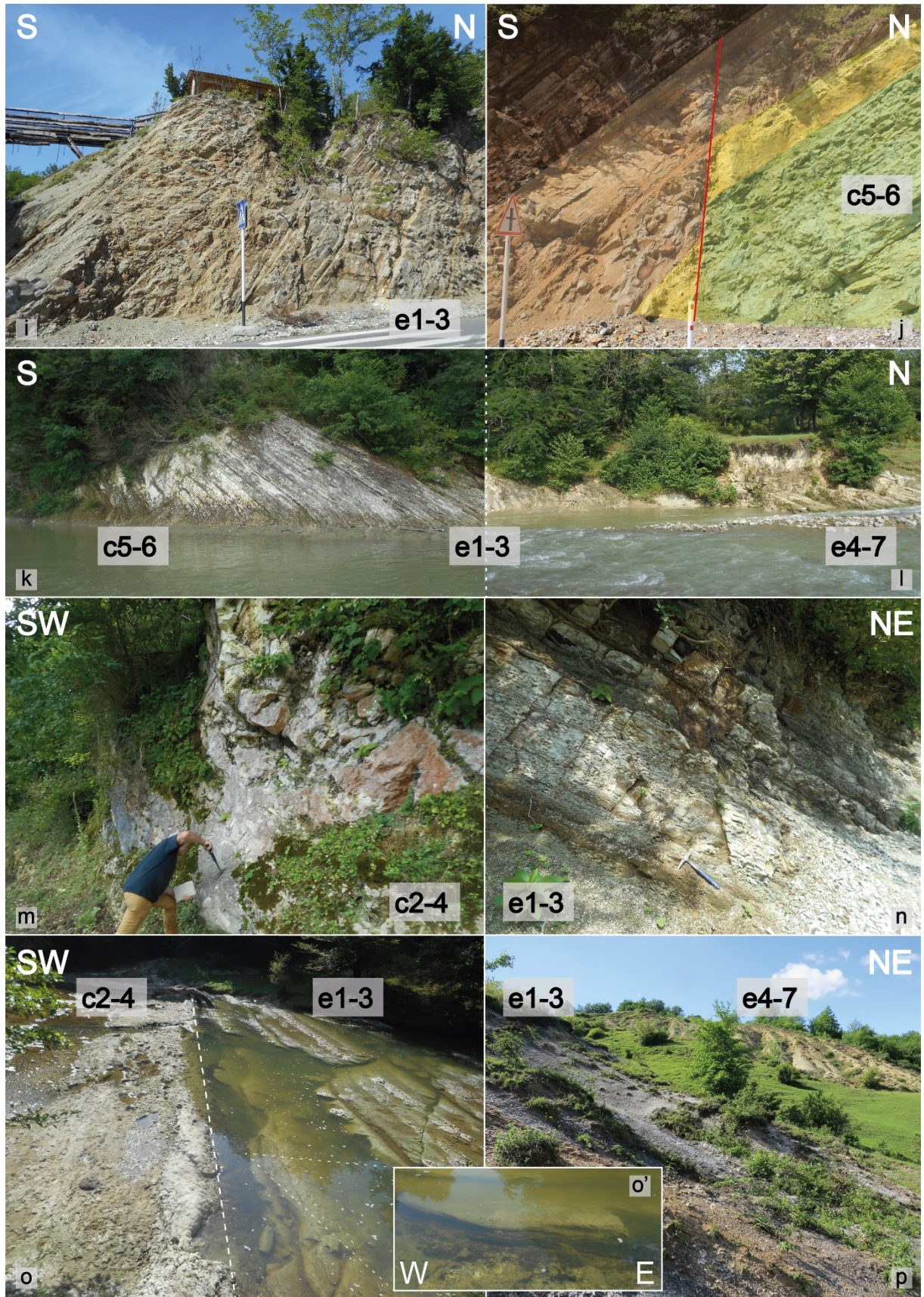


Figure III.6: Pictures of the area of Tsaishi. i and j: Pictures of the Paleogene deposits of the frontal part of the Gakhomela anticline. K-l: Pictures of the Paleogene deposits on the backlimb of the Tsaishi anticline in its western termination. m: Picture of the last Cretaceous deposits observed at the back

of the central Tsaishi anticline before the Paleogene deposits. n: Picture of the Paleogene deposits situated back of the Tsaishi anticline, further N from the picture m. o-o': Pictures of the hardground observed at the limit between Upper Cretaceous and Paleogene deposits at the back of the Tsaishi anticline. p: Picture of the transition of Palaeocene (marls)-Eocene (sandy) deposits.

An old seismic line across the Tsaishi anticline (Fig. III. 7) offers also some insights into the deeper architecture of the fold, including the geometry of the Paleogene deposits. The Palaeocene and Eocene deposits form growth strata, especially to the backlimb of the anticline which propagates to the south. The Oligocene deposits show an unconformity onto the Mesozoic deposits. Some secondary folds, <500m of wavelength are observed in the Oligocene deposits and also affect the Neogene deposits (Fig. III. 7). However, these folds are not observed in the Palaeocene and Eocene, nor the Mesozoic deposits. The origin of these folds remains unclear. These could be thin-skinned folds into the Maykopian shales deposits, but it could also be some folds linked to the diapirism of salted-evaporitic deposits of the Maykopian. The Maykopian deposits observed near the folds does not include much salts, however, since their thickness is more important far from the anticlines, the possibility of salt-tectonic can't be put aside.

## Central Tsaishi old seismic interpretation

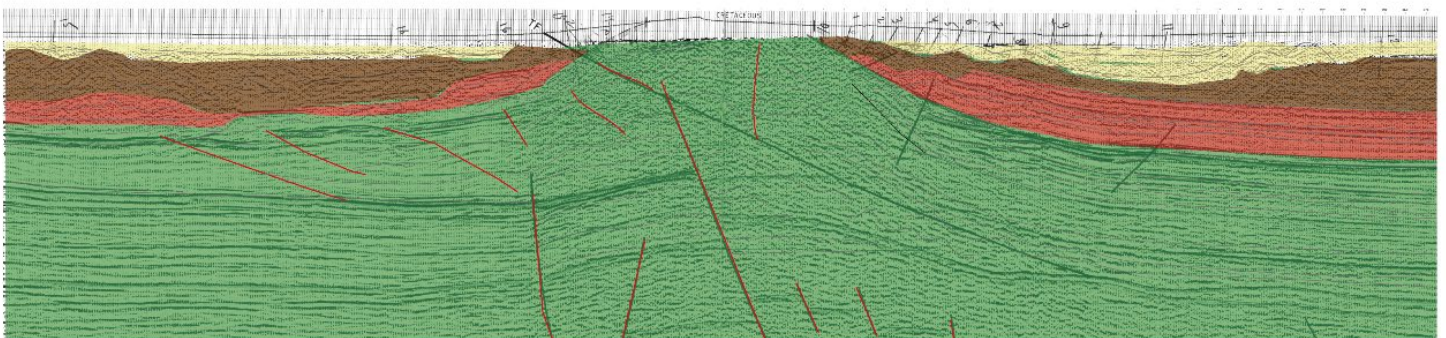


Figure III.7: Interpreted scan of the Tsaishi old seismic line. The green horizon is interpreted to be Mesozoic deposits, red horizon includes the Paleocene and Eocene deposits, the brown horizon includes the Oligocene deposits, and the yellow horizon the Neogene deposits. (Legend in Fig. III.14)

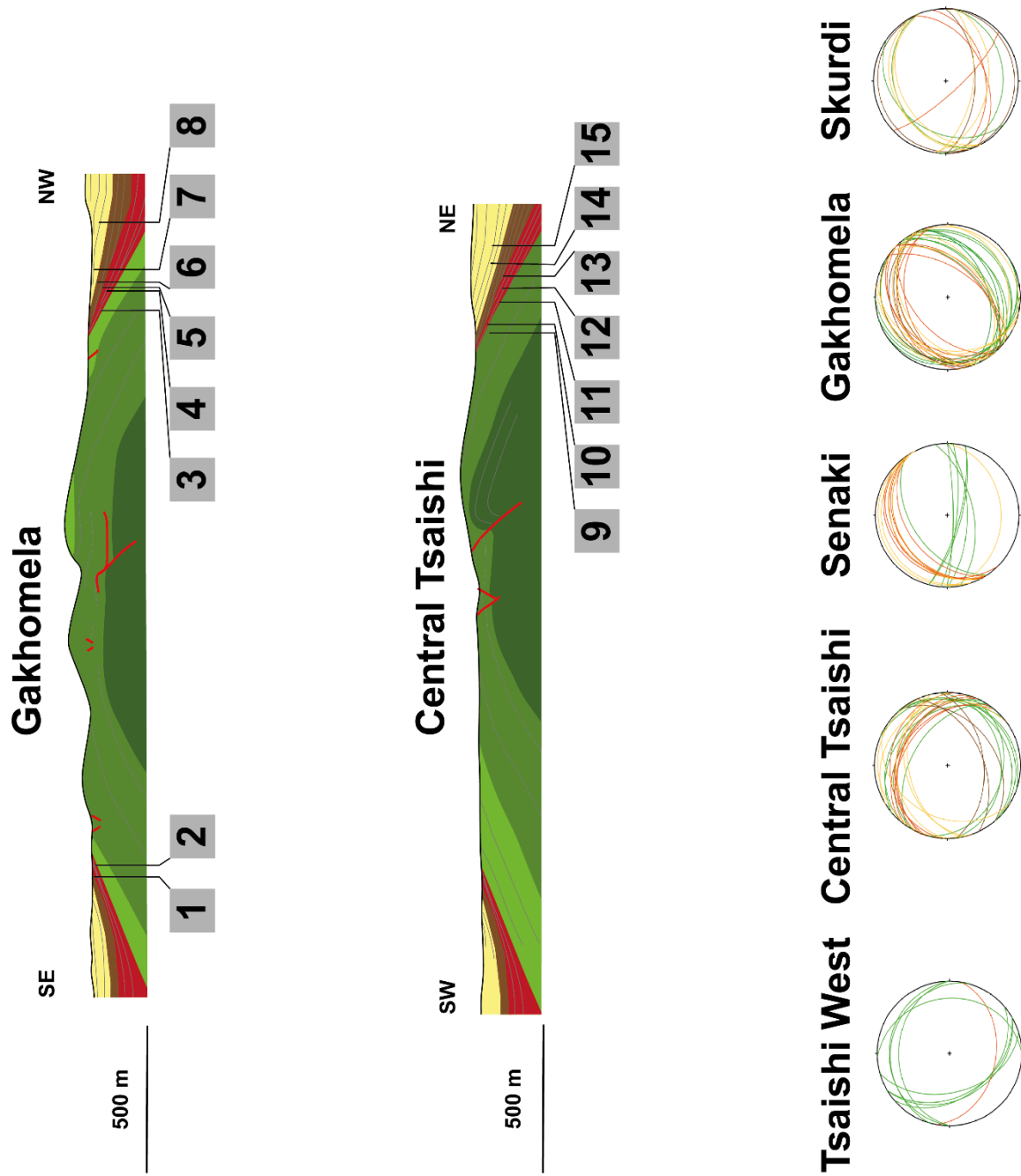


Figure III.8: Cross sections of the Gakhomela and Tsaishi anticlines. The pictures are localized along the sections. Several stereonet present the dipping data of the different folds of the Tsaishi area (see Fig. III. 1 for location, Ts, TsC, Snk, Gk, Sk in Fig. III.1). The green colors are the data in the Mesozoic deposits, the red ones are the Paleogene deposits and the yellow ones are the Neogene deposits. (See Fig. III.14 for legend)



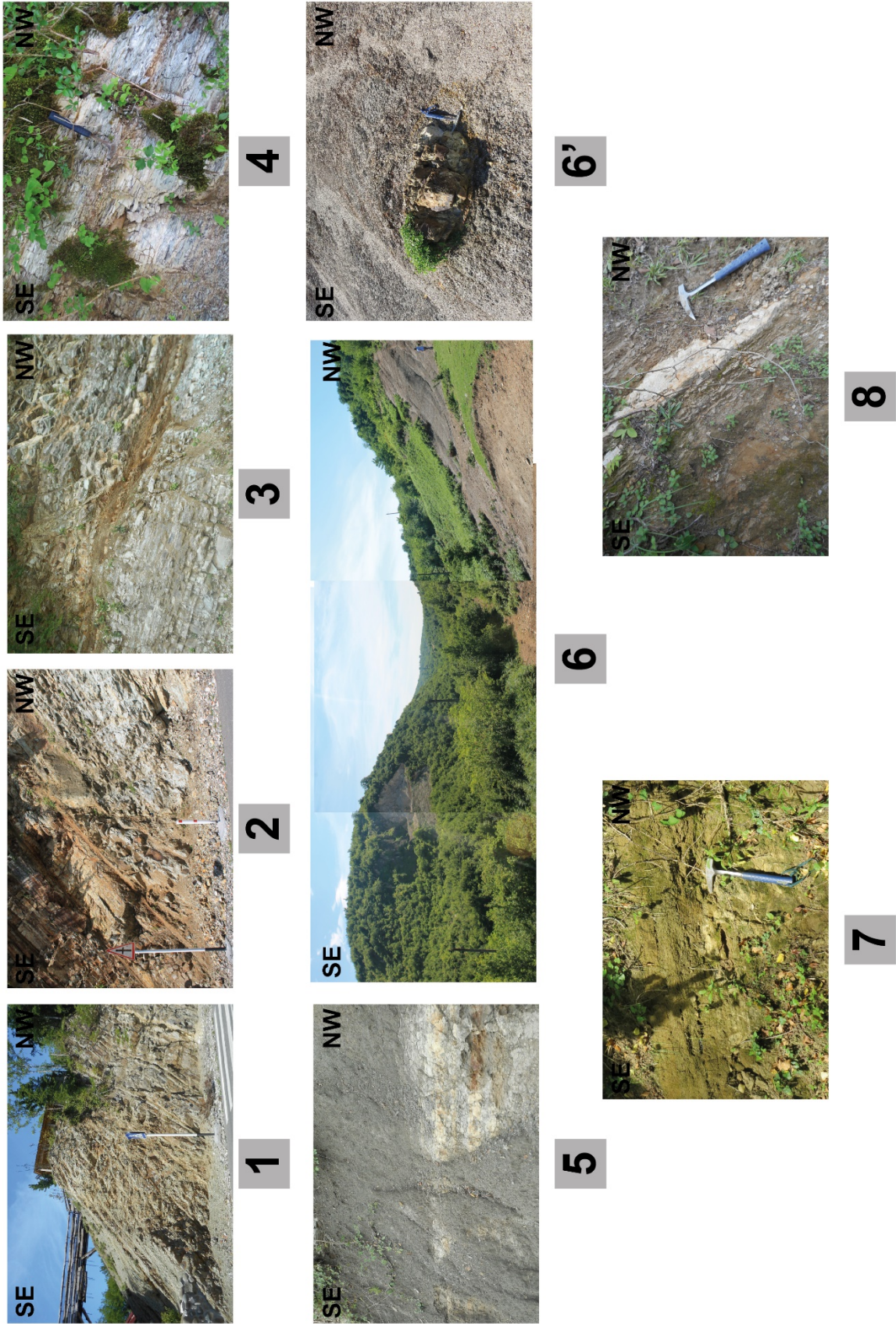


Figure III.8 bis: Pictures along the cross section of Fig. III. 8. 1 and 2: Palaeocene deposits evolution

from the Upper Cretaceous (2 is Fig. III. 6, j), 3-5: Palaeocene deposits evolution on the backlimb of the Gakhomela anticline, 6: maykopian Oligocene deposits, 7 and 8: Middle to Upper Miocene deposits

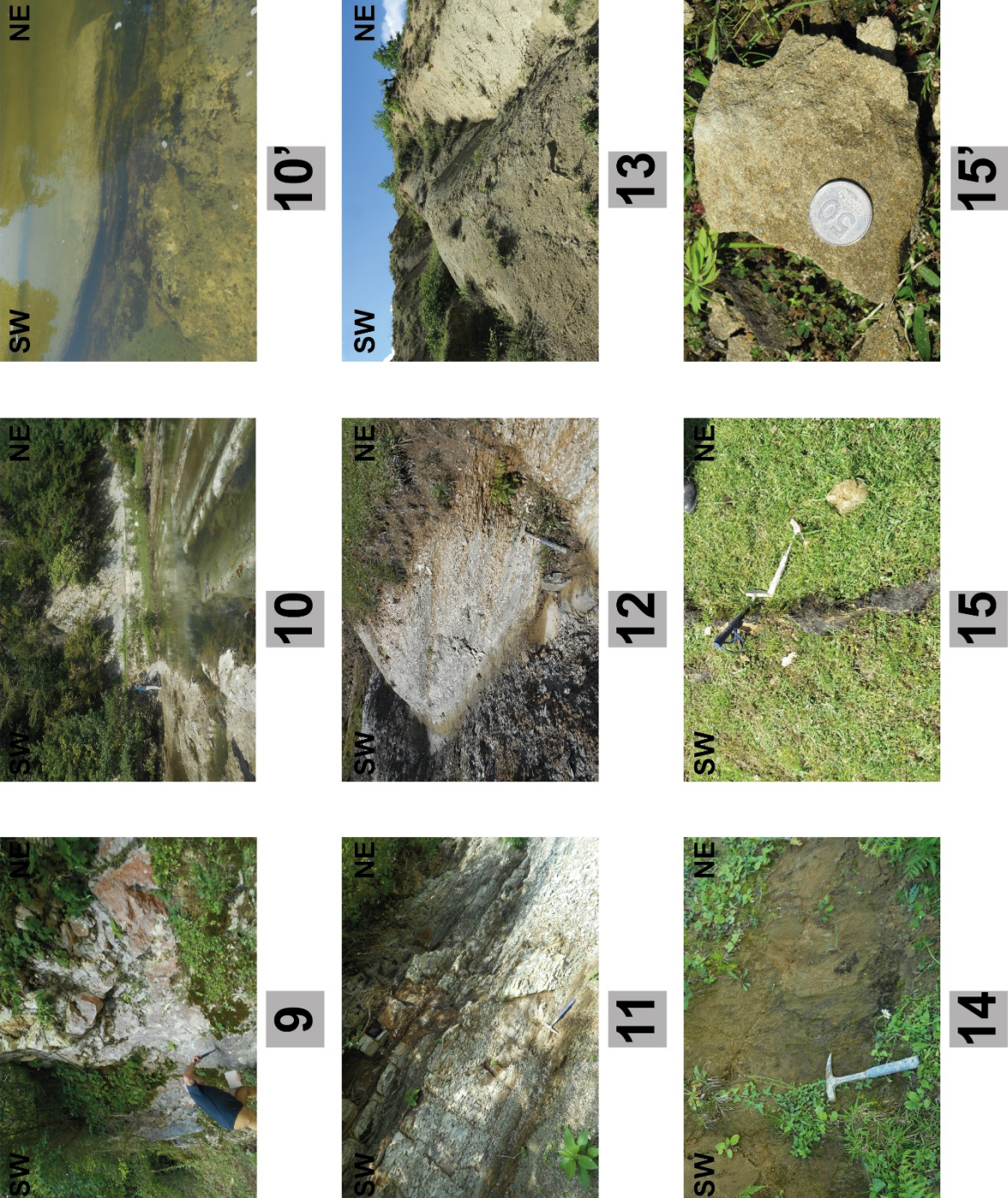


Figure III.8 bis bis: Pictures along the cross section of Fig. III. 8. 9: Upper Cretaceous deposits, 10: the hardground observed at the boulder Upper Cretaceous – Palaeocene, 11 to 13: Palaeocene to Eocene

deposits, 14: Lower to Middle Miocene deposits. The amount of clays in these deposits shows that it is near the Maykopian deposits, 15: Upper Miocene deposits

#### e- Kura Foreland basin

To the east, near Ananauri (An in Fig. III.1), north of Tbilisi on the “Military road”, we can observe the Paleogene deposits in the frontal deformation of the southern GC.

The olistostrome (Fig. III. 9, q) which reworks Mesozoic sediments is not dated because of detrital/reworked material without any fauna. We can only assume that it represents a syn-orogenic deposit such as a wildflysch. South of Ananauri, these are unconformably deposited onto the Mesozoic series (Fig. III. 10) and the Palaeocene deposits which are observed between fault-propagating folds composed of Cretaceous deposits (Fig. III. 9) (Fig. III. 11-13). Consequently, this olistostrome could be Eocene in age or younger at least syn-kinematic.

The Ananauri area is situated at the front of the frontal fold of the Greater Caucasus (Fig. III. 9v and 9w) (Fig. III. 10). In the Zhinvali area (Fig. III. 12-13), we observe the repetition of the Turonian red beds of the GC (fig 9, s). The Cenomanian deposits, made of argillite and shales, can be the decollement layer of the thin-skinned tectonic made up of duplexes with a southward propagation (see Fig. III. 11-13).

The observations at the limits between the duplexes show Palaeocene deposits (Abesadze *et al.*, 2004). These deposits are intensely deformed (Fig III. 9) and display a south-verging kinematics. These deposits are observed in the area, but they disappear to the east under the Alazani piggy-back basin where the Neogene deposits unconformably cover the structures. The frontal part of this duplex seems to be, if we follow the structure to the east about 5km of the Alazani anticline, where we observe the same Mesozoic deposits of the GC. Consequently, the deformation occurs during the Palaeocene to the Eocene. This compression can be related to the collision into the Lesser Caucasus.

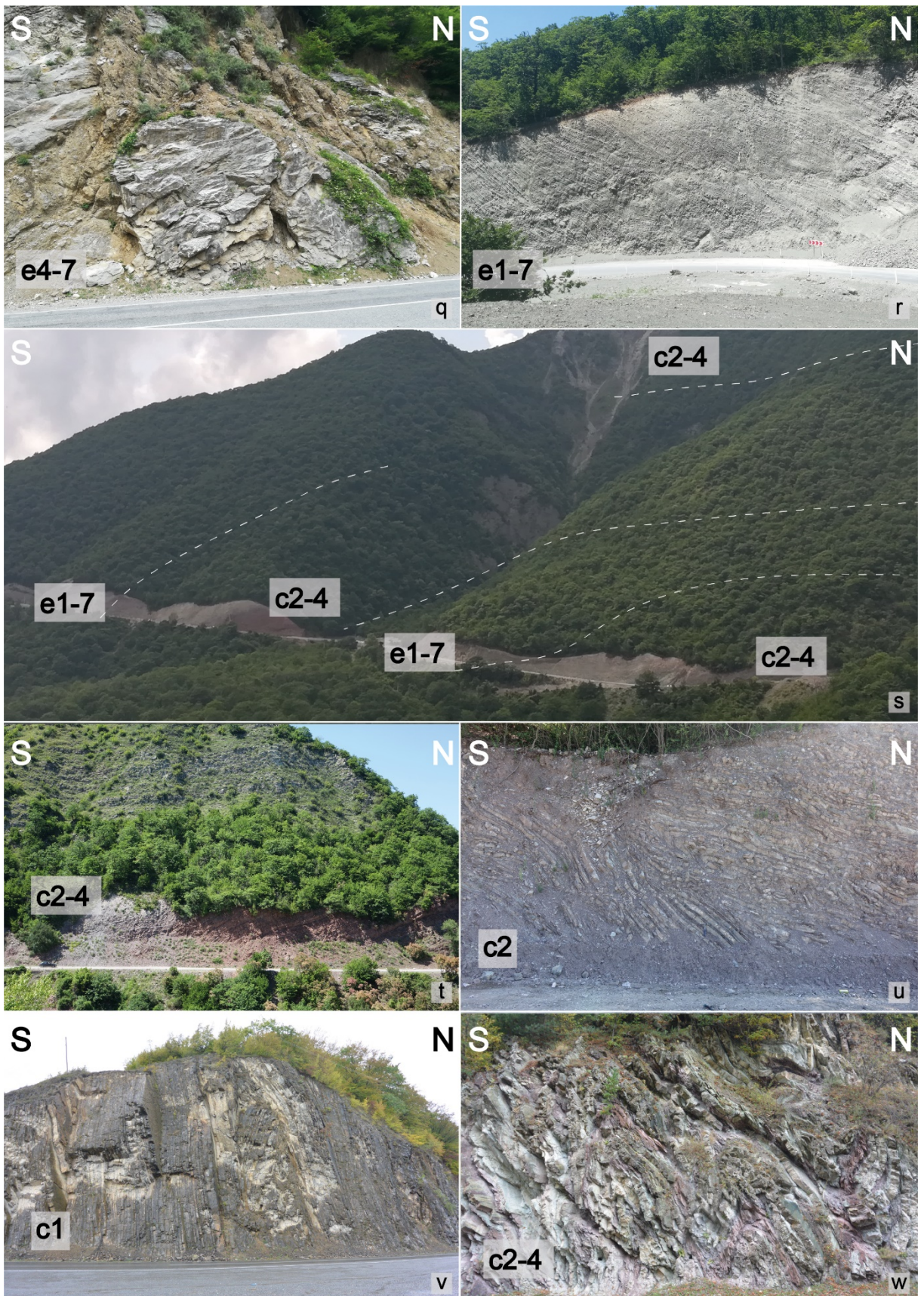


Figure III.9: Pictures in the frontal deformation of the Greater Caucasus in the Kura area (see Fig. III. 1 for location).q: Picture of a block in the wildflysh of Eocene age. r: Picture of the Paleocene deposits in the Zhinvali area s: Picture of the landscape of the Zhinvali area where the Turonian-Santonian deposits are good markers to observe the duplication of the serie. Paleocene and Eocene deposits are observed in between the Cretaceous deposits duplex. t: Picture of the Turonian-Santonian deposits in the Zhinvali area. u: Slumps in the Lower Turonian deposits in the Zhinvali area. v: Picture of the Cenomanian deposit in Ananauri. w: Picture of the Turonian-Santonian deposits north of Ananauri.

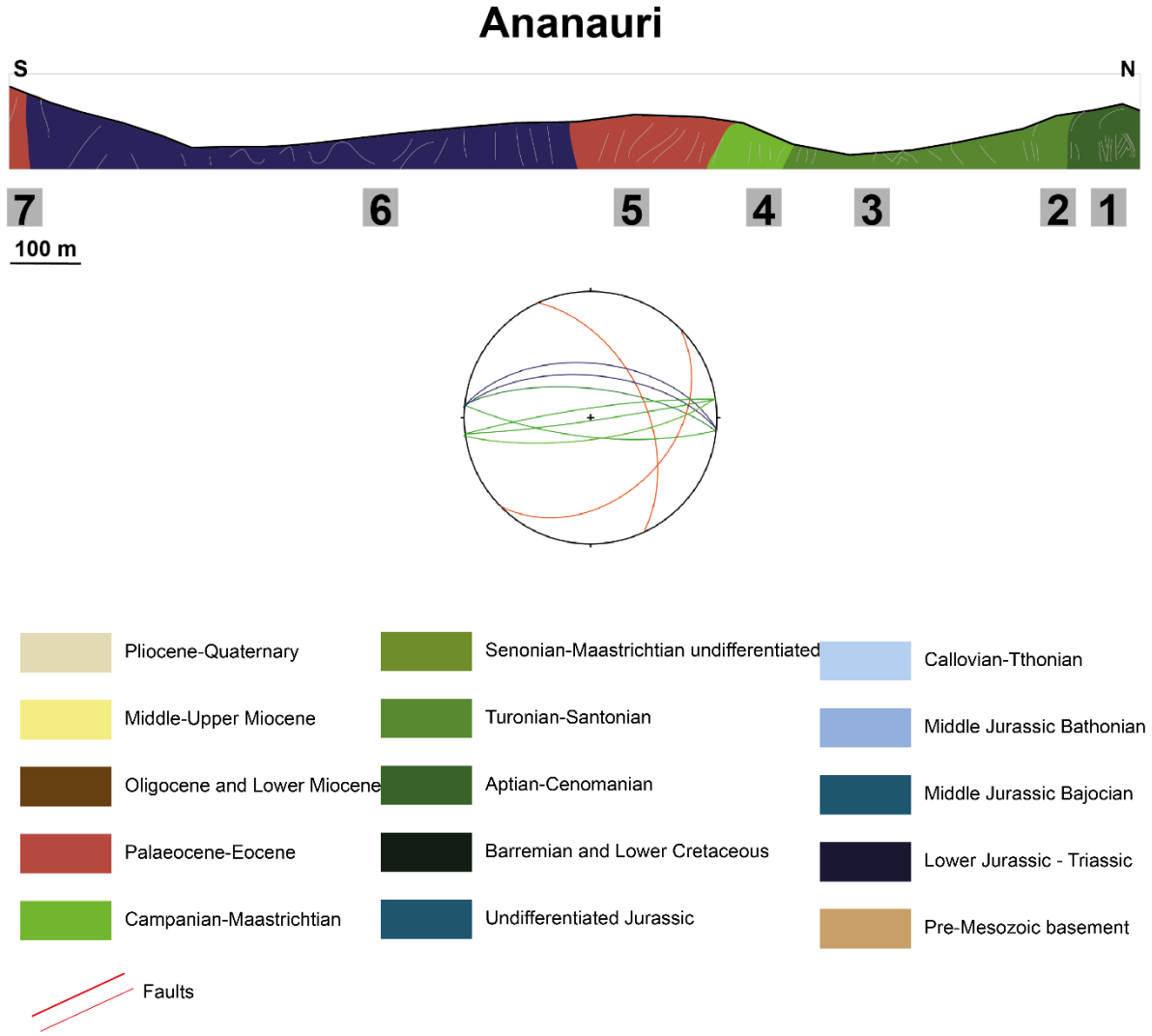


Figure III.10: Cross section of the Ananauri area with the stereonet of bedding from the data along the section. The pictures are located on the section

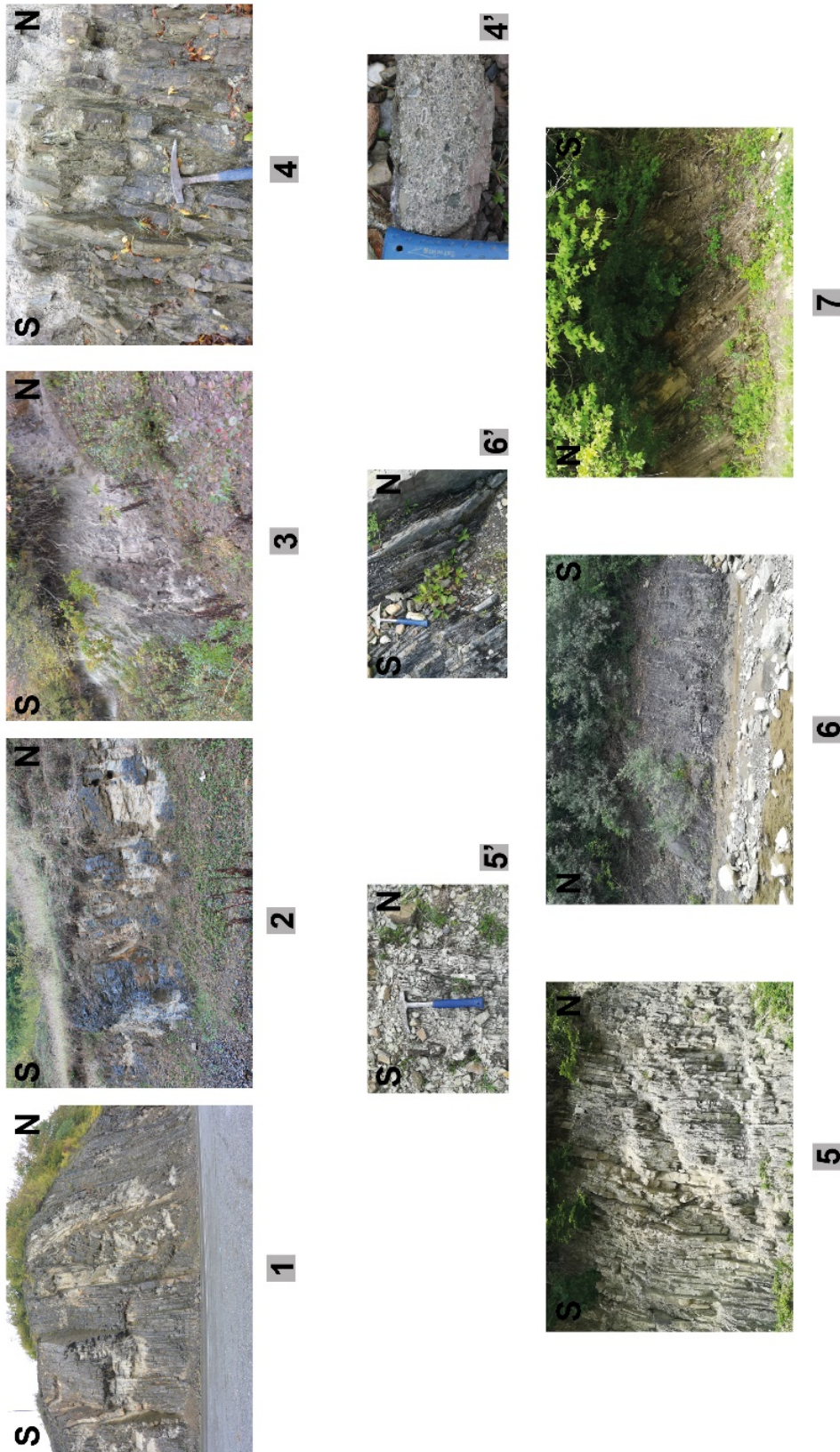


Figure III.10 bis: Pictures along the cross section of Fig. III. 10. 1: Cenomanian deposits, 2 and 3: Turonian-Santonian deposits, 4: Campanian deposits, 5 : Palaeocene deposits, 6 : Lower Jurassic deposits, 7 : Eocene deposits

# Zhinvali



Figure III.11: Cross section of the Zhinvali area with the stereonet from the bedding planes measurement along the section. The pictures are located on the section.

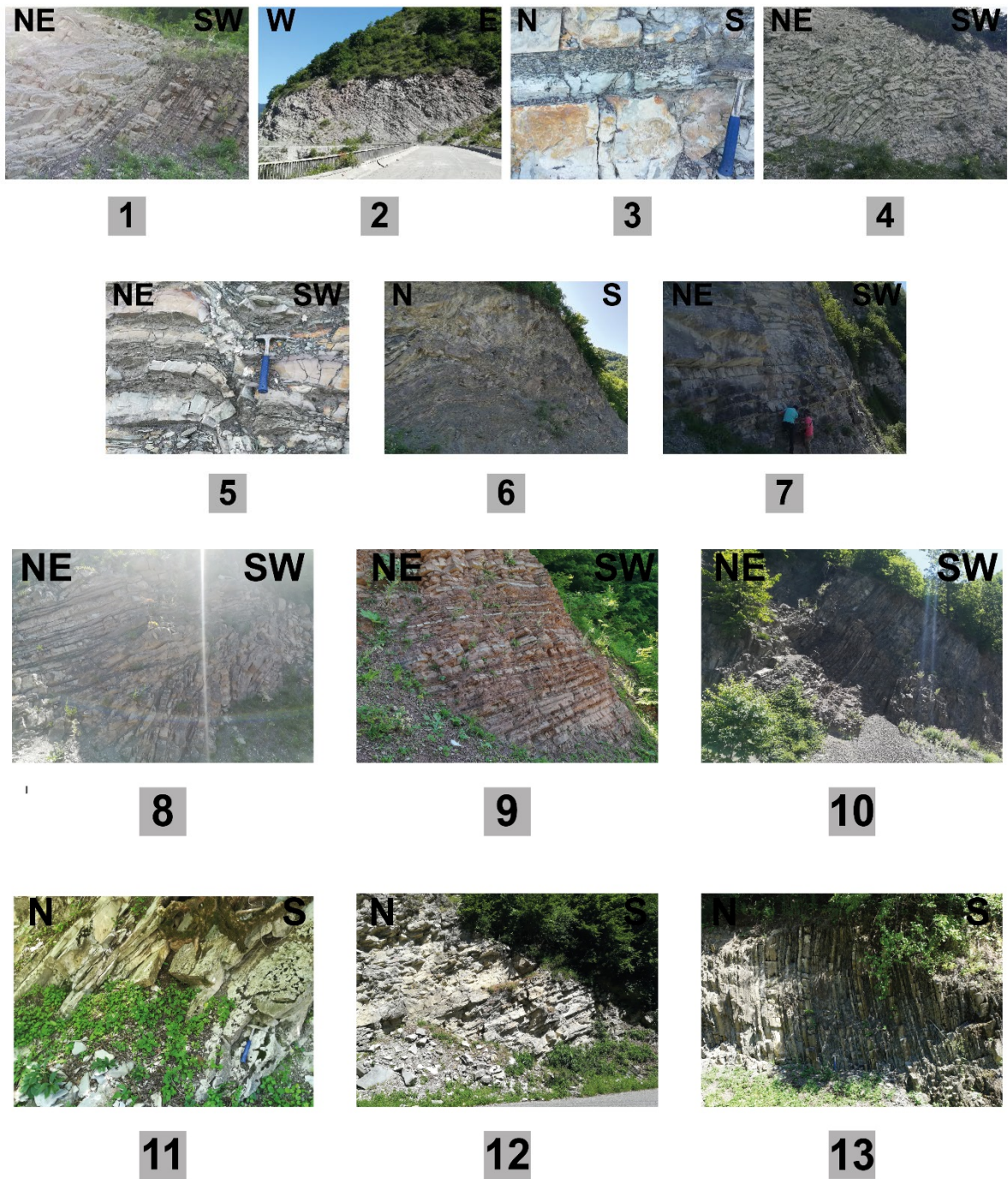


Figure III.11 bis: Pictures along the cross section of Fig. III. 11. 1: Cenomanian to Turonian deposits, 2: Palaeocene deposits, 3, Upper Cretaceous deposits, 4: Palaeocene deposits, 5: Cenomanian deposits with normal fault, 6: Turonian-Santonian deposits, 7: Campanian-Maastrichtian deposits, 8 and 9: Turonian-Santonian deposits, 10: Cenomanian deposits, 11 and 12: Campanian Maastrichtian deposits, 13: Cenomanian deposits



# Zhinvali bis

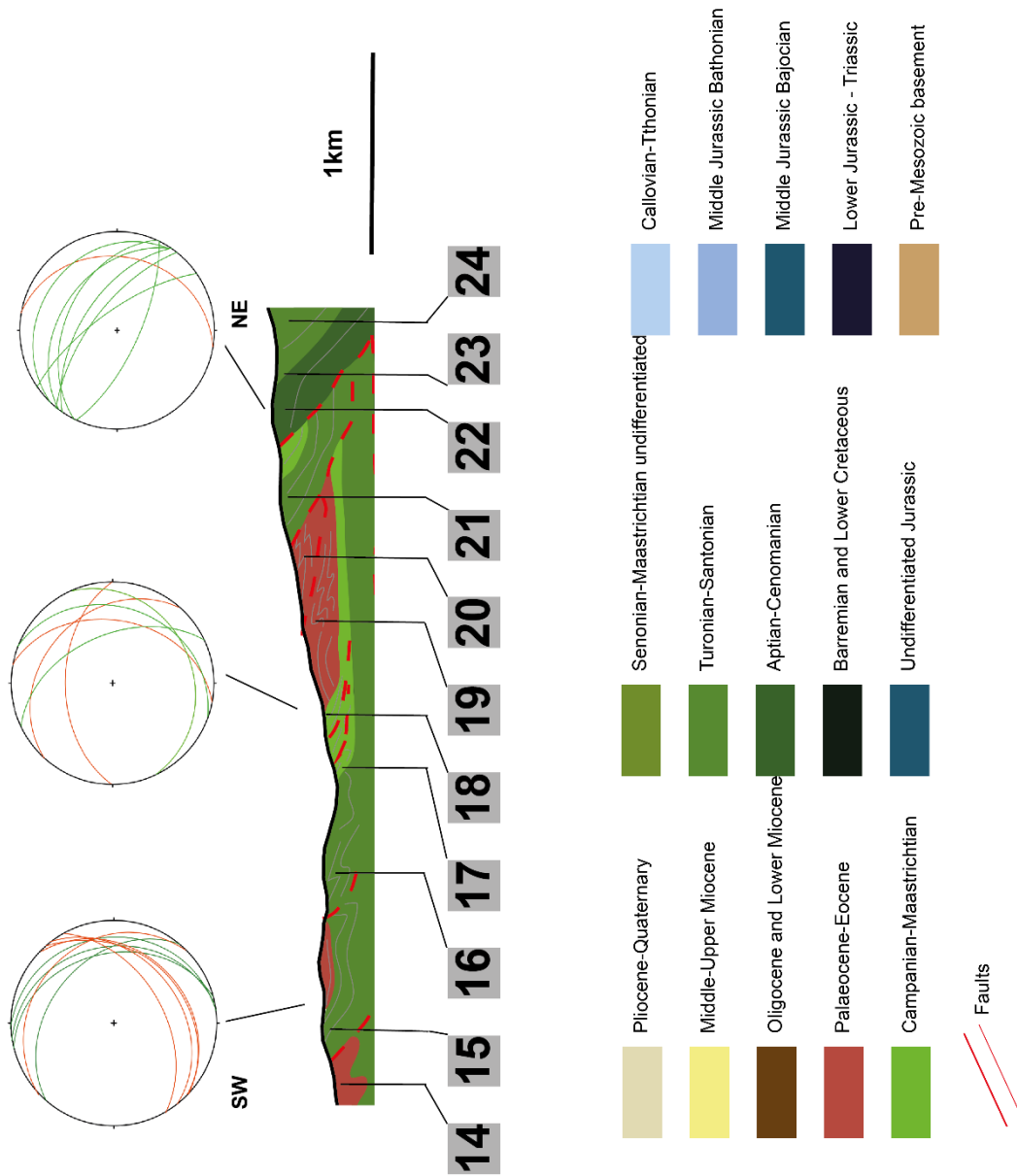


Figure III.12: Cross section of the Zhinvali area on the eastern part of the mountains with the stereonet from the bedding data along the section. The pictures are located on the section.



14



15



16



17



18



19



20



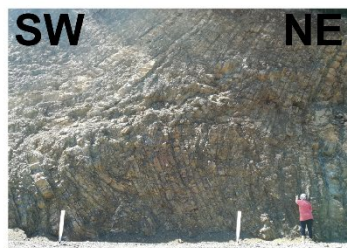
21



22



23



24

Figure III.12 bis: Pictures along the cross section of Fig. III. 12. 14: Palaeocene deposits with decollement levels, 15 and 16: Turonian-Santonian deposits, 17 : Upper Cretaceous deposits, 18 : transition from Upper Cretaceous to Palaeocene, 19 and 20: Palaeocene deposits, 21: Turonian-Santonian deposits, 22: Cenomanian deposits, 23: Cenomanian to Turonian deposits, 24: Turonian-Santonian deposits

## 2- The Neogene deposits

The Paleogene deposits are different from W to E, however the Neogene deposits show the same kind of structures with the growth strata during the Sarmatian. After the Oligocene, where sedimentation indicates a calm deposition environment, the Neogene deposits show the evidence of syn-deposition compression (Alania *et al.*, 2009, 2017; Forte *et al.*, 2010, 2013, 2015; Vincent *et al.*, 2011; Vincent, Stephen *et al.*, 2016). During Miocene time, the deposits are more detrital, coarser, and evolve from marine to continental in the Kura foreland basin, while they remain marine in the Rioni foreland basin. We describe here our observations from west to east to reconstruct the tectonic evolution from the Mesozoic in both areas.

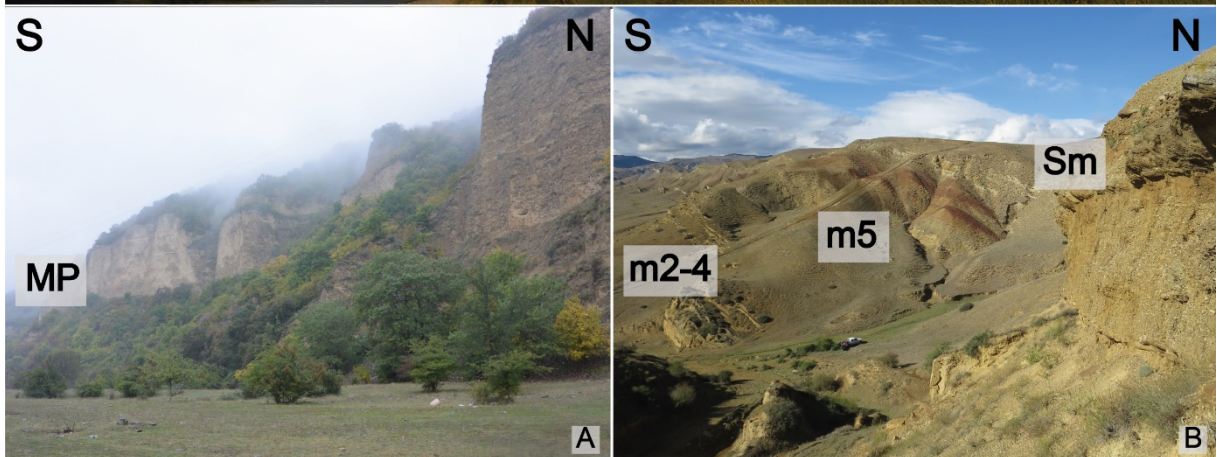
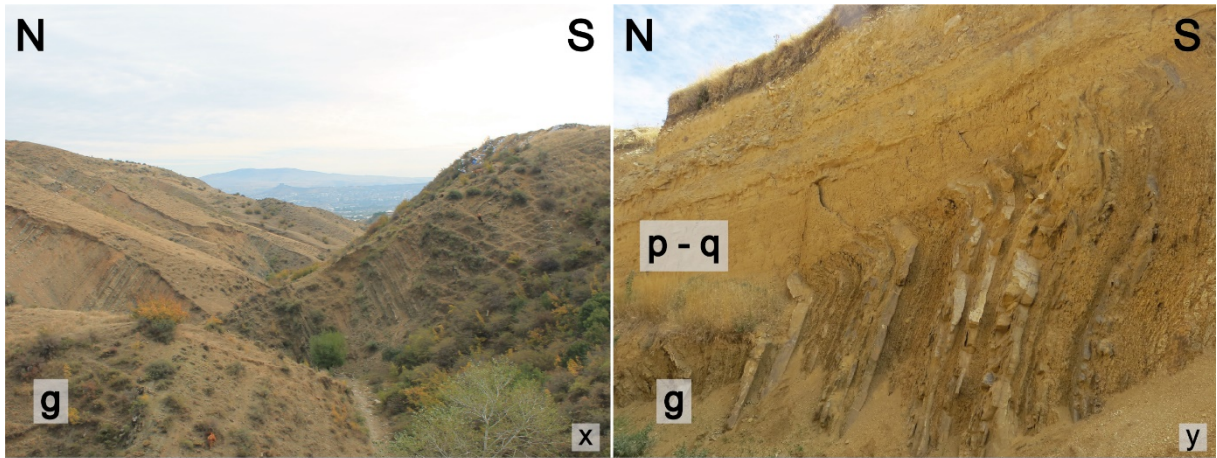


Figure III.13: Pictures of the deposits in the Kura and Kartli foreland basins. See Fig. III. 1 for locations. x and y: pictures of the folded and tilted Oligocene deposits in the Adjara-Trialeti synclines, covered unconformably by quaternary channel flows in y. z: Picture of the Landscape of the Kartli foreland basin, north of the Adjara-Trialeti fold-and-thrusts belt. The Sarmatian deposits show a growth-strata geometry. A: Picture of the undeformed Meotis-Pontian deposits south of Ananauri deposits. B: Picture of the Neogene deposits in the Kartli foreland basin where the Sarmatian (Upper Miocene) deposits are made of growth strata. C: Picture of the Neogene deposits south of the Kura foreland where the folds are still south-verging and not constrained by the Adjara-Trialeti fold-and-thrust belt. We notify the Pliocene-Quaternary undeformed deposits onto the folded Sarmatian deposits and the Meotis-Pontian (= Messinian) growth strata.

#### a. Rioni-Ambrolauri

At the Southern border of the GC into the Rioni FB, near Jvari and Ambrolauri, the Upper Miocene deposits are deformed and inclined (fig III. 4, pictures 1, 2, 8, 9 and Fig. III. 5, picture 8 and 9). The deposits are nearly vertical onto the forelimb of the major south-verging folds. The propagation of the deformation continues toward the south in both foreland basins. In the Ambrolauri, squeezed in a triangular zone between the south-verging GC structures and the GB north-verging folds, the Miocene deposits are shortened. The older deposits deformed in the central part of the flexural basin are the Oligocene deposits. It is possible that the Oligocene deposits are the decollement level in this area and that the deformation is thin-skinned.

North and south of the Tsaishi anticline, the foreland basin develops mostly during Neogene. The Upper Miocene deposits are deformed on the forelimb and the backlimb of the folds (Fig. III. 8, pictures 7, 8 and 14, 15) (and observed by many authors (Banks *et al.*, 1998; Morariu & Noual 2009; Adamia *et al.*, 2010; Tibaldi *et al.*, 2017b,a; Tari *et al.*, 2018). On the interpretation of the old seismic line (Fig. III. 7), the Neogene deposits are folded where the Oligocene deposits are folded but the older deposits are not. We observe that the Oligocene deposits are the basis of the deformations (decollement level or salt tectonic?) which infer some deformations north of the Tsaishi anticline: formation of north-verging duplex.

This duplexing results in the thickening of the Neogene deposits in the basin. The overlying Meotis-Pontian deposits are nearly not deformed which means that this deformation takes place before the Meotis-Pontian.

### b. Kura and Kartli basins

To the east of the Dzirula massif the structures show the Miocene deposits made of coarse detrital sediments folded within the basin, forming south-verging folds. The Upper Miocene deposits form growth-strata (fig III.14, B) with onlaps on the back of the folds showing the progression of thin-skinned tectonic related deformation (Chap. 1 (Ahmadi *et al.*, 2013)). The Oligocene deposits are the most probable decollement layer in the area (Maykop fm) and are also very deformed (Fig. III. 14, x, y). The MP deposits are also forming growth strata more to the back of the folds (fig 14, z, C).

The unconformity between the Upper Miocene and the Meotian-Pontian deposits can be linked to the Messinian crisis during which there is no deposit and likely erosion. If the deformation continues without any sedimentary record, the angular unconformity seems to appear. This does not imply a double stage of compression (Fig. III. 14, z). In the Kura basin, the Alazani piggy-back basin shows the same type of deformation onto the major fold of Cretaceous age (Philip *et al.*, 1989; Alania *et al.*, 2017). To the south, the propagation is as in the Kartli basin with the formation of south-verging thin-skinned structures (Fig. III. 14, C). The Pliocene deposits observed in the Kura foreland basin show an unconformity at the base of the Pliocene over the deformed Upper Miocene and MP sediments (fig III. 14, C).

### c. The AT FT belt

As observed, the inversion of the GC created the GC fold-and-thrust belt which delimits the north of the foreland basins.

During the Neogene, the foreland basins were delimited to the south by the AT FTB (AT in Fig. III.1). This concerns directly the Rioni and the Kartli basins, between Batumi and Tbilisi at least. The AT tectonic unit is described as a volcanic arc during Paleogene, however during the Neogene the NS convergence led to create north-verging folds which themselves deformed the foreland basin in their southern border.

All along its northern border, the AT presents major north-verging folds and thrusts and along its onto the forelimbs of the folds to the south and the north and mark some growth strata (Fig. III. 14: x, y, z are near AT).

These deposits present the same growth strata as in the Kartli FB. Near Tbilisi, the Neogene sediments are deposited into synclines, and are also squeezed between the anticlines formed in the AT, with Oligocene decollement level forming duplex structures (Fig. III. 14: x, y).

Toward the east of Tbilisi, the foreland basin develops toward the south without the north-verging deformation caused by the AT FTB.

#### IV. Interpretations

The observations of the post-Mesozoic deposits in the flexural basins reveals some syn-tectonic geometries in the Palaeocene-Eocene deposits and also in the Upper Miocene deposits. The identification of these deposits as growth strata or flysch allows to constrain the magnitude and spatial extent of the tectonic events during Paleogene and Neogene. Since the observations are different in the Rioni and Ambrolauri basins in one hand, and in the Kura and Kartli basins in the other hand, we will interpret them separately.

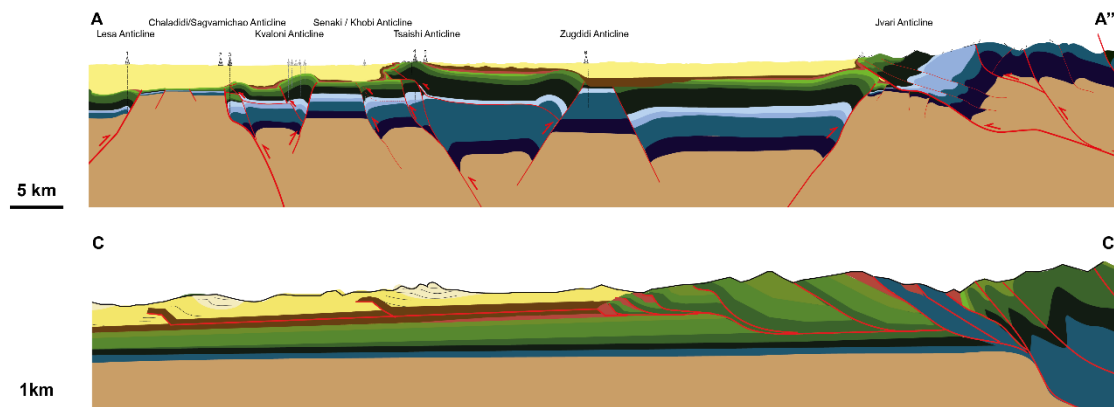


Figure III.14: cross sections located in Fig. III. 1. We can compare the style of deformation, depending on the inherited structures. The structures in the western cross section are driven by the inherited normal faults, while the eastern cross-section is deformed by thin-skinned tectonic. (Legend is after Fig. III.16)

##### 1. In the Rioni-Ambrolauri flexural basins

The Rioni flexural basins offers the possibility to observe the Palaeocene to Oligocene deposits near the Tsaisi anticline especially on the backlimb, and near the Gakhomela anticline (Fig.

III. 8) on the forelimb and the backlimb. The Jvari anticline offers the possibility to observe the Palaeocene deposits and the Oligocene deposits (Fig. III. 4). In the Ambrolauri flexural basin, the Kenashi fold offers the same possibility (Fig. III. 5). The maps (Abesadze *et al.*, 2004) show the unconformities along these folds, as well as along the Tsageri fold, the Ambrolauri fold and the Senaki and Tsaishi folds (chapter 2).

The Neogene deposits are filling the whole basins and we can interpret the pre-, syn- and post-tectonic behaviour of the deposits along the same folds as for the Paleogene.

#### a. The Paleogene deposits

The Palaeocene deposits, shown in brown in Fig. III. 15, are deposited onto the Upper Cretaceous conformably with a progression from chalky limestones to alternance of sandy-argillite detrital deposits and marly limestones, and finally into marls. This transition is observed on both flanks of the Gakhomela fold (Fig. III. 8). The transition from the chalky Maastrichtian limestones to the marly Palaeocene (Fig. III. 6: k, l) is observed at the western periclinal termination of the Tsaishi fold, while in its central part (TsC in Fig. III.1) the Maastrichtian limestones evolve toward detrital deposits. The difference tends to show that the environment is more energetic in the central part, with more materials, thus more erosion. Moreover, the hardground at the transition with the detrital deposits onto the hard and recrystallised red reef limestones define an unconformity (Fig. III.8). Near Jvari, the transition is different because onto the marly limestones is the olistostrome deposits which rework the Upper Cretaceous limestones into the matrix, before we can observe the marls (Fig. III. 4).

To resume, the Palaeocene deposits are more detrital in the central part of the fold than the more carbonated/marly deposits. Some syn-sedimentary normal faults are observed in these deposits (Fig. III. 6, j, l) and witness a subsidence on both flanks of the folds.

The Eocene deposits are observed only on the backlimb of the folds in Rioni and are deposited with onlaps onto the Palaeocene (Fig. III. 7). On the forelimb of the folds, the Eocene deposits are usually covered by the Oligocene which comes onto the Eocene, Palaeocene, and Mesozoic deposits. The detrital materials of the Eocene deposits imply that there was some erosion in the upstream area of these basins.

The Oligocene-Lower Miocene Maykopian series are then deposited with onlap onto the Eocene, the Palaeocene or directly onto the Upper Cretaceous (Abesadze *et al.*, 2004). The



unconformity highlights a shape of the post-tectonic deposits. The lithologies of the Oligocene show some close evaporitic basins with some detrital material, but with calm environment. As observed at the back of the Gakhomela or the western Tsaishi anticlines (Fig. III. 8), the growth strata are identified as Palaeocene and Eocene. We can follow them at the front of the fold on the maps (Abesadze *et al.*, 2004) but like in Jvari, the unconformity is then erased by the Neogene deposits (Fig. III. 4: 1,2).

We can interpret this to be linked to a first compression stage during the Palaeocene and Eocene. The folding creates subsidence on the flank of anticlines as they grow, and this controls the deposition of the growth strata. The detrital materials should thus come from the erosion of the topography created by the folding.

During the Oligocene, the tectonic stops and the environment returns to a calmer setting. The folds created now isolate the basins where the Maykopian series were deposited (Fig. III. 16).

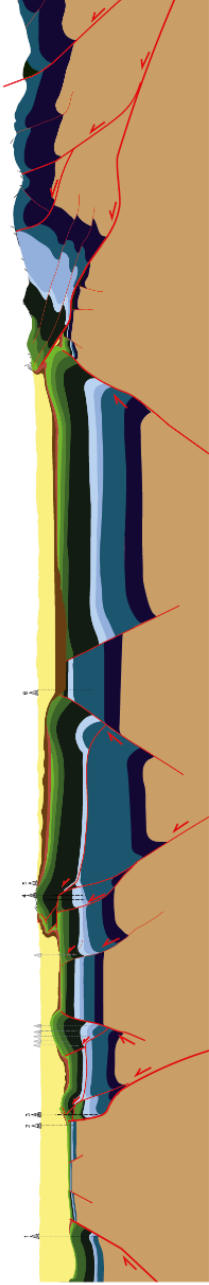
#### b. The Neogene deposits

The Neogene deposits constitute the second part of the Maykopian series during the Lower Miocene. The Middle Miocene deposits are still marine and made of sand. The Sarmatian deposits are deposited in piggy-back basins at the back of the Tsaishi-Gakhomela anticlines. These deposits are all folded until the Meotis-Pontian deposits which delimit the post-tectonic sequence in the Rioni-Am foreland basin.

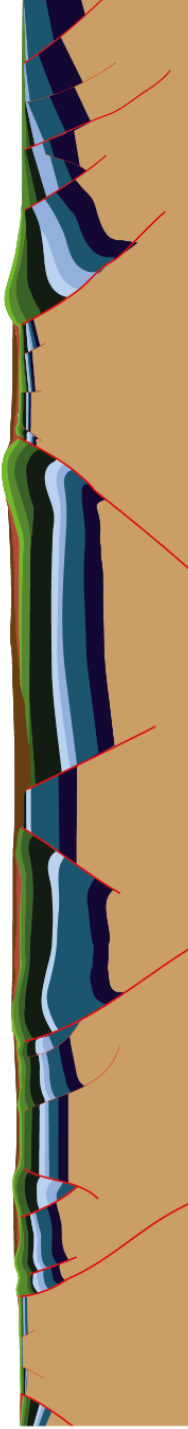
The deformation of the Maykopian series is interpreted as resulting from a second compression event that occurred during the Upper Miocene and was sealed by the deposition of the Meotis Pontian formations.

However, in some places like in the north of the Tsaishi anticline and to the eastern prolongation of the Gakhomela anticline or near the Jvari anticline we observed that the tectonic was and remain active as evidenced tilted quaternary conglomerate deposits. This is also well documented in Tibaldi *et al.*, 2017.

**Present**  
**5 km**



**Oligocene**



**Upper Cretaceous**

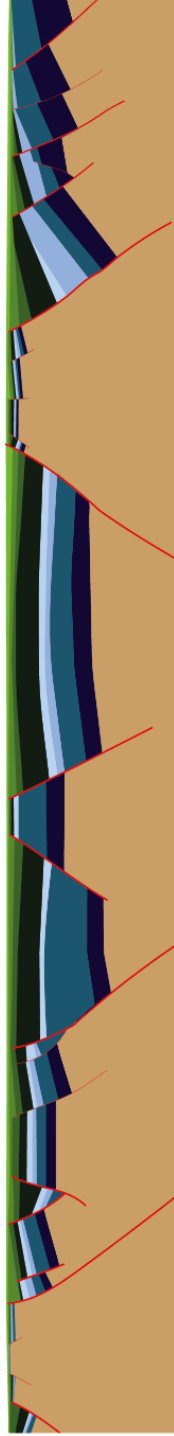


Figure III.15: Reconstitution of the cross-section in the Rioni FB after the Mesozoic. The first compression takes place during the Palaeocene, Eocene and is controlled by thick-skinned tectonic (interpretation from the geometry of the growth strata of the Paleocene-Eocene). The Oligocene period mark a post-compression stage with the subsidence in the foreland basins, separated by the folds which make the basin closed and forming an euxinic environment. The second compression is the well-studied Upper Miocene deformation, which can be related to the thin-skinned and thick-skinned deformations. The thin-skinned deformation take also place in the Neogene deposits. The deformation is known to be still active, even if the Meotis-Pontian deposits mark a difference between the tectonic activity during the Upper Miocene Sarmatian, and the present day tectonic. (Legend is after Fig. III.16)

## 2. In the Kura-Kartli flexural basins

In the Kura and Kartli flexural basins the Paleogene deposits are observed only on the “Military Road” near Ananauri. Neogene deposits are filling the rest of the Kura FB.

### a. the Paleogene deposits

The Paleogene deposits are made of turbidites, with large blocks in the Eocene parts which constitute an olistostrome. The location of these deposits is very important: they are situated between the different thrusts at the southern deformation front of the Greater Caucasus. They are also situated between duplexes of Upper Cretaceous sediments which developed thanks to a probable decollement layer located within the Cenomanian sediments. Near the biggest thrusts, the occurrence of olistostromes highlights the high energetic deposits in this area, that could be related to high deformation and slope.

The Oligocene sediments are deposited only south of the south-verging thrust front. The deposits are made of the Maykopian evaporitic series until the Lower Miocene. In the Kura FB, the Maykopian deposits are richer in evaporitic deposits witnessing the higher evaporation and thus the isolation of this anoxic basin.

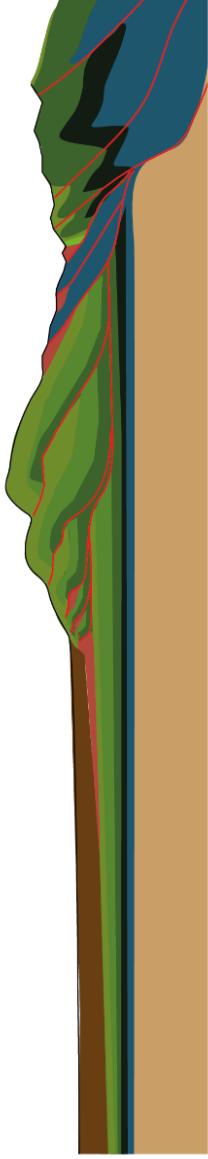
The Palaeocene and Eocene deposits are much alike other known example of syn-collision flysch, like in the Alps and the Oligocene deposits are the post-tectonic deposits following the first phase of convergence. As for the Rioni FB, the Oligocene deposits are constrained geographically by the topography created by the first phase of the compression.

We interpret that there is a major compression stage which implies thrusting and duplexing at the frontal part of the Greater Caucasus during the Palaeocene and Eocene (after the Danian which is still muddy and marks sedimentation in a calm environment). During the Oligocene, the deposits are at the frontal part of the deformation. The high topographic levels due to the compression can isolate the basin and offer the possibility to make it a close evaporitic euxinic basin (Fig. III. 17).

**Present**  
1 km



**Oligocene**



**Upper Cretaceous**

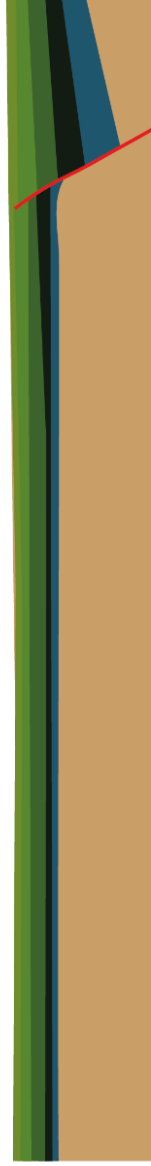
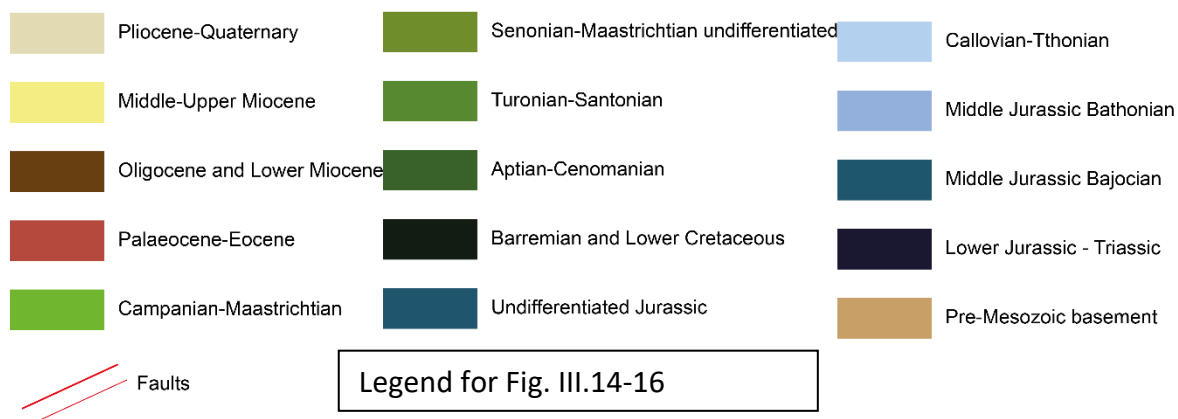


*Figure III. 16:* Reconstitution of the cross-section in the Kura FB after the Mesozoic. The first compression takes place during the Palaeocene, Eocene and is controlled by thin-skinned tectonic with a south progression of the duplex structure. The Oligocene period mark a post-compression stage with the subsidence in the foreland basins, separated by the folds which make the basin closed and forming an euxinic environment (on the figure erosion is not represented in the wedge made of horses). The second compression is the well-studied Upper Miocene deformation, which can be related to the thin-skinned deformations. The thin-skinned deformation takes place in the Neogene deposits probably onto/in the Maykopian deposits. The Meotian Pontian deposits are well deformed in the Kura FB. The deformation is known to be still active, even if the Pli-Pleistocene deposits mark a difference between the tectonic activity during the Upper Miocene, and the present day tectonic. (Legend on next page)



### b. The Neogene deposits

The Lower and Middle Miocene deposits are onto the Maykopian series and are marine detrital sediments (Adamia et al., 2010, 2011, a). The Upper Miocene Sarmatian deposits show growth strata in different places (Fig. III. 14: z, A-C). The Meotis-Pontian deposits are also deformed but show an angular unconformity onto the Sarmatian deposits. This unconformity evidences two stages of compression, but it could also be due to the absence of sedimentation during the transition that occurred during the famous Messinian crisis that affected all the Mediterranean system. Indeed, if the Messinian crisis affected the area while the compression was ongoing, the angular unconformity could then be a biased feature. We chose to talk about only one stage of compression during the Neogene since no “post- stage 2”, nor “pre- stage 3” deposits are observed, and no differences in the convergence directions (Alania *et al.*, 2009, 2017; Forte *et al.*, 2010, 2013, 2015). We can say that these observations are also observed at the frontal part of the Adjara-Trialeti. The post-compression deposits are thus the Plio-Pleistocene deposits, observed in the Kura foreland basins (Fig. III. 14: C).

## V. Discussion, comparison from west to east

### 1. The Paleogene deposits

The Paleogene deposits from west to east are similar in a way because the detrital materials input increases compared to the Upper Cretaceous chalky limestones. However, regarding the lithologies, the eastern part sediments witness a way more energetic deposition environment than in the Rioni flexural basin. There, the only place where the environment seems to be highly energetic is in the alternations of sand-marly limestones observed at the back of the

Tsaishi anticlines in its central part, and at the front and the back of the Ghakhomela anticline, but even then, the stratigraphic record shows that the energy of the deposition environment is certainly not comparable to the Ananauri-Zhinvali area. In both parts, these deposits are deformed by syn-sedimentary normal faults (Fig. III. 8 and Fig. III. 12) evidencing an active tectonic subsidence during the basin formation.

Regarding the Palaeocene marls situated in the Rioni foreland basin, to our knowledge there is no equivalent in the eastern part, except for the calm Danian deposits. The Palaeocene flyschs in the Kura foreland basin highlight a more energetic environment, more materials (related to more erosion?). Based on our observations of differences in the style and the intensity of deformation from west to east, we propose that the reason for more energetic deposits can be related to a higher deformation rate or to a different style of deformation.

We have observed that in the western part the tectonic is more linked to thick-skinned and thin-skinned tectonic, but there is no nappe formation. However, in the eastern part the thin-skinned tectonic is the main style of deformation and the material is moved toward the south implying intense shortening by duplex and thus, the syn-tectonic deposits are made of flysch into the deformation while in the Rioni FB, deformed with thick-skinned tectonic, the syn-tectonic deposits are deposited in growth-strata geometry forming onlaps.

The Oligocene Lower Miocene deposits of Maykopian series are similar but slightly different from west to east. Indeed, to the west these are more detrital and less evaporitic. We argue that in the western part, according to the figure 1, the basin is smaller because it is delimited by several folds and so the detrital material comes from all around the basin. In the eastern area near Kura/Kartli the basin is also closed but larger and so the detrital materials are localised at the borders while in the central part of the basin, the subsidence and the distance from the source of coarse detrital material promotes evaporitic and/or much finer detrital deposits. Such setting offers a great environment to create a calm and euxinic basin where evaporation can take place.

The evaporitic layers should be more present in the central part and thus can offer more possibilities to form a decollement level and create thin-skinned tectonic in the basins, or salt-tectonic deformation as well. This is observed in the syncline of the Eastern AT where the Oligocene deposits are folded.

## 2. The Neogene deposits

From the west to the east the Middle to Upper Miocene deposits are not very different in their nature. Some variations of continental to marine environment are described (Adamia, 2002, 2011a) and point that the western part is longer an open marine environment linked to the Black Sea.

However, the main difference is that in the western part the Meotis-Pontian deposits are poorly affected by the tectonic while the same deposits to the east are forming well deformed growth-strata.

This could be related to a higher rate of deformation in the eastern part during the Late Miocene and younger ages while in the western part the compression stage has a low rate of deformation after the Upper Miocene.

## Conclusion

We have observed in the field the post-Mesozoic deposits in the foreland basins of Rioni and Kura. The particularity is that these are formed at the front of the Greater Caucasus during its inversion. The tracking of the Palaeocene deposits offers us to observe some variations along the folds in the Rioni foreland, and to highlight the unconformity of the Oligocene deposits onto the Palaeocene-Eocene formations. This major unconformity shows a geometry of growth strata, allowing us to consider the Mesozoic deposits as pre-tectonic deposits, the Palaeocene and Eocene deposits as syn-tectonic deposits, and the Oligocene-Lower Miocene deposits as post-tectonic deposits. The tectonic setting during Palaeocene-Eocene is compressional and coincides with the collision between the Eurasian Plate and the TASAM during which the folds of Tsaishi and its eastern prolongation as in Gakhomela formed. The Jvari area and the southern GC are also impacted at this time by folding. The style of deformation we identified seems to be thick-skinned driven tectonic, even if some decollement levels are observed as in Tsaishi onto the Upper Jurassic, as well as in the Gakhomela anticline into the Upper Cretaceous.

Near Ananauri, to the east, at the Kartli and Kura basins transition, the observations are made on the frontal part of the Greater Caucasus. At this place the tectonic style shows some duplexes and is triggered by thin-skinned tectonic deformation. The thin-skinned tectonic involves formation of flysch and olistostrome deposits during the Palaeocene and Eocene. The

Oligocene deposits are then deposited at the frontal part of the deforming region and mark also the post-tectonic stage.

The timing of the Palaeocene-Eocene compression is the same from the west to the east but is marked by a difference in the style of deformation. The role of the Mesozoic normal faults (chapter 2) in the Rioni FB could be interesting to study. The difference on the convergence rate and amount of shortening is not well constrained in this study.

The second compression stage which take place during the Upper Miocene stopped or at least slowed down in the Rioni FB after the Sarmatian, while it was still very active during the Meotis-Pontian in the Kura FB. In both places some active tectonic is described in present days.

This study offers two major conclusions: the first is that, as it is observed around in the Caucasus area, a major compression stage takes place during the Palaeocene and Eocene. The second is that the style of deformation can be triggered by the inherited structures and plays a role in the style syn-tectonic deposits geometries and lithologies.

The differences from western to eastern Georgia can be related to these inherited structures, however the question about the possibility to have a different deformation/shortening rate along the Caucasus is interesting because of the rotational tectonic observed in the whole area (which could make a higher rate in the eastern area).



## *Chapter 4: The structure of the Adjara-Trialeti Fold-and-thrusts belt*

## I : Introduction

The Cenozoic Adjara-Trialeti Fold-and-thrusts belt (AT in Fig. IV 1) borders the southern part of the foreland basins of Rioni and Kura (RFB, KuFB in Fig. IV 1) and the northern part of the Lesser Caucasus range (LC in Fig. IV 1 inset). The southern border of the AT is covered by quaternary volcanic deposits (lavas, tuffs) and thus the location of the southern border of the AT cannot be well defined. Moreover, the relation between the AT and the LC (that includes some outcrops of the variscan basement) cannot be observed in the field.

The northern part of the AT shows some north-verging thrusts into the foreland basins. The north-verging thrusts are observed in the whole northern part of the AT. However, exposed terrains in the southern part of the AT are dominated by south-verging thrusts. The AT is thus a bi-verging fold-and-thrusts belt (see Fig. IV 1). The different interpretations in the literature suggest two contrasting mechanisms to explain the large-scale structure of the AT belt: some authors propose a thin-skinned tectonic deformation model with some major decollement levels and a structure made of major duplex structures with a decollement level in the Upper Cretaceous deposits (Banks *et al.*, 1998; Adamia *et al.*, 2010, 2011; Alania *et al.*, 2017b, 2020). Others propose a thick-skinned tectonic deformation model which results from the inversion of the basin (Khain 1975; Sosson *et al.*, 2010, 2013; Adamia *et al.*, 2011). Both interpretations imply important differences regarding the amount of shortening. The origin of the north-verging folds and thrusts that delimits the northern AT depends also on the interpretations on the style of deformation. The thick-skinned deformation style depends on the normal faults inherited from a Paleogene basin. The thin-skinned deformation style implies that the north-verging folds and thrusts are related to retro-thrusting with respect to the general vergence of the LC (Alania *et al.*, 2017b).

The geometry of the belt is elongated in an E-W to NE-SW direction. It is thinner at the eastern end, near Tbilisi. To the West, the belt is wider and take a NE-SW direction. During the Cretaceous and Paleogene, the AT is interpreted to be a volcanic arc (Banks *et al.*, 1998; Alania *et al.*, 2017b). The continuity or the relation with the Eastern Black Sea (EBS in Fig. IV 1) is still matter of debate: while some link the AT with the EBS (Adamia *et al.*, 2010, 2011), others tend to link the AT with the Pontides volcanic arc (Nikishin *et al.*, 2013; Sosson *et al.*, 2010; Sosson *et al.*, 2016) and Meijers *et al.*, (2017) interpret the belt as an orocline composed of the LC and the Pontides.

We propose to take a closer look into the AT, with a comparison between the western and the eastern parts, in order to observe whether the EBS has a link with the western AT, and to better constrain the role of the AT during the tectonic evolution of the Caucasus since the Cretaceous.

The general structure of the AT belt will be constrained by field observations and seismic lines (access for the interpretation from TOTAL, Paris).

In the first hand, the structure of the AT belt before the compression will be constrained by the variation in lithologies and thicknesses of the Cenozoic series, through field observations and wells data in the western area.

In the another hand, the style of deformation in the belt will be constrained through a thorough description of our structural observations: the thin-skinned tectonic deformations and the small-scale deformation will be pointed out, as well as the lithologies that might operate as decollement levels to create the thin-skinned tectonic deformations.

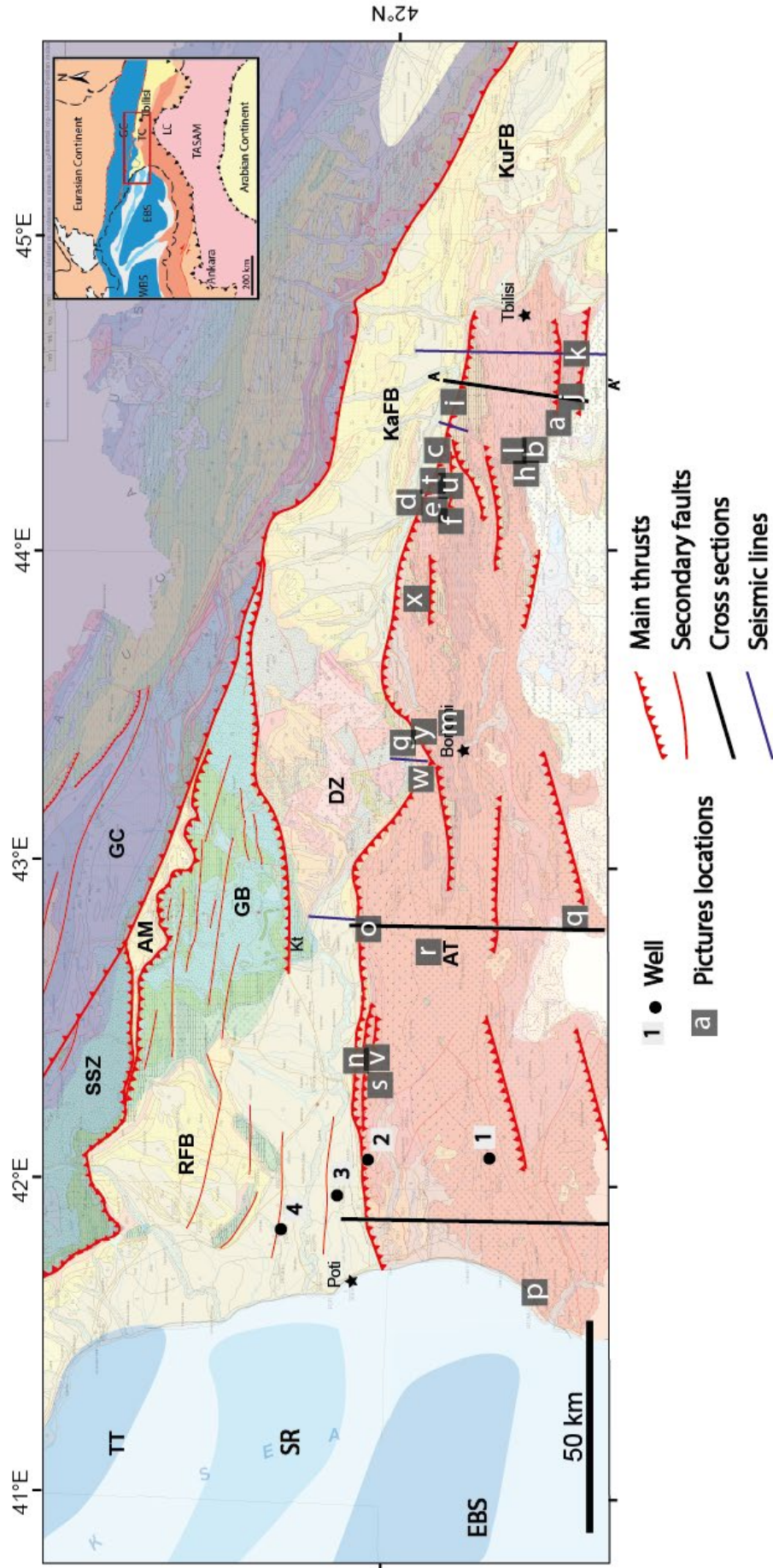


Figure IV.1: Tectonic map of the Adjara-Trialeti fold-and-thrusts belt and the neighbouring areas. TT: Tuapsee Ridge, SR: Shatsky Ridge, EBS: Eastern Black Sea basin, SSZ: Southern Slope Zone of the GC: Greater Caucasus basin. GB: Georgian block, AM: Amrbolauri foreland basin RFB: Rioni foreland basin, DZ: Dzirula massif, AT: Adjara-Trialeti fold-and-thrusts belt, KaFB: Kartli foreland basin, KuFB: Kura foreland basin.

## II. Geological Setting

The AT is mostly constituted of Paleogene deposits, especially in the central and the western parts. However, the Paleogene deposits present thickness variations and where the deposits are thinner (at the borders and in the eastern part) the core of anticlines can bring Cretaceous deposits at the surface allowing us to make some direct observations. The figure IV 2 shows how the AT deposits vary from Eastern to Central and Western parts. The Lower Cretaceous Barremian deposits are only known in the western part, where wells (see Fig. IV 4) go through the younger deposits. These deposits are made of dolomitized limestones, as described in the Rioni area (chap. 2). The Aptian-Cenomanian deposits in the western-central part are 650 to 1700m thick and constituted of volcanics and clayish limestones. In the Eastern part we observe a 100 to 200m thick deposits of Lower Cretaceous marls, clays and marine turbidites (Fig. IV 3 e). The Upper Cretaceous (Turonian-Maastrichtian) deposits are 500 to 900m thick limestones and sandy limestones in the western-central part of the AT, and are 200 to 300m thick limestones in the eastern part, locally known as “Tetriskaro limestones”. Palaeocene to Lower Eocene deposits are 600 to 1200m thick terrigenous turbidites in the western-central part of the AT, and from 50 (or even less near the borders) to 1200m in the eastern part. These deposits are known as “Borjomi flysch” and are deformed by syn-depositional normal faults (see section 3). The Middle Eocene deposits are of volcanic origin and are 1600 to 2800m thick in the western-central part. These latter deposits can be separated in three formations (Likani, Kvabishkhevi and Dviri formations), see Adamia et al., (2011a). Here, these formations will not be separate. In the Eastern part, the Middle Eocene deposits are from 50 to 500m thick and constituted of tuffturbidites, volcano-related lithologies, and olistostromes and terrigenous turbidites (especially to the eastern ending of the AT). The Upper Eocene deposits in the western and central parts are constituted of 50 to 200m thick terrigenous turbidites. In the eastern part, the Upper Eocene deposits are made of 500 to 1000m thick interbedded marls and terrigenous turbidites (especially near Tbilisi).

The Oligocene deposits, already described in chapter 3 within the Rioni and the Kura FB, are constituted of mainly evaporitic and clay deposits in euxinic environment. The thickness varies from 50 to 400m in the western part (in the synclines in the western part near Choloki and Batumi), and from 600 to up to 1000m in the eastern part, especially in the synclines at the eastern extremity of the belt near Tbilisi. We have to point that some duplex structures are

described (Alania et al., 2012) in the eastern part in the Oligocene deposits (see chapter 3), and this could bias the thickness interpretation in this area.

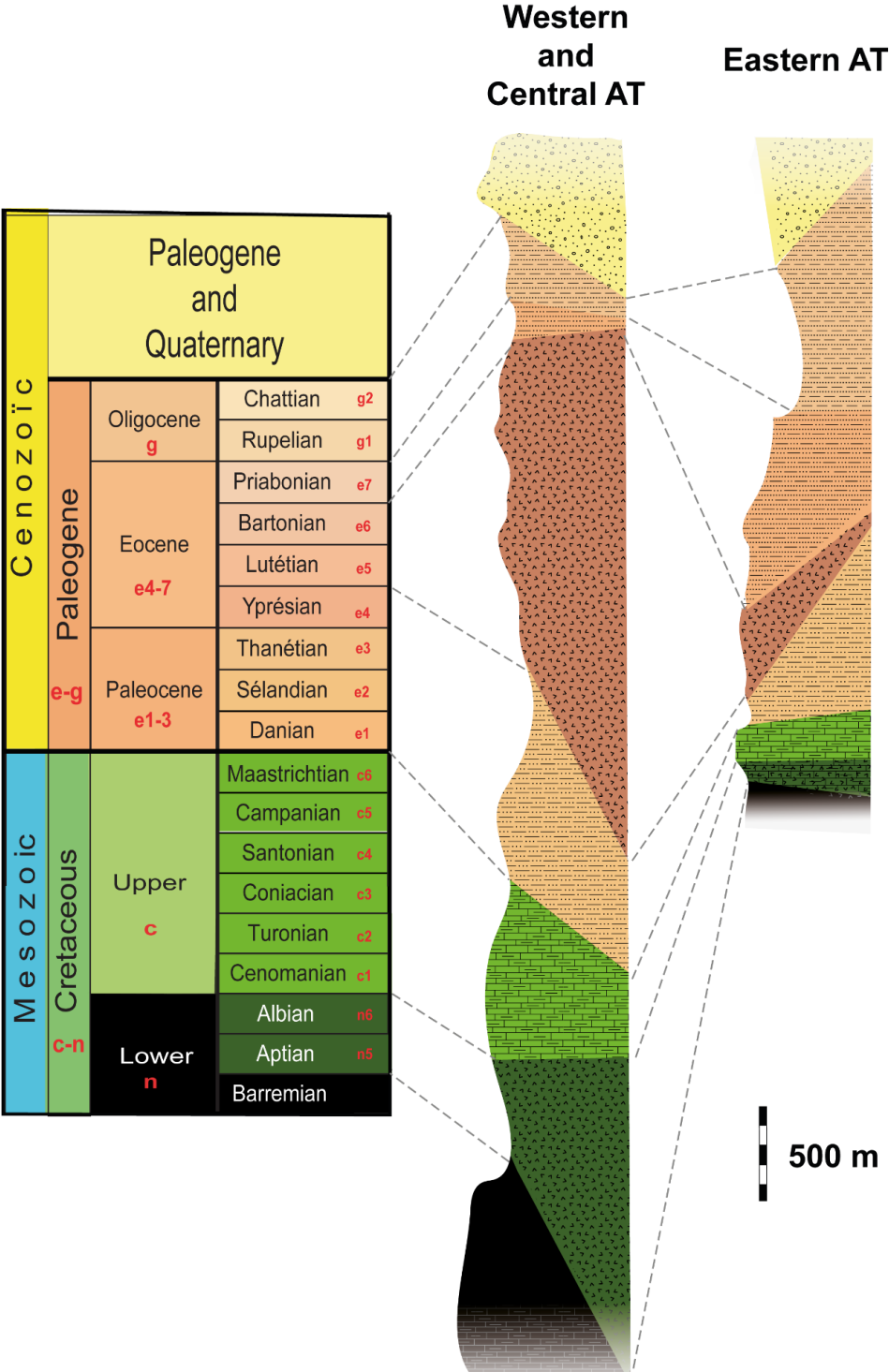


Figure IV.2: Stratigraphic log with thickness variations, modified after Adamia et al., (2011a). The colors and frames are used to separate the ages, for the nature of the deposits see the text.

### III. Observations

#### 1. Nature and thickness of the deposits along the AT

##### a- The Cretaceous deposits

The oldest deposits observed in the Eastern AT are the Aptian-Cenomanian deposits made of green clays and marls (Fig. IV 3, e). These are observed in the central part of an anticline located in the eastern part of the AT (see location d, e and f in Fig. IV 1). This lithology is interesting because it could be a possible decollement level consistent with the interpretations of thin-skinned deformation models. These deposits evolve into white sandy-marly limestones deformed by syn-depositional normal faults, and soft pebbles which are deformed (Fig. IV 3, d). The normal faults tend to show a deepening toward the west (see location of the picture on Fig. IV 1). The Maastrichtian-Campanian deposits are constituted of white chalky limestones with some intercalation of lenses of chert which are intruded and alternate with interbedded lavas flows (Fig. IV 3, c), and volcanic deposits (Fig. IV 3, a). These deposits evolve into more marly deposits which become reddish until Danian age (Fig. IV 3, b).

The oldest deposits observed toward the west are only observed on the southern border of the Dzirula massif and have been described in detail in chap. 2. The Aptian-Cenomanian deposits are made of clays and marls which alternate with marly limestones (Fig. IV 3, f). The Upper Cretaceous deposits are made of sandy and marly limestones (Fig. IV 3, g) with reddish cherts, as observed near the Tsaishi folds (chap. 2) (see the structure of the southern border of Dzirula in the further section). Towards the west we have not observed the Cretaceous deposits however these can be present deeper as observed with the wells data (Fig. IV 6).

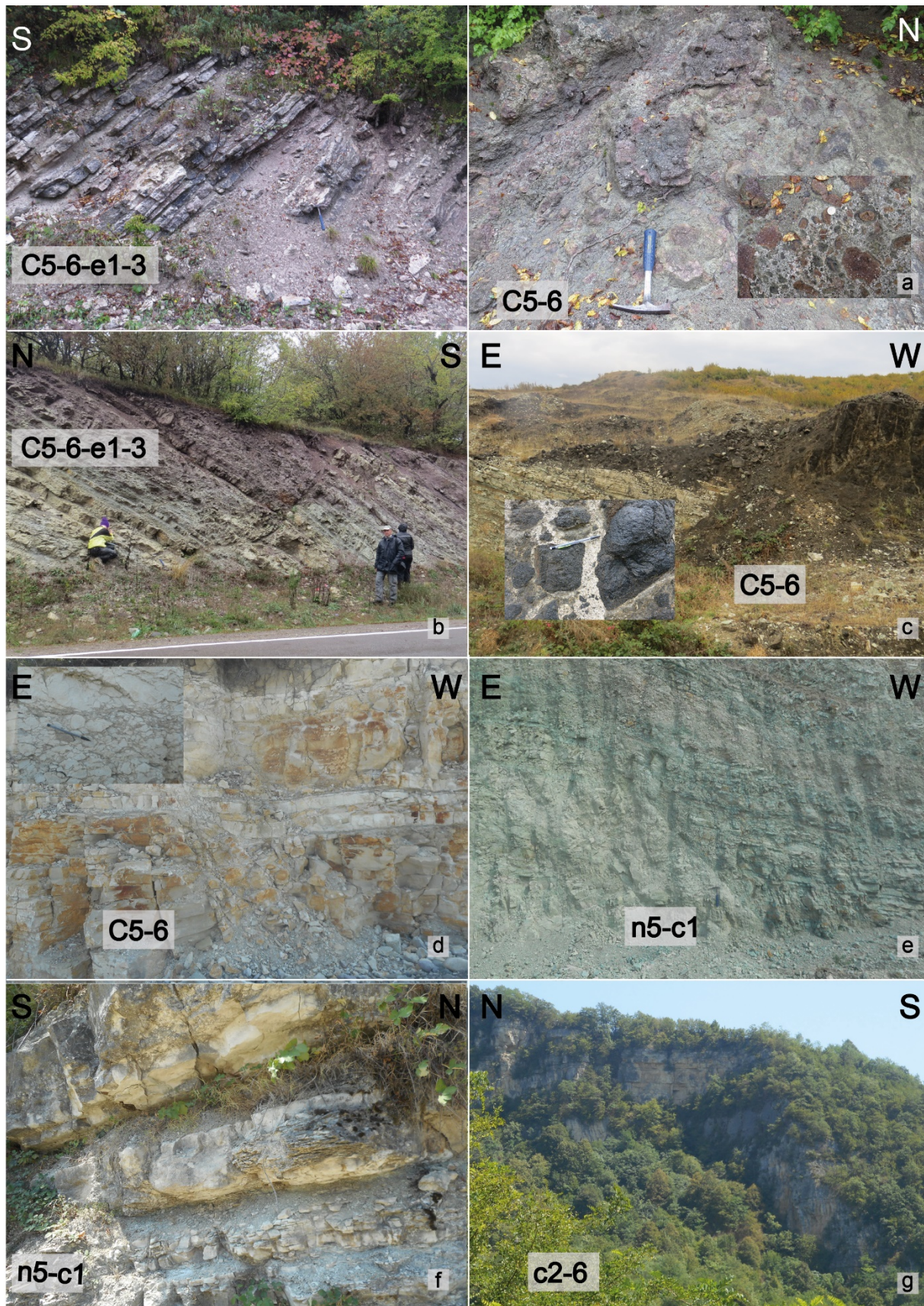


Figure IV.3: Pictures of the Mesozoic deposits observed along the AT. See Fig. IV 1 for the location of the deposits. a: Upper Cretaceous Campanian-Maastrichtian deposits which alternates with limestones, marls and volcano-related deposits, the two pictures show the evolution of the deposits,



and the zoom in the volcanoclastic deposits, b: end of the Upper Cretaceous - Danian deposits (reddish deposits). We observe some normal faults in this area. c: Campanian-Maastrichtian deposits which are intruded and alternates with volcano-related deposits and a picture of the details from the intrusion between the lavas and the sedimentary deposits. d: Campanian-Maastrichtian deposits with gravity deformations, e: Aptian-Cenomanian deposits of greenish clayish deposits. f: Aptian-Cenomanian deposits south of the Dzirula massif. These deposits cover unconformably the Variscan basement (or onto the Jurassic deposits). g: The Upper Cretaceous deposits in the southern Dzirula massif.

#### b- The Paleogene deposits

In the Eastern AT, the Paleogene deposits are thinner than in the western and in the central parts. In the folds situated at the northern and southern borders, the deposits thicken toward the central part (several hundred meters) of the AT and are thinner at the borders (several tens of meters) (Fig. IV, 2 Eastern AT).

The Palaeocene-Lower Eocene deposits are made of turbidites/flysch and are deformed by normal faults (Fig. IV 4, h, Fig. IV 5, m). The Palaeocene deposits can also be thinner as observed in Fig. IV 4, i. The Palaeocene marly-sandy deposits evolve in Middle Eocene volcano-related deposits (Fig. IV4, i). The Middle Eocene tuff-turbidites and volcano-related deposits (volcano-sedimentary deposits and lavas flows) cover the Lower Eocene clayish-marly deposits (Fig. IV 4, i, j and Fig. IV 5, n). The Middle Eocene can be made of olistostrome (Fig. IV 4, k) or by volcano-related deposits (Fig. IV 5, o, p, q, r). These deposits can be several thousand of meters thick as in the central part of the AT where most of the highs are made of the Middle Eocene volcano-related deposits (Fig. IV 2). The Upper Eocene deposits are more detrital and can be made of sandstones (more orange) with some oil content (Fig. IV 4, k, l, Fig. IV 5, s).

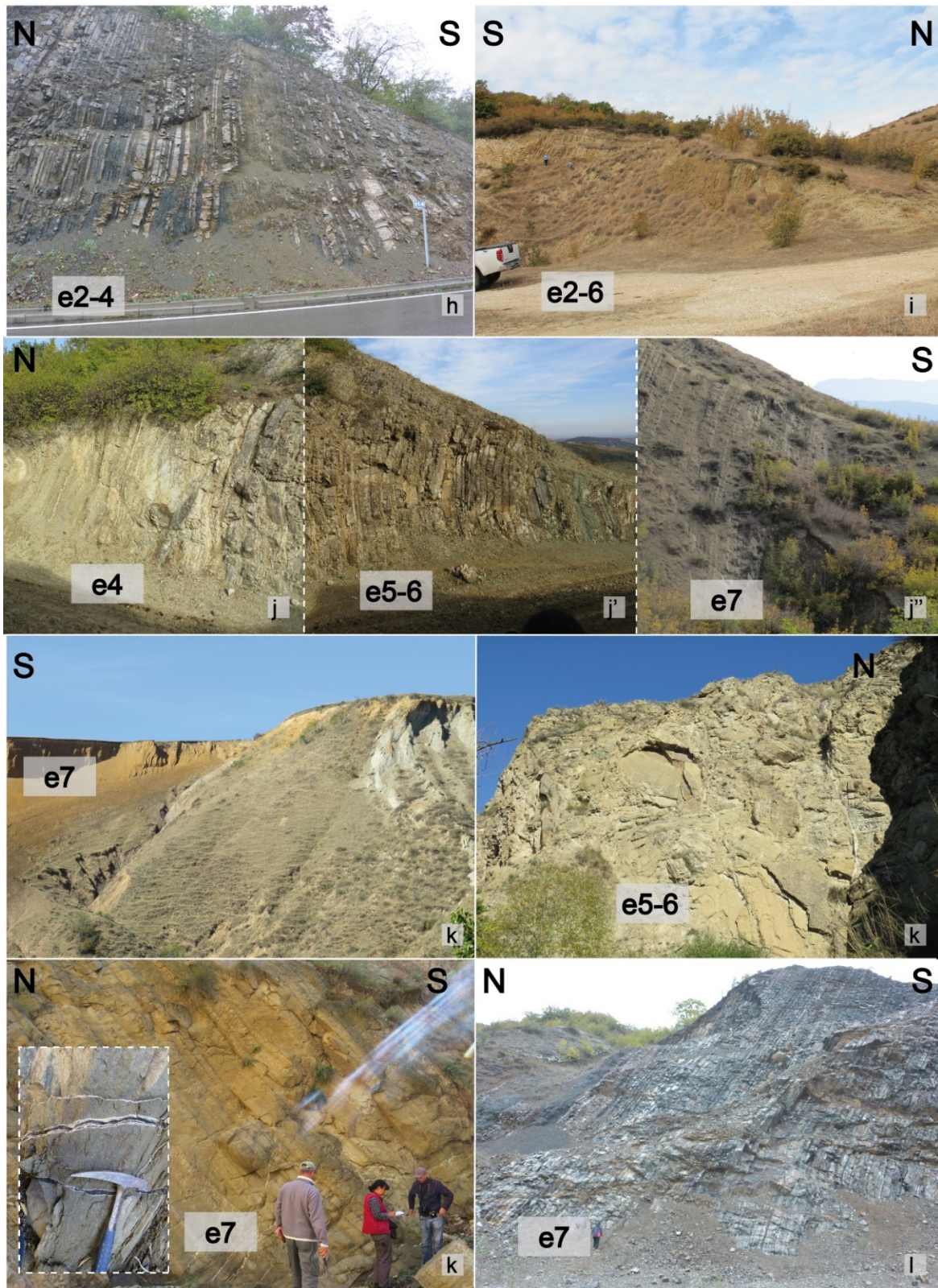


Figure IV.4: Pictures of the Paleogene deposits in the Eastern AT. See locations of the pictures in Fig. IV 1. h: Palaeocene-Lower Eocene deposits deformed by a normal fault and then folded, i: Palaeocene marly-sandy deposits to Middle Eocene volcano-related deposits in the north eastern AT j: Lower Eocene marls and clays, Middle Eocene more sandy deposits and Upper Eocene sandy deposits k: Middle Eocene Olistostrome, Upper Eocene sandstones (more orange) with picture of the oil content in detail l: Upper Eocene turbidites- sandstones, with oil-rich veins.

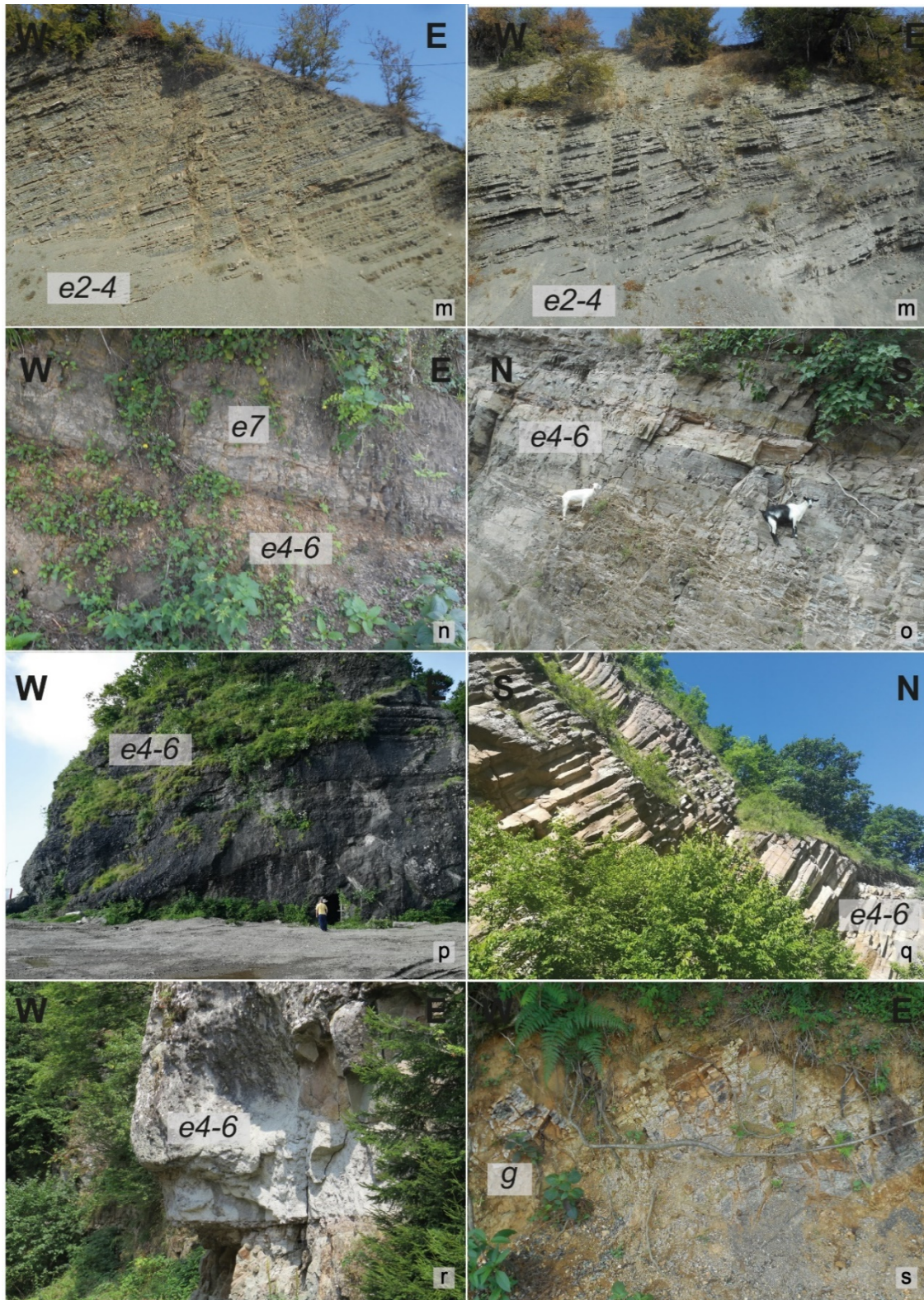


Figure IV.5: Pictures of the Paleogene deposits in the Western and central AT. See locations of the pictures in Fig. IV 1. m: Palaeocene-Lower Eocene typical Borjomi flysch deformed by normal faults. This formation can be very thick (Fig. IV 2, Fig. IV 6). n: contact of the Middle Eocene tufturbidites onto the Lower Eocene more sandy turbidites o: Middle Eocene tufturbidites p: Middle Eocene lava flows along the southern Black Sea coast q: Middle Eocene andesitic lava flows with columns r: pyroclastic flows onto tuff turbidites into the Middle Eocene deposits: Upper Eocene deposits (near the Oligocene maykopian deposits)

### c- Wells data in the Western-Central AT

We have also ten wells logs (see location in Fig. IV 1), which are presented in Fig. IV 4. Choloki 1 is consistent with Choloki 2 and 3, Chokatauri 4 is consistent with Chokatauri 5, Lesa 5 is consistent with Lesa 3, 6 and 12. To see wells data to the north, see chapter 2. Wells Shromisub 58 and 59, situated west of the Chokatauri wells, are filled by more than 3000m of Neogene deposits and do not bring any information about Paleogene or Mesozoic deposits.

We observe the sedimentary succession from south to north. The Choloki wells in the western-central part of the AT are comminated with Middle Eocene volcanic deposits that are more than 5000m thick and covered by Neogene deposits (without Oligocene deposits). The Chokatauri wells show nearly the same succession, but the Oligocene deposits (made of clays and marls) are deposited onto the Middle Eocene volcanic deposits. The older deposits are not reached in these wells. Further to the north, the Lesa wells show that the Neogene deposits are directly deposited onto the Mesozoic deposits without Paleogene deposits. This reveals a major difference between the well 2 and 3 (Chokatauri and Lesa) about the AT. However, Lesa 5 compared to Sagv. 6, as we have observed in chapter 2, show thicker Aptian-Cenomanian and Barremian deposits. Moreover, the wells data offer some details about the Aptian-Cenomanian deposits where some volcanic deposits (of andesitic composition) are observed in the clayish limestones, while the Barremian deposits are, as observed toward the north in the chapter 2, dolomitized limestones.

## 2. The structures

To better constrain the structure of the AT and to understand why the models of thin and thick-skinned are opposed we will separate our observations in two parts. In the first one, we present our observations of thin-skinned and small-scale tectonic deformations with the identification of potential decollement levels. This part will thus illustrate the observations that can fit with the thin-skinned model. In the second part, we will focus on the general structure of the AT to try to understand why it is bivergent and nearly symmetrical and to see if the main fold/thrust can be related to inherited structures. These observations will help us to discuss the thick-skinned model.

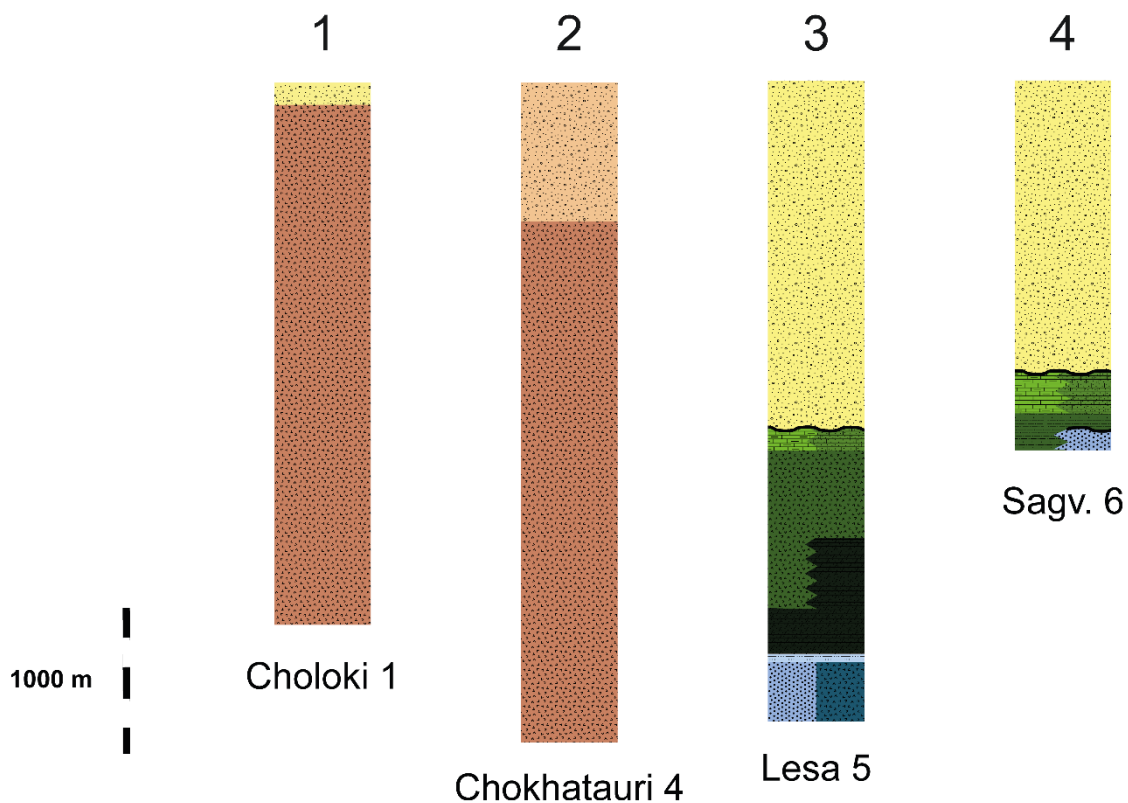


Figure IV.6: Wells data in the Western-Central part of the AT, illustrated in stratigraphic log with thickness. See location in Fig. IV 1, and legend in Fig. IV 2 and II 2 for the Jurassic colors.

### 3. Thin-skinned and small-scale tectonic

We have observed some small-scale deformations that can be the origin of some decollement level or at least some thin-skinned tectonic deformations. As observed in Fig. IV 3, e, the green clayish deposits of the Aptian-Cenomanian deposits can be a decollement level. Moreover, we have observed some deformations into the Upper Cretaceous deposits of tens of meters scale (see Fig. IV 7 t, u). The Upper Cretaceous deposits are also deformed in small-scale into the major folds at the borders (Fig. IV 7, v) and near the Dzirula massif (Fig. IV 7, w). For a comparison, the deposits are less deformed in the Georgian Block (chap. 2 and 3). The Palaeocene deposits of the Borjomi flysch are deformed by normal faults and are folded. At a larger scale, as in Fig. IV 4, h, we can observe that the whole formation that is tilted, but in Fig. IV 7, m, we observe that the deposits are deformed by the normal faults in an EW/NESW direction and are also deformed by decametres folds in a N-S direction. On the borders of the

AT, the Palaeocene deposits are also deformed in small-scale as observed in Fig. IV 7, x, y; while these deposits are part of main folds/thrusts which define the AT borders.

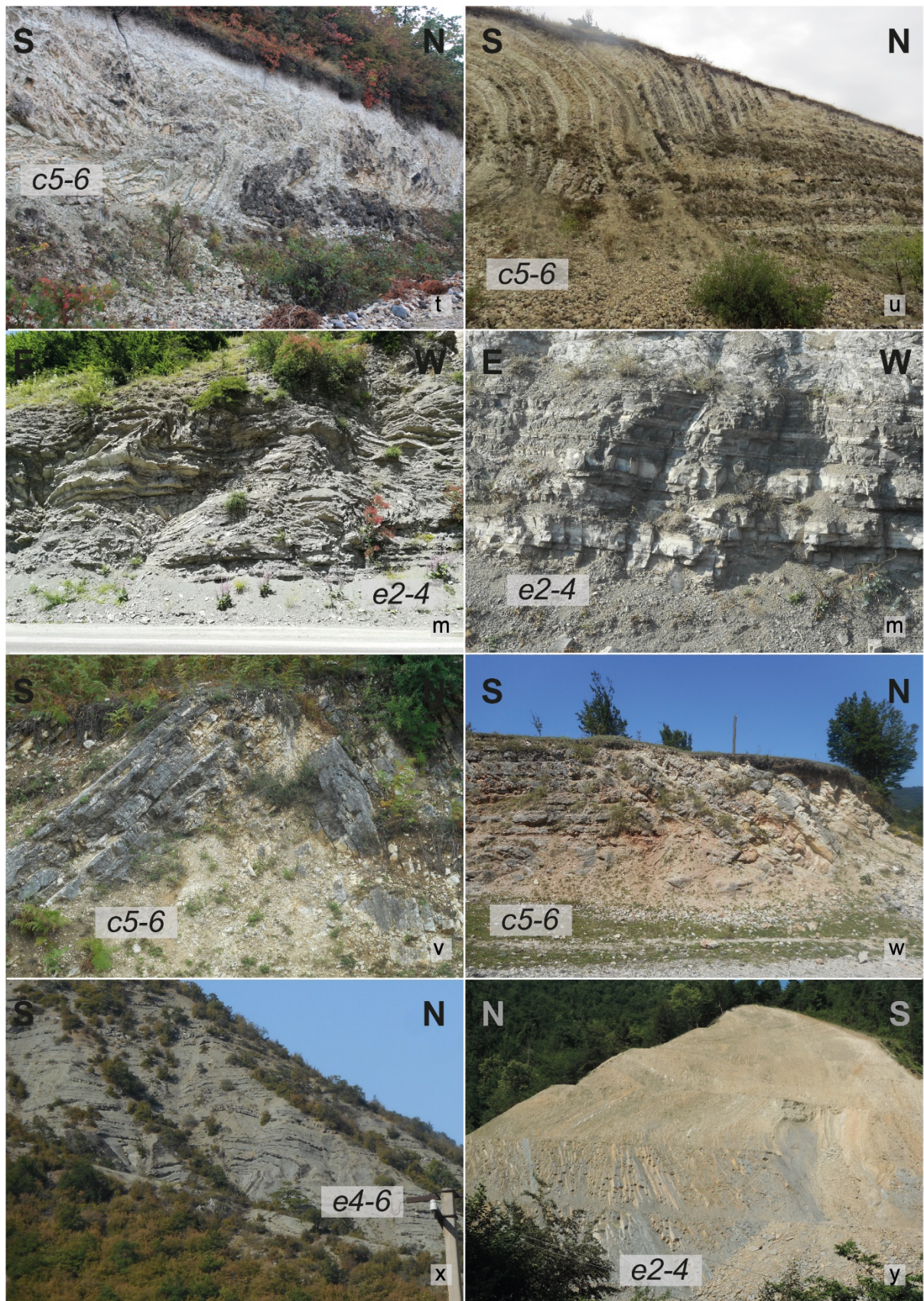


Figure IV.7: Pictures of small-scale deformations in different deposits along the AT. See locations of the pictures in Fig. IV 1. t and u: folds observed in the Upper Cretaceous deposits along the northern border of the eastern

AT, v: fold observed in Upper Cretaceous along the northern border of the western-central AT, w: thrust observed in the Upper Cretaceous deposits south of the Dzirula massif, x: folds observed in the Middle Eocene volcanic tuffturbidites into the central AT, y: folds observed in the Palaeocene deposits of the AT, south of the Dzirula massif.

#### 4. Thick-skinned tectonic and major fold-and-thrust structures of the belt

The AT presents a structure that can be highlighted directly on the geological maps (Abesadze *et al.*, 2004) as well as on the aerial pictures or satellite's pictures. Google Earth imagery offers a great opportunity to outline the major structure (Fig. IV 8). The structure is bivergent and show major anticlines to the north, and to the south, with a symmetry which separates both vergences in an E-W direction.

##### a- The borders

The borders are easier to study since we can observe the variations in the deposits from the Cretaceous to the Neogene, but the major anticlines observed into the AT show the same kind of structures with a gentle dipping at the back of the folds, and a very steep to reverse dipping at the frontal part. The Fig. IV 8 illustrates these observations. Thin-skinned small-scale deformations are observed, with normal faults into the Palaeocene and Eocene deposits, and small-scale folds in the Cretaceous deposits. The small-scale folds can be observed also in the Palaeocene-Eocene deposits (Fig. IV 7, m, x). The change of deposits near the borders allows us to highlight the important thickness variations from the border (front of the anticline) toward the central AT. The second cross-section of the Fig. IV 8 shows also the unconformity of the younger deposits onto the older that are more tilted. This remind us the "fan-shapes" with the onlaps observed in the chapter 2 in the Georgian Block, at the major anticlines.



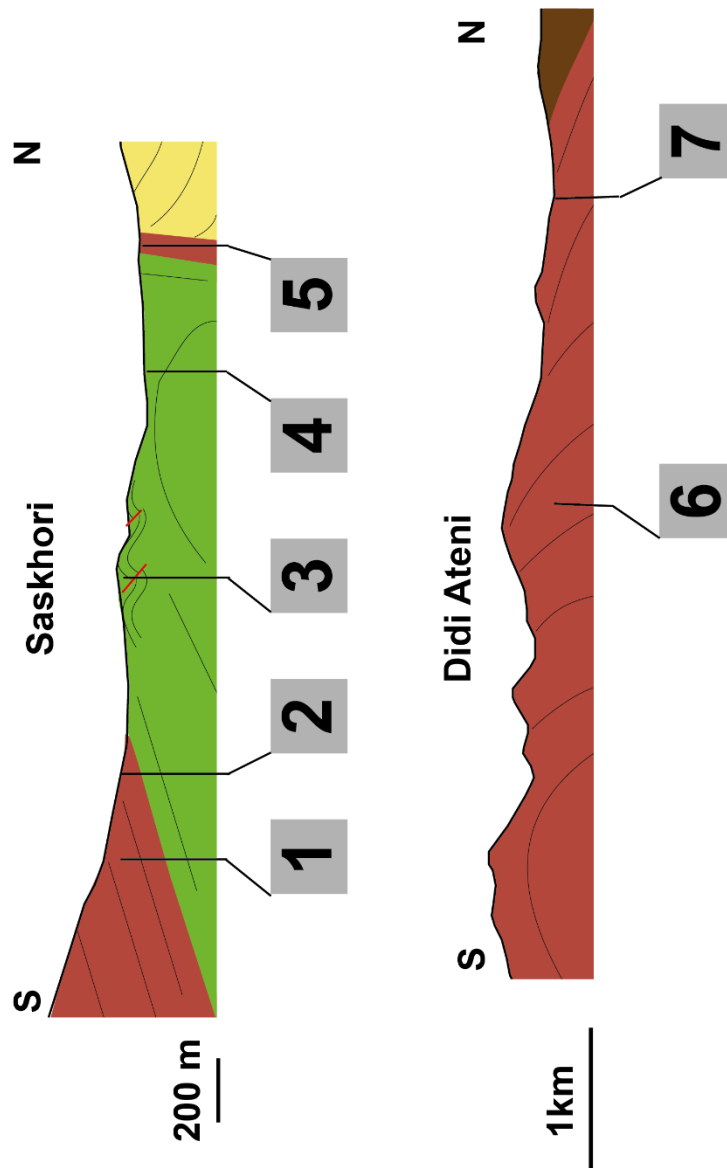
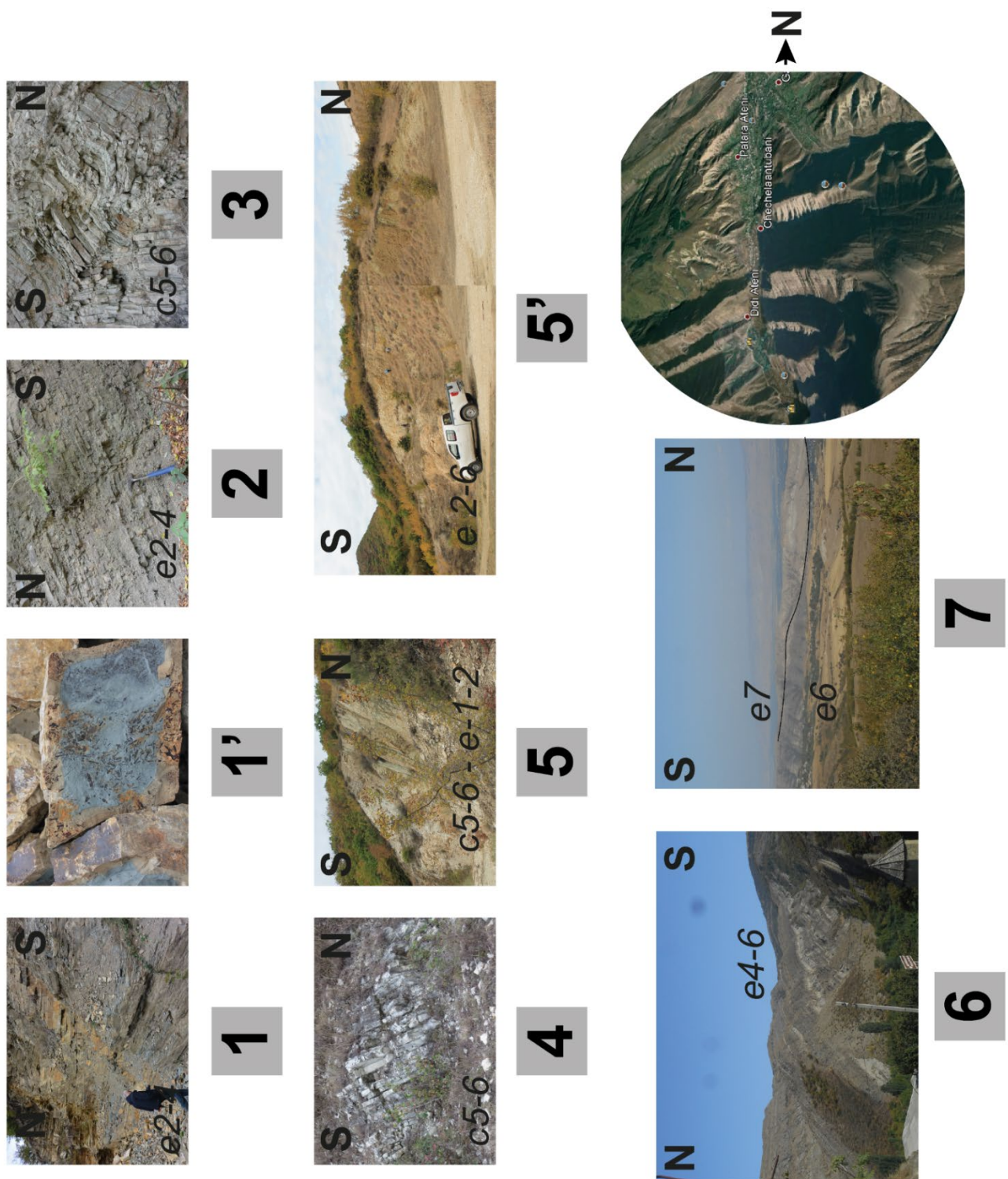


Figure IV.8: Cross sections on the northern border of the AT with associated pictures (see Fig. IV 8 bis) of the northern border of the AT (see locations in Fig. IV 1). The Saskhori cross sections is situated more to the eastern ending of the AT than the Didi Ateni which is more central. The main difference is the thickness of the Palaeocene-Eocene deposits and the growth-strata observed in the Didi Ateni cross section. Legend see Fig. IV.10.



**FIGURE IV.8 BIS: THE GOOGLE EARTH SCREENSHOT SHOWS THE WELL IDENTIFIED ANTICLINE. THE OPPORTUNITY TO OBSERVE THE MAJOR FOLDS IN THE AT HAS BEEN USED TO CONSTRAIN THE STRUCTURES. PICTURES: 1: PALAEOCENE TURBIDITES AFFECTED BY NORMAL FAULTS. THE DETAILS (1') SHOWS SOME FOSSIL TRACES OF LEAVES. 2: NORMAL FAULT AFFECTING THE PALAEOCENE TURBIDITES. 3 AND 4: THE MAASTRICHTIAN DEPOSITS, DEFORMED BY SMALL-SCALE FOLDS. 5: THE TRANSITION FROM UPPER CRETACEOUS TO MIDDLE EOCENE DEPOSITS. PICTURES OF THE DIDI ATENI CROSS-SECTION ARE THE LANDSCAPE OF THE CROSS SECTION WHERE WE CAN OBSERVE THE MIDDLE EOCENE TO UPPER EOCENE DEPOSITS.**

## b- Dzirula

The Dzirula massif borders also the northern AT (Fig. IV 1). However, the structure is slightly different from the other borders and the major structures situated in the AT. Here, there is the opportunity to see the structure that separates the AT tectonic units from the Dzirula massif, interpreted as a horst in the chapter 2. It is important to constrain the tectonic behaviour of the southern part of the Dzirula massif in order to compare with the tectonic behaviour of its northern part (chap. 2 and 3). We observe in the Dzirula massif the Mesozoic deposits, with unconformities of the Lower or Upper Cretaceous onto the variscan basement or the Bajocian volcanic deposits. The Palaeocene deposits, observed onto the Upper Cretaceous deposits, are the same deposits as observed in chapter 2 in the Georgian Block/Rioni foreland basin: grey marls and detrital deposits (picture 2 in Fig. IV 9). The Upper Cretaceous deposits are deformed with small-scale thin-skinned thrusts. To the south, the Palaeocene-Eocene deposits, typical of the AT basin are thrust and sheared against the Dzirula Massif.

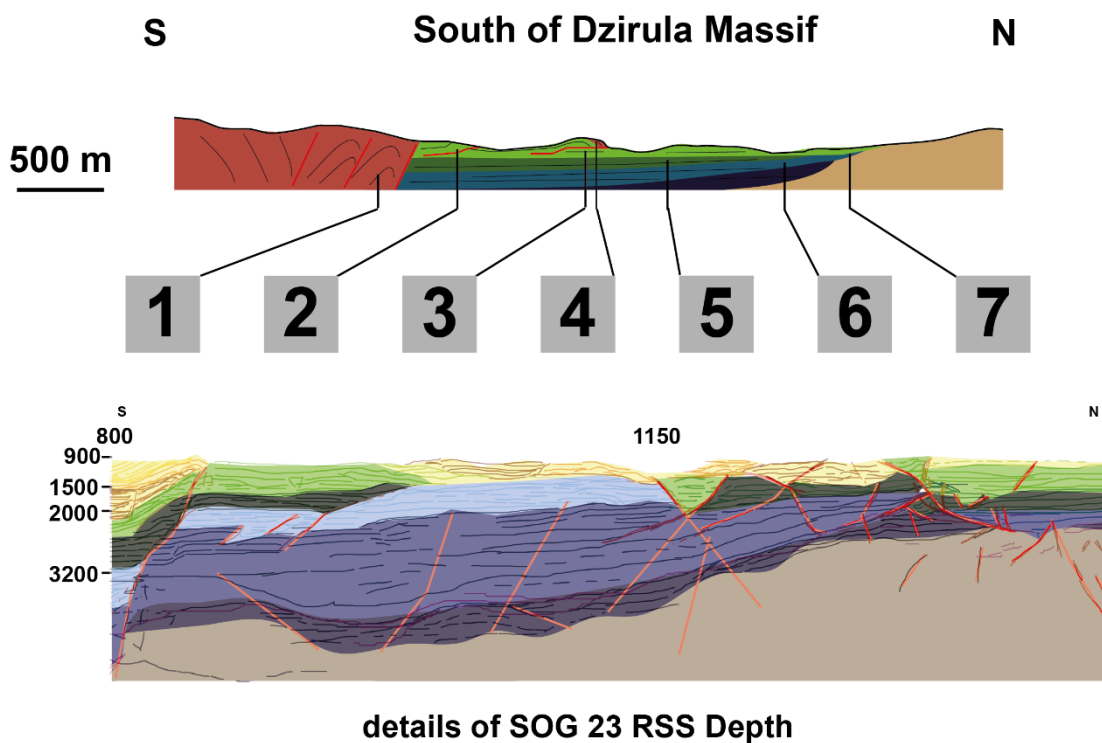


Figure IV.9: Cross section south of the Dzirula massif, at the transition with the AT with associated pictures (see Fig. IV 9 bis). See location in the Fig. IV 1. interpreted seismic line (see chapter 2). Legend see Fig. IV.10.



1



2



3



4



4'



5



6



7

Figure IV.9 bis: Pictures: 1: Sheared and folded Palaeocene deposits, 2: Upper Cretaceous deposits affected by thrusts. 3-4 transition from Upper Cretaceous to Palaeocene deposits. 5 are the Lower Cretaceous deposits onto the 6: Bajocian deposits, and 7 is the picture of the Upper Cretaceous deposits onto the Bajocian deposit.

## IV. Interpretations - discussion

### 1. The general structure of the belt

Based on the observations, the general structure of the belt is interpreted to be mainly driven by normal faults located on the borders which define the structure of the AT basin during the Palaeocene-Eocene (Fig. IV 10 and 11). These normal faults are active during the Palaeocene-Eocene in the basin, but the wells data of the Fig. IV 6 offer the possibility to show that the ones situated southward from the Lesa anticline are active during the Aptian-Cenomanian and Barremian. The seismic interpretation of the SOG 23 seismic line (Fig. IV 9) seems to go in the same way of interpretation south of the Dzirula Massif. The interpretation can't be made further to the east since no evidence of extension have been observed in the Cretaceous deposits. The volcanism observed could be related to the arc, or to the rifting. No geochemistry is already published, but this is a work to follow (Sadradze and colleagues) and some geochemistry has been interpreted in the Eastern Pontides (Hässig *et al.*, 2020) where the interpretation tends to show that the geochemical signature of the volcanism evolves from west to east of the Pontides during the Paleogene. The interpretation is based on the opening of the Eastern Black Sea and we have proposed that the western AT is rifting during the same time. We propose that the AT evolves during the Paleogene, in a superimposed basin that is not the same as the Eastern Black Sea which rifted during the Mesozoic. The interpretation of the seismic line "05 XIA" (Fig. IV 11) help us to observe some major decollement levels at the basis of the Upper Cretaceous, into the Lower Cretaceous (?), and in the Palaeocene-Eocene deposits. The Oligocene deposits are even more affected by the thin-skinned tectonic deformations. These observations imply that the model must be improved by thin-skinned deformations together with the major thick-skinned deformation due to the reactivation by tectonic inversion of normal faults. The decollement levels seem to connect with the normal faults. During the line drawing, the main normal faults were interpreted to flatten at depth, which is not usually observed. This is interpreted to be the decollement level (thin-skinned tectonic deformation), which connect then with the normal

faults. This interpretation is interesting because the inherited normal faults drive the major structure, but the decollement levels in the deposits are a way to deform more the deposits. A question is to understand how to equilibrate the shortening between the deposits at depth which are deformed by the normal faults, while the younger deposits are deformed by some thin-skinned tectonic, involving a higher shortening rate. A track to follow is that the deposits syn-extensional would need a higher shortening than the pre-extension deposits if the final shortening is to “come” back to the pre-extension size of the AT unit. This implies a “box effect” of the syn and post-extension deposits. The major thin-skinned deformations observed in the Oligocene deposits could be thus the result of this “box effect”.

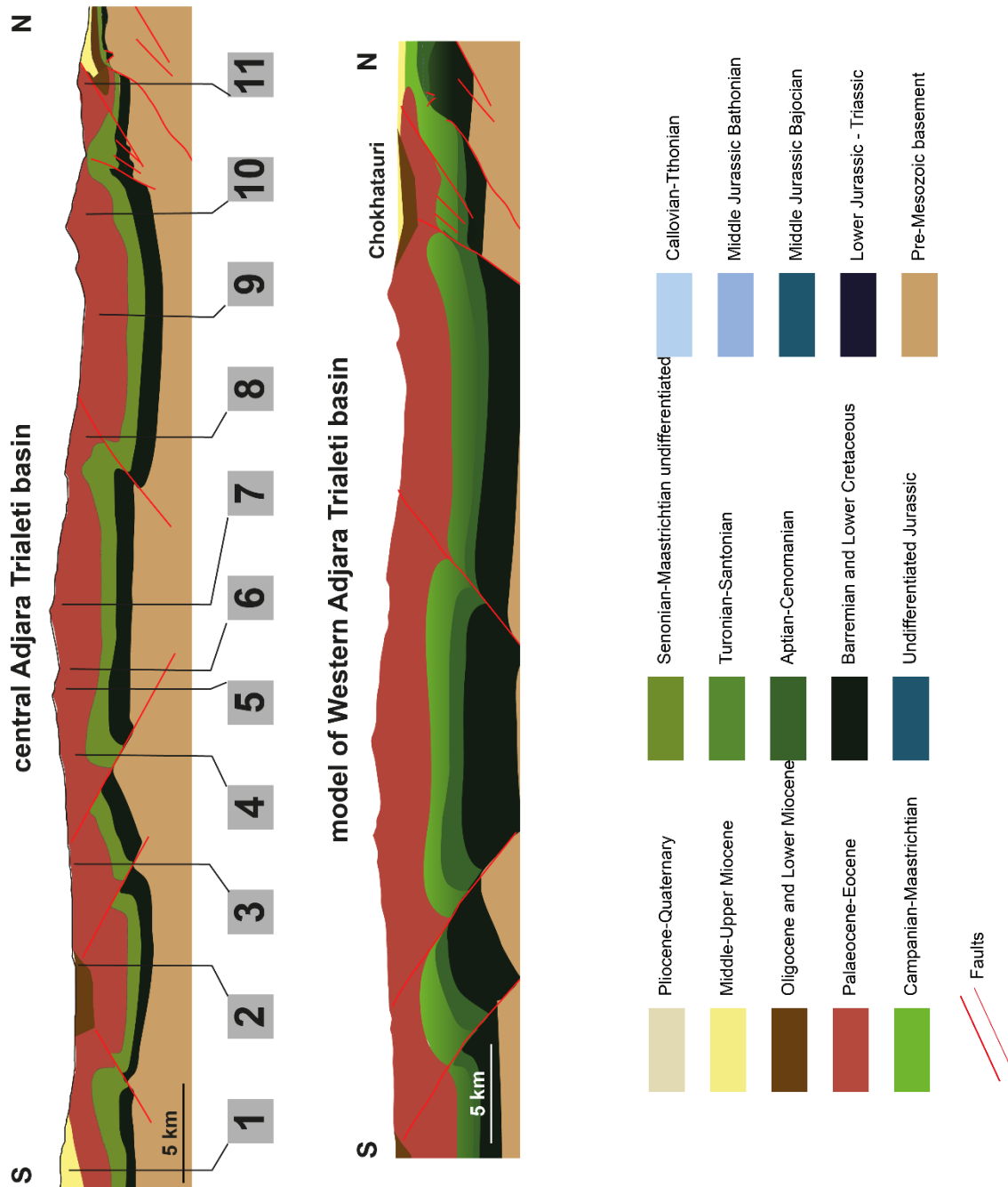


Figure IV.10: Cross section of the central AT with the relative pictures (see Fig. IV 10 bis) and the Western continuation interpreted to be larger (observed on the map) and with thicker Cretaceous and Palaeocene-Eocene deposits (interpretation based on the wells data in Fig. IV 6). See location in Fig. IV 1. Here the thick-skinned tectonic model is chosen because we have not enough observations to constrain the thin-skinned deformations, however, these are present. Legend see Fig. IV.10.

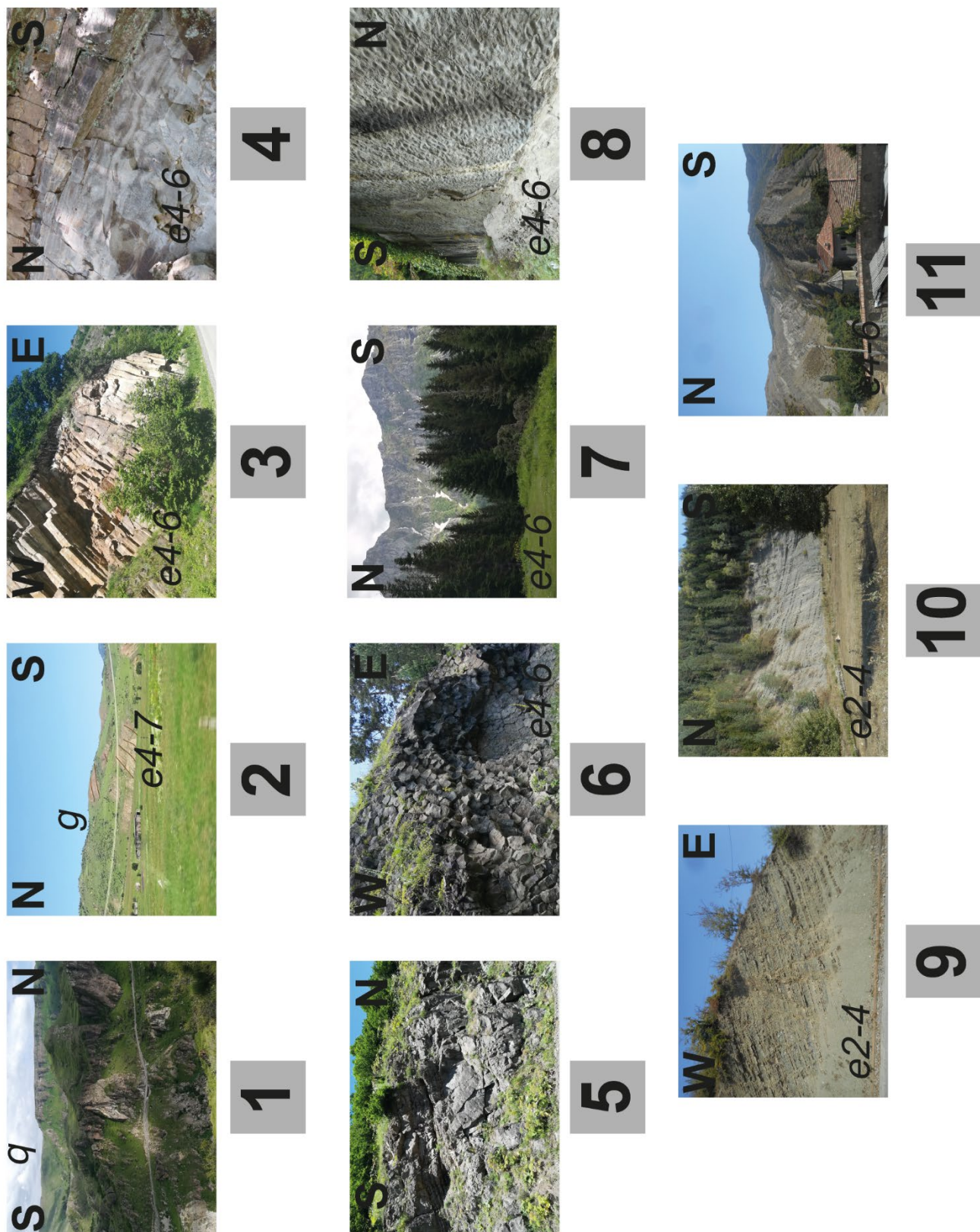


Figure IV.10 bis: Pictures: 1: Quaternary lavas of the southern AT. 2: Oligocene deposits unconformably covering the Middle-Upper Eocene deposits. 3 to 8 are the Middle Eocene volcano-related deposits. 9 and 10 are the Palaeocene-Lower Eocene flyschs, and 11 is the Middle to Upper Eocene deposits at the frontal part of the northern AT.



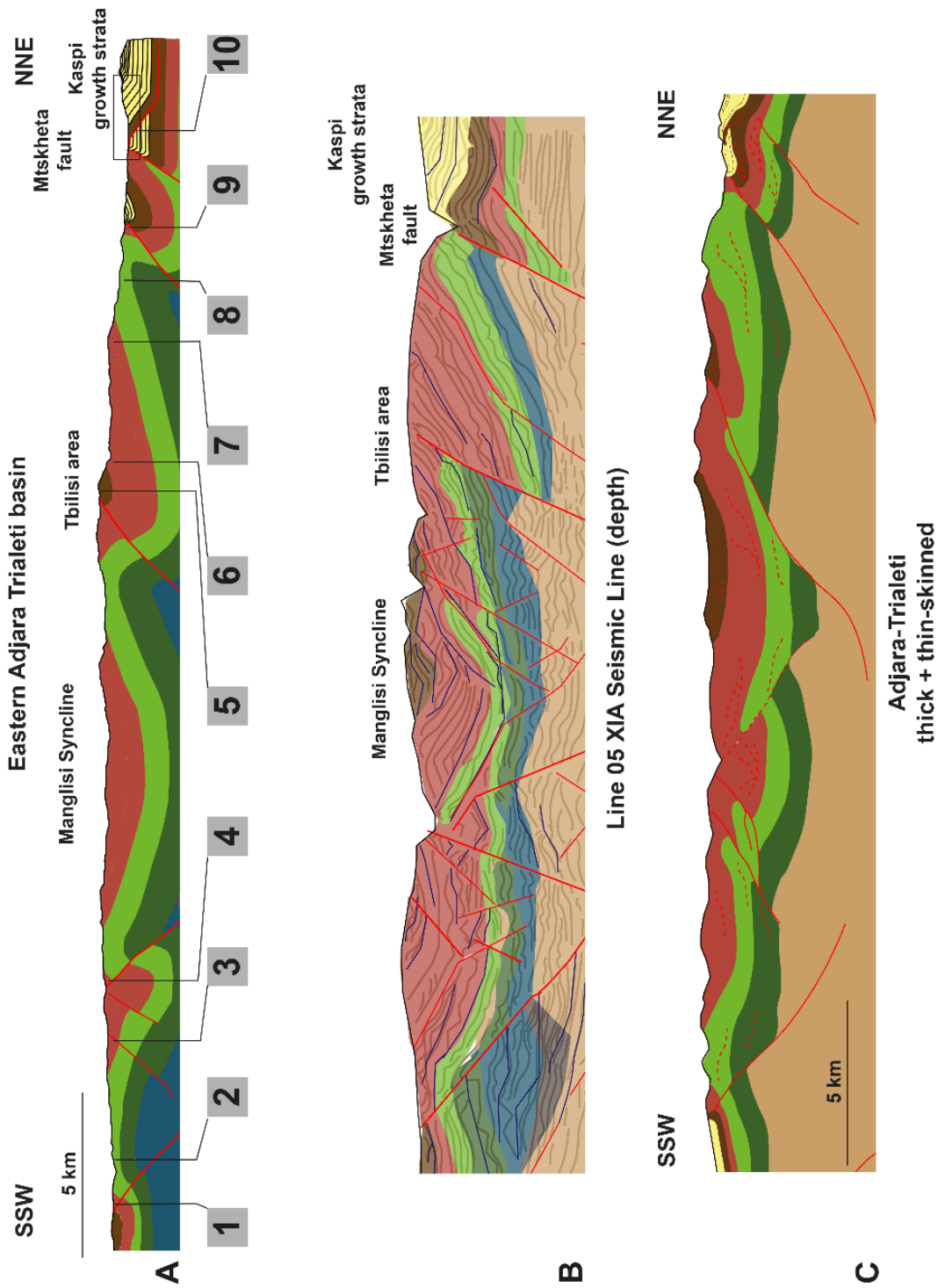


Figure IV.11: Cross section and relative pictures (see Fig IV. 11 bis) of the Eastern AT. The thick-skinned model is used since the thin-skinned deformation are not constrained enough in this cross-section. The seismic interpretation of the 05 XIA seismic line (depth) show the major thick-skinned structure, but some thin-skinned deformations are observed. The last cross-section is modified after the seismic interpretation. See locations in Fig. IV 1. Legend see Fig. IV.10.

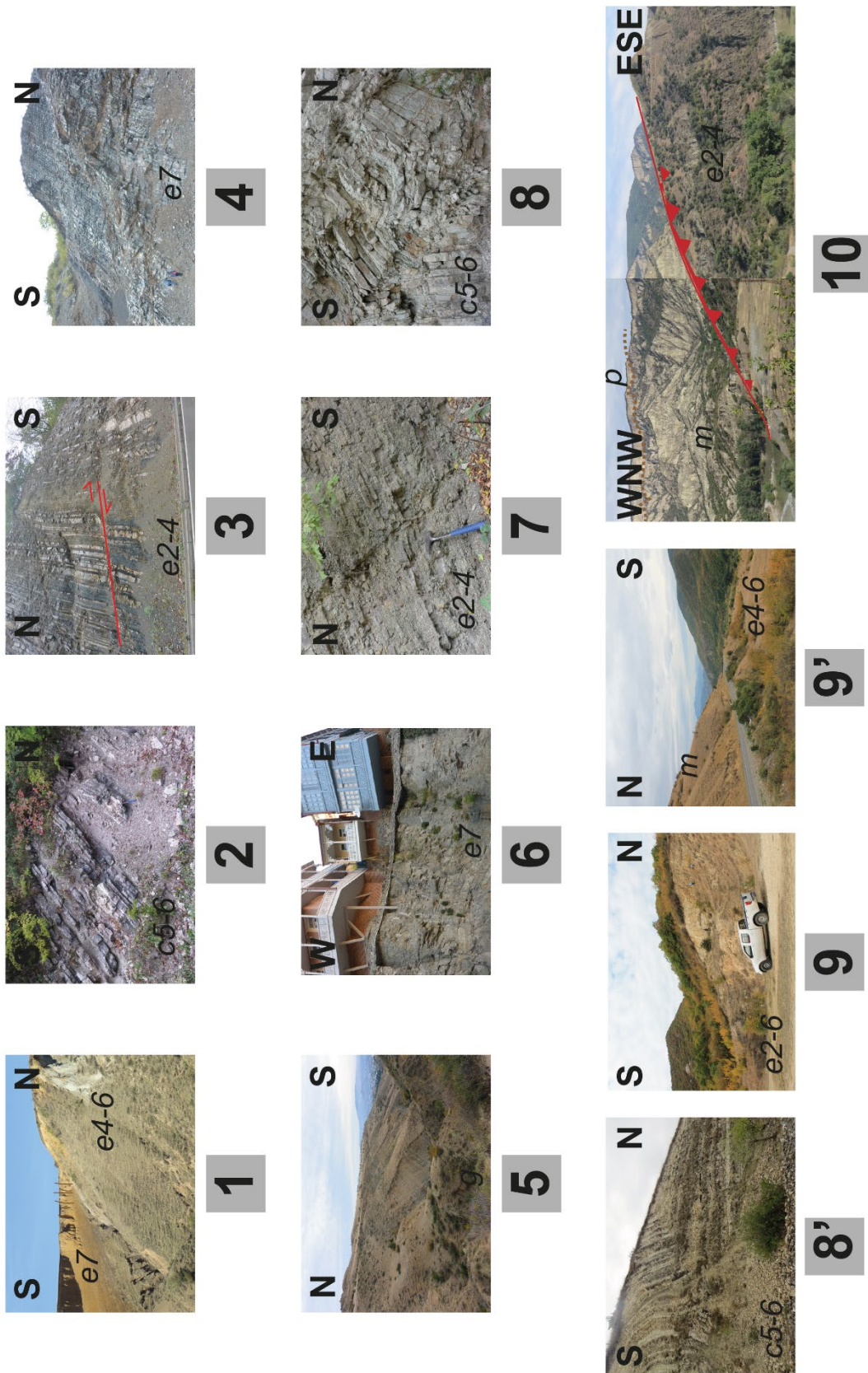


Figure IV.11 bis: Pictures: 1 is the transition from the Middle to Upper Eocene deposits to the southern border of the AT, where olistostrome are observed. 2-3 are the Palaeocene-Lower Eocene deposits, deformed by normal faults. 4 is the oil-bearing Upper Eocene deposits. 5 is the Oligocene folded

deposits, 6 is the Upper Eocene deposits observed in Tbilisi. 7 is the Palaeocene-Lower Eocene flysch deformed by normal faults, 8 and 8' are the small-scale and thin-skinned deformations that affect the Upper Cretaceous deposits. 9 and 9' are the transition from the thrust Palaeocene-Eocene deposits to the Neogene deposits. The Picture 10 shows this transition (with the Mtskheta fault) in the landscape. The Kaspi Growth strata are documented in the chapter 3.

## 2. Reconstitutions

### a- Adjara-Trialeti during the Mesozoic

The wells data as well as the Cretaceous deposits observed on surface highlight that the western Adjara-Trialeti basin is deformed by normal faults during the Lower Cretaceous (Barremien, Aptian-Cenomanian). The Cenomanian deposits are made of Andesitic-basaltic volcanic formations. We interpret this extension to affects the AT basin toward the east until the Dzirula Massif. More to the east, we do not have any geological evidence to justify extension during the Cretaceous, but the deposits are likely to show a deepening toward the west (Fig. IV 3, g). The Upper Cretaceous are quite homogeneous and are post-extension in the whole area. We note that in the eastern part volcanism takes place during the Campanian-Maastrichtian (Fig. IV 12) (Fig. IV 3, a, c).

### b- Adjara-Trialeti during the Paleogene

During the Paleogene, after the calm Danian period (mudstones and clays), the Adjara-Trialeti basin is deformed in extension. The Paleocene-Lower Eocene terrigenous flyschs are already affected by normal faults. The basin has the same borders than the fold-and-thrusts belt. To the west, the northern border is situated about 5km south of the Cretaceous normal faults (Fig. IV 6). During the Middle Eocene a major magmatism event occurred in the basin. Syn-deposition normal faults are not known in the Upper Eocene detrital and terrigenous deposits which evolve with time in the Maykopian deposits during Oligocene (-Lower Miocene). As discussed in the chapter 3, the Maykopian deposits are linked to a calm environment, closed and euxinic which create evaporitic deposits. The closure could be linked to subsidence or only to the uplift situated to the south with the collision in the Lesser Caucasus, and to the north with the first evidence of uplift and compression during the Paleocene-Eocene, isolating the zone between both compression belts (see Fig. IV 12).

### c- Adjara-Trialeti during the Neogene compression

The basin is then deformed during the Upper Miocene compression and isolate the Kartli basin (western part of the Kura basin), with the formation of a triangular zone. The style of deformation is important here: the triangular zone is made of south-verging thin-skinned deformations coming from the Greater Caucasus and deforming the Kura and Kartli basins with major decollement level in the Oligocene deposits. Toward the west, the south-verging deformation is constrained as discussed in the chapter 2 by the inversion of inherited normal faults in the Rioni and the “Georgian Block”, but we observe some thin-skinned tectonic too.

The Adjara-Trialeti, which ends west of Tbilisi, does not constrain the deformations east of Tbilisi where the decollement levels and the south-verging deformations continues toward the Caspian Sea.

The Adjara-Trialeti basin evolves in a fold-and-thrusts belt, constrained by the location of major normal faults. However, the thick-skinned tectonic caused by the inheritance evolves in decollement levels near the normal faults. The younger deposits seem to be more deformed by the thin-skinned tectonic deformations. The Oligocene deposits are post-rift deposits and can form a decollement level. These post-rift deposits are then constrained by the normal faults which could create some border effects and constrain the younger deposits to be shortened with thin-skinned tectonic.

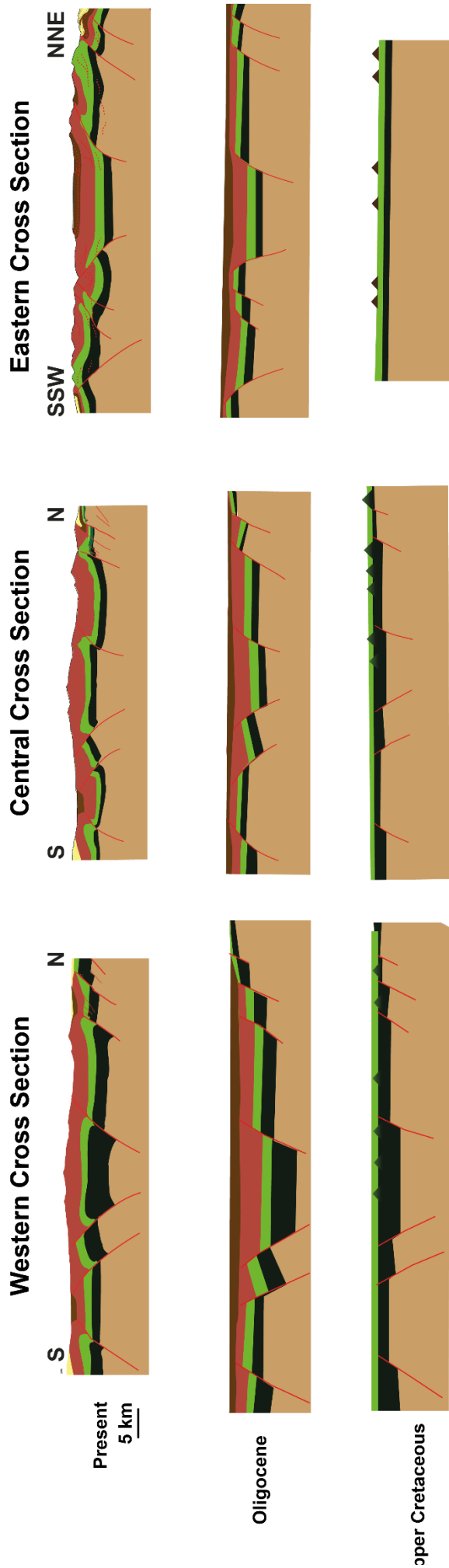
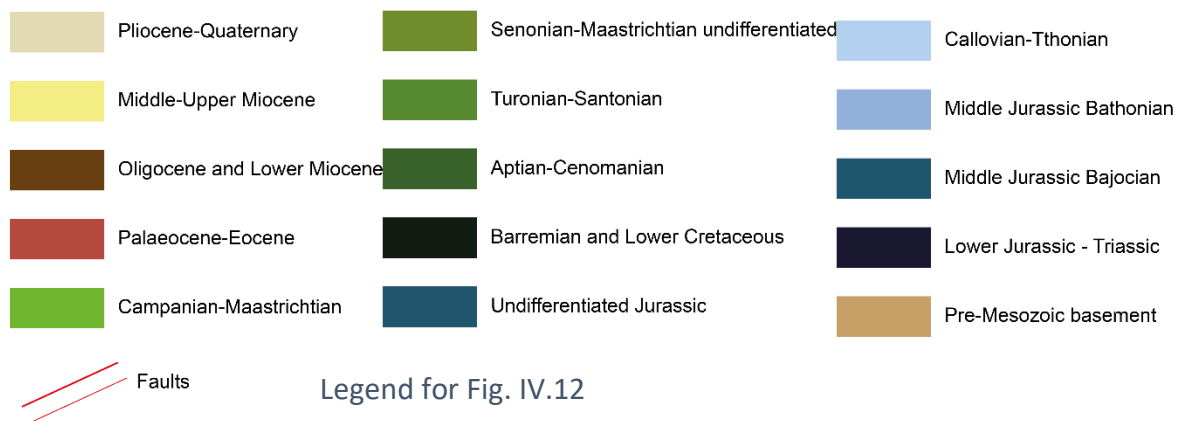


Figure IV.12: Reconstitutions of the Adjara-Trialeti basin since the Upper Cretaceous from the Eastern to the Western part. Legend is the same as in chap. 3.



## V. Conclusion

This chapter offers some new observations concerning the Adjara-Trialeti fold-and-thrust belt. We show that during the Early Cretaceous the western part of the Adjara-Trialeti FTB is concerned by the opening of a basin, situated south of the Dzirula horst during the Lower Cretaceous (Barremian and Aptian-Cenomanian). The continuation toward the west into the Eastern Black Sea basin can be supposed. However, the deposits east of the Dzirula massif do not show an extension but only a deepening toward the west.

We show that the main extension then takes place during the Palaeocene-Middle Eocene in the whole Adjara-Trialeti basin. The basin formed during this stage is superimposed onto the Cretaceous basin in the western AT. The Palaeocene-Lower Eocene is more detrital and constituted of flyschs. The Middle Eocene indicates a major volcanism event, and the origin is still poorly constrained. However, it is a volcanism syn-rift according to the extensional tectonic we demonstrated.

After the extension, the Upper Eocene until the Oligocene is made of an euxinic basin which creates terrigenous deposits and then the Maykopian formation. The closed and euxinic environment is likely to be because the belts of the Lesser Caucasus situated to the south, and the belt of the Greater Caucasus situated to the north make the location in between closed and cut off from the open seas, making a great environment to create evaporitic deposits.

Finally, we have observed that the inherited Mesozoic-to-Palaeocene normal faults constrain the location and the style of the deformation during the Neogene compression. However, some thin-skinned tectonic take place also in the fold-and-thrust belt, as proposed by many authors in literature (Banks *et al.*, 1998; Alania *et al.*, 2017a, 2020)



*Chapter 5: Discussion and Conclusion*



## I. Introduction

The style of deformation interpreted from observed structures can lead to very different reconstitutions and is thus critical for the tectonic interpretation of an area as well as the estimation of its resources endowment. Fold-and-thrusts belts can be deformed by thin-skinned, thick-skinned or a large panel of interactions of both styles, and even both styles together.

One of the parameters that can control the style of deformation is the occurrence of inherited structures involved in the deformation. A good example can be a rifted basin which is affected later by some compression. This example can be found in the paleo-back-arc area where extension occurs during the subduction. During the collision, the basins will be deformed by a compressional tectonic regime and the normal faults reactivated. The reactivation of such faults controls the whole structure of a mountain belt: the faults are steeper than the thrusts, the thickness of the syn-extension deposits change across the belt. The way the normal faults are reactivated can lead to the deformation of the basement and create thick-skinned tectonic. The Caucasus offers a great case study of such process: since Triassic, the Eurasian plate was bordered to the south by an active margin. The back-arc area was shaped by lateral partitioning of rifting depressions accommodating differential extensions resulting in isolated sub-basins.

The northern branch of the Neotethys ocean, after following an obduction phase during the Late Cretaceous onto the Taurides-Anatolides-South-Armenian Microcontinent (TASAM), closed during the Palaeocene-Eocene. Then during the Late Miocene the southern branch of Neotethys ocean closed and as the result the Arabian Plate collided with the TASAM already jointed with the Eurasian plate (Barrier *et al.*, 2018).

This two-stages collision offers the possibility to evaluate the role of the inherited basins in the Caucasus on the structure of the mountain belt since the last stage of collision. The Greater Caucasus inverted basin is elongated from NW to SE. The Black Sea and the Southern Caspian basins are situated southward of the Greater Caucasus. The structures between the Eastern Black Sea to the west, and the Southern Caspian basin to the east, located in the so-called Transcaucasus area are not well constraint and the lateral continuity or the evolution of the structures is subject to debate and many uncertainties. The timing of the tectonic stages related to the collisions (Eurasia, TASAM, Arabia) does not correspond to the timing observed in the areas nearby. This could be due to different tectonic processes, or to lack of observations leading to errors in the evaluation of the timing in the Transcaucasus area.

This leads us to take the Transcaucasus area, from the Rioni to the Kura foreland basins for our study. The style of deformation and the timing of the tectonic stages is the axis of this study.

## II. The main results of the study

### 1- Interpretation of tectonic events during the Mesozoic

#### a- The Rioni foreland basin and the Georgian Block: the western section

The Rioni foreland basin, and to the east its prolongation in the Georgian Block, is the first unit we have studied. The Mesozoic deposits that are observed in the anticlines in the Rioni foreland basin are interpreted to continue into the Georgian Block. The area is limited to the north by the Greater Caucasus and the Ambrolauri flexural basin, and to the south by the Adjara-Trialeti and the Dzirula Massif. To the west it is limited by the Eastern Black Sea basin, and to the east by the Greater Caucasus deformation front.

Along the chapter 2, we have highlighted the Mesozoic tectonic stages in the Rioni area. This was evidenced by the occurrence of angular unconformities and by observation and analyses of tectonic structures in the sediments beneath the unconformities.

- The unconformity of the Lower Cretaceous formations onto the Bajocian-Bathonian: this unconformity covers sediments deposited in an extensional tectonic regime during the Bajocian (syn-rift) followed by Bathonian to End of Jurassic of shallow marine, lagoonal environment (post-rift)
- Unconformity of the Upper Cretaceous onto the Lower Cretaceous series: extension during the Barremian followed by extension more localized along the normal faults during the Albian-Cenomanian and followed by some subsidence during the Turonian-Senonian (deposits syn-rift). The Campanian-Maastrichtian deposits mark the post-extension stage with calm platform (deposits post-rift).

In more details, the tectonic unit which is deformed by the extensional events described above is delimited by what we interpret as horst structures: to the north, the horst is located below the Neogene Ambrolauri flexural basin and its western prolongation, and to the south by the Variscan basement of the Dzirula massif. The interpretation to continue the EBS structures toward the east in the Rioni area was proposed by Nikishin *et al.*, (2015), Tari *et al.*, (2018) with the continuation of the Shatsky Ridge below the Rioni foreland basin.

#### b- The Kura foreland basin and the central Greater Caucasus – the Eastern section

The Mesozoic deposits are not observed in the Kura foreland basin. The observations of Mesozoic deposits concern only the southern Central GC and are related to the East flysch basin (Adamia *et al.*, 2011b) of the Greater Caucasus basin.

## 2- Interpretation of post-Mesozoic tectonic events

The chapter 3 focused on the Rioni and Kura foreland basins to better constrain the timing of the Greater Caucasus' compression. The Paleogene and Neogene deposits are observed at the deformation front of the Greater Caucasus not within the belt itself.

### a- In the western section

In the western section, two compressional stages have been highlighted. The first one takes place after Danian, during the Palaeocene and Eocene. Palaeocene and Eocene deposits in the Rioni area are made of growth strata constituted of marls and detrital deposits. The Oligocene sediments mark the post-compression stage and witness a calm and euxinic depositional environment. The reason that the environment is closed is interpreted to be linked to the first compressional stage which created high topography to the north in the Greater Caucasus and inverted the "Georgian Block basin", and to the south by the suture zone of the Lesser Caucasus. The Neogene deposits mark a major erosional event producing a lot of detrital sediments in the foreland and flexural basins (Rioni and Ambrolauri FB). The Upper Miocene (Sarmatian) deposits are made of growth strata. The unconformity between the Sarmatian and the Meotis-Pontian deposits could be related to the Messinian crisis and is possible to interpret without "2-stages" of compression.

### b- In the eastern section

In the eastern section, we can observe Paleogene deposits in the southern GC. The Paleogene deposits are observed in the duplex formation which involves the southern slope zone deposits of the Greater Caucasus.

The two compression stages are also highlighted in the eastern section.

The first one takes place after Danian, during the Palaeocene and Eocene. In the Kura area, the deposits are some flyschs trapped in the nappes in duplex structure.

The Oligocene deposits mark the post-compression stage and are in a calm environment and formed an evaporitic and euxinic basin. The interpretation of the reason that the environment is closed can be the same in the eastern section as in the western section: the first compression stage which create high topography to the north in the Greater Caucasus and to the south by the suture zone of the Lesser Caucasus. We have notified that these deposits are

thicker in the Kura foreland basin and contain more evaporitic deposits (more gypsum into the clays).

The Neogene deposits mark a major erosion event producing a lot of detrital deposits. The Upper Miocene (Sarmatian) deposits are made of growth strata which continue during the Meotis-Pontian in the Kura foreland basin. As interpreted in the western section, the unconformity between the Sarmatian and the Meotis-Pontian deposits could be related to the Messinian crisis and is possible to interpret without “2-stages” of compression.

### 3- Differences from west to east

#### a- Differences during the Mesozoic

The main difference from west to east during the Mesozoic is that during the Early Cretaceous, the eastern Greater Caucasus is affected by the basin formation and that the frontal Greater Caucasus is part of this rifting. The western section shows a different evolution because the southern slope zone deposits can be correlated to the deposits observed in the Georgian Block. The southern GC situated north of Ambrolauri presents also a structure related to the main GC basin, but with less subsidence than in the eastern section. This means that another basin takes place south of the Greater Caucasus in the western section location (Rioni-Koutaissi area) (chap. 2), while nothing is observed to the east. The shape of the northern Dzirula Massif together with the eastward evolution of the Lower and Middle Cretaceous deposits make us interpret that the Georgian Block basin is the eastern limit of a basin situated south of the southern Greater Caucasus.

#### b- Differences after the Mesozoic

We have observed that from west (in the Rioni foreland basin) to east (in the Kura foreland basin) the compression stages are not expressed in the same way. The nature of the deposits (marls/sandstones to the west, flysch and olistostrome to the east) is different, and also the structure where these deposits are observed: some thick-skinned tectonic is observed to the west, with the growth strata observed at the front of the deformations, and also at the back in the Rioni foreland basin, while to the east, the deposits are observed in the thin-skinned deformation which are due to the duplex' formation along a Cenomanian decollement level.

The style of the deformations during the collision are different. The inherited structures of the normal faults observed to the west seem to be a reason that the deformation is thick-skinned in this area while to the east, the decollement levels seem to control the deformation.

#### 4- The Adjara-Trialeti: from basin to fold-and-thrust belt

The Adjara-Trialeti fold-and-thrust belt borders the southern part of the studied area. Its structure made of bivergent fold-and-thrust belt implies that the tectonic history of this unit is related to the one of the foreland basins Rioni and Kura. Moreover, this unit and the relation with the Eastern Black Sea has also to be constrained.

##### a- The tectonic history of the AT fold-and-thrust belt

The observations made in the Adjara-Trialeti fold-and-thrust belt confirm that the belt was active during the Palaeocene and Lower Eocene affected by an extension which creates the basin. During the Middle Eocene the basin is still the major structure, but a major volcanic event takes place. During the Upper Eocene and Oligocene, the tectonic is quiescent, and an euxinic-closed environment developed as observed in the Rioni and Kura foreland basins.

Toward the western part, the Lower Cretaceous history of the basin predating the fold-and-thrust belt is similar to the one proposed for the “Rioni and the Georgian Block”, as well the Eastern Black Sea basin.

During the Palaeocene-Eocene the tectonic and the volcanism observed in the AT seems to correlate with the Pontides, situated west of the AT.

During the Neogene, the basin is inverted during the compression, and foreland basins developed south and north of the belt.

##### b- The structures of the AT FTB

The Adjara-Trialeti fold-and-thrust belt structure is interpreted to be strongly influenced by the Adjara-Trialeti basin structure and architecture. The limit to the east is well defined west of Tbilisi, where the deposits are more detrital, and thinner. Toward the west, the basin is wider from north to south and keep increasing until the Pontides limit.

The structures where the deformation of the belt is localised during the Neogene compression, are interpreted to be the inherited normal faults from the Paleogene extension. This is thus interpreted to be deformed with a thick-skinned style of deformation. However, some decollement levels are also observed (Lower-Upper Cretaceous limit, into the Eocene, and

most of all, into the Oligocene deposits) and show that some thin-skinned deformation is also present in this structure (Banks *et al.*, 1998; Alania *et al.*, 2017).

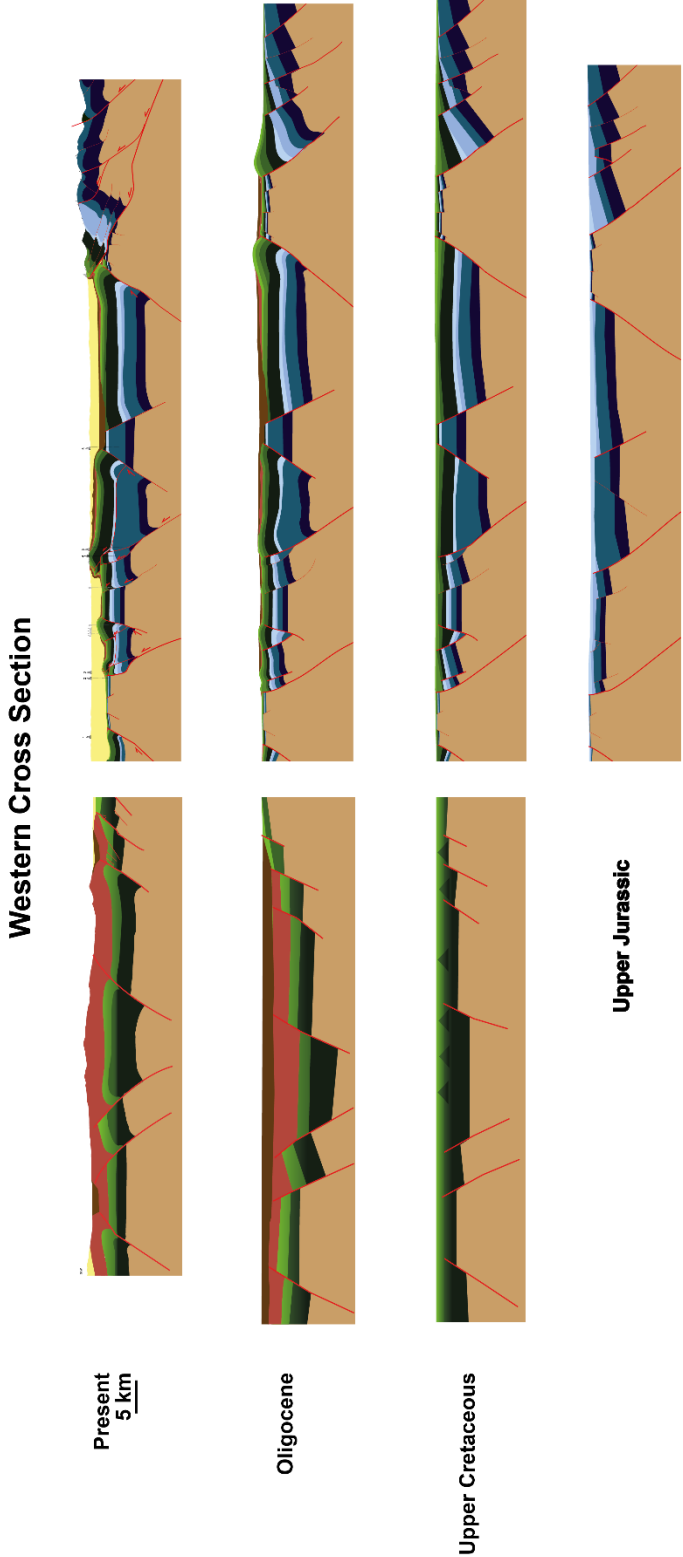


Figure V.1: Evolutive cross-section of the Western Transcaucasus area, from the Adjara-Trialeti section, the Rioni foreland basins and southern Greater Caucasus

## Central Cross Section

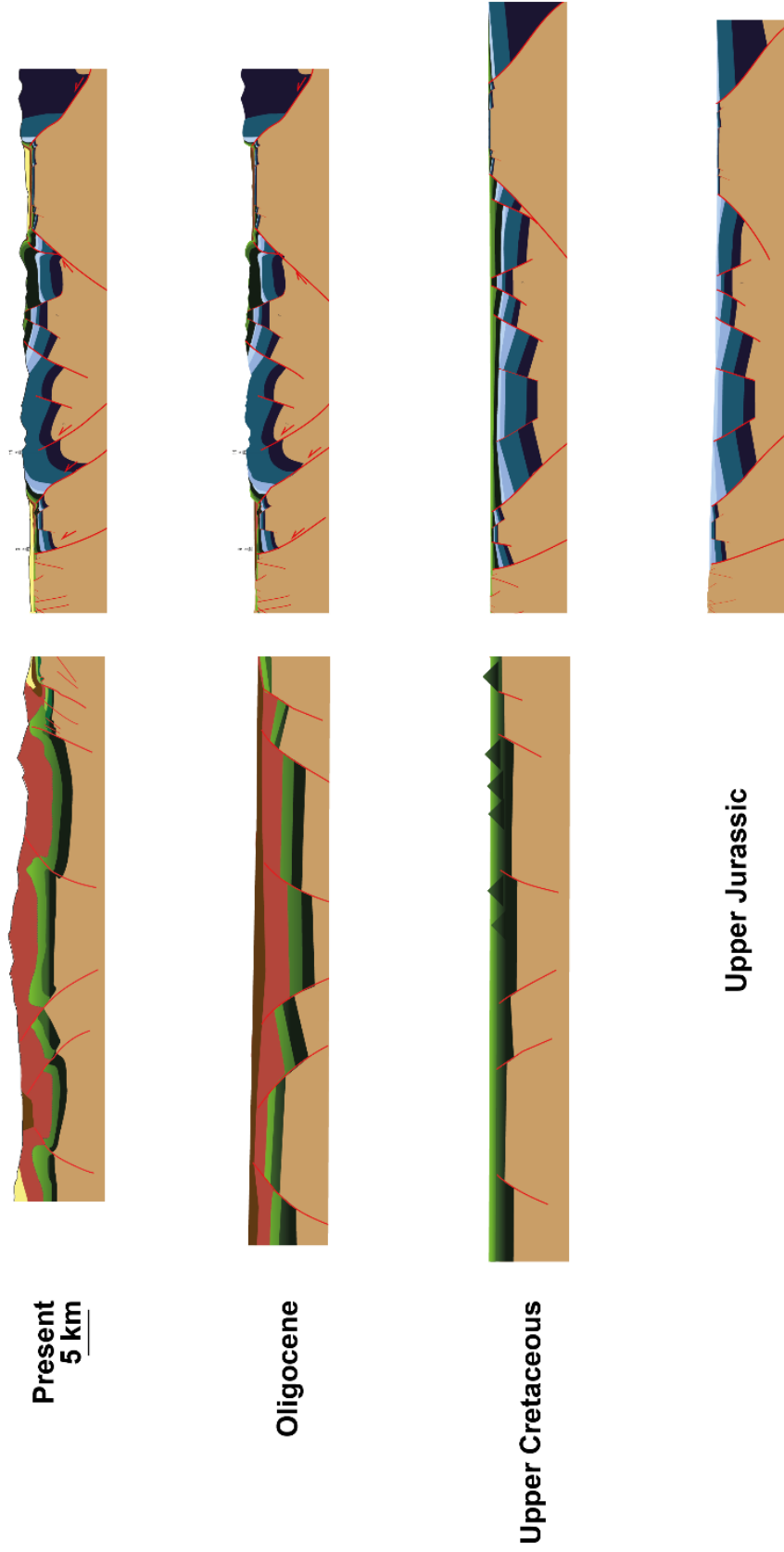


Figure V.2: Evolutionary cross-section of the Central Transcaucasus area, from the Adjara-Trialeti section, the Dzirula horst, the Georgian Block "basin", the Ambrolauri horst / foreland basin and the southern Greater Caucasus

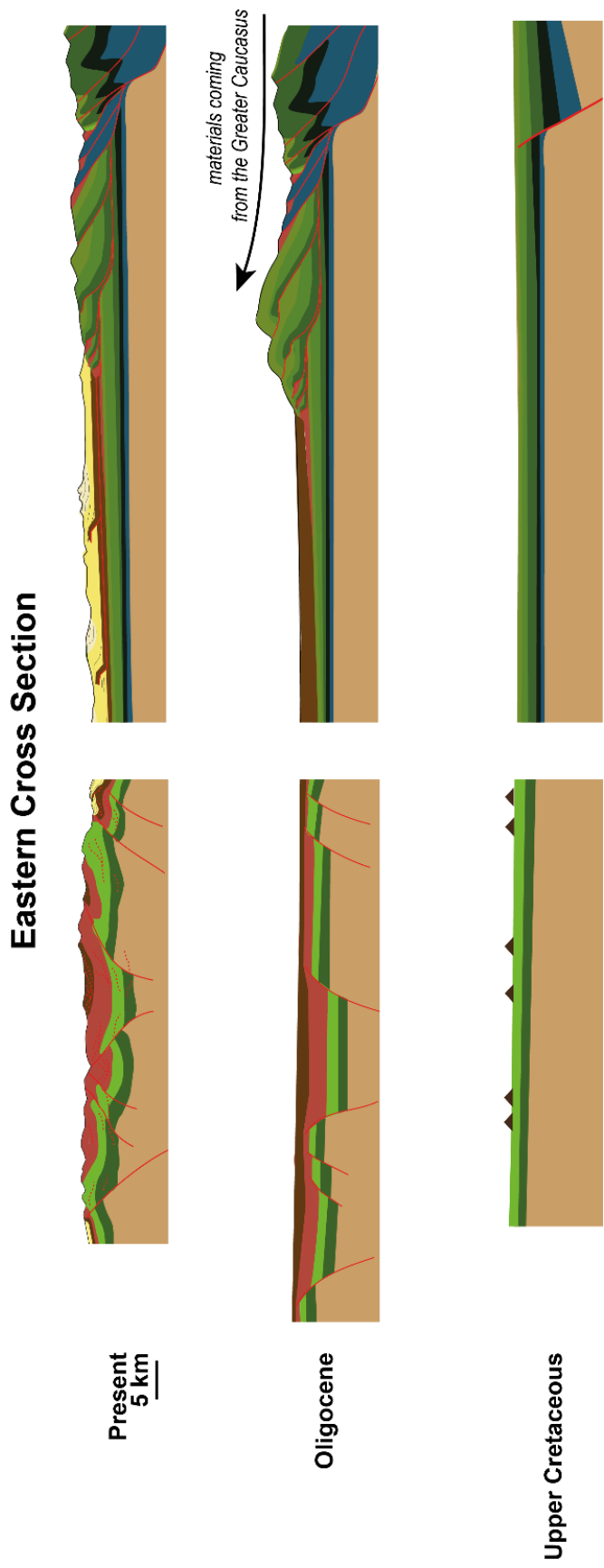
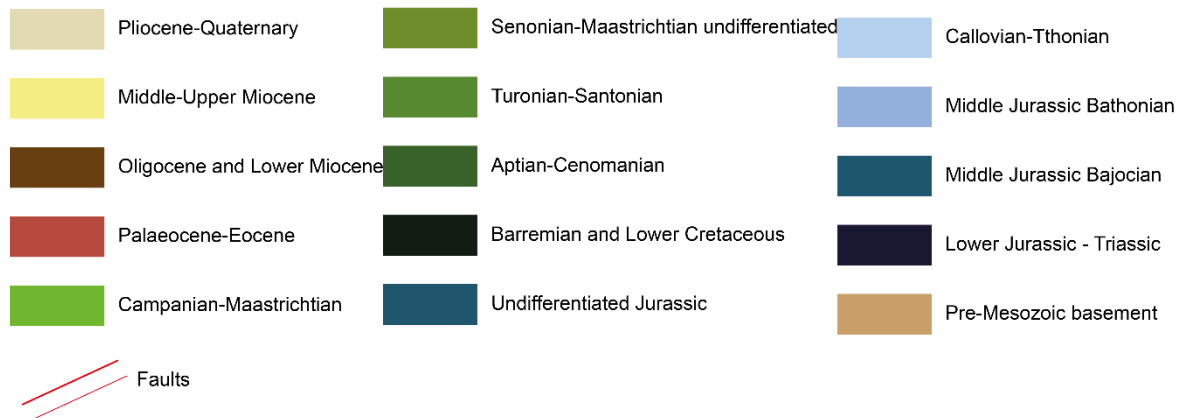


Figure V.3: Evolutionary cross-section of the Eastern Transcaucasus area, from the Adjara-Trialeti section, the Kura foreland basins an southern Greater Caucasus





Legend for Fig. V. 1-3

### III. The flexural basins of the GC in Georgia: highlights of the tectonic history

#### 1- Reconstitutions

The tectonic reconstructions offer us the possibility to put in perspective the deformations at a larger scale.

- During the Jurassic, the subduction zone implies major extension in the back-arc area.
- During the Early Cretaceous, we observe that the main extension takes place in the Georgian Block and in the western Adjara-Trialeti. This highlights the southward transition of the extensional stage, only in the western GC and EBS. The extension in the Eastern GC is not affected by this evolution toward the south (fig.V.1) and is still localised in the “East Flysch Basin” (Adamia *et al.*, 2011b). The western Transcaucasus is thus affected by thick-skinned tectonic during the Early Cretaceous, while the eastward continuity of the Transcaucasus is not concerned by thick-skinned deformations.
- During the Late Cretaceous, the tectonic is calm and the platform takes place in the area.
- During the Palaeocene-Eocene, the collision in the LC involves active compression in the GB and the GC. The inversion of the basins involves some thick-skinned tectonic deformation to the west, and some thin-skinned and duplex formation to the east. However, southward, near the subduction zone, the Adjara-Trialeti is affected by a major extensional stage (fig. V.1) at the same time.

- During the Oligocene, the Maykopian evaporitic-euxinic environment takes place in the area between the GC and the LS which are defined by high topographic levels.
- Finally, during the Late Miocene, the compression consistent with the timing of the collision between the TASAM and the Arabian continent in Zagros affects the Caucasus area. During this compression, the inherited normal faults play a major role in the localisation of the deformation: some thick-skinned tectonic deformations are observed, but also some thin-skinned tectonic with decollement near the normal faults as observed in the Rioni foreland basin and in the AT fold-and-thrust belt (fig. V.1).

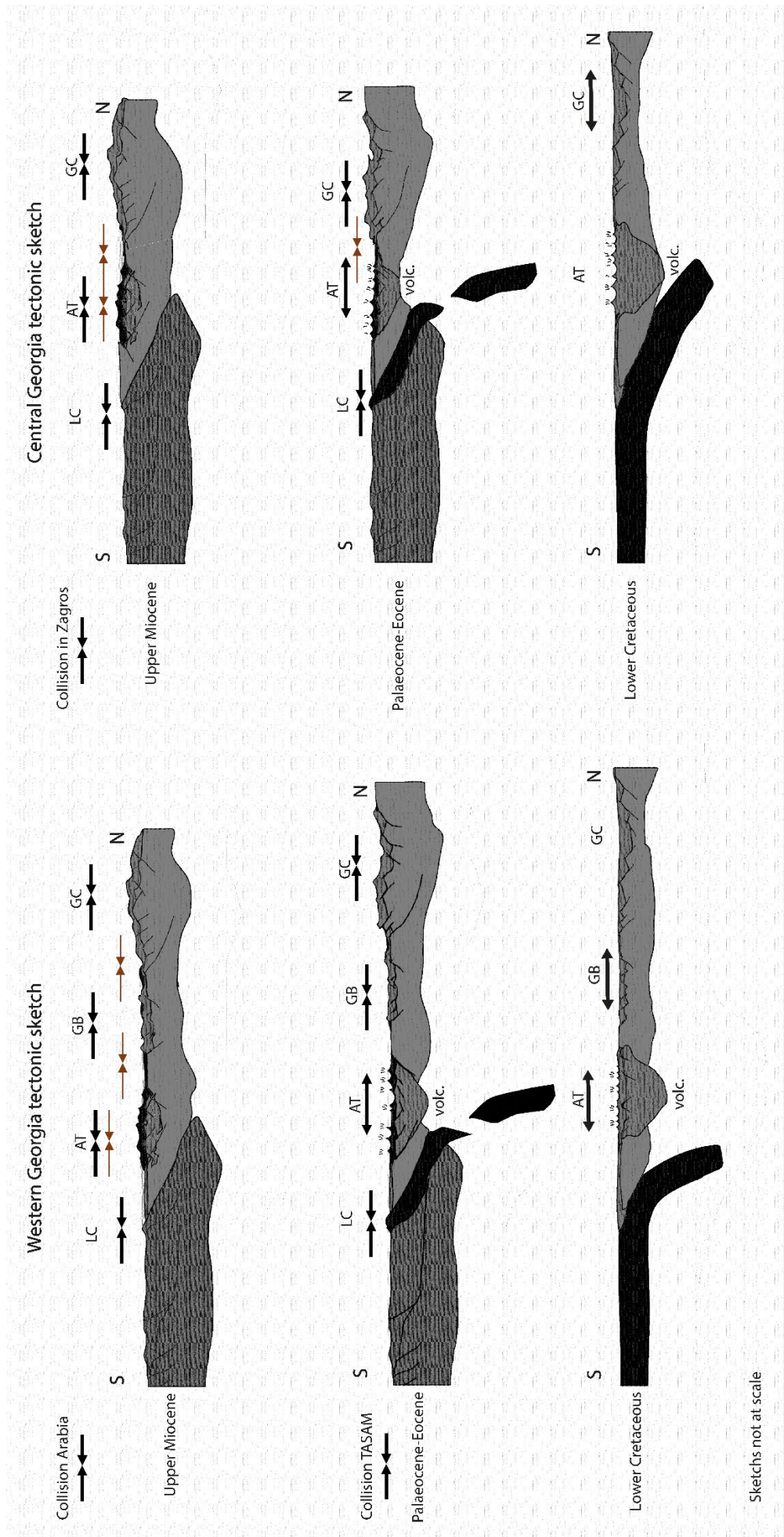


Figure V.4: Tectonic reconstitution sketches of the western and central Georgia during the Lower Cretaceous, the Palaeocene-Eocene and the Upper Miocene. The arrows show the location of the tectonic events: extension or compression.

## 2- Tectonic units and tectonic stages in space

In the figure V.4, we want to show the geometries of the different units described in this study to show the lateral relations.

- We observe that during the Jurassic, the internal zone is affected by the back-arc tectonic setting.
- During the Early Cretaceous extension, we observe to the west the opening of the Eastern Black Sea, the Adjara-Trialeti, the Georgian Block to the west, and the Greater Caucasus to the East (fig. V.4).
- During the Late Cretaceous, while some subsidence takes place in the basins and then more calm tectonic setting takes place in the studied area, the Lesser Caucasus is affected by the obduction (Sosson et al., 2010).
- During the Palaeocene-Eocene, while the Lesser Caucasus is affected by the collision between the TASAM and the Eurasian continent, the compression deformation is driven by the inherited structures located in the internal zone. The Adjara-Trialeti shape show a larger extension toward the west and a change in the orientation of the unit: from an E-W trend at the eastern end to a SW-NE trend in the western part. The shape is kind of triangular (fig. V.4 and IV.1).

We observe that these orientations are the same during the Cretaceous and then Palaeocene.

## IV. Highlights of the open questions pointed out and discussion

The conclusions about the tectonic events, their evolution in term of timing and the style of deformation show important new results for the area. However, a lot of questions remain. We want to talk about the major ones, some can have some interesting answers or perspectives, and some are even more uncertain.

Western Transcaucasus			Western Adjara-Trialeti			
Timing	Observations	Interpretation	Tectonic setting	Observations	Interpretation	Tectonic setting
Pliocene	sandstones to conglomerates	compression? and uplift		sandstones, conglomerates undeformed (uplifted) volcanism to the south	compression? and uplift	
Upper Miocene	<b>U7: unconformity or undeveloped Meotis Pontian</b> sandstones to conglomerates	compression thick and thin-skinned tectonic		sandstones to conglomerates	compression inversion of normal faults	
Middle Miocene	<b>U6: unconformity Up Miocene growth strata</b> sandstones and detrital deposits	erosion		sandstones and detrital deposits	erosion	
Oligocene-Lower Miocene	clays, little gypsum, septaria, detrital	calm and closed environment delimited by topography flexural subsidence?		clays, gypsum, septaria, detrital	calm and closed environment delimited by topography flexural subsidence?	
Eocene	<b>U5: unconformity Oligocene</b> fasciès variations: marls, turbidites flyschs, olistostrome	Growth strata: compression inversion of normal faults products or erosion of the topography		detrital deposits (e7) Thick turbidites flysch Thick volcanics deposits	basin formation rifting active volcanism	
Paleocene	Shaly limestones and mudstone	Calm platform		undifferentiated shaly limestones and detrital limestones	Calm platform and deltaic deposits (possible erosion + subsidence)	
Danian	<b>U4: unconformity Up K</b> detrital limestones, volcanics in south	subsidence and erosion arc?		flyschs marls, volcanics thick dolomitized limestones	extension - rifting? extension in deltaic environment	
Campanian-Maastrichtian	<b>U3: unconformity Turonian</b> flyschs turbidites marls/limestones	localised extension (near normal faults)		?	?	
Turonian-Santonian	<b>U2: unconformity Low K</b> thick dolomitized limestones	extension in deltaic environment				
Aptian-Cenomanian	<b>U1: unconformity Bathonian</b> evaporites, conglomerates	Localised subsidence, calm environment				
Berriasian-Barremian	<b>U1: unconformity Up J</b> sandstones and coal	Deltaic extension localised				
Callovian-Tithonian	Volcanics, thick	rifting?				
Bathonian						
Bajocian						

Figure V.5: Recapitulative table of the observations and interpretations resulting of the study for the eastern Transcaucasus area

## 1. Eastern Black Sea structures continuation

### a. The Adjara-Trialeti basin, Dzirula and the Georgian Block basin

During the late Early Cretaceous, extensional tectonic regime deformed the Georgian Block and the western Adjara-Trialeti units. The shape of these units (fig. IV.1) together with the timing of the extension, which is consistent in these units, bring the possibility that the AT and the GB are the eastern continuation of the Eastern Black Sea. According to Nikhishin *et al.*, 2015 the rifting stage is documented from Late Barremian to Albian, with an evolution in ocean opening between Cenomanian to Mid Santonian (Finetti *et al.*, 1988; Görür 1988; Hippolyte *et al.*, 2010; Stephenson & Schellart 2010; Nikishin *et al.*, 2013, 2015).

Nevertheless, other authors documented the rifting stage of the EBS during the Cenozoic (Robinson *et al.*, 1996; Cloetingh *et al.*, 2003; Monteleone *et al.*, 2019; Maynard & Erratt 2020). The Ambrolauri and the Dzirula Massif can then be the continuation of the main horsts/ridges as the Shatsky Ridge and a northward other horst not observed. The continuation of the Shatsky Ridge to Dzirula was already proposed by Nikishin *et al.*, (2003, 2015), while Tari *et al.*, (2018) proposes that the continuation is beneath the Rioni FB.

Some interesting questions if this assumption is confirmed is the relation with the Tuapsee Through. This unit is usually interpreted to be a Paleogene/Neogene flexural basin situated northeast of the Shatsky Ridge and thrust by the southern (Saintot & Angelier 2002; Nikishin *et al.*, 2010, 2015; Tari & Simmons 2018).

We have observed that the borders of the inherited basins are the location of the frontal deformations where the foreland basins develop. The south-verging thrusting of the GC onto the Georgian Block near Jvari makes the lateral transition difficult to constrain concerning the relation with the Tuapsee Through. The study of Guo *et al.*, (2011) point also the question about the tectonic behaviour of the Tuapsee Through during the Mesozoic (specifically during the Late Jurassic), to know if it is shallow marine (and the continuation of the High, or if it is deeper and could be part of the Black Sea basins. Khain (2007) interprets the structure to be the continuation of the Transcaucasus accretionary complex of a continental subduction beneath the GC since the Jurassic (Khain 2007, 2009; Gamkrelidze *et al.*, 2015, 2018; Mumladze *et al.*, 2015; Cowgill *et al.*, 2016). Based on the studies cited in this paragraph, no observations seem to reflect a potential horst/high beneath the Tuapsee Through.

### b. The Ambrolauri horst

It seems that a horst (Ambrolauri horst) is located beneath a Paleocene flexural basin. This interpretation is constrained by the presence of Lower Jurassic deposits covered by

Cretaceous and Cenozoic deposits, east of Ambrolauri (Abesadze *et al.*, 2004) as well as the north vergence of the folds from the “Georgian Block” to the south, and the southern vergence of the folds from the Greater Caucasus to the north. The south-verging fold from the Greater Caucasus is not debated. The north-verging fold from the GB is more problematic. Our structural analyses and related interpretation show that south of this fold, the volcanic Bajocian deposits as well as the unconformable Upper Cretaceous limestones covering the whole structure, are nearly horizontal and poorly deformed. Northward, in the fold, the bedding is more and more vertical, describing the fan-shape of the onlapping younging Cretaceous deposits. The geometry is difficult to be interpreted with south-verging fold all along the southern border of Ambrolauri. One possibility could be a fault-bend-fold, where we could use the evaporitic deposits as decollement level. The Bajocian and Bathonian are deformed. So, the decollement should be deeper. Moreover, it would be difficult to “cut” or preserve the onlapping fan-shape of the Cretaceous described in the chapter 2.

## 2. The relation of the Jvari area and the Greater Caucasus

A question remains also about the Jvari area. The Jvari area is the south-verging frontal structural zone situated north of the Rioni foreland basin. Structurally, this seems to be part of the south-verging Greater Caucasus chain. However, the lithologies observed in the Lower to Upper Cretaceous deposits are much more similar to those observed in the BS and in the GB: these are made of more sandy limestones than the lithologies observed in the GC north of the Ambrolauri flexural basin. The deposits situated north of the Ambrolauri flexural basin are less detrital and offer the view of the southern slope of the GC basin. This difference has already been pointed in the literature by Adamia (Adamia *et al.*, 1977, 1981, 2011a,b) as the “Western Greater Caucasus Southern Slope Zone”. The deposits observed toward the east are different from the ones described in the Western Greater Caucasus Slope Zone: these deposits are similar to those observed in the southern GC situated north of the Ambrolauri flexural basin. The difference between both areas (eastern section and the Ambrolauri section) is observed in the style of deformation: the GC deposits north of the Ambrolauri FB are verticalized toward the south while the GC deposits in the eastern section are intensively folded and thrust toward the south.

## 3. The superimposed basins in Adjara-Trialeti

The western Adjara-Trialeti basin could be related to the EBS during the Early Cretaceous. The volcanism occurs in AT during the Cenomanian (chap. 4), and during the Albian in the Shatsky Ridge ((Nikishin *et al.*, 2015). We have observed some magmatic rocks (volcanoclastic deposits and lavas flows of basaltic to andesitic nature) within the Eastern AT

Upper Cretaceous deposits. We interpret this magmatic activity as a magmatic arc. The deposits are also interpreted to be from a shallower environment. However, during the Palaeocene-Eocene extension, the structure seems to be redefined by the tectonic event. To the west, the normal faults inherited from the Lower Cretaceous extension near Lesa were not reactivated during this new stage of extension. As described in chap. 4, the Lesa wells show that the thickness of the Lower Cretaceous series increases toward the south, but the Paleogene deposits are not thick in this place. The thickening toward the south is situated more to the south. This means that these normal faults inherited from the Cretaceous, are not used during the Paleogene. The normal faults that are active during the Paleogene are situated more southward (chap. 4).

The AT unit is thus taking a new path which differs from the Eastern Black Sea. In the western section the northern border of the AT is situated southward compared to the EBS structures, even if it could have used some inherited normal faults active during the Lower Cretaceous extensive event in the EBS. The southern border of the AT is also situated more to the south than what is considered as the southern border of the EBS as described in (Espurt *et al.*, 2014). In the Eastern section, the EBS has not been observed, and the AT seems to be linked to new structures. This let us propose that the AT is a superimposed basin, that could use some of the inherited structure of the EBS basin but is the result of new deformations. The structures, together with the intense volcanic activity could be related to the Pontides situated on the western AT.

Some interpret the EBS to open during the Palaeocene-Eocene as the AT basin (Adamia *et al.*, 1981; Robinson *et al.*, 1996). That involves a model of a unique basin (EBS and the AT basins) affected by multiple tectonic stages, while our model involves superimposed basins with different tectonic evolutions.

#### 4. Tectonic during the Paleogene

##### a. Relations between the Paleogene Eastern Black Sea and Rioni basins

The Palaeocene-Eocene compression stage was not proposed in the Rioni area before our study, but was observed further to the north-west (Saintot & Angelier 2002). The relation between the Rioni foreland and the Black Sea during this period is interesting. The Paleogene deposits are called “syn-orogenic” by Nikishin *et al.*, (2015), but are sometimes interpreted to be linked to a basin/oceanic area (Cowgill *et al.*, 2016) (Okay *et al.*, (1994) for the Rioni area) which can subduct beneath the GC (Khain 2007, 2009; Gamkrelidze *et al.*, 2015, 2018; Mumladze *et al.*, 2015; Cowgill *et al.*, 2016). This interpretation could thus link the Rioni foreland basin to the EBS. Based on our observations, despite the growth strata geometries on the folds, the Paleogene deposits are not likely basin environment or of oceanic area. The



lithologies are detrital (marls to sandstones to evaporitic euxinic environment), and the Palaeocene and Eocene deposits have limited thickness. The Paleogene deposits in the EBS are thicker and are not interpreted as growth strata (Tari *et al.*, 2018; Tari & Simmons 2018), and interpreted as post-rift deposits (Nikishin *et al.*, 2015). In (Tari *et al.*, 2018) we can observe that the Palaeocene-Eocene deposits have the growth-strata geometry in the seismic interpretations in the Rioni Foreland basin but are not interpreted with the tectonic. The difference between the EBS and the RFB/GB during the Palaeocene-Eocene could be linked to the deeper basin in the EBS, and because of the localized deformations on the borders of the EBS while the basin is much narrower in the GB and beneath the Rioni FB.

#### b. Extensional stage during the Palaeocene Eocene collision

The occurrence of extensional tectonic during the Palaeocene-Eocene, in a global compressional tectonic regime, is still debated today. The location of the extension must be important to understand the role/the cause of this tectonic event and the geodynamic process which caused it.

The AT basin is located southeast or nearly juxtaposed onto the Lower Cretaceous back-arc basin\* Eastern BS Basin. We have to point that Okay *et al.*, (1994) proposed that the EBS continued to open until the Miocene while they proposed the compression in the GC also from the Eocene until Miocene, so even if we don't agree on the specific interpretations, the possible tectonic setting which involve extension near the active margin while more to the north the compression is observed is not new in the area.

The suture zone of the LC is situated south of the AT basin. The Fig. V.5 and V.6 shows well the global compression stage in the whole area while the AT is affected by the extension. In the presentations of (Gamkrelidze *et al.*, 2015, 2018), the AT is interpreted as an intra-arc rift. A possibility is that the extension is due to the response of the slab during the collision. The slab motion affects the area situated above: from arc formation, compression and extension when it is rolling back, the slab is the main control on the surface response (references) . Kaz'min & Tikhonova (2006) interpret the different back-arc basins (the GC, the BS and the Caspian Sea), to open during the Palaeocene-Mid. Eocene time while the collision occurs in the Taurides plate.

We have shown that the BS and the GC are in compression during this period. The extension of the AT situated southward and closer to the suture zone is thus interesting regarding the geodynamic. We interpret this as the results of the intense steepening/detachment of the slab beneath the Eurasian plate. A such geodynamical process was also described by Sosson *et al.*, (2010, 2016) to explain in the Lesser Caucasus the presence of an Eocene basin unconformably overlying the Neotethys suture zone, Eurasia and the TASAM.

Finally, we want to point out that the Alborz basin shows some similarity in the tectonic evolution, but with a NNW/SSE direction (previous basin during the Mesozoic, inverted during the Palaeocene to the north with the Caspian basin border, and then rifted basin with volcanic activity during the Eocene (Brunet *et al.*, 2007; Shahidi *et al.*, 2011)). The Neogene compression affects it and inverts the basin (Brunet *et al.*, 2007; Shahidi *et al.*, 2011). They interpret this as a back-arc during the Eocene too.

\* We talk about “back-arc” basin, but the cause of this extension is not accepted and still matter of debate (Okay *et al.*, 1994; McCann *et al.*, 2010; Sosson *et al.*, 2016; Tari *et al.*, 2020)). The Greater Caucasus seems to be the back-arc basin, but then, during the Lower Cretaceous-early Upper Cretaceous, the extension jumps toward the south in the BS area while it stays in the GC toward the east.

#### c. The Oligocene deposits

During the Oligocene (and Lower Miocene), the lithologies of “Maykopian series” evidence an euxinic environment which created evaporites (Adamia *et al.*, 2010). We have proposed to explain this palaeoenvironment by the role of the Palaeocene-Eocene collision in the LC, which creates uplift of the suture zone and propagation off the compressional deformation which caused the basins inversion in the internal zone (GC). This constrains only the north and the south of the area. The Dzirula massif creates a high which separates the Rioni from the Kura area, but the AT is not separated here. We cannot constrain the lateral borders of the Maykopian evaporitic basin. Eastward near the Caspian Sea Van der Boon *et al.*, (2017) propose that the Maykopian deposits are “syn-collision”. The question is here the age of “the Maykopian” deposits which are more defined as a facies, but (Milanovsky & Khain 1963) were already talking about the syn-collisional Maykopian deposits.

#### d. Styles of deformation variations from west to east along the belt and relation with the inherited structures

(Somin 1996) was not considering the plate tectonics in the area but had some observations which we have interpreted in modern interpretations. Where the basement is deformed (interpreted as geosynclinal, regional diapirism), our observations are interpreted to be thick-skinned tectonic (the GB between Koutaissi and Ambrolauri). However, he interpreted a “diapir” to be made of Liassic rocks, and this could be interpreted as thin-skinned tectonic. We don’t have any observation of the Lias deposits that could lead us to interpret it as a decollement level.

The structures along the deformational front of the GC were interpreted as the result of a thin-skinned tectonic, in the east (as observed in this study) (Forte *et al.*, 2010, 2013; Alania *et al.*, 2017), but also toward the west in lateral continuity of the eastern structures (Gamkrelidze *et al.*, 2018, n.d.). This lateral and cylindrical interpretation was already contested (Khain 2007, 2009; Trexler *et al.*, 2020). These authors pointed the differences from west to east, because of occurrence of major strike-slip faults cutting the main structures of the front or by the presence or not of inherited structures. Khain's (1975) interpretations are based on non-plate tectonics have nevertheless some interesting points: he interpreted every structure to be inherited structures, with thick-skinned tectonic dominance. This interpretation has evolved (Khain 2007, 2009), however, some of its observations were interesting regarding the role of the inherited structures we point in the study, and the role on the variations in styles from west to east. In the Eastern area (Kura), (Allen *et al.*, 2004) shows that the along-strike variations in style of deformation could also be triggered by the syn-tectonic deposits, the erosion and the amount of shortening in the area (involving some differences in the rate of shortening along strike as a trigger).

We have highlighted that during the compressional tectonic regime, especially during the Palaeocene-Eocene one, the tectonic response difference between the Rioni and the Kura area seems to be mostly related to the presence of inherited structures. The occurrence of pre-existing normal faults related to the rifting phases (Barremian, Aptian-Cenomanian Fig. V.5, V.6) interpreted in chap. 2 based on the observations of the unconformities, the shape of the Lower to Upper Cretaceous deposits, and their thickness variations in the BS-GB area, seem to control the location of the deformations. Moreover, as observed in chap. 3, the style of the deformation in thick-skinned or a combination of thick-skinned and then thin-skinned tectonic is due to the inherited faults. Toward the east, these normal faults are not observed, and the formation of duplex and decollements are the evolution of the thin-skinned tectonic deformation (decollement levels can be the Oligocene Maykopian deposits, as proposed in this study, and/or the Middle Miocene deposits and the Sarmatian deposits (Forte *et al.*, 2010, 2013; Alania *et al.*, 2017).

This result involves a difference of shortening rate between the western and eastern GC. According to Khain (2009), the eastern part tectonic front of the GC presents folds and thrusts structures deformed by higher rate of deformation. (Philip *et al.*, 1989; Mosar *et al.*, 2010) show that the tectonic evolution is heterogeneous along the southern GC and interpret that the strain partitioning is vertical (uplift amount/rate) and horizontal (shortening rates). Trexler *et al.*, (2020) propose also some differences in the rates of deformation and their location along the GC, especially in the western part.

Moreover, differences between the western and the eastern structural style could be related to changes in the shortening rate: it could be more intense in the eastern part (as also proposed by Mosar *et al.*, (2010) where the major thick-skinned deformations related to the GC result in major thin-skinned deformations at the frontal part and in the foreland basin.

This can also be observed during the Upper Miocene compression during the Meotian Pontian (MP), as proposed by Mosar *et al.*, (2010), when an acceleration of shortening took place. In the western area in the Rioni foreland basin, the deformations are localized on inherited normal faults (chap. 2 and 3). The deformations are not observed further from the major anticlines. The location of the MP deposits in the Rioni foreland basins is in the undeformed areas. We can't thus argue if these deposits are poorly deformed because the deformation is far or if it is not active during the MP. The studies of Tibaldi *et al.*, (2017) and Trexler *et al.*, (2020) show that the tectonic is still active in the western part, so we can say that the MP are just too far from the deformed area and remain undeformed.

The role of the AT FTB/basin should be a key to understand the differences between changes in the structures of the GC front belt from west to east. Indeed, the AT FTB could be the cause of a change in the shortening rate from west to east.

The AT basin presents a westward enlargement (chap. 4) which could have had an impact onto the distribution of the shortening rate due to the collision in the Lesser Caucasus. The AT basin was narrow and thinner eastward (near Tbilisi). Consequently, we can propose that the compression initiated from the Lesser Caucasus compression to the GC inversion was continuous in the eastern part of The AT Basin, while westward, where the basin is wider, the compression was decreasing in the Rioni foreland basin.

## V. Limits and perspectives

### 1. Styles of deformation variations from west to east and relations with strike-slips structures (inherited or neofomed)

A question about the W-E differences is if it is the consequences of strike-slip and rotational movements, or if the differences linked to the different deformations styles can result in different rates of shortening and thus create some strike-slips movement to accommodate these deformations.

Eastern Transcaucasus and southern Greater Caucasus		Eastern Adjara-Trialeti	
Timing	Observations	Interpretation	Tectonic setting
Pliocene	sandstones to conglomerates	compression thin-skinned tectonic uplift in GC and AT: products of erosion	
Upper Miocene	<b>U7: unconformity or undeveloped Meotis Pontian</b> sandstones to conglomerates	compression thin-skinned tectonic	
Middle Miocene	<b>U6: unconformity Up Miocene</b> sandstones and detrital deposits	erosion calm and closed environment delimited by topography flexural subsidence?	
Oligocene-Lower Miocene	clays, gypsum, septaria, detrital		
Eocene Paleocene	<b>U5: unconformity Oligocene</b> marls, turbidites, olistostrome	flysch syn-duplex formation	
Danian Campanian-Maastrichtian	Limestones and mudstone	Calm platform	
Aptian-Cenomanian	flyschs turbidites argillites and shales	extension	
Turonian-Santonian			

Extension/rifting  
 Subsidence  
 Localised extension  
 Localised subsidence  
 Calm environment

Compression: thick+thin-skinned  
 Compression: thick-skinned  
 Compression: thin-skinned  
 Uplift - compression  
 - - - - Unconformity

Figure V.6: Recapitulative table of the observations and interpretations resulting of the study for the western Transcaucasus area

The differences from west to east takes place during the whole tectonic evolution of these domains since the Early Cretaceous when the extensional deformations create the opening of basins. The Eastern Black Sea is not the structural continuation of the Western Black Sea and does not continues eastward of the Dzirula Massif. The superimposed AT basin onto the southern EBS opened during the Paleogene and ends near Tbilisi.

In order to explain the lateral variation of tectonic regime transpression and transtension and rotational tectonic are proposed in many studies (Philip *et al.*, 1989; Rebaï *et al.*, 1993; Okay *et al.*, 1994; Allen *et al.*, 2003, 2004; McCann *et al.*, 2010; Lefebvre *et al.*, 2013; Nikishin *et al.*, 2015; Meijers *et al.*, 2017; Tibaldi *et al.*, 2017). The change in the main directions of shortening, as for the southern Black Sea proposed by Hippolyte *et al.*, (2015) who proposed a NNE direction of shortening before the escape of the Anatolian plate resulting in a NW direction for the main shortening during the Neogene. The occurrence of rotational tectonic has not been considered in our study. The role of strike-slips tectonic should have been taken in account. For example, the Zugdidi dextral fault affects the Rioni foreland basin. The variation of the bedding from W to E in the Jvari area could be due to this fault zone (chapter 2). The difference of the tectonic response in the Georgian Block and in the Rioni foreland could also be related to major strike-slip motion, as well as the shape of the Dzirula massif, which can be interpreted as a rigid unit where limited deformation occur (Trexler *et al.*, 2020). However we haven't taken it into account and it can have an importance, especially with the rotational tectonic (as observed in the Black Sea by e.g. (Okay *et al.*, 1994) (Korniyenko-Sheremet *et al.*, 2021) and in the whole Anatolides-Taurides-Pontides area (Lefebvre *et al.*, 2013), or the West-East differences. The AT fold-and-thrust belt global structure can also be affected by strike-slip tectonic.

There is no doubt about the importance of the strike slip regime of deformation to explain the variation of the tectonic evolution in the region and especially regarding the importance to the south of the LC (Avagyan *et al.*, 2008, 2010) and toward the west in Turkey as proposed by Koçyiğit *et al.*, (2001): the main thrusting could evolve during the Pliocene in the sutures zones in major strike-slip movements (and related transpression). The effect of a punching/indenting effect of the Arabia and the TASAM into the Eurasia which evolves in escaping of the TASAM toward the west should have major consequences (Philip *et al.*, 1989; Koçyiğit *et al.*, 2001; Adamia *et al.*, 2011a; Hippolyte *et al.*, 2015, 2018).

The modalities of the opening of the Black Sea basins debate is also related to these questions for those who try to constrain the Western basin and the Eastern basin: from the creation to the inversion, the tectonic in the area seems to be very affected by rotational tectonic (except

if we interpret the Black Sea as an asymmetrical back-arc basin (Stephenson & Schellart 2010), but this interpretation does not take in account that the Eastern Greater Caucasus is still opening during the late Early Cretaceous. The questions about the opening of the Black Sea as an active rifting (asymmetric) or passive rifting (with transtension) as described in (Stampfli *et al.*, 1991) is a key problem in the area, but our study does not improve the problem at this scale.

## 2. What controls the style of deformation?

Finally, this study also has interesting results about the style of deformations and the role of the inherited structures.

The ancient normal faults can play a role on the location of the deformation during the compression stages and the location of the flexural basins on the borders of the rifted basins. As observed in chap. 2 and 3, the frontal deformations in the western area are localized on the inherited normal faults that bordered the basins, while the central normal faults are not reactivated by the compression (observed in the central cross section). The flexural basins are in this situation, located above horst structures. This is also proposed in the southern BS by Espurt *et al.*, (2014), Hippolyte *et al.*, (2015, 2018) in the Pontides area where the deformation is localized on ancient normal faults related to the rifting phases, while the “strong and cold” BS basin is not deformed. The northern margin is also affected by localised deformations and possible transpressive and strike-slip movements along the borders (Angelier *et al.*, 1994; Saintot & Angelier 2002; Gobarenko *et al.*, 2016; Korniyenko-Sheremet *et al.*, 2021). The localisation of the deformation on the borders of the basin is also observed in the Caspian basin (Allen *et al.*, 2003, 2004) where some strike-slip movement draw the contour of the basin. (Adamia *et al.*, 2010) opposes the rigid platform where no or limited deformation occur, and the fold-and-thrusts belts where most of the deformation is localised. In the same idea, Trexler *et al.*, (2020) propose that the Dzirula Massif behaviour is the same as a rigid block too.

The thick-skinned tectonic deformations are not the only ones driven by the occurrence of the inherited normal faults: these faults can also control the location of the thin-skinned deformations.

In the AT FTB, the locations where most of the décollements occur are in the synclines in the post-rift deposits. The “box effect” could be interesting to study with software used to make equilibrate cross section, such as MOVE. The model without thin-skinned tectonic results in an excess of post-extension deposits. This seems to support that the post-extension deposits have to be deformed by thin-skinned tectonic. The décollement levels offer the possibility to deform the post-rift deposits “inside the box” delimited by the normal faults that border the AT

basin. Because the inverted basins of the internal zone of the Caucasus (Georgian Block, the AT basin) are constrained to the north and to the south, the deposits cannot be displaced in a long way: we have observed this in the Rioni foreland basin where the normal faults, active at least until the early Late Cretaceous, affect the decollement level situated in the Upper Jurassic (chap. 2).

The controls onto the thin-skinned tectonic can also be the occurrence of possible decollement levels. The difference between the GB (Koutaissi-Ambrolauri) and the Rioni foreland basin deformations show that in the GB, where the Upper Jurassic deposits are not observed near Koutaissi, thin-skinned tectonic does not take place, while the Tsaishi anticline for example, is affected by the thin-skinned tectonic onto the Upper Jurassic deposits decollement level. The Upper Jurassic evaporites and clays and the Albian-Cenomanian clays and marls deposits are the possible deposits in the GB, and also the Maykopian shales and gypsum in the Rioni foreland basin. In the Kura foreland basin, the marls and clays Cenomanian is the decollement level along the southern GC, and the Maykopian shales and gypsum below the Kura foreland basin. In the AT FTB, the main decollement levels are the Albian-Cenomanian clays and marls deposits, some parts in the Palaeocene-Eocene are not well defined but observed in the seismic profile, and in the Oligocene Maykopian shales and gypsum deposits mostly (observed in the seismic profile and in the field).

The amount of deposits that has to be transported above the decollement level can also controls the occurrence of the decollement (Lacombe & Bellahsen 2016). Since the seismic profiles is situated in the Eastern AT FTB, there is thus a possibility that the style of deformation varies westward in the central part of the basin.

### 3. Salt tectonic in the Maykopian deposits

Finally, the occurrence of possible diapirism – salt-tectonic in the Maykopian deposits has not been taken in account into this study. The seismic line in Rioni could be interpreted with salt-tectonic that could deform the Neogene deposits. We don't have focused on these deformations because these were not significant regarding the scale of the major folds (<1km of wavelength, see the seismic interpretation in chap. 3 where the Neogene deposits are deformed above the Oligocene deposits while the older deposits remain undeformed). The very important occurrence of such tectonic in the Pontides show however that this possibility could have been more important. (Khain 2007) describes some mud-clays diapirism in Eastern Georgia as well.



#### 4. The shortening rate

The different units are not deformed by a unique style of deformation. We have observed that the western Georgia is more affected by thick-skinned tectonic and some thin-skinned tectonic in some places, while the Central Georgia is mainly affected by thin-skinned tectonic. The style of deformation differs also depending on the tectonic units, from north to south, the GC, the GB and the Rioni FB, the Kura FB, and the AT to the south. The BS and its eastern continuation the GB show mainly thick-skinned deformation. (Espurt *et al.*, 2014) who has studied the southern part of the EBS, situated west of our study proposed that the thick-skinned deformations localized on the borders of the EBS results in about 33% shortening. It can also vary in a same structural unit as in between the Rioni FB and the GB, especially during the Late Miocene compression because of the style of deformation observed. This is also an argument that the strike-slip role in the area must be studied.

The GC shows intense deformation, and results in a thin-skinned deformation at the eastern border, but the western are (ex. North of the Ambrolauri area), it is more in thick-skinned deformation.

The AT is thick-and-thin-skinned tectonic and show a differential rate shortening in the different deposits (pre-syn-post extension) but results in an inversion of the basin to get closer to the size before the extension.

An interesting application to these observations could be to calculate the different shortening amount in all the structural units separately, and then compare the total amount of shortening from west to east. This could reflect the real difference in shortening along the GC. To consider the shortening and extending amount in the whole area could be also very interesting to highlight the role of the extensive structures during the collisions.

#### 5. Resources

The known source rocks are the Upper Eocene deposits in the Eastern Black Sea (Robinson *et al.*, 1996) and with its interpretation of the EBS, should be also in the AT.

The Jurassic and Mesozoic deposits were interpreted to be too deep by Robinson *et al.*, (1996). However, the GB in the Rioni area is from a more deltaic environment, situated at the end of the eastern continuation of the basin. The Bathonian coal observed in the Koutaissi-Ambrolauri area (GB) show that the environment was a good environment to cumulate organic matters. However, the question which remains it rest of the tectonic history of these deposits to creates oils and gas.

The structures observed in the Koutaissi-Ambrolauri area are thick-skinned tectonic. However, toward the west, where the deposits could have been buried deeper and be source of oil/gas, the deformation style combine thick and thin-skinned tectonic (see previous paragraph for the parameters proposed to control the deformation). The occurrence of the Upper Jurassic evaporitic deposits allows to have the thin-skinned tectonic, and there are not too many deposits to block the thin-skinned deformation (EBS). This is the reason why the Tsaishi anticline is such studied. The combination of the thick-skinned tectonic in the area could have trigger some bias in the evolution of the oil/gas contents. The Maykopian series can be also sources rocks.

The inherited structure have an important role on the resources (Stampfli *et al.*, 1991; Robinson *et al.*, 1996; Tari & Simmons 2018; Tari *et al.*, 2020). The inherited structures of the Eastern Black Sea are thus very important on the interpretation of the potential resources in the Transcaucasus and our interpretation to make the normal fault inversion during the Paleocene has consequences. We don't have observed the fault propagation into the Palaeocene or Eocene deposits, which has the consequence that these deposits cover the fault. If some studies are made keeping in head that the normal fault have been inverted, the location and the role of the propagation of the fault is important. If the fault would cut the Paleogene deposits, the Maykopian deposits will be very important as a reservoir.

## VI. Conclusion

To conclude, this study gives new highlights concerning the structures and their lateral variations in the Transcaucasus area.

The Rioni foreland basin develops onto an extensive basin opened by rifting during the Early Cretaceous. The inherited structures of this basin are inverted during the Palaeocene and Eocene and then is deformed during the Miocene by thin-skinned tectonic based on an Upper Jurassic decollement level. Eastward, the thin-skinned deformation does not occur. We observe that this basin localised the deformations on the borders and create the main foreland basins at the fronts: onto the horsts. The geometry of the basin is thus the main driver for the geometries of the structures during the compression stages and could explain the shape of the Dzirula massif which separates the Rioni from the Kura foreland basins.

Toward the east, the thin-skinned tectonic is the main deformation style.

An exception is the style of deformation observed in the Adjara-Trialeti fold-and-thrust belt which is also an inverted basin that ends near Tbilisi. This basin is deformed by thick-skinned tectonic and the normal faults locations controls the localisation of the deformation. However, some decollement levels are observed and thin-skinned tectonic occurs along these normal faults.

The timing of the tectonic stages highlighted in this study is consistent with the observations made all around the Transcaucasus area and confirms that there is no different evolution in this area regarding the tectonic of the global Caucasus area.



## Bibliography

- Abesadze, G., Adamia, S., Beradze, R., Bukia, S., Gamkrelidze, M., Gujabidze, G., Geguchadze, Sh., Devdariani, E., Vashakidze, I., Edilashvili, V., Torozov, R., Kandelaki, N., Kandelaki, Dj., Metreveli, I., Papava, D., Sepashvili, O., Pruidze, M., Kipiani, Y., Chichua, G., Shirashvili, O. & Jigauri, D. 2004. Geological map of Georgia.
- Adamia, S., Alania, V., Ananiashvili, G.D., Bombolakis, E.G., Chichua, G., GIRSIASHVILI, D., MARTIN, R. & TATARASHVIL, L. 2002. Late Mesozoic-Cenozoic geodynamic evolution of the Eastern Georgian oil-gaz bearing basin (Transcaucasus).
- Adamia, S., Alania, V., Chabukiani, A., Chichua, G., Enukidze, O. & Sadradze, N. 2010. Evolution of the Late Cenozoic basins of Georgia (SW Caucasus): a review. *Geological Society, London, Special Publications 340*, 239–259. DOI 10.1144/SP340.11
- Adamia, S., Zakariadze, G., Chkhotua, T., Sadradze, N., Tsereteli, N., Chabukiani, A. & Gventsadze, A. 2011a. Geology of the Caucasus: a review. *Turkish Journal of Earth Sciences 20(5)*, 489–544.
- Adamia, S., Alania, V., Chabukiani, A., Kutelia, Z. & Sadradze, N. 2011b. Great Caucasus (Cavcasioni): a long-lived north-Tethyan back-arc basin. *Turkish Journal of Earth Sciences 20(5)*, 611–628.
- Adamia, S., Alania, V., Gventsadze, A., Enukidze, O., Sadradze, N., Tsereteli, N. & Zakariadze, G.S. 2017. Tethyan evolution and continental collision in SW Caucasus (Georgia and adjacent areas).
- Adamia, S.A., Chkhotua, T., Kekelia, M., Lordkipanidze, M., Shavishvili, I. & Zakariadze, G. 1981. Tectonics of the Caucasus and adjoining regions: implications for the evolution of the Tethys ocean. *Journal of Structural Geology 3(4)*, 437–447.
- Adamia, S.A., Chkhotua, T.G., Gvartadze, T.T., Lebanidze, Z.A., Lursmanashvili, N.D., Sadradze, N.G., Zakaraia, D.P. & Zakariadze, G.S. 2015. Tectonic setting of Georgia–Eastern Black Sea: a review. *Geological Society, London, Special Publications 428(1)*, 11–40. DOI 10.1144/SP428.6
- Adamia, Sh.A., Lordkipanidze, M.B. & Zakariadze, G.S. 1977. Evolution of an active continental margin as exemplified by the Alpine history of the Caucasus. *Tectonophysics 40(3–4)*, 183–199. DOI 10.1016/0040-1951(77)90065-8

- Ahmadi, R., Mercier, E. & Ouali, J. 2013. Growth-strata geometry in fault-propagation folds: a case study from the Gafsa basin, southern Tunisian Atlas. *Swiss Journal of Geosciences* 106(1), 91–107. DOI 10.1007/s00015-013-0122-z
- Alania, V., Bukhsianidze, M., Chabukiani, A., Chagelkhvili, R. & E nukidze, O. 2009. The kinematic evolution of Kura foreland fold and thrust belt, Eastern Georgia.
- Alania, V., Beridze, T., E nukidze, O., Le banidze, Z., Razmadze, A., Sadradze, N. & Tevzadze, N. 2020. Structural Model of the Frontal Part of the Eastern Achara-Trialeti Fold-and-Thrust Belt: the Results of Seismic Profile Interpretation. 14(2), 8.
- Alania, V.M., Chabukiani, A.O., Chagelishvili, R.L., E nukidze, O.V., Gogrichiani, K.O., Razmadze, A.N. & Tsereteli, N.S. 2017a. Growth structures, piggy-back basins and growth strata of the Georgian part of the Kura foreland fold–thrust belt: implications for Late Alpine kinematic evolution. *Geological Society, London, Special Publications* 428(1), 171–185. DOI 10.1144/SP428.5
- Alania, V.M., Sosson, M., E nukidze, O.V., Asatiani, N., Beridze, T., Candaux, Z., Chabukiani, A., Giorgadze, A., Gventsadze, A., Kvavadze, N., Kvintradze, G. & Tsereteli, N. 2017b. Structural architecture of the eastern Achara-Trialeti fold and thrust belt, Georgia: Implications for kinematic evolution. *South Caucasus Geosciences*(4). DOI 10.1144/SP428.5
- Allen, M., Jackson, J. & Walker, R. 2004. Late Cenozoic reorganization of the Arabia-Eurasia collision and the comparison of short-term and long-term deformation rates: ARABIA-EURASIA COLLISION. *Tectonics* 23(2), n/a-n/a. DOI 10.1029/2003TC001530
- Allen, M.B., Vincent, S.J., Alsop, G.I., Ismail-zadeh, A. & Flecker, R. 2003. Late Cenozoic deformation in the South Caspian region: effects of a rigid basement block within a collision zone. *Tectonophysics* 366(3–4), 223–239. DOI 10.1016/S0040-1951(03)00098-2
- Angelier, J., Gushtenko, O., Saintot, A., Ilyin, A., Rebetsky, Y., Vassiliev, N., Yakovlev, F. & Malutin, S. 1994. Relations entre champs de contraintes et déformations le long d’une chaîne compressive-décrochante: Crimée et Caucase (Russie et Ukraine) - Relationships between stress fields and deformation along a compressive strike-slip belt: Caucasus and Crimea (Russia and Ukraine). *Comptes Rendus de l’Académie des sciences*, 341–348.
- Banks, C.J., Robinson, A.G. & Williams, M.P. 1998. Structure and regional tectonics of the Achara-Trialeti fold belt and the adjacent Rioni and Kartli foreland basins, Republic of Georgia. *MEMOIRS-AMERICAN ASSOCIATION OF PETROLEUM GEOLOGISTS*, 331–346.

- Barrier, E. & Vrielynck, B. 2008. Middle East Basins Evolution Programme.
- Barrier, E., Vrielynck, B., Brouillet, J.F. & Brunet, M.-F. 2018. *Paleotectonic Reconstruction of the Central Tethyan Realm. Tectonono-Sedimentary-Palinspastic Maps from Late Permian to Pliocene*. CCGM/CGMW.
- Bauville, A. & Schmalholz, S.M. 2015. Transition from thin- to thick-skinned tectonics and consequences for nappe formation: Numerical simulations and applications to the Helvetic nappe system, Switzerland. *Tectonophysics* 665, 101–117.
- Brunet, M.-F., Shahidi, A., Barrier, E., Muller, C. & Saidi, A. 2007. Geodynamics of the South Caspian Basin southern margin now inverted in Alborz and Kopet Dagh (Northern Iran). In: *Geophysical Research Abstracts – EGU*.
- Butler, R.W.H., Tavarnelli, E. & Grasso, M. 2006. Structural inheritance in mountain belts: An Alpine–Apennine perspective. *Journal of Structural Geology* 28(11), 1893–1908. DOI 10.1016/j.jsg.2006.09.006
- Castelltort, S., Pochat, S. & Van den Driessche, J. 2004. How reliable are growth strata in interpreting short-term (10 s to 100 s ka) growth structures kinematics? *Comptes Rendus Geoscience* 336(2), 151–158. DOI 10.1016/j.crte.2003.10.020
- Cloetingh, S., Spadini, G., Van Wees, J.D. & Beekman, F. 2003. Thermo-mechanical modelling of Black Sea Basin (de)formation. *Sedimentary Geology* 156(1–4), 169–184. DOI 10.1016/S0037-0738(02)00287-7
- Cowgill, E., Forte, A.M., Niemi, N., Avdeev, B., Tye, A., Trexler, C., Javakhishvili, Z., Elashvili, M. & Godoladze, T. 2016. Relict basin closure and crustal shortening budgets during continental collision: An example from Caucasus sediment provenance: Greater Caucasus Relict Basin Closure. *Tectonics* 35(12), 2918–2947. DOI 10.1002/2016TC004295
- Davis, D., Suppe, J. & Dahlen, F.A. 1983. Mechanics of fold-and-thrust belts and accretionary wedges. *Journal of Geophysical Research* 88(B2), 1153. DOI 10.1029/JB088iB02p01153
- Epard, J.-L. & Groshong, Jr., R.H. 1993. Excess area and depth to detachment. *The American Association of Petroleum Geologists Bulletin* 77(8), 1291–1302.

- Epard, J.-L. & Groshong, Jr., R.H. 1995. Kinematic model of detachment folding including limb rotation, fixed hinges and layer-parallel strain. *Tectonophysics* 247, 85–103. DOI SSDI 0040-1951(94)00266-5
- Erdős, Z., Huismans, R.S. & Van der Beek, P. 2015. First-order control of syntectonic sedimentation on crustal-scale structure of mountain belts. *J. Geophys. Res. Solid Earth* 120, 5362–5377. DOI 10.1002/2014JB011408.
- Espurt, N., Hippolyte, J.-C., Kaymakci, N. & Sangu, E. 2014. Lithospheric structural control on inversion of the southern margin of the Black Sea Basin, Central Pontides, Turkey. *Lithosphere* 6(1), 26–34. DOI 10.1130/L316.1
- Finetti, I., Bricchi, G., Del Ben, A., Pipan, M. & Xuan, Z. 1988. Geophysical study of the Black Sea. *Bollettino di Geofisica Teorica ed Applicata* 30(117–118), 197–324.
- Forte, A.M., Cowgill, E., Bernardin, T., Kreylos, O. & Hamann, B. 2010. Late Cenozoic deformation of the Kura fold-thrust belt, southern Greater Caucasus. *Geological Society of America Bulletin* 122(3–4), 465–486.
- Forte, A.M., Cowgill, E., Murtuzayev, I., Kangarli, T. & Stoica, M. 2013. Structural geometries and magnitude of shortening in the eastern Kura fold-thrust belt, Azerbaijan: Implications for the development of the Greater Caucasus Mountains: STRUCTURAL GEOMETRIES OF KURA FTB. *Tectonics* 32(3), 688–717. DOI 10.1002/tect.20032
- Forte, A.M., Sumner, D.Y., Cowgill, E., Stoica, M., Murtuzayev, I., Kangarli, T., Elashvili, M., Godoladze, T. & Javakhishvili, Z. 2015. Late Miocene to Pliocene stratigraphy of the Kura Basin, a subbasin of the South Caspian Basin: implications for the diachroneity of stage boundaries. *Basin Research* 27(3), 247–271. DOI 10.1111/bre.12069
- Gaetani, M., Garzanti, E., Riccardo, P., Kiricko, Y., Korsakhov, S., Cirilli, C., Nicora, A., Rettori, R., Larghi, C. & Bucefalo Palliani, R. 2005. Stratigraphic evidence of Cimmerian events in NW Caucasus (Russia).
- Gamkrelidze, I., Koiava, K. & Mosar, J. 2015. Geological Structure of Georgia and Geodynamic Evolution of the Caucasus. , 3.



- Gamkrelidze, Irakli, Koiava, K., Mosar, J., Kvaliashvili, L. & Mauvilly, J. 2018. Main features of geological structure and a new tectonic map of Georgia. In: *EGU General Assembly Conference Abstracts*. 5040.
- Gamkrelidze, I.P. 1964. Geology of the USSR. Georgian SSR. *Moscow 'Nedra' X*, 1–655.
- Gamkrelidze, I.P. 1986. GEODYNAMIC EVOLUTION OF THE CAUCASUS AND ADJACENT AREAS IN ALPINE TIME. *Tectonophysics* 127, 261–277. DOI 0040-1951/86/
- Gamkrelidze, I.P. 1991. Tectonic nappes and horizontal layering of the Earth's crust in the Mediterranean belt (Crpathians, Balkanides and Caucasus).
- Gamkrelidze, I. P., Koiava, K., Mosar, J., Kvaliashvili, L. & Mauvilly, J. 2018. Main features of geological structure and a new tectonic map of Georgia.
- Gamkrelidze, I.P., Koiava, K. & Mosar, J. n.d. Geological Structure of Georgia and Geodynamic Evolution of the Caucasus.
- Gobarenko, V.S., Murovskaya, A.V., Yegorova, T.P. & Sheremet, E.E. 2016. Collision processes at the northern margin of the Black Sea. *Geotectonics* 50(4), 407–424. DOI 10.1134/S0016852116040026
- Görür, N. 1988. Timing of opening of the Black Sea basin. *Tectonophysics* 147(3–4), 247–262. DOI 10.1016/0040-1951(88)90189-8
- Guo, L., Vincent, S.J. & Lavrishchev, V. 2011. Upper Jurassic reefs from the Russian western Caucasus: Implications for the eastern Black Sea. *Turkish Journal of Earth Sciences* 20(5), 629–653.
- Hässig, M., Rolland, Y. & Sosson, M. 2015. From seafloor spreading to obduction: Jurassic–Cretaceous evolution of the northern branch of the Neotethys in the Northeastern Anatolian and Lesser Caucasus regions. *Geological Society, London, Special Publications* 428(1), 41–60. DOI 10.1144/SP428.10
- Hässig, M., Moritz, R., Ulianov, A., Popkhadze, N., Galoyan, G. & Enukidze, O. 2020. Jurassic to Cenozoic Magmatic and Geodynamic Evolution of the Eastern Pontides and Caucasus Belts, and Their Relationship With the Eastern Black Sea Basin Opening. *Tectonics* 39(10). DOI 10.1029/2020TC006336

- Hippolyte, J.-C., Muller, C., Kaymakci, N. & Sangu, E. 2010. Dating of the Black Sea Basin: new nannoplankton ages from its inverted margin in the Central Pontides (Turkey). *Geological Society, London, Special Publications 340(1)*, 113–136. DOI 10.1144/SP340.7
- Hippolyte, J.-C., Espurt, N., Kaymakci, N., Sangu, E. & Müller, C. 2015. Cross-sectional anatomy and geodynamic evolution of the Central Pontide orogenic belt (northern Turkey). *International Journal of Earth Sciences*. DOI 10.1007/s00531-015-1170-6
- Hippolyte, J.-C., Murovskaya, A., Volfman, Y., Yegorova, T., Gintov, O., Kaymakci, N. & Sangu, E. 2018. Age and geodynamic evolution of the Black Sea Basin: Tectonic evidences of rifting in Crimea. *Marine and Petroleum Geology 93*, 298–314. DOI 10.1016/j.marpetgeo.2018.03.009
- Kaz'min, V.G. & Tikhonova, N.F. 2006. Late Cretaceous-Eocene marginal seas in the Black Sea-Caspian region: Paleotectonic reconstructions. *Geotectonics 40(3)*, 169–182. DOI 10.1134/S0016852106030022
- Khain, V.E. 1975. Structure and main stages in the tectono-magmatic development of the Caucasus: an attempt at geodynamic interpretation.
- Khain, V.E. 2007. Mesozoic-Cenozoic accretionary complexes of the Greater Caucasus. *Doklady Earth Sciences 413(2)*, 376–379. DOI 10.1134/S1028334X07030129
- Khain, V.E. 2009. On the role of the Transcaucasian transverse uplift in preorogenic Alpine evolution of the Greater Caucasus. *Doklady Earth Sciences 426(1)*, 532–533. DOI 10.1134/S1028334X09040047
- Koçyiğit, A., Yilmaz, A., Adamia, S. & Kuloshvili, S. 2001. Neotectonics of East Anatolian Plateau (Turkey) and Lesser Caucasus: implication for transition from thrusting to strike-slip faulting. *Geodinamica Acta 14(1–3)*, 177–195.
- Korniyenko-Sheremet, Y., Sosson, M., Murovskaya, A., Gobarenko, V. & Yegorova, T. 2021. Palaeo-stress regimes and structural framework during the Mesozoic-Cenozoic tectonic evolution of the Crimean Mountains (the northern margin of the Black Sea). *Journal of Asian Earth Sciences 211*, 104704. DOI 10.1016/j.jseaes.2021.104704
- Lacombe, O. & Bellahsen, N. 2016. Thick-skinned tectonics and basement-involved fold–thrust belts: insights from selected Cenozoic orogens. *Geological Magazine 153(5–6)*, 763–810. DOI 10.1017/S0016756816000078

- Lefebvre, C., Meijers, M.J.M., Kaymakci, N., Peynircioğlu, A., Langereis, C.G. & van Hinsbergen, D.J.J. 2013. Reconstructing the geometry of central Anatolia during the late Cretaceous: Large-scale Cenozoic rotations and deformation between the Pontides and Taurides. *Earth and Planetary Science Letters* 366, 83–98. DOI 10.1016/j.epsl.2013.01.003
- Maynard, J.R. & Erratt, D. 2020. The Black Sea, a Tertiary basin: Observations and insights. *Marine and Petroleum Geology* 118, 104462. DOI 10.1016/j.marpetgeo.2020.104462
- McCann, T., Chalot-Prat, F. & Saintot, A. 2010. The Early Mesozoic evolution of the Western Greater Caucasus (Russia): Triassic-Jurassic sedimentary and magmatic history. *Geological Society, London, Special Publications* 340(1), 181–238. DOI 10.1144/SP340.10
- Meijers, M.J.M., Smith, B., Pastor-Galán, D., Degenaar, R., Sadradze, N., Adamia, S., Sahakyan, L., Avagyan, A., Sosson, M., Rolland, Y., Langereis, C.G. & Müller, C. 2017. Progressive orocline formation in the Eastern Pontides–Lesser Caucasus. *Geological Society, London, Special Publications* 428(1), 117–143. DOI 10.1144/SP428.8
- Mercier, E., Rafini, S. & Ahmadi, R. 2007. Folds Kinematics in “Fold-and-Thrust Belts” the “Hinge Migration” Question, a Review. In: Lacombe, O., Roure, F., Lavé, J. & Vergés, J. (eds) *Thrust Belts and Foreland Basins*. Springer Berlin Heidelberg, Berlin, Heidelberg, 135–147.
- Milanovsky, E.E. & Khain, V.E. 1963. Geological structure of the Caucasus.
- Monteleone, V., Minshull, T.A. & Marin-Moreno, H. 2019. Spatial and temporal evolution of rifting and continental breakup in the eastern Black Sea basin revealed by long-offset seismic reflection data. *Tectonics* 38(8), 2646–2667.
- Morariu, D. & Noual, V. 2009. Cretaceous play - new exploration potential in the Eastern Georgia.
- Mosar, J., Kangarli, T., Bochud, M., Glasmacher, U.A., Rast, A., Brunet, M.-F. & Sosson, M. 2010. Cenozoic-Recent tectonics and uplift in the Greater Caucasus: a perspective from Azerbaijan. *Geological Society, London, Special Publications* 340(1), 261–280. DOI 10.1144/SP340.12
- Mumladze, T., Forte, A.M., Cowgill, E.S., Trexler, C.C., Niemi, N.A., Burak Yılmaz, M. & Kellogg, L.H. 2015. Subducted, detached, and torn slabs beneath the Greater Caucasus. *GeoResJ* 5, 36–46. DOI 10.1016/j.grj.2014.09.004
- Nalpas, T. 1994. *Inversion Des Grabens Du Sud de La Mer Du Nord. Données de Sub-Surface et Modélisation Analogique*. Université de Rennes I.

- Nikishin, A.M. & Cloetingh, S. 1998. Scythian Platform, Caucasus and Black Sea region: Mesoizoic-Cenozoic tectonic history and dynamics.
- Nikishin, A.M., Korotaev, M.V., Ershov, A.V. & Brunet, M.-F. 2003. The Black Sea basin: tectonic history and Neogene–Quaternary rapid subsidence modelling. *Sedimentary Geology* 156(1), 149–168.
- Nikishin, A.M., Ershov, A.V. & Nikishin, V.A. 2010. Geological history of Western Caucasus and adjacent foredeeps based on analysis of the regional balanced section. *Doklady Earth Sciences* 430(2), 155–157. DOI 10.1134/S1028334X10020017
- Nikishin, A.M., Ziegler, P.A., Bolotov, S.N. & Fokin, P.A. 2012. Late Paleozoic to Cenozoic Evolution of the Black Sea-Southern Eastern Europe Region: A View from the Russian Platform.
- Nikishin, A.M., Khotylev, A.O., Bychkov, A.Yu., Kopaevich, L.F., Petrov, E.I. & Yapaskurt, V.O. 2013. Cretaceous volcanic belts and the evolution of the Black Sea Basin. *Moscow University Geology Bulletin* 68(3), 141–154. DOI 10.3103/S0145875213030058
- Nikishin, A.M., Okay, A.I., Tüysüz, O., Demirer, A., Amelin, N. & Petrov, E. 2015a. The Black Sea basins structure and history: New model based on new deep penetration regional seismic data. Part 1: Basins structure and fill. *Marine and Petroleum Geology* 59, 638–655. DOI 10.1016/j.marpetgeo.2014.08.017
- Nikishin, A.M., Okay, A.I., Tüysüz, O., Demirer, A., Wannier, M., Amelin, N. & Petrov, E. 2015b. The Black Sea basins structure and history: New model based on new deep penetration regional seismic data. Part 2: Tectonic history and paeogeography.
- Nikishin, A.M., Wannier, M., Alekseev, A.S., Almendinger, O.A., Fokin, P.A., Gabdullin, R.R., Khudoley, A.K., Kopaevich, L.F., Mityukov, A.V., Petrov, E.I. & Rubtsova, E.V. 2017. Mesozoic to recent geological history of southern Crimea and the Eastern Black Sea region. *Geological Society, London, Special Publications* 428(1), 241–264. DOI 10.1144/SP428.1
- Okay, A.I. & Nikishin, A.M. 2015. Tectonic evolution of the southern margin of Laurasia in the Black Sea region. *International Geology Review* 57(5–8), 1051–1076. DOI 10.1080/00206814.2015.1010609
- Okay, A.I., Celal Şengör, A.M. & Görür, N. 1994. Kinematic history of the opening of the Black Sea and its effect on the surrounding regions. *Geology* 22(3), 267. DOI 10.1130/0091-7613(1994)022<0267:KHOTOO>2.3.CO;2

- Okay, A.I., Altiner, D. & Kiliç, A.M. 2015. Triassic limestone, turbidites and serpentinite—the Cimmeride orogeny in the Central Pontides. *Geological Magazine* 152(03), 460–479. DOI 10.1017/S0016756814000429
- Pfiffner, O.A. 2017. *Thick-Skinned and Thin-Skinned Tectonics: A Global Perspective*. EARTH SCIENCES, preprint. DOI 10.20944/preprints201707.0020.v2
- Philip, H., Cisternas, A., Gvishiani, A. & Gorshkov, A. 1989. The Caucasus: an actual example of the initial stages of continental collision. *Tectonophysics* 161, 1–21.
- Pochat, S., Castelltort, S., Choblet, G. & Van Den Driessche, J. 2009. High-resolution record of tectonic and sedimentary processes in growth strata. *Marine and Petroleum Geology* 26(8), 1350–1364. DOI 10.1016/j.marpetgeo.2009.06.001
- Rebai, S., Philip, H., Dorbath, L., Borissoff, B., Haessler, H. & Cisternas, A. 1993. Active tectonics in the Lesser Caucasus: coexistence of compressive and extensional structures.
- Ricou, L.E., Braud, J. & Brunn, J.A. 1977. Le Zagros. *Memoire Société Géologique de France Hors Serie(8)*, 33–52.
- Ricou, L.E., Dercourt, J., Geyssant, J., Grandjacquet, C., Lepvrier, C. & Biju-Duval, B. 1986. Geological constraints on the alpine evolution of the Mediterranean Tethys. *Tectonophysics* 123(1–4), 83–122. DOI 10.1016/0040-1951(86)90194-0
- Robertson, A., Parlak, O., Ustaömer, T., Taslı, K., İnan, N., Dumitrica, P. & Karaoğlan, F. 2013. Subduction, ophiolite genesis and collision history of Tethys adjacent to the Eurasian continental margin: new evidence from the Eastern Pontides, Turkey. *Geodinamica Acta* 26(3–4), 230–293. DOI 10.1080/09853111.2013.877240
- Robertson, A.H.F., Dixon, J.E., Brown, S., Collins, A., Morris, A., Pickett, E., Sharp, I. & Ustaömer, T. 1996. Alternative tectonic models for the Late Palaeozoic-Early Tertiary development of Tethys in the Eastern Mediterranean region. *Geological Society, London, Special Publications* 105(1), 239–263. DOI 10.1144/GSL.SP.1996.105.01.22
- Robertson, A.H.F., Parlak, O. & Koller, F. 2009. Tethyan tectonics of the Mediterranean region: Some recent advances. *Tectonophysics* 473(1–2), 1–3. DOI 10.1016/j.tecto.2008.10.036
- Robinson, A.G., Rudat, J.H., Banks, C.J. & Wiles, R.L.F. 1996. Petroleum geology of the Black Sea.

- Rolland, Y. 2017. Caucasus collisional history: Review of data from East Anatolia to West Iran. *Gondwana Research* 49, 130–146. DOI 10.1016/j.gr.2017.05.005
- Rolland, Y., Sosson, M., Adamia, Sh. & Sadradze, N. 2011. Prolonged Variscan to Alpine history of an active Eurasian margin (Georgia, Armenia) revealed by 40Ar/39Ar dating. *Gondwana Research* 20(4), 798–815. DOI 10.1016/j.gr.2011.05.007
- Rolland, Y., Perincek, D., Kaymakci, N., Sosson, M., Barrier, E. & Avagyan, A. 2012. Evidence for ~80–75Ma subduction jump during Anatolide–Tauride–Armenian block accretion and ~48Ma Arabia–Eurasia collision in Lesser Caucasus–East Anatolia. *Journal of Geodynamics* 56–57, 76–85. DOI 10.1016/j.jog.2011.08.006
- Rolland, Y., Hässig, M., Bosch, D., Meijers, M.J.M., Sosson, M., Bruguier, O., Adamia, Sh. & Sadradze, N. 2016. A review of the plate convergence history of the East Anatolia-Transcaucasus region during the Variscan: Insights from the Georgian basement and its connection to the Eastern Pontides. *Journal of Geodynamics* 96, 131–145. DOI 10.1016/j.jog.2016.03.003
- Saintot, A. & Angelier, J. 2002. Tectonic paleostress fields and structural evolution of the NW-Caucasus fold-and-thrust belt from Late Cretaceous to Quaternary. *Tectonophysics* 357, 1–31. DOI 0040-1951/02
- Saintot, A., Brunet, M.-F., Yakovlev, F.L., Sebrier, M., Stephenson, R., Ershov, A.V., Chalot-Prat, F. & McCann, T. 2006. The Mesozoic–Cenozoic tectonic evolution of the Greater Caucasus. In: *European Lithosphere Dynamics*. Geological Society, London, Memoirs, 32, 277–289.
- Scisciani, V., Patruno, S., Tavarnelli, E., Calamita, F., Pace, P. & Iacopini, D. 2019. Multi-phase reactivations and inversions of Paleozoic–Mesozoic extensional basins during the Wilson cycle: case studies from the North Sea (UK) and the Northern Apennines (Italy). *Geological Society, London, Special Publications* 470(1), 205–243. DOI 10.1144/SP470-2017-232
- Şengör, A.M.C. 2003. East Anatolian high plateau as a mantle-supported, north-south shortened domal structure. *Geophysical Research Letters* 30(24). DOI 10.1029/2003GL017858
- Shahidi, A., Barrier, E., Brunet, M.-F. & Saidi, A. 2011. Tectonic Evolution of the Alborz in Mesozoic and Cenozoic. *Scientific Quarterly Journal, GEOSCIENCES* 21(8).
- Sheremet, Y., Sosson, M., Ratzov, G., Sydorenko, G., Voitsitskiy, Z., Yegorova, T., Gintov, O. & Murovskaya, A. 2016a. An offshore-onland transect across the north-eastern Black Sea basin

- (Crimean margin): Evidence of Paleocene to Pliocene two-stage compression. *Tectonophysics* 688, 84–100. DOI 10.1016/j.tecto.2016.09.015
- Sheremet, Y., Sosson, M., Muller, C., Gintov, O., Murovskaya, A. & Yegorova, T. 2016b. Key problems of stratigraphy in the Eastern Crimea Peninsula: some insights from new dating and structural data. *Geological Society, London, Special Publications* 428(1), 265–306. DOI 10.1144/SP428.14
- Sokhadze, G., Floyd, M., Godoladze, T., King, R., Cowgill, E.S., Javakhishvili, Z., Hahubia, G. & Reilinger, R. 2018. Active convergence between the Lesser and Greater Caucasus in Georgia: Constraints on the tectonic evolution of the Lesser–Greater Caucasus continental collision. *Earth and Planetary Science Letters* 481, 154–161. DOI 10.1016/j.epsl.2017.10.007
- Somin, M.L. 1996. Advection hypothesis of fold formation in the Greater Caucasus in light of data on deformation of its basement (On the occasion of the paper by V. N. Sholpo, ‘Advection hypothesis and structure of the core complexes in the inversion anticlinoria of the Greater Caucasus’. *Geotectonics* 28(5). DOI 0016-8521/96/2805-0009\$18.00/1
- Sosson, M., Kaymakci, N., Stephenson, R., Bergerat, F. & Starostenko, V. 2010a. Sedimentary basin tectonics from the Black Sea and Caucasus to the Arabian Platform: introduction. *Geological Society, London, Special Publications* 340(1), 1–10. DOI 10.1144/SP340.1
- Sosson, M., Rolland, Y., Müller, C., Danelian, T., Melkonyan, R., Kekelia, S., Adamia, S., Babazadeh, V., Kangarli, T., Avagyan, A., Galoyan, G. & Mosar, J. 2010b. Subductions, obduction and collision in the Lesser Caucasus (Armenia, Azerbaijan, Georgia), new insights. *Geological Society, London, Special Publications* 340(1), 329–352. DOI 10.1144/SP340.14
- Sosson, M., Adamia, S., Muller, C., Sadradze, N., Rolland, Y., Alania, V., Enukidze, O. & Hassig, M. 2013. From Greater to Lesser Caucasus: new insights from surface and subsurface data along a N-S Trending Transect (Georgia): Thick-Skin versus Thin-Skin tectonics. *Darius News*.
- Sosson, M., Stephenson, R., Sheremet, Y., Rolland, Y., Adamia, S., Melkonian, R., Kangarli, T., Yegorova, T., Avagyan, A., Galoyan, G., Danelian, T., Hässig, M., Meijers, M., Müller, C., Sahakyan, L., Sadradze, N., Alania, V., Enukidze, O. & Mosar, J. 2016a. The eastern Black Sea-Caucasus region during the Cretaceous: New evidence to constrain its tectonic evolution. *Comptes Rendus Geoscience* 348(1), 23–32. DOI 10.1016/j.crte.2015.11.002
- Sosson, M., Stephenson, R., Sheremet, Y., Rolland, Y., Adamia, S., Melkonian, R., Kangarli, T., Yegorova, T., Avagyan, A., Galoyan, G., Danelian, T., Hässig, M., Meijers, M., Müller, C., Sahakyan, L.,

- Sadradze, N., Alania, V., Enukidze, O. & Mosar, J. 2016b. The eastern Black Sea-Caucasus region during the Cretaceous: New evidence to constrain its tectonic evolution. *Comptes Rendus Geoscience* 348(1), 23–32. DOI 10.1016/j.crte.2015.11.002
- Sosson, M., Stephenson, R. & Adamia, S. 2017a. Tectonic Evolution of the Eastern Black Sea and Caucasus: an introduction. *Geological Society, London, Special Publications* 428(1), 1–9. DOI 10.1144/SP428.16
- Sosson, M., Stephenson, R. & Adamia, S. 2017b. Tectonic Evolution of the Eastern Black Sea and Caucasus: an introduction. *Geological Society, London, Special Publications* 428(1), 1–9. DOI 10.1144/SP428.16
- Stampfli, G., Marcoux, J. & Baud, A. 1991. Tethyan margins in space and time. *Palaeogeography, Palaeoclimatology, Palaeoecology* 87(1–4), 373–409. DOI 10.1016/0031-0182(91)90142-E
- Stampfli, G.M. & Borel, G.D. 2002. A plate tectonic model for the Paleozoic and Mesozoic constrained by dynamic plate boundaries and restored synthetic oceanic isochrons. *Earth and Planetary Science Letters* 196, 17–33. DOI 0012-821X / 02 / \$
- Stephenson, R. & Schellart, W.P. 2010. The Black Sea back-arc basin: insights to its origin from geodynamic models of modern analogues. *Geological Society, London, Special Publications* 340(1), 11–21. DOI 10.1144/SP340.2
- Suppe, J. 1983. Geometry and kinematics of fault-bend folding. *American Journal of Science* 283, 684–721.
- Suppe, J. 1997. Bed-by-bed fold growth by kink-band migration: Sant Llorenç de Morunys, eastern Pyrenees. *Journal of Structural Geology* 19(3–4), 443–461. DOI 0191-8141/97\$ 17.00+0.00
- Suppe, J. & Medwedeff, D.A. 1990. Geometry and kinematics of fault-propagation folding. *Eclogae geol. Helv.* 83(3), 409–454. DOI 0012-9402/90/030409-46 S 1.50 + 0.20/0
- Suppe, J., Chou, G.T. & Hook, C. 1992. Rates of folding and faulting determined from growth strata.
- Tari, G., Vakhania, D., Tatishvili, G., Mikeladze, V., Gogritchiani, K., Vacharadze, S., Mayer, J., Sheya, C., Siedl, W., Banon, J.J.M. & Trigo Sanchez, J.L. 2018. Stratigraphy, structure and petroleum exploration play types of the Rioni Basin, Georgia. *Geological Society, London, Special Publications* 464(1), 403–438. DOI 10.1144/SP464.14



- Tari, G., Arbouille, D., Schlöder, Z. & Tóth, T. 2020. Inversion tectonics: a brief petroleum industry perspective. *Solid Earth* 11(5), 1865–1889. DOI 10.5194/se-11-1865-2020
- Tari, G.C. & Simmons, M.D. 2018. History of deepwater exploration in the Black Sea and an overview of deepwater petroleum play types. *Geological Society, London, Special Publications* 464(1), 439–475. DOI 10.1144/SP464.16
- Tibaldi, A., Russo, E., Bonali, F.L., Alania, V., Chabukiani, A., Enukidze, O. & Tsereteli, N. 2017a. 3-D anatomy of an active fault-propagation fold: A multidisciplinary case study from Tsaishi, western Caucasus (Georgia). *Tectonophysics* 717, 253–269. DOI 10.1016/j.tecto.2017.08.006
- Tibaldi, A., Alania, V., Bonali, F.L., Enukidze, O., Tsereteli, N., Kvavadze, N. & Varazanashvili, O. 2017b. Active inversion tectonics, simple shear folding and back-thrusting at Rioni Basin, Georgia. *Journal of Structural Geology* 96, 35–53. DOI 10.1016/j.jsg.2017.01.005
- Trexler, C., Cowgill, E., Spencer, J.Q.G. & Godoladze, T. 2020. Rate of active shortening across the southern thrust front of the Greater Caucasus in western Georgia from kinematic modeling of folded river terraces above a listric thrust.
- van der Boon, A., Kuiper, K.F., Villa, G., Renema, W., Meijers, M.J.M., Langereis, C.G., Aliyeva, E. & Krijgsman, W. 2017. Onset of Maikop sedimentation and cessation of Eocene arc volcanism in the Talysh Mountains, Azerbaijan. *Geological Society, London, Special Publications* 428(1), 145–169. DOI 10.1144/SP428.3
- Vergés, J., Marzo, M. & Muñoz, J.A. 2002. Growth strata in foreland settings. *Sedimentary Geology* 146, 1–9. DOI 0037-0738/02/\$
- Vincent, S.J., Morton, A.C., Carter, A., Gibbs, S. & Barabadze, T.G. 2007. Oligocene uplift of the Western Greater Caucasus: an effect of initial Arabia-Eurasia collision. *Terra Nova* 19(2), 160–166. DOI 10.1111/j.1365-3121.2007.00731.x
- Vincent, S.J., Carter, A., Lavrishchev, V.A., Rice, S.P., Barabadze, T.G. & Hovius, N. 2011. The exhumation of the western Greater Caucasus: a thermochronometric study. *Geological Magazine* 148(01), 1–21. DOI 10.1017/S0016756810000257
- Vincent, S.J., Hyden, F. & Braham, W. 2014. Along-strike variations in the composition of sandstones derived from the uplifting western Greater Caucasus: causes and implications for reservoir

quality prediction in the Eastern Black Sea. *Geological Society, London, Special Publications* 386(1), 111–127. DOI 10.1144/SP386.15

Vincent, Stephen J, Braham, W., Lavrishchev, V., Maynard, J.R. & Harland, M. 2016. The formation of inversion of the western Greater Caucasus Basin and the uplift of the western Greater Caucasus: implications for the wider Black Sea region.

Yilmaz, A., Adamia, S. & Yilmaz, H. 2013. Comparisons of the suture zones along a geotraverse from the Scythian Platform to the Arabian Platform.